Elucidating the Physiological and Genomic Underpinnings of Lipid-Related Metabolic Disorders and Leveraging Farm Data Streams to Predict Disorder Cases

By

Ryan Selz Pralle

A dissertation submitted in partial fulfillment

of the requirements for the degree of

Doctor of Philosophy

(Dairy Science)

at the

UNIVERSITY OF WISCONSIN – MADISON

2020

Date of final oral examination: 07/30/2020

The dissertation is approved by the following members of the Final Oral Committee:

Heather M. White, Associate Professor, Dairy Science
Kent A. Weigel, Professor, Dairy Science
Randy D. Shaver, Emeritus Professor, Dairy Science
Garrett R. Oetzel, Professor, School of Veterinary Medicine
Wenli Li, Dairy Scientist, United States Dairy Forage Research Center
Robert H. Fourdraine, Adjunct Professor, Dairy Science

This dissertation is dedicated to my grandfathers,
John Selz & Earl Pralle

ACKNOWLEDGEMENTS

This dissertation represents years of work that would not have been possible without the support of many individuals. Foremost, I would like to thank my major adviser, Dr. Heather White, for the support, guidance, and patience she has provided all these years. I cannot thank her enough for shaping me into the scientist I am today and for championing my achievements. Additionally, I would like to thank the remaining members of my Ph.D. committee, Drs. Kent Weigel, Randy Shaver, Gary Oetzel, Robert Fourdraine, and Wenli Li. They have been instrumental to my personal growth as both mentors and research collaborators.

A special thank you to Sandy Bertics, the heart and soul of the Dairy Science nutrition group. I will be forever grateful to Sandy for hiring me as a student hourly and introducing me to Heather, which made all of this possible. Also, I am grateful that she always made time for me and so many other students, sharing her boundless knowledge and wisdom.

Thank you to my friends and colleagues in the Dairy Science nutrition group for the long hours of work, study, and discussion we put in together over the years. They made every moment joyful and precious. I would especially like to thank Henry, Kristina, Rafael, Sophia, and Tawny for tolerating my antics over the years.

Finally, I would like to thank my family for the love and support they gave me throughout my years of education. The constant encouragement from my parents, Scott and Pam, helped keep me motivated and they were constant reminders of the mission of my research. Meanwhile, Jessica and Nicole, my sisters, have always kept me humble with our playful banter. Above all, I thank Brooke, my loving and patient wife, for being my constant companion and keeping me grounded.

TABLE OF CONTENTS

LIST OF TABLES

CHAPTER 2

CHAPTER 3

CHAPTER 6

LIST OF FIGURES

CHAPTER 2

CHAPTER 5

CHAPTER 6

CHAPTER 7

LIST OF ABBREVIATIONS

ABHD5 = abhydrolase domain containing 5

AGEFC = age at first calving

ANN = artificial neural network

ANT = antigen

ANT● = oxidized antigen

aPNPLA3 = adipose patatin-like phospholipase domain-containing protein 3

ATGL = adipose triglyceride lipase

AUC = area under the curve

BCS = body condition score

BHB = β-hydroxybutyrate

BOLA-DQB = bovine lymphocyte antigen – DQB

BW = body weight

CCC = concordance correlation coefficient

CI = confidence interval

CK = cytokine

COL14A1 = collagen type XIV alpha 1 chain

CP = crude protein

CTL = control

DAVID = Database for Annotation, Visualization and Integrated Discovery

DEG = differentially expressed gene

DEPTOR = DEP domain-containing mTOR-interacting protein

DHI = dairy herd improvement

DIM = day in milk

DM = dry matter

DMI = dry matter intake

DRTC = days relative to calving

EC = eicosanoid

EE = ether extract

EMP = enriched metabolic pathway

ENPP2 = ectonucleotide pyrophosphatase/phosphodiesterase 2

F:P = fat to protein ration

FA = fatty acid

FE = fold enrichment

FFselect = feature forward selection

FLI = fatty liver induction

FLS = fatty liver syndrome

FPKM = fragments per kilobase of transcript

FTIR = Fourier-transform infrared

GBLUP = genomic best linear unbiased prediction

GC = GC vitamin D binding protein

GHR1A = growth hormone receptor 1A

GSH = glutathione

GWAS = genome-wide association study

GWIS = genome-wide interaction study

HYK = hyperketonemia

HYS = herd-year-season

IFI = the interferon inducible protein

IFN = interferon

IGF-1 = insulin-like growth factor 1

KEGG = Kyoto encyclopedia of genes and genomes

LCFA = long chain fatty acid

LMM = linear mixed model

lPNPLA3 = liver patatin-like phospholipase domain-containing protein 3

LR = less resistant

LRMD = lipid-related metabolic disorder

LS = less susceptible

LSM = least squares mean

MCFA = medium chain fatty acid

mFTIR = milk Fourier-transform infrared

MHC = major histocompatibility complex

MITO = mitochondria

MLR = multiple linear regression

MR = more resistant

MRPL13 = mitochondrial ribosomal protein L13

MS = more susceptible

MSE = mean squared error

mTest = milk composition and producer-reported data

MUFA = monounsaturated fatty acid

MUN = milk urea nitrogen

NAFLD = non-alcoholic fatty liver disease

NDF = neutral detergent fiber

NEB = net energy balance

NEL = net energy of lactation

NFC = non-fiber carbohydrate

NPFFR2 = neuropeptide FF receptor 2

NPV = negative predictive value

OAA = oxaloacetate

PC = pyruvate carboxylase

PCK = phosphoenolpyruvate carboxykinase

PLACT = previous lactation

PLS = partial least squares regression

PME305 = previous 305-day mature equivalent milk

PNPLA3 = patatin-like phospholipase domain-containing protein 3

POX = peroxisome

PPV = positive predictive value

PUFA = polyunsaturated fatty acid

R2 = coefficient of determination

RMSE = root mean squared error

ROS = reactive oxygen species

SAA = serum amyloid A

SCC = somatic cell count

SCFA = short chain fatty acid

SE = standard error

SFA = saturated fatty acid

SLC4A4 = solute carrier family 4 member 4

SnF = solids not fat

SNP = single nucleotide polymorphism

T2D = type 2 diabetes mellitus

TCA = tricarboxylic acid

TG = triglyceride

TRIM36 = tripartite motif containing 36

TRT = treatment

VIF = variable inflation factor

VLDL = very-low density lipoproteins

ΔBCS = body condition score change

ΔBW = body weight change

ABSTRACT

Dairy cows must orchestrate whole-body physiological and metabolic adaptations during the rapid transition from a gravid, non-lactating state to a non-gravid, lactating state. The complexity and importance of these adaptations is underscored by the substantial prevalence of unfavorable health outcomes peripartum. Hyperketonemia (**HYK**) and fatty liver syndrome (**FLS**), comorbid metabolic disorders related to the metabolism of endogenous lipids, have subclinical prevalences of approximately 50% during the first 21 d postpartum. These disorders have substantial economic impact on dairy production systems due to their frequency and association with reduced lactation performance, impaired fertility, greater risk of comorbidities, and greater risk of involuntary culling. Therefore, investigations into the pathophysiology of these lipid-related metabolic disorders (**LRMD**) and innovations in the identification of disorder cases have potential for tremendous beneficial impact on dairy production systems. This dissertation has two major hypotheses: 1) LRMD pathology is influenced by individual variation in the expression of key regulatory genes and metabolic pathways in the liver and 2) the data streams readily available within dairy production systems can be leveraged to identify biological features of HYK and develop convenient, high throughput prediction tools for HYK diagnosis.

Key aspects of whole-animal and liver metabolism pertinent to the peripartum transition period and animal health are reviewed in Chapter 1. In Chapter 2, we hypothesized patatin-like phospholipase domain-containing protein 3 (**PNPLA3**), a lipase and novel candidate gene for bovine FLS, would maintain lipolysis of liver triglyceride (**TG**) peripartum and that the downregulation of liver PNPLA3 at parturition promotes the accumulation of liver TG. Additionally, we hypothesized that PNPLA3 is present in bovine adipose tissue and would have greater abundance during adipose TG mobilization. Thus, we investigated the relationship

between tissue PNPLA3 protein abundance and liver triglyceride accumulation *in vivo* via a fatty liver induction (**FLI**) protocol in multiparous dairy cows peripartum. Results demonstrated a negative association between liver PNPLA3 protein abundance and liver triglyceride content in peripartum dairy cows, while adipose PNPLA3 protein abundance was not associated with blood fatty acid concentration or liver triglyceride content. Future investigations should leverage *in vitro* bovine hepatocyte models to determine a causal relationship between PNPLA3 and liver TG accumulation.

Recognizing that there was a range in metabolic response to the dietary treatments imposed in Chapter 2, we hypothesized that LRMD pathology is regulated by individual variation in metabolic pathways conferring susceptibility (disposition to LRMD occurrence during typical conditions) and resistance (disposition to LRMD onset and severity when presented a challenge). To discover these underlying pathways within the liver of dairy cows, we clustered cows based on postpartum lipid metabolite concentrations (*i.e.* blood fatty acid and liver TG) within the control and FLI dietary treatments in Chapter 3. We identified groups of cows with differential susceptibility to LRMD within the control treatment, as well as with differential resistance to LRMD within the FLI treatment. Comparing the liver transcriptomes among these groups revealed numerous differentially expressed genes related to the innate immune response and inflammation, potentially mediating the adaptation to oxidative stress peripartum. The inferred differential metabolism supports unique roles for glutathione metabolism and eicosanoid metabolism for modulating LRMD susceptibility and resistance, respectively. Additionally, major histocompatibility complex molecules and interferon inducible proteins appear to participate in the metabolic control of susceptibility and resistance to LRMD.

Overall, this research provided novel insights into the role of immunometabolism in LRMD pathology and suggests potential for unique control points for LRMD progression and severity.

Although research presented in Chapters 2 and 3 are basic in nature, progressing our understanding of the liver metabolism associated with LRMD, this work uniquely poses us to also identify the markers that can be used in more applied settings to identify cows with metabolic challenges. Chapter 4 reviews the rapidly advancing use of readily available data streams, or "big data", to manage HYK through prediction. We leveraged farm genetic data in Chapter 5, with the hypothesis that genomic markers routinely utilized for dairy cow genetic evaluations are associated with HYK susceptibility and that some of these associations are dependent on parity group (primiparous vs. multiparous), a HYK risk factor. Therefore, we conducted a cross-sectional epidemiological study where blood β-hydroxybutyrate (**BHB**) concentration was intensively sampled, producing an accurate HYK phenotype. Then, we aligned phenotypes to imputed single nucleotide polymorphism genotypes and utilized a novel linear mixed model methodology to test for genotype and parity group-dependent genotype associations. Our analysis revealed several novel polymorphism genotypes associated with hyperketonemia susceptibility. Genes annotated to the associated genotypes and the pathways they enriched suggested overlap in HYK pathology and the pathology of human metabolic syndrome: insulin resistance, non-alcoholic fatty liver disease, type II diabetes mellitus, and obesity. These genomic associations and implicated pathways may be utilized to improve genomic prediction of HYK susceptibility and provide novel hypotheses for reductionist research, respectively.

Although the causal relationship is not completely understood, there are differences in the chemical composition of milk associated with HYK. In Chapter 6, we hypothesized that

advanced prediction methods, specifically artificial neural networks, and multiple data streams collected routinely during dairy herd improvement testing can produce an accurate, high-throughput tool for diagnosing and monitor hyperketonemia. To evaluate this hypothesis, we cross-validated models predicting blood BHB using multiple linear regression, partial least squares regression, and artificial neural network methodologies for fitting different data stream combinations: dairy herd improvement data, milk Fourier-transform infrared spectra, and those data in combination. We concluded that the artificial neural network models were generally more effective at diagnosing HYK regardless of data stream utilized. The use of data streams in combination may have marginally better predictions. In summary, this work provided several high throughput options for HYK diagnosis that do not require more labor intensive and invasive blood BHB testing.

The work presented in this dissertation significantly contributed to our understanding of LRMD pathology and data-driven approaches to managing HYK. We provided *in vivo* evidence for liver PNPLA3 protein abundance to contribute to the control of liver TG accumulation peripartum. Furthermore, we discovered novel divergence in immunometabolism regulation that was associated with LRMD risk and severity. Based on genomic markers routinely used for cow genetic evaluation, we identified candidate markers and inferred genes associated with human metabolic syndrome that contribute to genetic susceptibility to HYK. Finally, we developed advanced prediction equations based on data streams available to dairy herds as a less invasive and high throughput option for monitoring and managing HYK. While this dissertation provides novel insights into the respective physiological and data science orientated hypotheses, it did not directly address how these bodies of work can be integrated into scientific discovery and data-driven husbandry schemes. Future progress in the integration of biological research into dairy

herd data collection and development of data-based management tools has tremendous potential to improve animal husbandry and can provide opportunities for the precision management of cow metabolic health.

CHAPTER 1: LITERATURE REVIEW PART 1: PHYSIOLOGY OF PERIPARTURIENT DAIRY COWS AND THE ETIOLOGY OF LIPID-RELATED METABOLIC DISORDERS IN EARLY LACTATION

INTRODUCTION

The coordinated physiological and metabolic adaptions that underpin the transition to lactation, or periparturient, period of dairy cows are pivotal determinants of lactation cycle success and farm profitability. Notably, periparturient cows must adapt to the negative net energy and nutrient balance that often occurs due to an expeditious increase in milk production and a lagging increase in voluntary feed intake following parturition (Grummer et al., 2004). This imbalance of nutrient supply has generally been considered the principal challenge to periparturient dairy cows and the maladaptation to this challenge is frequently regarded as the progenitor of poor lactation performance, reduced fertility, and unfavorable health outcomes (Cameron et al., 1998; Herdt, 2000; Dann et al., 2005; Esposito et al., 2014).

Among the unfavorable health outcomes associated with negative net nutrient status, the lipid-related metabolic disorders hyperketonemia (**HYK**) and fatty liver syndrome (**FLS**) have received considerable attention in the last 20 years (Bobe et al., 2004; White, 2015; Overton et al., 2017). Elevated concentrations of β-hydroxybutyrate (**BHB**) and liver TG are the diagnostic biomarkers for HYK and FLS, respectively (Grummer, 1993; Bobe et al., 2004; Overton et al., 2017). These comorbid disorders have received this attention due to large-scale epidemiological studies, which highlighted their substantial prevalence in early lactation dairy cows, reported as 43.2 to 53.2% for HYK and 50.0% for FLS (Jorritsma et al., 2001; McArt et al., 2012; Mahrt et al., 2015). Concern over the prevalence of these disorders is exacerbated by the serious financial

burden they impose due to productive losses and health consequences (Bobe et al., 2004; McArt et al., 2015). Thus, noting the importance of these metabolic disorder to contemporary animal agriculture, this review will summarize our present understanding of periparturient cow nutritional physiology with special attention given to our understanding of HYK and FLS etiology.

PHYSIOLOGICAL AND METABOLIC ADAPTATIONS DURING THE PERIPARTURIENT PERIOD

An adage in dairy cow nutrition is, "the dairy cow is an appendage of the mammary gland." This is never truer than during the weeks following parturition, when the periparturient cow has made homeorhetic adaptions to support milk production. Many of these physiological and metabolic adaptations pertain to partitioning the limited supply of dietary and endogenous nutrients to the mammary gland, supporting milk synthesis and the supply of nutrition to the neonate. These adaptive mechanisms have been extensively reviewed by others (Bauman and Currie, 1980; Grummer, 1993; Bobe et al., 2004; White, 2015; Bradford and Swartz, 2020). With the principal interest of this review being the coordinated efforts to adapt to the net nutrient deficiency often occurring in dairy cows, brief summaries of specific peripartum adaptations will be provided in that context, including nutrient and energy status, endocrine status, immunological status, gluconeogenesis, and lipid metabolism.

Nutrient and Energy Status

Peripartum dairy cows often undergo a reduction in voluntary feed intake in the weeks prior to and after parturition (Bertics et al., 1992; Vazquez-Añon et al., 1994; Greenfield et al., 2000). On a dry matter basis, feed intake declines approximately 25% and 50% for primiparous and multiparous cows, respectively, in the 14 d preceding parturition (Marquardt et al., 1977).

This depression in voluntary intake before calving is followed by the expeditious increase in energy and nutrient requirements to support lactation after parturition, resulting in a net negative energy and nutrient status (Ingvartsen and Andersen, 2000; Grummer et al., 2004; Mann et al., 2015). Therefore, early lactation cows become dependent on the mobilization of endogenous nutrient stores to meet lactation requirements, such as stored adipose triglycerides (**TG**) for energy, skeletal muscle for protein, and bone for calcium (Bauman and Bruce Currie, 1980; Herdt, 2000; Wilkens et al., 2020). The myriad of physiological changes peripartum make it difficult to isolate causative factors for the reduction in feed intake (Ingvartsen and Andersen, 2000). The predominant factors for feed intake regulation in mid- to late lactation cows are the satisfaction of productive requirements (*i.e.* lactation and maintenance energy requirements) and the physical filling effects of diet ingredients (Conrad et al., 1964; Mertens, 1987; Allen, 1996). For peripartum cows, a prevailing theory of intake regulation is the hepatic oxidation theory where the oxidation of substrate, particularly endogenous fatty acids (**FA**) liberated from adipose tissue, can induce firing of the vagal afferent nerves and hypothalamus mediated intake suppression (Allen et al., 2009; Allen, 2020).

Endocrine Status

Homeorhetic mechanisms for modulating whole-cow physiological state are mediated by hormones or other products secreted from endocrine glands into the blood supply. The principal endocrine hormones for regulating energy status include glucagon, insulin, and somatotropin (Bauman and Bruce Currie, 1980). Insulin and glucagon are pancreatic peptide hormones that are the most well known for their regulation of fed and fasted states. Considered the main anabolic hormone, insulin is secreted from pancreatic β-cells in response to the postprandial increase in blood concentrations of nutrients, particularly glucose, to promote the uptake, oxidation, and

sequestering of nutrients by insulin sensitive tissues (*i.e.* adipose, skeletal muscle, and liver; Brockman, 1979). Conversely, glucagon promotes catabolism of endogenous nutrient stores during fasted states, such as adipose TG lipolysis and muscle protein mobilization, in support of gluconeogenesis (Brockman, 1979). Blood insulin concentration decreases postpartum and achieves nadir at approximately 2 wk postpartum (Herbein et al., 1985; Radcliff et al., 2003a; Rhoads et al., 2004). Meanwhile, glucagon appears to maintain its blood concentration from late-pregnancy through the early postpartum period, but does increase around 6 to 8 wk postpartum (Herbein et al., 1985; Osman et al., 2010). These observations suggest a reduced ratio of insulin to glucagon at the onset of lactation, promoting a fasted-like state and catabolism of body nutrient reserves. Somatotropin is a hormone secreted from the anterior pituitary gland and is regarded as the primary hormone for maintenance of lactation in dairy cows. The general effects of somatotropin on physiology include increased amino acid uptake and protein anabolism, lipolysis of adipose TG, oxidation of FA, and hepatic gluconeogenesis, as well as reduced uptake and oxidation of glucose by insulin sensitive tissues (*i.e.* adipose and skeletal muscle). During the final week of gestation, circulating somatotropin concentration will increase and that increase will be maintained postpartum (Goff and Horst, 1997; Rhoads et al., 2004). Interestingly, an uncoupling of the hypothalamic-pituitary-somatotropic axis occurs postpartum due to a reduction in hepatic growth hormone receptor 1A (**GHR1A**) expression that begins about one-week prepartum. Loss of GHR1A expression prevents the downstream signaling that promotes the synthesis and secretion of hepatic insulin-like growth factor 1 (**IGF-1**; Radcliff et al., 2003a; b). Thus, the primary negative feedback signaling mechanism that maintains somatotropin homeostasis, IGF-1 secretion, is attenuated. Based on the resumption of hepatic GHR1A expression and the concomitant increase in circulating IGF-1, this feedback mechanism is not

reestablished until approximately 2 wk after parturition (Radcliff et al., 2003a; b; Rhoads et al., 2004). Overall, the early postpartum hormonal adaptations support lactation through the mobilization of body nutrient reserves and partitioning of these nutrients towards the mammary gland for milk production. This homeorhetic adaptation is essential considering the negative net nutrient status that is often experienced by dairy cows (Ingvartsen and Andersen, 2000; Grummer et al., 2004; Mann et al., 2015).

Immunological and Inflammatory Status

The contributions of the immune system and inflammatory response to the adaptation to lactation has only recently received significant attention in periparturient dairy cows. Of particular interest, the question raised is to what extent does the inflammatory tone of tissues contribute to metabolic regulation and health? After parturition, cows typically experience a degree of immunosuppression including reductions in serum immunoglobulin G concentration, lymphocyte concentration and blastogenetic response, and neutrophil phagocytosis (Ishikawa, 1987; Kehrli et al., 1989; Saad et al., 1989). Additionally, the circulating concentrations of acute phase proteins, such as haptoglobin and serum amyloid A, increase immediately postpartum, as well as a variety of pro-inflammatory cytokines (Humblet et al., 2006; Pohl et al., 2015; Cui et al., 2019). These data suggested an immunosuppressed and proinflammatory state during early lactation. However, the interaction with the nutritional status and health of dairy cows is still a growing field.

Gluconeogenesis

Lactose is the primary carbohydrate in milk, which is synthesized in the mammary gland; 1 mol of lactose requires 2 mol of glucose. Thus, at the initiation of lactation, glucose requirements increase dramatically for dairy cows to support milk production (Aschenbach et al.,

2010). Hepatic gluconeogenesis is the primary mechanism to satisfy the glucose requirement because dietary sugars and starch are anaerobically fermented in the rumen to volatile FA (Russell and Hespell, 1981). The gluconeogenesis pathway produces glucose through the conversion of intermediates extracted from the tricarboxylic acid (**TCA**) cycle and other intermediates to glucose. Metabolic substrates that support anaplerosis of TCA in support of gluconeogenesis include propionate, lactate, and amino acids (Lomax and Baird, 1983). Propionate —the predominate gluconeogenic substrate— is converted to propionyl-CoA by propionyl-CoA carboxylase and enters TCA cycle as succinyl-CoA via methylmalonyl-CoA mutase. Lactate and some glucogenic amino acids enter TCA cycle through conversion of their carbon skeletons to pyruvate and are subsequently carboxylated to oxaloacetate (**OAA**) by pyruvate carboxylase (**PC**). Cataplerosis of TCA to support gluconeogenesis is mediated by phosphoenolpyruvate carboxykinase (**PCK**), decarboxylating OAA to phosphoenolpyruvate (White, 2015). Reverse reactions of glycolysis mediate the remainder of gluconeogenesis, with fructose bisphosphatase and glucose-6-phosphatase catalyzing the committal reactions (Aschenbach et al., 2010). Glycerol enters gluconeogenesis during these reverse reactions through its conversion to dihydroxyacetone phosphate by glycerol phosphate dehydrogenase. Energy supporting the anabolism of glucose is provided by the oxidation of FA, including rumen volatile FA and preformed FA either from the diet or adipose tissue (Bauman and Currie, 1980).

Lipid Metabolism

Lipids serve a variety of biological functions including energy storage, signaling, and acting as a structural component in cell membranes. The major classes of lipids referred to in the nutrient regulation of the transition period and etiology of lipid-related metabolic disorders are

FA and glycerolipids, particularly TG (Grummer, 1993; Bobe et al., 2004). This section will focus on the postabsorptive metabolism of these substrates within key tissues: adipose and liver.

Lipogenesis is the anabolic pathway for synthesis of FA from dietarily sourced substrates as a method to store excess dietary energy during the postprandial state. In dairy cows, this occurs predominately in adipose tissue during periods of positive net energy balance (*i.e.* late pregnancy) and the mammary gland during lactation (Bauman and Bruce Currie, 1980). The bovine liver is considered to have limited *de novo* lipogenesis (Pullen et al., 1990). Acetate and butyrate produced by anerobic fermentation of carbohydrates in the ruminant gastrointestinal tract serve as the primary substrates for lipogenesis in adipose tissue and within the mammary gland (Bauman and Currie, 1980). First, acetate and butyrate must be activated with coenzyme A. Then, acetyl-CoA carboxylase catalyzes the first step of *de novo* synthesis forming malonyl-CoA from two acetyl-CoA. Condensation of additional acetyl-CoA units onto the growing FA chain is catalyzed by FA synthetase; however, *de novo* FA chains cannot elongate beyond 18 carbons (9 acetyl-CoA units; St. John et al., 1991). Preformed FA from the diet, generally ≥16 carbon chains, can be utilized by adipose tissue and the mammary gland after transport mediated by FA translocases, FA binding protein, and acyl-CoA synthetases (Stremmel et al., 2001; Digel et al., 2009). Both preformed and *de novo* FA are esterified for storage in adipose tissue or secretion from the mammary gland as glycerolipids, predominately TG, by the successive addition of FA to glycerol phosphate (Coleman et al., 2000). The major enzymes responsible for esterification are glycerol-3-phosphate acyltransferase, 1-acyclglycerol-3-phosphate acyltransferase, and diacylglycerol acyltransferase, successively (Coleman et al., 2000). The resulting TG are stored as lipid droplets within adipose tissue and coated with lipid droplet-associated proteins; notably, perilipin coats the droplet, preventing enzyme access and

breakdown of TG (Tansey et al., 2004; Koltes and Spurlock, 2011). Uptake, esterification, and storage of FA as TG does occur in the liver of dairy cows by the same mechanisms; however, this occurs during the peripartum period and other periods of negative net energy balance. These FA stored in the liver are predominately sourced from lipolysis of adipose tissue (Grummer, 1993; White, 2015).

Lipolysis is the enzyme mediated catabolism of lipids into monomeric units for further utilization by tissues. This is most prominent in the adipose tissue of peripartum dairy cows, where negative energy balance promotes the use of endogenous nutrient stores. Phosphorylation cascades induced by fasting signals (*i.e.* glucagon) result in the phosphorylation of perilipin coating adipocyte lipid droplets, inducing conformational changes that promote lipase access to the lipid droplet and releases the co-localized protein abhydrolase domain containing 5 (**ABHD5**; Tansey et al., 2004; Koltes and Spurlock, 2011). Additionally, the lipases hormone sensitive lipase and adipose triglyceride lipase (**ATGL**) become activated by phosphorylation and ABHD5, respectively (Koltes and Spurlock, 2011; De Koster et al., 2018). These lipases mediate the cleavage of FA from TG and other glycerolipids for metabolism within adipose tissue or secretion into blood circulation for use as energetic substrate in other tissues. In nonruminants, ATGL has become knowns as the rate-limiting step in lipolysis (De Koster et al., 2018). While aspects of this cascade are similar to human and nonruminant physiology, it is less clear what the key rate-limiting enzyme is in bovine since ATGL is decreased at parturition when lipolysis is at the peak (Koltes and Spurlock, 2011).

Interestingly, there is limited knowledge on the role of lipases in the liver, particularly in the clearance of stored liver TG as cows enter progressively more positive energy balance around peak lactation (White, 2020). The activity of the lipase patatin-like phospholipase domain-

containing protein 3 (**PNPLA3**) has been found to be key to the regulation of liver TG accumulation in humans and the pathology of nonalcoholic fatty liver disease (Ruhanen et al., 2014, 3; Pingitore and Romeo, 2019). Additionally, liver mRNA expression of *PNPLA3* is reduced immediately postpartum in dairy cows when peak liver TG accumulation occurs (McCann et al., 2014). This makes liver lipases, specifically PNPLA3, interesting candidates for the regulation of the net accumulation of liver TG postpartum, as well as the pathology and recovery from FLS in dairy cows.

Uptake and utilization of blood FA liberated from adipose tissue occurs in a variety of other tissues, including the mammary gland, skeletal muscle, and the liver (Bauman and Currie, 1980). We will focus on the metabolic fates of these FA in the liver because it is central to the pathology of HYK and FLS. During the peripartum period, the liver manages the substantial liberation of FA through uptake of approximately 20% of the circulating FA (Thompson and Darling, 1975; Emery et al., 1992). Again, blood FA uptake is mediated by FA translocases, FA binding protein, and acyl-CoA synthetases (Stremmel et al., 2001; Digel et al., 2009) and seems to be proportional to the concentration of blood FA (Stremmel and Theilmann, 1986). After liver uptake, FA have four possible fates: complete oxidation to CO_2, incomplete oxidation to ketones, storage in the liver as TG, or export as TG in very-low density lipoproteins (**VLDL**). Oxidation of FA begins with a committal activation of the FA with coenzyme A, producing acyl-CoA. Then, acyl-CoA undergoes β-oxidation within the cell mitochondria or peroxisomal oxidation; both pathways yield acetyl-CoA units proportional to FA carbon chain length. From here, acetyl-CoA can be completely oxidized by entering the TCA cycle through condensation with OAA, yielding CO_2 and energy equivalents (*i.e.* adenosine triphosphate and reduced nicotinamide adenine dinucleotide). Alternatively, acetyl-CoA can undergo ketogenesis through the

condensation of two acetyl-CoA units to acetoacetyl-CoA (White, 2015). The end products of ketogenesis are the ketone bodies acetoacetate, BHB, and acetone, which are secreted into the blood circulation. While the rumen epithelial wall can convert butyrate to BHB (Reynolds et al., 1988), incomplete oxidation of acetyl-CoA to ketone bodies only occurs in the liver. These ketone bodies, except acetone, can be used by extrahepatic tissues as an alternative energy source, especially during fasting or other negative energy balance conditions (Andersson, 1988; Herdt, 2000). As previously mentioned, esterification of the endogenously sourced FA to glycerolipids can occur in the liver during negative energy balance (Grummer, 1993). These glycerolipids can be stored in the liver or secreted into the blood circulation as VLDL. Secretion of VLDL is apparently limited in ruminant species compared to monogastrics in tissue culture (Kleppe et al., 1988).

PATHOLOGY OF LIPID-RELATED METABOLIC DISORDERS

Failure to properly orchestrate the physiological and metabolic adaptations supporting early lactation energy and nutrient requirements can result in numerous pathologies, including the lipid-related metabolic disorders HYK and FLS. These disorders are considered co-morbid because they often develop concurrently and are thought to be the result of similar metabolic imbalances (Grummer, 1993; Bobe et al., 2004; White, 2015). In particular, the substantial increase in FA liberation from adipose tissue early postpartum and the apparent linear uptake of circulating FA by hepatocytes promotes an increasingly large pool of hepatic FA that needs to be metabolized. Ideally, these FA would be oxidized (peroxisomal or mitochondrial β-oxidation), and the resulting acetyl-CoA products would be completely oxidized via the TCA cycle (White, 2015). However, an imbalance in the TCA cycle capacity, FA supply, or both promotes alternative metabolic fates of these FA: ketogenesis or storage as TG in hepatic lipid droplets

(Grummer, 1993; Bobe et al., 2004; White, 2015). Continued peroxisomal or β-oxidation of FA in excess of the TCA capacity results in an increasingly large pool of acetyl-CoA, which will be redirected towards ketogenesis. Ketone body production and their secretion into biological fluids (*i.e.* milk, urine, and blood) of cows will result in elevated concentrations of these ketone bodies which is the diagnostic hallmark of HYK (Andersson, 1984, 1988; Overton et al., 2017). Insufficient oxidation of preformed FA taken up by the TCA cycle or ketogenesis, as well as the insufficient secretion via VLDL, is thought to redirect the excess FA towards re-esterification to TG for temporarily storage within hepatocyte lipid droplets (Grummer, 1993; White, 2015). Thus, net accumulation of hepatic TG occurs and may progress to FLS (Bobe et al., 2004). There are several competing theories regarding which principal insult(s) shift endogenous FA metabolic fates towards ketogenesis and storage as TG. This section will briefly highlight three predominant theories: oxaloacetate shortage, insulin resistance, and inflammation.

Oxaloacetate Shortage

Capacity of the TCA cycle has been a suggested limitation for the complete oxidation of endogenous FA to energy molecules (Aschenbach et al., 2010; White, 2015). As previously mentioned, complete oxidation of the acetyl-CoA derived from FA β-oxidation is dependent on its condensation with OAA. Also, cataplerosis of TCA cycle intermediates for gluconeogenesis is mediated by PCK decarboxylation of OAA. This depletion of OAA for glucose production can be exacerbated by the decline in dietary intake peripartum, which limits the supply of anaplerotic substrate to regenerate the OAA pool (*i.e.* propionate and lactate). Thus, the OAA pool may be insufficient for FA derived acetyl-CoA oxidation if there is substantial acetyl-CoA availability (Baird, 1982; Aschenbach et al., 2010; White, 2015). In turn, this may promote an accumulation

of acetyl-CoA that is redirected to ketogenesis, potentially inhibits FA β-oxidation (Schulz, 1994), and may promote partitioning of FA to re-esterification and storage in liver lipid droplets.

Insulin Resistance

Dairy cows experience a degree of insulin resistance postpartum to promote the mobilization of body nutrient reserves in support of lactation. In particular, insulin resistance will reduce the anti-lipolytic signaling in adipose tissue and allow greater mobilization of FA from adipose lipid droplets (De Koster and Opsomer, 2013). There is a question of whether "over-mobilization" of adipose can occur due to excessive insulin resistance where more FA is liberated than required to meet energy requirement (Metz and Bergh, 1977; Grummer, 1993; Drackley and Cardoso, 2014). An oversupply of FA would occur in the liver which may saturate the TCA cycle oxidative capacity and VLDL secretory capacity of the liver. The resulting accumulation of FA and acetyl-CoA would then promote the pathology of HYK and FLS through greater liver re-esterification and storage of FA, as well as ketogenesis (White, 2015). Additionally, there is potential for a metabolic health cycle were insulin resistance mediated adipose over-mobilization promotes greater insulin resistance (Pires et al., 2007) and reduces cow feed intake (Allen et al., 2009), reducing the OAA pool. Intravenous glucose tolerance tests and indexes of insulin resistance have suggested cows with HYK have greater insulin resistance than non-HYK contemporaries (Kerestes et al., 2009; Xu et al., 2014; Djoković et al., 2017).

Immunity and Inflammation

There is a burgeoning interest in the role of the immune response and inflammation in the pathogenesis of lipid-related metabolic disorders. Macrophage invasion of adipose tissue has been demonstrated in early lactation and feed restricted dairy cows (Contreras et al., 2015; 2016). Furthermore, greater degrees of adipose macrophage invasion have been associated with

greater body condition loss peripartum (Newman et al., 2019). These data suggest that immune cells and response are involved in the coordination of lipolysis to support early lactation energy requirement. Additionally, greater concentrations of the inflammatory biomarkers serum amyloid A, haptoglobin, and lipopolysaccharide binding protein have been associated with ketotic cows (Abuajamieh et al., 2016) and tissue transcript profiling has revealed inflammatory states in liver and adipose tissue in the first week of lactation (Loor et al., 2005; Sadri et al., 2010; Saremi et al., 2012). Again, these data are suggestive of some association between the inflammatory response with metabolic health. The interrelationships between metabolic health, immunity, and inflammatory response currently are speculative, but warrant further investigation.

CONCLUSIONS

Dairy cows undergo several physiological adaptations during the peripartum period to support the expeditious increase in lactation energy requirements postpartum while voluntary nutrient intake is insufficient. These adaptations include homeorhetic programming, the reduction of insulin to glucagon ratio and uncoupling of the somatotropic axis, that promotes the liberation of endogenous nutrient reserves to meet the energetic demands of lactation. In particular, the metabolism of endogenous lipid stores is important to meet the energetic demands of gluconeogenesis, milk synthesis, and maintenance. Maladaptation to the peripartum transition can impact lipid metabolism by promoting metabolic fates less ideal than complete oxidation of liberated FA, such as ketogenesis and liver TG accumulation. This can result in the metabolic disorders HYK and FLS, which are prevalent in early lactation dairy cows. Presently, the pathology of these comorbid disorders has been attributed to an insufficient pool of OAA, insensitivity to insulin, and inflammation. There has been limited inquiry into the role of liver lipases in the pathology and recovery from these disorders; specifically, PNPLA3 should be of

substantial interest due to its central role in non-alcoholic fatty liver disease in human beings. Additionally, systems-level research utilizing Omics technology may implicate novel genes and metabolic pathways instrumental to the pathology of HYK and FLS, as highlighted in subsequent chapters.

REFERENCES

Abuajamieh, M., S.K. Kvidera, M.V.S. Fernandez, A. Nayeri, N.C. Upah, E.A. Nolan, S.M. Lei, J.M. DeFrain, H.B. Green, K.M. Schoenberg, W.E. Trout, and L.H. Baumgard. 2016. Inflammatory biomarkers are associated with ketosis in periparturient Holstein cows. Res. Vet. Sci. 109:81–85. https://doi.org/10.1016/j.rvsc.2016.09.015.

Allen, M.S. 1996. Physical constraints on voluntary intake of forages by ruminants. J. Anim. Sci. 74:3063–3075. https://doi.org/10.2527/1996.74123063x.

Allen, M.S. 2020. Review: Control of feed intake by hepatic oxidation in ruminant animals: integration of homeostasis and homeorhesis. Animal 14:s55–s64. https://doi.org/10.1017/S1751731119003215.

Allen, M.S., B.J. Bradford, and M. Oba. 2009. Board Invited Review: The hepatic oxidation theory of the control of feed intake and its application to ruminants. J. Anim. Sci. 87:3317–3334. https://doi.org/10.2527/jas.2009-1779.

Andersson, L. 1984. Concentrations of blood and milk ketone bodies, blood isopropanol and plasma glucose in dairy cows in relation to the degree of hyperketonaemia and clinical signs. Zentralbl. Veterinarmed. A 31:683–693. https://doi.org/10.1111/j.1439-0442.1984.tb01327.x.

Andersson, L. 1988. Subclinical ketosis in dairy cows. Vet. Clin. North Am. Food Anim. Pract. 4:233–251. https://doi.org/10.1016/s0749-0720(15)31046-x.

Aschenbach, J.R., N.B. Kristensen, S.S. Donkin, H.M. Hammon, and G.B. Penner. 2010. Gluconeogenesis in dairy cows: The secret of making sweet milk from sour dough. IUBMB Life 62:869–877. https://doi.org/10.1002/iub.400.

Baird, G.D. 1982. Primary ketosis in the high producing dairy cow: Clinical and subclinical disorders, treatment, prevention, and outlook. J. Dairy Sci. 65:1–10. https://doi.org/10.3168/jds.S0022-0302(82)82146-2.

Bauman, D.E., and W. Bruce Currie. 1980. Partitioning of nutrients during pregnancy and lactation: A review of mechanisms involving homeostasis and homeorhesis. J. Dairy Sci. 63:1514–1529. https://doi.org/10.3168/jds.S0022-0302(80)83111-0.

Bertics, S.J., R.R. Grummer, C. Cadorniga-Valino, and E.E. Stoddard. 1992. Effect of prepartum dry matter intake on liver triglyceride concentration and early lactation. J. Dairy Sci. 75:1914–1922. https://doi.org/10.3168/jds.S0022-0302(92)77951-X.

Bobe, G., J.W. Young, and D.C. Beitz. 2004. Invited review: Pathology, etiology, prevention, and treatment of fatty liver in dairy cows. J. Dairy Sci. 87:3105–3124. https://doi.org/10.3168/jds.S0022-0302(04)73446-3.

Bradford, B.J., and T.H. Swartz. 2020. Review: Following the smoke signals: Inflammatory signaling in metabolic homeostasis and homeorhesis in dairy cattle. Animal 14:s144–s154. https://doi.org/10.1017/S1751731119003203.

Brockman, R.P. 1979. Roles for insulin and glucagon in the development of ruminant ketosis -- a review. Can. Vet. J. 20:121–126.

Cameron, R.E., P.B. Dyk, T.H. Herdt, J.B. Kaneene, R. Miller, H.F. Bucholtz, J.S. Liesman, M.J. Vandehaar, and R.S. Emery. 1998. Dry cow diet, management, and energy balance as risk factors for displaced abomasum in high producing dairy herds. J. Dairy Sci. 81:132–139. https://doi.org/10.3168/jds.S0022-0302(98)75560-2.

Coleman, R.A., T.M. Lewin, and D.M. Muoio. 2000. Physiological and nutritional regulation of enzymes of triacylglycerol synthesis. Annu. Rev. Nutr. 20:77–103. https://doi.org/10.1146/annurev.nutr.20.1.77.

Conrad, H.R., A.D. Pratt, and J.W. Hibbs. 1964. Regulation of feed intake in dairy cows. I. Change in importance of physical and physiological factors with increasing digestibility. J. Dairy Sci. 47:54–62. https://doi.org/10.3168/jds.S0022-0302(64)88581-7.

Contreras, G.A., E. Kabara, J. Brester, L. Neuder, and M. Kiupel. 2015. Macrophage infiltration in the omental and subcutaneous adipose tissues of dairy cows with displaced abomasum. J. Dairy Sci. 98:6176–6187. https://doi.org/10.3168/jds.2015-9370.

Contreras, G.A., K. Thelen, S.E. Schmidt, C. Strieder-Barboza, C.L. Preseault, W. Raphael, M. Kiupel, J. Caron, and A.L. Lock. 2016. Adipose tissue remodeling in late-lactation dairy cows during feed-restriction-induced negative energy balance. J. Dairy Sci. 99:10009–10021. https://doi.org/10.3168/jds.2016-11552.

Cui, L., H. Wang, Y. Ding, J. Li, and J. Li. 2019. Changes in the blood routine, biochemical indexes and the pro-inflammatory cytokine expressions of peripheral leukocytes in postpartum dairy cows with metritis. BMC Vet. Res. 15. https://doi.org/10.1186/s12917-019-1912-y.

Dann, H.M., D.E. Morin, G.A. Bollero, M.R. Murphy, and J.K. Drackley. 2005. Prepartum intake, postpartum induction of ketosis, and periparturient disorders affect the metabolic status of dairy cows. J. Dairy Sci. 88:3249–3264. https://doi.org/10.3168/jds.S0022-0302(05)73008-3.

De Koster, J., R.K. Nelli, C. Strieder-Barboza, J. de Souza, A.L. Lock, and G.A. Contreras. 2018. The contribution of hormone sensitive lipase to adipose tissue lipolysis and its regulation by insulin in periparturient dairy cows. Sci. Reports 8:13378. https://doi.org/10.1038/s41598-018-31582-4.

De Koster, J.D., and G. Opsomer. 2013. Insulin resistance in dairy cows. Vet. Clin. North Am. Food Anim. Pract. 29:299–322. https://doi.org/10.1016/j.cvfa.2013.04.002.

Digel, M., R. Ehehalt, W. Stremmel, and J. Füllekrug. 2009. Acyl-CoA synthetases: Fatty acid uptake and metabolic channeling. Mol. Cell. Biochem. 326:23–28. https://doi.org/10.1007/s11010-008-0003-3.

Djoković, R., V. Dosković, M. Cincović, B. Belić, N. Fratrić, B. Jašović, and M. Lalović. 2017. Estimation of insulin resistance in healthy and ketotic cows during an intravenous glucose tolerance test. Pak. Vet. J. 37:387-392.

Drackley, J.K., and F.C. Cardoso. 2014. Prepartum and postpartum nutritional management to optimize fertility in high-yielding dairy cows in confined TMR systems. Animal 8:5–14. https://doi.org/10.1017/S1751731114000731.

Emery, R.S., J.S. Liesman, and T.H. Herdt. 1992. Metabolism of long chain fatty acids by ruminant liver. J. Nutr. 122:832–837. https://doi.org/10.1093/jn/122.suppl_3.832.

Esposito, G., P.C. Irons, E.C. Webb, and A. Chapwanya. 2014. Interactions between negative energy balance, metabolic diseases, uterine health and immune response in transition dairy cows. Anim. Reprod. Sci. 144:60–71. https://doi.org/10.1016/j.anireprosci.2013.11.007.

Goff, J.P., and R.L. Horst. 1997. Physiological changes at parturition and their relationship to metabolic disorders. J. Dairy Sci. 80:1260–1268. https://doi.org/10.3168/jds.S0022-0302(97)76055-7.

Greenfield, R.B., M.J. Cecava, T.R. Johnson, and S.S. Donkin. 2000. Impact of dietary protein amount and rumen undegradability on intake, peripartum liver triglyceride, plasma metabolites, and milk production in transition dairy cattle. J. Dairy Sci. 83:703–710. https://doi.org/10.3168/jds.S0022-0302(00)74932-0.

Grummer, R.R. 1993. Etiology of lipid-related metabolic disorders in periparturient dairy cows. J. Dairy Sci. 76:3882–3896. https://doi.org/10.3168/jds.S0022-0302(93)77729-2.

Grummer, R.R., D.G. Mashek, and A. Hayirli. 2004. Dry matter intake and energy balance in the transition period. Vet. Clin. North Am. Food Anim. Pract. 20:447–470. https://doi.org/10.1016/j.cvfa.2004.06.013.

Herbein, J.H., R.J. Aiello, L.I. Eckler, R.E. Pearson, and R.M. Akers. 1985. Glucagon, insulin, growth hormone, and glucose concentrations in blood plasma of lactating dairy cows. J. Dairy Sci. 68:320–325. https://doi.org/10.3168/jds.S0022-0302(85)80828-6.

Herdt, T.H. 2000. Ruminant adaptation to negative energy balance. Influences on the etiology of ketosis and fatty liver. Vet. Clin. North Am. Food Anim. Pract. 16:215–230, https://doi.org/10.1016/s0749-0720(15)30102-x.

Humblet, M.-F., H. Guyot, B. Boudry, F. Mbayahi, C. Hanzen, F. Rollin, and J.-M. Godeau. 2006. Relationship between haptoglobin, serum amyloid A, and clinical status in a survey of dairy herds during a 6-month period. Vet. Clin. Pathol. 35:188–193. https://doi.org/10.1111/j.1939-165X.2006.tb00112.x.

Ingvartsen, K.L., and J.B. Andersen. 2000. Integration of metabolism and intake regulation: A review focusing on periparturient animals. J. Dairy Sci. 83:1573–1597. https://doi.org/10.3168/jds.S0022-0302(00)75029-6.

Ishikawa, H. 1987. Observation of lymphocyte function in perinatal cows and neonatal calves. Accessed April 8, 2020. https://www.semanticscholar.org/paper/Observation-of-lymphocyte-function-in-perinatal-and-Ishikawa/474b587d085bd79e51f0b74428af18841bc0fd3c#paper-header.

Jorritsma, R., H. Jorritsma, Y.H. Schukken, P.C. Bartlett, T. Wensing, and G.H. Wentink. 2001. Prevalence and indicators of post partum fatty infiltration of the liver in nine commercial dairy herds in the Netherlands. Livest. Prod. Sci. 68:53–60. https://doi.org/10.1016/S0301-6226(00)00208-6.

Kehrli, M.E., B.J. Nonnecke, and J.A. Roth. 1989. Alterations in bovine lymphocyte function during the periparturient period. Am. J. Vet. Res. 50:215–220.

Kerestes, M., V. Faigl, M. Kulcsar, J. Foeldi, and G. Huszenicza. 2009. Insulin resistance in different forms of hyperketonemia and in cows affected by puerperal metritis.

Kleppe, B.B., R.J. Aiello, R.R. Grummer, and L.E. Armentano. 1988. Triglyceride accumulation and very low density lipoprotein secretion by rat and goat hepatocytes in vitro. J. Dairy Sci. 71:1813–1822. https://doi.org/10.3168/jds.S0022-0302(88)79750-7.

Koltes, D.A., and D.M. Spurlock. 2011. Coordination of lipid droplet-associated proteins during the transition period of Holstein dairy cows. J. Dairy Sci. 94:1839–1848. https://doi.org/10.3168/jds.2010-3769.

Lomax, M.A., and G.D. Baird. 1983. Blood flow and nutrient exchange across the liver and gut of the dairy cow: Effects of lactation and fasting. Br. J. Nutr. 49:481–496. https://doi.org/10.1079/BJN19830057.

Loor, J.J., H.M. Dann, R.E. Everts, R. Oliveira, C.A. Green, N.A.J. Guretzky, S.L. Rodriguez-Zas, H.A. Lewin, and J.K. Drackley. 2005. Temporal gene expression profiling of liver from periparturient dairy cows reveals complex adaptive mechanisms in hepatic function. Physiol. Genomics 23:217–226. https://doi.org/10.1152/physiolgenomics.00132.2005.

Mahrt, A., O. Burfeind, and W. Heuwieser. 2015. Evaluation of hyperketonemia risk period and screening protocols for early-lactation dairy cows. J. Dairy Sci. 98:3110–3119. https://doi.org/10.3168/jds.2014-8910.

Mann, S., F.A.L. Yepes, T.R. Overton, J.J. Wakshlag, A.L. Lock, C.M. Ryan, and D.V. Nydam. 2015. Dry period plane of energy: Effects on feed intake, energy balance, milk production, and composition in transition dairy cows. J. Dairy Sci. 98:3366–3382. https://doi.org/10.3168/jds.2014-9024.

Marquardt, J.P., R.L. Horst, and N.A. Jorgensen. 1977. Effect of parity on dry matter intake at parturition in dairy cattle. J. Dairy Sci. 60:929–934. https://doi.org/10.3168/jds.S0022-0302(77)83965-9.

McArt, J.A.A., D.V. Nydam, and G.R. Oetzel. 2012. Epidemiology of subclinical ketosis in early lactation dairy cattle. J. Dairy Sci. 95:5056–5066. https://doi.org/10.3168/jds.2012-5443.

McArt, J.A.A., D.V. Nydam, and M.W. Overton. 2015. Hyperketonemia in early lactation dairy cattle: A deterministic estimate of component and total cost per case. J. Dairy Sci. 98:2043–2054. https://doi.org/10.3168/jds.2014-8740.

McCann, C.C., M.E. Viner, S.S. Donkin, and H.M. White. 2014. Hepatic patatin-like phospholipase domain-containing protein 3 sequence, single nucleotide polymorphism presence, protein confirmation, and responsiveness to energy balance in dairy cows. J. Dairy Sci. 97:5167–5175. https://doi.org/10.3168/jds.2014-7910.

Mertens, D.R. 1987. Predicting intake and digestibility using mathematical models of ruminal function. J. Anim. Sci. 64:1548–1558. https://doi.org/10.2527/jas1987.6451548x.

Metz, S.H., and S. van den Bergh. 1977. Regulation of fat mobilization in adipose tissue of dairy cows in the period around parturition. Neth. J. Argic. Sci. 25:198-211. https://doi.org/10.18174/njas.v25i3.17132.

Newman, A.W., A. Miller, F.A. Leal Yepes, E. Bitsko, D. Nydam, and S. Mann. 2019. The effect of the transition period and postpartum body weight loss on macrophage infiltrates in bovine subcutaneous adipose tissue. J. Dairy Sci. 102:1693–1701. https://doi.org/10.3168/jds.2018-15362.

Osman, M.A., P.S. Allen, G. Bobe, J.F. Coetzee, A. Abuzaid, K. Koehler, and D.C. Beitz. 2010. Chronic metabolic responses of postpartal dairy cows to subcutaneous glucagon injections, oral glycerol, or both. J. Dairy Sci. 93:3505–3512. https://doi.org/10.3168/jds.2009-2712.

Overton, T.R., J.A.A. McArt, and D.V. Nydam. 2017. A 100-Year Review: Metabolic health indicators and management of dairy cattle. J. Dairy Sci. 100:10398–10417. https://doi.org/10.3168/jds.2017-13054.

Pingitore, P., and S. Romeo. 2019. The role of PNPLA3 in health and disease. Biochimica et Biophysica Acta (BBA) Mol. Cell Biol. Lipids 1864:900–906. https://doi.org/10.1016/j.bbalip.2018.06.018.

Pires, J.A., A.H. Souza, and R.R. Grummer. 2007. Induction of hyperlipidemia by intravenous infusion of tallow emulsion causes insulin resistance in Holstein cows. J. Dairy Sci. 90:2735–2744. https://doi.org/10.3168/jds.2006-759.

Pohl, A., O. Burfeind, and W. Heuwieser. 2015. The associations between postpartum serum haptoglobin concentration and metabolic status, calving difficulties, retained fetal

membranes, and metritis. J. Dairy Sci. 98:4544–4551. https://doi.org/10.3168/jds.2014-9181.

Pullen, D.L., J.S. Liesman, and R.S. Emery. 1990. A species comparison of liver slice synthesis and secretion of triacylglycerol from nonesterified fatty acids in media. J. Anim. Sci. 68:1395–1399. https://doi.org/10.2527/1990.6851395x.

Radcliff, R.P., B.L. McCormack, B.A. Crooker, and M.C. Lucy. 2003a. Plasma hormones and expression of growth hormone receptor and insulin-like growth factor-I mRNA in hepatic tissue of periparturient dairy cows. J. Dairy Sci. 86:3920–3926. https://doi.org/10.3168/jds.S0022-0302(03)74000-4.

Radcliff, R.P., B.L. McCormack, B.A. Crooker, and M.C. Lucy. 2003b. Growth hormone (GH) binding and expression of GH receptor 1A mRNA in hepatic tissue of periparturient dairy cows. J. Dairy Sci. 86:3933–3940. https://doi.org/10.3168/jds.S0022-0302(03)74002-8.

Reynolds, C.K., G.B. Huntington, H.F. Tyrrell, and P.J. Reynolds. 1988. Net metabolism of volatile fatty acids, D-β-hydroxybutyrate, nonesterified fatty acids, and blood gasses by portal-drained viscera and liver of lactating Holstein cows. J. Dairy Sci. 71:2395–2405. https://doi.org/10.3168/jds.S0022-0302(88)79824-0.

Rhoads, R.P., J.W. Kim, B.J. Leury, L.H. Baumgard, N. Segoale, S.J. Frank, D.E. Bauman, and Y.R. Boisclair. 2004. Insulin increases the abundance of the growth hormone receptor in liver and adipose tissue of periparturient dairy cows. J. Nutr. 134:1020–1027. https://doi.org/10.1093/jn/134.5.1020.

Ruhanen, H., J. Perttilä, M. Hölttä-Vuori, Y. Zhou, H. Yki-Järvinen, E. Ikonen, R. Käkelä, and V.M. Olkkonen. 2014. PNPLA3 mediates hepatocyte triacylglycerol remodeling. J. Lipid Res. 55:739–746. https://doi.org/10.1194/jlr.M046607.

Russell, J.B., and R.B. Hespell. 1981. Microbial rumen fermentation. J. Dairy Sci. 64:1153–1169. https://doi.org/10.3168/jds.S0022-0302(81)82694-x.

Saad, A.M., C. Concha, and G. Aström. 1989. Alterations in neutrophil phagocytosis and lymphocyte blastogenesis in dairy cows around parturition. Zentralbl. Veterinarmed. Reihe B 36:337–345. https://doi.org/10.1111/j.1439-0450.1989.tb00612.x.

Sadri, H., R.M. Bruckmaier, H.R. Rahmani, G.R. Ghorbani, I. Morel, and H.A. van Dorland. 2010. Gene expression of tumour necrosis factor and insulin signalling-related factors in subcutaneous adipose tissue during the dry period and in early lactation in dairy cows. J. Anim. Physiol. Anim. Nutr. (Berl.) 94:e194-202. https://doi.org/10.1111/j.1439-0396.2010.01005.x.

Saremi, B., A. Al-Dawood, S. Winand, U. Müller, J. Pappritz, D. von Soosten, J. Rehage, S. Dänicke, S. Häussler, M. Mielenz, and H. Sauerwein. 2012. Bovine haptoglobin as an adipokine: Serum concentrations and tissue expression in dairy cows receiving a conjugated linoleic acids supplement throughout lactation. Vet. Immunol. Immunopathol. 146:201–211. https://doi.org/10.1016/j.vetimm.2012.03.011.

Schulz, H. 1994. Regulation of fatty acid oxidation in heart. J. Nutr. 124:165–171. https://doi.org/10.1093/jn/124.2.165.

St. John, L.C., D.K. Lunt, and S.B. Smith. 1991. Fatty acid elongation and desaturation enzyme activities of bovine liver and subcutaneous adipose tissue microsomes. J. Anim. Sci. 69:1064–1073. https://doi.org/10.2527/1991.6931064x.

Stremmel, W., L. Pohl, A. Ring, and T. Herrmann. 2001. A new concept of cellular uptake and intracellular trafficking of long-chain fatty acids. Lipids 36:981–989. https://doi.org/10.1007/s11745-001-0809-2.

Stremmel, W., and L. Theilmann. 1986. Selective inhibition of long-chain fatty acid uptake in short-term cultured rat hepatocytes by an antibody to the rat liver plasma membrane fatty acid-binding protein. Biochimica et Biophysica Acta (BBA) Lipids Lipid Metabol. 877:191–197. https://doi.org/10.1016/0005-2760(86)90134-7.

Tansey, J., C. Sztalryd, E. Hlavin, A. Kimmel, and C. Londos. 2004. The central role of perilipin A in lipid metabolism and adipocyte lipolysis. IUBMB Life 56:379–385. https://doi.org/10.1080/15216540400009968.

Thompson, G.E., and F. Darling. 1975. The hepatic uptake of individual free fatty acids in sheep during noradrenaline infusion. Res. Vet. Sci. 18:325–327. https://doi.org/10.1016/S0034-5288(18)33586-0.

Vazquez-Añon, M., S. Bertics, M. Luck, R.R. Grummer, and J. Pinheiro. 1994. Peripartum liver triglyceride and plasma metabolites in dairy cows. J. Dairy Sci. 77:1521–1528. https://doi.org/10.3168/jds.S0022-0302(94)77092-2.

White, H.M. 2015. The role of TCA cycle anaplerosis in ketosis and fatty liver in periparturient dairy cows. Animals (Basel) 5:793–802. https://doi.org/10.3390/ani5030384.

White, H.M. 2020. ADSA Foundation Scholar Award: Influencing hepatic metabolism: Can nutrient partitioning be modulated to optimize metabolic health in the transition dairy cow? J. Dairy Sci. 103:P6741-6750. https://doi.org/10.3168/jds.2019-18119.

Wilkens, M.R., C.D. Nelson, L.L. Hernandez, and J.A.A. McArt. 2020. Symposium review: Transition cow calcium homeostasis—Health effects of hypocalcemia and strategies for prevention. J. Dairy Sci. 103:P2909-2927. https://doi.org/10.3168/jds.2019-17268.

Xu, C., S. Shu, C. Xia, B. Wang, H. Zhang, and B. Jun. 2014. Investigation on the relationship of insulin resistance and ketosis in dairy cows. J. Vet. Sci. Technol. 5:2-4. https://doi.org/10.4172/2157-7579.1000162.

CHAPTER 2: PROTEIN ABUNDANCE OF LIVER PATATIN-LIKE PHOSPHOLIPASE DOMAIN-CONTAINING PROTEIN 3, BUT NOT ADIPOSE, WAS NEGATIVELY ASSOCIATED WITH PERIPARTUM LIVER TRIGLYCERIDE IN DAIRY COWS

ABSTRACT

Fatty liver syndrome is a prevalent metabolic disorder in peripartum dairy cows that unfavorably impacts lactation performance and health. Patatin-like phospholipase domain-containing protein 3 (**PNPLA3**) is a lipase that plays a central role in human non-alcoholic fatty liver disease etiology but has received limited attention in bovine fatty liver research. Thus, we investigated the relationship between tissue PNPLA3 expression and liver triglyceride (**TG**) accumulation *in vivo* via a fatty liver induction protocol in multiparous dairy cows peripartum. Multiparous cows were blocked by expected calving date and randomly assigned to a control (n=13) or fatty liver induction (FLI; n=12) treatment. Control cows were given *ab libitum* access to feed peripartum, while FLI cows were offered an additional 6 kg cracked corn top-dress prepartum and feed restricted to 80% *ad libitum* intake at +14 days relative to calving (**DRTC**) until blood β-hydroxybutyrate ≥ 3.0 m*M*. After achieving the β-hydroxybutyrate threshold, FLI cows were treated for ketosis and allowed *ad libitum* intake for the remainder of the study. Liver and adipose tissue biopsies were collected at -28, -14, +1, +14, and +56 DRTC. Additional liver biopsies were collected at +28 and +42 DRTC. Quantification of tissue PNPLA3 protein abundance via semi-quantitative Western blot was normalized to total sample protein. Statistical analysis was performed using the GLIMMIX procedure (SAS 9.4). Liver TG %, DM and tissue PNPLA3 abundance were $\log_{10}$ transformed. Linear mixed models included fixed effects of treatment, DRTC, and treatment × DRTC, as well as random intercepts of cow, block, and

repeated measures of cow across DRTC. The PNPLA3 models included the tissue abundance at -28 DRTC as a covariate. Liver PNPLA3 abundance was also regressed against liver TG. All FLI and 2 control cows had blood β-hydroxybutyrate ≥ 3.0 m*M*. Liver TG content did not differ between treatments ($P = 0.41$) but differed over time ($P < 0.01$). Prepartum liver TG was lower than postpartum; the postpartum maximum and nadir TG were at +14 and +56 DRTC ($P < 0.05$), respectively. No treatment difference was detected for liver PNPLA3 ($P = 0.29$) or adipose PNPLA3 abundance ($P = 0.56$). A time effect was observed ($P < 0.01$) with increasing PNPLA3 from -14 to +56 DRTC. The greatest liver PNPLA3 abundance was observed during the postpartum decrease of liver TG. Adipose tissue PNPLA3 abundance did not differ over time ($P = 0.35$). Liver PNPLA3 had an inverse relationship ($\beta = -0.31$; $P = 0.03$) when regressed against liver TG content. These results suggest liver PNPLA3 protein abundance was not altered by FLI but changed over time inversely compared to postpartum liver TG. Furthermore, regression analysis suggests that incremental increases in liver PNPLA3 may lessen TG accumulation peripartum.

INTRODUCTION

Accumulation of liver triglycerides (**TG**) is a common feature of the periparturient period in dairy cattle due to the negative energy balance and insulin resistance associated with the initiation of lactation (Bauman and Bruce Currie, 1980; Grummer, 1993; Bobe et al., 2004). Excessive accumulation of liver TG can result in clinical fatty liver syndrome (**FLS**), which has been associated with increased risk for other early lactation metabolic disorders, diseases, and impaired lactation performance (Bobe et al., 2004). With an estimated 50% of dairy cows experiencing some liver TG accumulation (Jorritsma et al., 2000, 2001), understanding the etiology of bovine FLS and developing liver TG mitigation strategies are of relevant interest to

dairy production systems. A surprising lacuna in our knowledge is the role of liver lipases to the onset, progression, and recovery of bovine FLS (White, 2020).

Patatin-like phospholipase domain-containing 3 (**PNPLA3**) is a lipase of interest in human medical research because of a genetic mutation (rs738409) associated with nonalcoholic fatty liver disease (**NAFLD**) and steatohepatitis (Romeo et al., 2008; Rotman et al., 2010; Namjou et al., 2019). Thought to be predominately lipolytic in its activity, PNPLA3 can act on mono-, di-, and tri-glycerides (Huang et al., 2011). Liver PNPLA3 has been proposed as a lipid droplet regulator in fed states by remodeling the lipid droplet FA profile (Ruhanen et al., 2014; Pingitore and Romeo, 2019). There has been little investigation into the expression, regulation, and role of PNPLA3 in lipid metabolism of dairy cows. Characterization of liver *PNPLA3* mRNA expression in dairy cows exhibited decreased expression at the time of parturition and during 50% feed restriction (McCann et al., 2014). This observation of decreased expression during natural and induced negative energy balance parallels *PNPLA3* responsiveness to fasting in mice (Polson and Thompson, 2003; Dubuquoy et al., 2011; Huang et al., 2011) and suggests that PNPLA3 may also play a role in liver TG accumulation in dairy cows. Adipose *PNPLA3* has not been strongly linked to the pathology of human NAFLD, but is responsive to nutritional status (Caimari et al., 2007; Oliver et al., 2012), glucose (Moldes et al., 2006; Rae-Whitcombe et al., 2010), and energy status related hormones (Moldes et al., 2006; Calvo and Obregon, 2009; Rae-Whitcombe et al., 2010). The dynamics of PNPLA3 protein abundance in the liver and adipose tissues of periparturient dairy cattle is still unknown.

We hypothesized that PNPLA3 protein maintains liver hydrolysis of TG and that liver PNPLA3 downregulation at parturition promotes accumulation of liver TG. Additionally, we hypothesized that PNPLA3 is present in bovine adipose tissue and would be greater during

adipose TG mobilization. The objectives of this work were 1) to elucidate the peripartum protein abundance of PNPLA3 in the liver and adipose of multiparous dairy cows subjected to a fatty liver induction protocol and 2) to explore the potential association between tissue PNPLA3 protein abundance and liver TG content peripartum.

MATERIALS AND METHODS

All animal use and handling protocols were approved by the University of Wisconsin-Madison College of Agricultural and Life Sciences Animal Care and Use Committee.

Animal Use and Handling

Multiparous Holstein cows (n = 25) were enrolled in the experiment conducted at the University of Wisconsin-Madison Dairy Cattle Instruction and Research Center. Cows were blocked by expected calving date and randomly assigned to a control (**CTL**; n =13) or a fatty liver induction (**FLI**; n = 12) treatment. Enrollment on to treatment began at -28 days relative to expected calving date. The CTL treatment was allowed *ad libitum* intake of rations formulated to meet the needs of dry or lactating cows, respectively (Table 2.1). Cows within the FLI treatment were subjected to a protocol similar to previous work (Drackley et al., 1992; Hippen et al., 1999; Oliveira et al., 2019). Our protocol offered 6 kg of dry, cracked corn as a daily top-dress in addition to *ad libitum* access to the dry cow ration (Table 2.1). After calving, FLI cows were offered *ad libitum* access to the lactating cow ration until +14 DIM, at which time feed intake was restricted to 80% of previous *ad libitum* intake. The previous *ad libitum* intake of a cow was calculated as the average voluntarily feed intake for the 3 d prior to the feed restriction period. Postpartum, whole-blood BHB was monitored daily for all cows with a BHBCheck meter (PortaCheck, Moorestown, NJ). Cows that achieved a whole-blood BHB $\geq$ 3.0 mmol/L were treated with intravenous dextrose (250 mL; Phoenix Scientific Inc., St. Joseph, MO; 50%

dextrose) and orally administered Propylene Advantage (300 mL/d for 3 to 5 days; TechMix LLC, Stewart, MN). In addition, FLI cows undergoing feed restriction that achieved BHB ≥ 3.0 mmol/L were re-alimented feed and allowed *ad libitum* intake for the remainder of the experiment. The median number of days FLI cows were feed restricted was 2 d and ranged from 0 to 12 d.

Sample Collection and Analysis

Daily feed offered and refused was recorded by trained herd staff and daily feed intakes were determined by calculation. Individual feed ingredients and total mixed ration samples were collected weekly. Feed ingredients were dried in a 55° C forced-air oven for 48 h, ground through a Wiley Mill, and composited by month. Composited samples were analyzed for composition by a commercial laboratory (Dairyland Labs, Arcadia, WI). Milk harvest occurred 2x daily with yield recorded at every harvest. For composition analysis, milk samples were collected at 4 consecutive harvests weekly and preserved with 2-bromo-2-nitropropane-1,3-diol. Milk composition of fat, protein, lactose, solids not fat, milk urea nitrogen (**MUN**), and somatic cell count (**SCC**) was determined by a DHIA laboratory (AgSource, Menominee, WI).

Body weights (**BW**) and body condition score (**BCS**), as well as blood and liver biopsies were collected at -28, -14, +1, +14, +28, +42, and +56 DRTC and additional blood samples were taken at -7, -5, -3, +3, +5, +7 DRTC. Adipose biopsies were performed on -28, -14, +1, +14, and +56 DRTC. Net energy balance was calculated using published prediction equations (NRC, 2001), as described by Koltes et al. (2011) for each sampling time point. Two trained individuals recorded BCS using a five-point scale (Wildman et al., 1982) and the scores were averaged within an observation.

Blood samples were collected by venipuncture of the coccygeal vessels before feeding at approximately 0800 hours into evacuated tubes with or without additive. Serum was separated from blood collected in tubes without additive (BD Vacutainer, Franklin Lakes, NJ) after centrifuging at 2,500 x *g* for 15 minutes at room temperature. Plasma was separated from blood collected in an evacuated tube containing potassium oxalate and 4% sodium fluoride (BD Vacutainer, Franklin Lakes, NJ) by centrifuging at 2,000 x *g* for 15 minutes at 4° C. Serum and plasma aliquots were stored at -20° C until metabolite analysis. Plasma glucose, serum BHB, and serum TG concentrations were quantified in their respective aliquots using Catachem VETSPEC reagents on the Catachem Well-T AutoAnalyzer (Catachem, Awareness Technologies, Oxford, CT). All standards were within expected, calibrated ranges provided by the manufacturer during the calibration event (Catachem, Oxford, CT). Samples were read by the autoanalyzer in cuvettes either in duplicate (plasma glucose, serum BHB) or triplicate (serum TG). Methods for glucose (C124-06, Catachem), BHB (C444-0A, Catachem), and TG (C116-0A, Catachem) are based on the work of León et al. (1977), Koch and Feidbruegge (1987), and Trinder (1969), respectively. A serial dilution (1:2) of a standard (NEFA Standard Solution, FUJIFILM Wako Diagnostics U.S.A., Mountain View, CA) was used to establish a standard curve for quantification of serum TG. Plasma FA concentration was quantified enzymatically using a plate adaptation of the Catachem assay (C514-0A; (Trout et al., 1960; Itaya and Ui, 1965; Novak, 1965). Subcutaneous adipose samples were collected from the tailhead region, sampling alternate sides of the tailhead over consecutive sampling dates. First, the tailhead region was shaved, including the sacral vertebrae, coccygeal vertebrae, and pins. The sacrococcygeal space was identified via palpation and an epidural (5 to 7 mL of lidocaine hydrochloride injectible-2%, Clipper Distribution Company, St. Joseph, MO) was given. When the cow's tail became limp, the surgical field was

prepared by alternating washes of povidone iodine (0.75% titratable iodine, First Priority, Elgin, IL) and 70% ethanol solution (3 washes with each solution). Local anesthetic (10 mL of lidocaine) was administered subcutaneously at the planned incision site. A straight-line incision was made (~3 cm) and a sterile 8 mm punch biopsy tool (Miltex model 33-57, Integra LifeSciences, Princeton, NJ) was used to collect adipose tissue (1 to 2 g). Then, the incision was sutured with a sterile non-absorbable suture material (USP 1, Braunamid white, Jorgensen Lab, Loveland, CO). The incision site and general health of the cow was monitored by the research staff and a veterinarian for 5 d post operation. Sutures were removed at 7 to 10 d post operation. Liver samples (~750 mg) were obtained by blind percutaneous biopsy as described previously (Lucy et al., 2009; Walker et al., 2016). Tissue biopsy samples were immediately rinsed with saline, aliquoted into tubes (~250 mg liver per tube; ~500 mg adipose per tube), frozen in liquid nitrogen, and stored at -80° C until further analysis of liver TG and protein abundance. As described by Caputo Oliveira et al. (2020), liver TG content was quantified by colorimetric assay of Folch-extracted product and expressed as a % of dry matter (Folch et al., 1957; Foster and Dunn, 1973; Oliveira et al., 2020). Intra-assay coefficient of variation was less than 10% for the quantification of the preceding blood fraction and liver metabolites. Inter-assay coefficients of variation were 5.9%, 6.5%, 5.6%, and 15.3%, for plasma glucose, plasma FA, serum BHB, and serum TG, respectively.

Semi-quantitative western blotting was used to analyze the abundance of PNPLA3 in liver and adipose tissue. Protein was isolated from tissue samples by homogenization in a lysis buffer: 1.0% nonidet P-40 substitute (US Biological, Salem, MA), 0.5% sodium deoxycholate (Sigma-Aldrich, St. Louis, MO), 0.1% sodium dodecyl sulfate (Sigma-Aldrich), and protease inhibitors (Halt^{TM} Protease and Phosphatase Inhibitor Cocktail, Thermo Scientific, Rockford,

IL). The homogenate was centrifuged at 14,000 x *g* at 4° C for 5 minutes, after which the supernatant was collected for further assay. Bicinchoninic assay (Pierce Biotechnology Inc., Rockford, IL) was used to determine protein content of the supernatant, allowing for a standardized total protein quantity of 25 µg to be used for gel loading.

Protein was isolated from 300 mg adipose tissue and 250 mg liver tissue by homogenization in a phosphate buffered saline lysis buffer with 1.0% nonidet P-40 substitute (US Biological, Salem, MA), 0.5% sodium deoxycholate (Sigma-Aldrich, St. Louis, MO), 0.1% sodium dodecyl sulfate (SDS; Sigma-Aldrich), and protease inhibitors (HaltTM Protease and Phosphatase Inhibitor Cocktail, Thermo Scientific, Rockford, IL). Homogenates were centrifuged at 14,000 x g at 4° C for 5 minutes, after which the supernatant was collected for protein quantification. When obtaining the supernatant from tissue, the fat cake was avoided. A tissue specific pool of samples was created from equal volumes as a quality control standard for Western Blot analysis. Bicinchoninic assay (Pierce Biotechnology Inc., Rockford, IL) was used to determine protein concentration of all samples and pools via the manufacturer's protocol. Samples originating from adipose tissue, but not liver tissue, were subjected to molecular weight concentrators of either 10 kDa or 30 kDa by following the manufacturer's protocol (88513 and 88502, respectively; Pierce, ThermoFisher, Rockford, IL). After the concentration step, adipose tissue samples were re-analyzed via bicinchoninic acid assay to determine concentration. Samples originating from liver tissue, but not adipose tissue, were diluted and re-assayed as necessary. Final concentrations of adipose and liver tissues fell within the standard curve of each plate and the coefficient of variation of standards and samples was less than 10%.

Western Blotting was completed to determine tissues PNPLA3 protein abundance. A standardized protein quantity of 25 µg was used for pool and experimental sample preparation in

Laemmili Buffer (161-0737; Bio-Rad Laboratories, Hercules, CA) and 0.2 M dithiothreitol (DTT25; Gold Biotechnologies, St. Louis, MO), then heated at 37° C for 30 min before gel loading. Prepared protein samples were loaded into a gradient gel of 4-20% Criterion TGX Stain-Free Protein Gels (Bio-Rad Laboratories) and proteins were separated by electrophoresis in Tris/Glycine/SDS Running Buffer (1610732; Bio-Rad Laboratories) for 40-45 min at 200 V. After electrophoresis, gels were activated on a ChemiDoc XRS+ imager (Bio-Rad Laboratories) for one minute and transferred to a polyvinylidene fluoride membrane utilizing the TransBlot Turbo transfer system at the "Midi, Mixed Molecular Weight" setting (Bio-Rad Laboratories). Membranes were blocked for 2 h at room temperature then incubated with a rabbit-derived primary antibody (ab81874; Abcam, Cambridge, MA). Primary PNPLA3 antibody incubation lasted 1 h at room temperature with dilutions of 1:250 and 1:500 for adipose and liver samples, respectively. Subsequently, blots were incubated with a goat-anti-rabbit secondary antibody for 1 h at room temperature diluted to 1:5,000 (ab97080, Abcam). After each antibody incubation, blots were washed with tris-buffered saline containing Tween 4 times for 5 min each. Blots were imaged on the ChemiDoc XRS+ (Bio-Rad Laboratories) using ImageLab 5.0 software (Bio-Rad Laboratories) for 1) Total Lane Protein image using the Stain-Free setting and no imaging substrate (Taylor and Posch, 2014) and 2) bands of interest image using the ChemiHi Sensitivity setting with administration of SuperSignal West Dura Extended Duration Substrate at a 1:1 ratio (Pierce Biotechnology, Thermo Scientific, Rockford, IL). Intra- and inter- assay CV of the pool on blots was less than 15%.

Statistical Analysis

Data analysis was performed using the SAS (version 9.4; SAS Institute Inc., Cary, NC) procedures UNIVARIATE for normality testing, CORR for spearman correlations, and

GLIMMIX for linear mixed models (**LMM**). Investigation of response variable distribution found several responses to have non-Gaussian distributions based on the Shapiro-Wilk test ($P < 0.05$). In those instances, the response variable data was systematically evaluated for transformations that provided Gaussian distributions empirically by Shapiro-Wilks test ($P > 0.05$) or subjectively by histogram visualization when empirical solutions were not found. Dry matter intake, serum TG, plasma FA, and calculated net energy balance had bimodal distributions due to different pre- and postpartum distributions; therefore, the data for these responses were subset by parturition status for further statistical analysis.

Linear mixed models were used to evaluate evidence for differential effects for all response variables. A systematic procedure was implemented for the development of the LMM for each response. Initially, a base model was fitted that incorporated the essential fixed and random effects for the response. The typical fixed effects included treatment, time, and treatment × time; the typical random effects included cow, block (expected calving date), cow nested within week of lactation (models with subsampling), and repeated measures of cow across time. After initial LMM fitting, responses were interrogated for the incorporation of covariates (*i.e.* previous lactation 305 d mature equivalent milk yield, parity, and -28 DRTC measurement), which were retained when there was sufficient evidence ($P < 0.10$) for a main effect or interaction with the treatment effect. Not all models had beneficial covariates and no models had sufficient evidence for more than one beneficial covariate. Following covariate fitting, the conditional studentized residuals were subjectively evaluated subjectively by plotting (*i.e.* linear predictor × studentized residuals, studentized residual quantile-quantile plot, effect × studentized residuals). When studentized residuals had a non-Gaussian distribution or unequal variance across linear predictors modeling heterogeneous variance was investigated. Potential

heterogeneous groups were determined based on plotting model variables by studentized residuals. Several groups were investigated for each LMM; the reported LMM had the lowest Bayes information criteria or improved studentized residual plots. We considered fixed effects with $P \leq 0.05$ as having significant evidence for differences and effects with $0.05 < P \leq 0.10$ as having marginal evidence for differences. Whenever a treatment × time effect had some evidence ($P \leq 0.15$) we made simple-effect comparisons of treatment within timepoint and corrected for multiplicity by the Bonferroni method. Treatment means are expressed as least squares means and the 95% confidence interval denoted as [lower limit, upper limit].

Preliminary associations between PNPLA3 protein abundance and other variables of interest were performed via Spearman correlations within expected DRTC. In addition, LMM were fitted to delineate the association between tissue specific PNPLA3 protein abundance and liver TG content, while accounting for experimental design and data structure. The mixed effect regression model was developed by fitting an initial model using final LMM model for liver TG with liver PNPLA3 abundance as a fixed effect. Inclusion of higher order interactions between liver PNPLA3 and the other fixed effects (*i.e.* treatment or DRTC) did not minimize BIC or provide evidence for effects ($P \leq 0.15$). We report the slope (**β**) and P-value of liver PNPLA3 abundance from the mixed effect regression model and consider evidence of an association significant or marginal when $P \leq 0.05$ or $0.05 < P \leq 0.10$, respectively.

RESULTS

Animal Performance

There was no evidence for treatment differences in BW ($P = 0.92$), BCS ($P = 0.17$), the prepartum change in BW and BCS ($P = 0.93$ and $P = 0.84$, respectively), and the postpartum change in BW ($P = 0.63$; Table 2.2). However, BW and BCS differed across the experimental

period ($P < 0.001$; Figure 2.1) and the postpartum loss in BCS was greater ($P = 0.03$) for FLI than CTL cows (Table 2). Prepartum DMI was greater ($P = 0.01$) for FLI cows than CTL and was differed across time ($P = 0.004$; Figure 2.2a). Meanwhile, a significant ($P = 0.002$) treatment × time effect was observed for postpartum DMI (Figure 2.2a), with significant ($P \leq 0.003$) simple effects detected at +3 and +4 weeks postpartum were lower DMI was observed for FLI cows (19.6 [17.7, 21.2] kg and 23.2 [21.8, 24.5] kg DMI for +3 and +4 weeks postpartum, respectively) than CTL cows (23.5 [22.2, 24.8] kg DMI and 25.7 [24.5, 26.8] DMI kg for +3 and +4 weeks postpartum, respectively). Marginal evidence ($P = 0.06$) was found for FLI cows to yield less milk than CTL cows, 35.0 [32.5, 37.5] kg and 31.4 [28.8, 34.1] kg respectively (Figure 2.2b**)**. Total milk yield, milk protein yield, and milk lactose yield were affected by time ($P < 0.0001$), increasing in quantity until 6 weeks postpartum. There was no evidence for treatment differences in milk protein ($P = 0.19$) or lactose yield ($P = 0.17$; Table 2.2). Milk fat yield had marginal evidence ($P = 0.08$) for a treatment × time difference with a marginal simple effect ($P = 0.08$) at +5 weeks postpartum. Milk energy yield had marginal evidence for a treatment × time difference ($P = 0.10$), but there was a lack of evidence for any simple effects ($P \geq 0.13$). Most milk composition variables had no treatment differences ($P \geq 0.19$), including the fat, lactose, solids not fat, milk urea nitrogen, and SCC (Table 2.2), but were altered ($P < 0.001$) across time, generally decreasing in content as milk volume increased over time. Milk protein composition had a treatment × time difference ($P = 0.04$), were marginal evidence ($P = 0.08$) was observed at +3 postpartum for greater protein content in FLI than CTL, 2.93 [2.82, 3.05] % protein and 2.80 [2.71, 2.90] % protein, respectively. Prepartum energy balance was greater ($P = 0.001$) in FLI cows than CTL (Table 2.2) and was affected by time ($P = 0.04$; Figure 2.2c). Postpartum energy balance had a treatment × time difference ($P = 0.04$; Figure 2.2c) with marginal evidence ($P =$

0.07) for a simple effect at +4 weeks postpartum with a more negative energy balance for FLI cows than CTL cows, -10.2 [-13.2, -7.2] Mcal and -6.5 [-9.3, -3.6] Mcal, respectively.

Blood Fraction and Liver Metabolites

Plasma glucose was not affected by treatment ($P = 0.61$; Table 2.3) but did differ over time ($P < 0.01$) with concentrations from +3 to +14 DRTC being generally lower than prepartum and later postpartum timepoints (Figure 2.3a). Serum BHB had some evidence ($P = 0.15$) for a DRTC dependent treatment effect were FLI cows had greater BHB concentrations than CTL at +28 ($P = 0.05$) and +42 DRTC ($P = 0.01$; Figure 2.3b). Prepartum plasma FA was lower for the FLI treatment than CTL ($P = 0.03$; Table 2.3) and increased ($P < 0.01$) approaching parturition date (Figure 2.3c). Postpartum plasma FA had marginal evidence ($P = 0.07$) for treatment × time differences, were FLI cows had greater FA than CTL on +14 ($P = 0.04$) and +28 DRTC ($P = 0.07$; Figure 3c). No effect of treatment was observed for prepartum ($P = 0.68$) or postpartum serum TG concentration ($P = 0.23$; Table 2.3). Postpartum serum TG did change over time ($P = 0.04$; Figure 2.3d). Liver TG content was not impacted by treatment ($P = 0.41$, Table 2.3), but did differ over time ($P < 0.01$; Figure 2.4a).

PNPLA3 Protein Abundance

Liver PNPLA3 was not altered by treatment ($P = 0.29$; Table 2.3) but was altered over time ($P < 0.001$; Figure 2.4b). Adipose PNPLA3 was not affected by treatment ($P = 0.56$; Table 2.3) or time ($P = 0.35$; Figure 2.4c). Spearman correlations between -28 DRTC PNPLA3 abundance and other timepoints were significant within tissues, with ranges of 0.62 to 0.77 ($P < 0.01$) and 0.40 to 0.55 ($P \leq 0.05$) for liver and adipose tissue, respectively (Table 2.4). Liver and adipose PNPLA3 were not correlated ($P \geq 0.18$; Table 2.5) within any timepoint. Serum BHB was negatively ($r = -0.48$; $P = 0.02$) correlated with liver PNPLA3 at -14 DRTC. Marginal

evidence (P = 0.10) for a positive correlation (r = 0.34) between plasma glucose and adipose PNPLA3 abundance was observed at -14 DRTC. Plasma FA was negatively correlated with liver PNPLA3 at -14 (r = -0.47; P = 0.02), +14 (r = -0.47; P = 0.02), and +42 DRTC (r = -0.38; P = 0.06). Liver TG content was negatively correlated with liver PNPLA3 abundance at -14 (r = -0.36; P = 0.08) and +14 DRTC (r = -0.50; P = 0.01), as well as adipose PNPLA3 at +56 DRTC (r = -0.37; P = 0.07). Mixed effect regression analysis elucidated a significant association between liver TG and liver PNPLA3 abundance (P = 0.04; β = -0.34; Figure 2.5), but no evidence of an association was found between liver TG and adipose PNPLA3 abundance (P = 0.76).

DISCUSSION

In this study, we examined the relationship of liver and adipose PNPLA3 protein abundances to liver TG content, as well as the associations of PNPLA3 to energy metabolites, over the transition to lactation period during a FLI protocol. The purpose of FLI was to simulate a poor physiological adaptation to lactation (e.g. negative energy balance and excessive mobilization of adipose TG), generating a range of ketosis and fatty liver phenotypes in order to investigate the role of PNPLA3 in liver TG accumulation and recovery. By design, the FLI treatment had a greater positive energy balance prepartum due to a corn top-dress and modest increase in DMI (Table 2.2). Concomitantly, plasma FA concentration was lower for FLI cows than CTL cows (Figure 2.2c). These findings are consistent with previous experiments investigating the impact of dietary energy prepartum on cow performance (Vandehaar et al., 1999; Janovick and Drackley, 2010; Janovick et al., 2011). Despite the greater prepartum energy intake, FLI cows did not have greater prepartum BW, BCS, or change in prepartum BW and BCS (Table 2.2, Figure 2.1), which would be expected based on the aforementioned studies

comparing different planes of prepartum dietary energy (Vandehaar et al., 1999; Janovick and Drackley, 2010; Janovick et al., 2011). The intentional reduction of postpartum DMI in FLI cows was verified statistically at +3 weeks postpartum with FLI cows consuming 83.4% of CTL cow intake. Furthermore, FLI cows had evidence for lower intake than CTL cows at +4 and +5 weeks postpartum (Figure 2.2a) even after the re-alimentation of their diet to *ad libitum*, which coincided with greater negative energy balance (Figure 2.2c), greater plasma FA concentration, and greater serum BHB concentration in FLI cows compared to CTL cows (Figure 2.3). The greater FA and BHB concentrations reflect the increased demand for endogenous energy stores to support lactation during the feed restriction period (Bauman and Bruce Currie, 1980; Grummer, 1993; White, 2015), which is further supported by the greater BCS loss observed for the FLI cows. Our primary biomarker for the FLI protocol was blood BHB concentration measured cowside with 100% (n = 12) of FLI cows and 15% (n = 2) of CTL cows achieving BHB 3.0 ≥ mmol/L. Reaching this threshold resulted in cessation of FLI protocol. Results in the current study demonstrate a range of liver TG accumulation; however, the lack of treatment effect on liver TG content suggests that accumulation may not be due solely to the FLI protocol. Previous epidemiological work has associated BCS loss with greater liver TG (Reid, 1980; Jorritsma et al., 2001). Considering the extent of BCS loss for both treatment groups was substantial (Table 2.2), it may be that CTL cows lost sufficient BCS to promote liver TG accumulation and prevent delineation of treatment differences.

Liver PNPLA3 protein abundance was not affected by dietary treatment. Temporally, liver PNPLA3 abundance increased as lactation progressed. This is contrary to the reduced liver PNPLA3 mRNA expression at +1 and +14 DRTC, relative to prepartum, and during feed restriction previously observed (McCann et al., 2014). Saturated (C16:0), monounsaturated

(C18:1), and polyunsaturated (C18:2) FA can extend PNPLA3 protein half-life in cultured cells (Huang et al., 2010). Considering the increased concentration of plasma FA immediately postpartum (Figure 2.3c), the efflux of the aforementioned FA from adipose tissue could have resulted in the maintained liver PNPLA3 protein abundance from -14 to +14 DRTC (Figure 2.4b; Rukkwamsuk et al., 2000). It is worth noting several negative correlations within DRTC were observed between liver PNPLA3 protein abundance and plasma FA concentration (Table 2.5), particularly at +14 DRTC, suggesting that transcriptional repression of *PNPLA3* expression by FA possibly occurred in the present study. This is consistent with the negative correlation between plasma FA concentration and liver *PNPLA3* mRNA expression in dairy cows previously observed (McCann et al., 2014). Additionally, these observations in dairy cows are consistent in other species and cell culture models, where expression of *PNPLA3* mRNA was reduced in fasting mice (Huang et al., 2010; Dubuquoy et al., 2011) and reduced *in vitro* for HepG2 cells exposed to unsaturated FA (Hao et al., 2014). Together, these data suggest contradictory roles for FA regulating *PNPLA3* mRNA transcription, translation, and its resulting protein degradation; however, the regulation of bovine liver PNPLA3 expression by FA merits further *in vitro* investigation of the exact mechanism.

Despite the absence of treatment differences in liver TG and PNPLA3 protein abundance (Table 2.2), mixed effect regression analysis and spearman correlations revealed liver PNPLA3 protein abundance was negatively associated with liver TG content (Figure 2.5). In addition, several within DRTC spearman correlations demonstrated a negative relationship between liver PNPLA3 and liver TG (Table 2.5). These data suggest that greater PNPLA3 abundance may inhibit liver TG accumulation. Due to the lipolytic activity of PNPLA3 (Huang et al., 2011), it is likely that liver PNPLA3 contributes to the “re-mobilization” of endogenous FA that were re-

esterified and stored in the bovine liver. Therefore, a greater abundance of liver PNPLA3 could liberate and redirect stored FA to other fates including reassembly and secretion within very-low density lipoproteins, β-oxidation within the mitochondria, and peroxisomal oxidation (Grummer, 1993; White, 2015). This may differ from the mechanism that liver PNPLA3, specifically the catalytically inactive I148M variant, contributes to NAFLD in humans. While reduced PNPLA3 mediated lipolysis is one potential pathway in which PNPLA3 contributes to NAFLD (Huang et al., 2011, 3; Li et al., 2012), recent work suggests PNPLA3 may indirectly inactivate the rate-limiting lipase adipose triglyceride lipase through competition for α/β hydrolase domain-containing 5 (Wang et al., 2019; Yang et al., 2019). Thus, further *in vitro* investigations are necessary to affirm a mechanistic relationship between liver PNPLA3 and liver TF, as well as delineate the potentially species-specific regulation of PNPLA3 and interrelationships with other lipid-droplet associated proteins.

The present investigation into adipose PNPLA3 is novel in dairy cows. The precise regulation of adipose tissue lipolysis around at parturition in dairy cows is not fully understood (Koltes and Spurlock, 2011) and given that PNPLA3 contributes to lipolysis in other species it was of interest to explore it within this experiment. Adipose PNPLA3 protein abundance did not appear to be influenced by treatment or have a significant temporal pattern. Furthermore, there were no considerable correlations with metabolites, energy status, or body composition observed for adipose PNPLA3 protein. Adipose *PNPLA3* mRNA responsiveness to energy status has been demonstrated in rodents (Polson and Thompson, 2003; Oliver et al., 2012), but posttranslational regulation of adipose PNPLA3 has not been confirmed. Nonetheless, the present lack of any significant associations with metabolites or energy status make it difficult to suggest responsiveness of adipose PNPLA3 protein in dairy cows. Several factors could contribute to the

lack of observed responsiveness. In mice, subcutaneous adipose depots had less *PNPLA3* mRNA expression compared to internal adipose depots and mice of relatively greater age (6 vs 3 months) had less basal PNPLA3 expression (Oliver et al., 2012). Therefore, it is possible that our lack of results for any PNPLA3 protein abundance differences may be due to our use of mature cows or sampling of subcutaneous adipose tissue. Additionally, adipose *PNPLA3* in mice with genetic-induced obesity and diet-induced obesity appeared to no longer respond to carbohydrate refeeding (Caimari et al., 2007; Oliver et al., 2012). Although we found no significant correlations between BCS and adipose PNPLA3, it is possible that our lack of control for adiposity between treatments made it difficult for us to delineate adipose PNPLA3 responses. We propose that future investigations into the contribution of adipose PNPLA3 to lipolysis should consider sampling from other adipose depots, primi- and multiparous cows, as well as ensuring a range of adiposity.

CONCLUSIONS

Patatin-like phospholipase domain-containing protein 3 is a lipase expressed in liver and adipose tissues that is responsive to energy status in humans and rodents. Previous work in dairy cows has demonstrated that liver PNPLA3 mRNA expression is responsive to energy status and dynamically expressed during the transition period. The present work provided several novel insights into tissue specific PNPLA3 protein abundance in peripartal, multiparous dairy cows. First, peripartum adipose PNPLA3 protein abundance remained constant from -14 to +56 DRTC, suggesting it was nonresponsive within our experimental conditions. Second, contrary to previous examination of liver PNPLA3 mRNA expression, the liver PNPLA3 protein abundance did not decrease after parturition in this study but was relatively increased from +28 to +56 DRTC. Third, liver PNPLA3 had a significant, negative association with liver TG content across

the peripartum period, which suggests its relevance in preventing liver TG accumulation and liver TG clearance postpartum. Future investigations *in vitro* are merited to further delineate the mechanistic relationship of liver PNPLA3 to liver TG, as well as the regulatory mechanisms that could be leveraged to promote PNPLA3 expression and its resulting protein abundance to prevent onset of, or accelerate recovery from, bovine FLS.

ACKNOWLEDGEMENTS

This chapter represents part of a larger research project that has resulted in a manuscript currently under review with the peer-reviewed journal Scientific reports; co-authors include S. J. Erb, H. T. Holdorf, and H. M. White. The authors acknowledge and appreciate the support of D. Rieman, manager at the UW-Madison Dairy Cattle Center, and the UW-Madison Dairy Cattle Instruction and Research Center staff (University of Wisconsin-Madison, Madison, WI). Furthermore, the authors recognize the valued assistance from H. M. White laboratory members T. L. Chandler, C. R. Seely, and M. R. Moede, as well as laboratory manager S. J. Bertics. This project was supported by the Agricultural Food Research Initiative of the National Institute of Food and Agriculture, USDA, Grant # 2016-67015-24573 and the USDA Hatch Grant # WIS01736.

REFERENCES

Bauman, D.E., and W. Bruce Currie. 1980. Partitioning of nutrients during pregnancy and lactation: A review of mechanisms involving homeostasis and homeorhesis. J. Dairy Sci. 63:1514–1529. https://doi.org/10.3168/jds.S0022-0302(80)83111-0.

Bobe, G., J.W. Young, and D.C. Beitz. 2004. Invited review: Pathology, etiology, prevention, and treatment of fatty liver in dairy cows. J. Dairy Sci. 87:3105–3124. https://doi.org/10.3168/jds.S0022-0302(04)73446-3.

Caimari, A., P. Oliver, and A. Palou. 2007. Regulation of adiponutrin expression by feeding conditions in rats is altered in the obese state. Obesity 15:591–599. https://doi.org/10.1038/oby.2007.563.

Calvo, R.M., and M.J. Obregon. 2009. Tri-iodothyronine upregulates adiponutrin mRNA expression in rat and human adipocytes. Mol. Cell. Endocrinol. 311:39–46. https://doi.org/10.1016/j.mce.2009.07.006.

Dubuquoy, C., C. Robichon, F. Lasnier, C. Langlois, I. Dugail, F. Foufelle, J. Girard, A.-F. Burnol, C. Postic, and M. Moldes. 2011. Distinct regulation of adiponutrin/PNPLA3 gene expression by the transcription factors ChREBP and SREBP1c in mouse and human hepatocytes. J. Hepatol. 55:145–153. https://doi.org/10.1016/j.jhep.2010.10.024.

Folch, J., M. Lees, and G.H. Sloane Stanley. 1957. A simple method for the isolation and purification of total lipids from animal tissues. J. Biol. Chem. 226:497–509.

Foster, L.B., and R.T. Dunn. 1973. Stable reagents for determination of serum triglycerides by a colorimetric Hantzsch condensation method. Clin. Chem. 19:338–340.

Grummer, R.R. 1993. Etiology of lipid-related metabolic disorders in periparturient dairy cows. J. Dairy Sci. 76:3882–3896. https://doi.org/10.3168/jds.S0022-0302(93)77729-2.

Hao, L., K. Ito, K.-H. Huang, S. Sae-tan, J.D. Lambert, and A.C. Ross. 2014. Shifts in dietary carbohydrate-lipid exposure regulate expression of the non-alcoholic fatty liver disease-associated gene PNPLA3/adiponutrin in mouse liver and HepG2 human liver cells. Metabolism 63:1352–1362. https://doi.org/10.1016/j.metabol.2014.06.016.

Huang, Y., J.C. Cohen, and H.H. Hobbs. 2011. Expression and characterization of a PNPLA3 protein isoform (I148M) associated with nonalcoholic fatty liver disease. J. Biol. Chem. 286:37085–37093. https://doi.org/10.1074/jbc.M111.290114.

Huang, Y., S. He, J.Z. Li, Y.-K. Seo, T.F. Osborne, J.C. Cohen, and H.H. Hobbs. 2010. A feed-forward loop amplifies nutritional regulation of PNPLA3. Proc. Natl. Acad. Sci. U. S. A. 107:7892–7897. https://doi.org/10.1073/pnas.1003585107.

Itaya, K., and M. Ui. 1965. Colorimetric determination of free fatty acids in biological fluids. J. Lipid Res. 6:16–20.

Janovick, N.A., Y.R. Boisclair, and J.K. Drackley. 2011. Prepartum dietary energy intake affects metabolism and health during the periparturient period in primiparous and multiparous Holstein cows. J. Dairy Sci. 94:1385–1400. https://doi.org/10.3168/jds.2010-3303.

Janovick, N.A., and J.K. Drackley. 2010. Prepartum dietary management of energy intake affects postpartum intake and lactation performance by primiparous and multiparous Holstein cows. J. Dairy Sci. 93:3086–3102. https://doi.org/10.3168/jds.2009-2656.

Jorritsma, R., H. Jorritsma, Y.H. Schukken, P.C. Bartlett, T. Wensing, and G.H. Wentink. 2001. Prevalence and indicators of post partum fatty infiltration of the liver in nine commercial dairy herds in the Netherlands. Livest. Prod. Sci. 68:53–60. https://doi.org/10.1016/S0301-6226(00)00208-6.

Jorritsma, R., H. Jorritsma, Y.H. Schukken, and G.H. Wentink. 2000. Relationships between fatty liver and fertility and some periparturient diseases in commercial Dutch dairy herds. Theriogenology 54:1065–1074. https://doi.org/10.1016/S0093-691X(00)00415-5.

Koch, D.D., and D.H. Feldbruegge. 1987. Optimized kinetic method for automated determination of beta-hydroxybutyrate. Clin. Chem. 33:1761–1766.

Koltes, D.A., and D.M. Spurlock. 2011. Coordination of lipid droplet-associated proteins during the transition period of Holstein dairy cows. J. Dairy Sci. 94:1839–1848. https://doi.org/10.3168/jds.2010-3769.

León, L.P., M. Sansur, L.R. Snyder, and C. Horvath. 1977. Continuous-flow analysis for glucose, triglycerides, and ATP with immobilized enzymes in tubular form. Clin. Chem. 23:1556–1562.

Li, J.Z., Y. Huang, R. Karaman, P.T. Ivanova, H.A. Brown, T. Roddy, J. Castro-Perez, J.C. Cohen, and H.H. Hobbs. 2012. Chronic overexpression of PNPLA3I148M in mouse liver causes hepatic steatosis. J. Clin. Invest. 122:4130–4144. https://doi.org/10.1172/JCI65179.

Lucy, M.C., G.A. Verkerk, B.E. Whyte, K.A. Macdonald, L. Burton, R.T. Cursons, J.R. Roche, and C.W. Holmes. 2009. Somatotropic axis components and nutrient partitioning in genetically diverse dairy cows managed under different feed allowances in a pasture system. J. Dairy Sci. 92:526–539. https://doi.org/10.3168/jds.2008-1421.

McCann, C.C., M.E. Viner, S.S. Donkin, and H.M. White. 2014. Hepatic patatin-like phospholipase domain-containing protein 3 sequence, single nucleotide polymorphism presence, protein confirmation, and responsiveness to energy balance in dairy cows. J. Dairy Sci. 97:5167–5175. https://doi.org/10.3168/jds.2014-7910.

Moldes, M., G. Beauregard, M. Faraj, N. Peretti, P.-H. Ducluzeau, M. Laville, R. Rabasa-Lhoret, H. Vidal, and K. Clément. 2006. Adiponutrin gene is regulated by insulin and glucose in human adipose tissue. Eur. J. Endocrinol. 155:461–468. https://doi.org/10.1530/eje.1.02229.

Namjou, B., T. Lingren, Y. Huang, S. Parameswaran, B.L. Cobb, I.B. Stanaway, J.J. Connolly, F.D. Mentch, B. Benoit, X. Niu, W.-Q. Wei, R.J. Carroll, J.A. Pacheco, I.T.W. Harley, S. Divanovic, D.S. Carrell, E.B. Larson, D.J. Carey, S. Verma, M.D. Ritchie, A.G. Gharavi, S. Murphy, M.S. Williams, D.R. Crosslin, G.P. Jarvik, I.J. Kullo, H. Hakonarson, R. Li, eMERGE Network, S.A. Xanthakos, and J.B. Harley. 2019. GWAS and enrichment analyses of non-alcoholic fatty liver disease identify new trait-associated genes and pathways across eMERGE Network. BMC Med. 17:135-153. https://doi.org/10.1186/s12916-019-1364-z.

Novak, M. 1965. Colorimetric ultramicro method for the determination of free fatty acids. J. Lipid Res. 6:431–433.

Oliveira, R.C., S.J. Erb, R.S. Pralle, H.T. Holdorf, C.R. Seely, and H.M. White. 2020. Postpartum supplementation with fermented ammoniated condensed whey altered nutrient partitioning to support hepatic metabolism. J. Dairy Sci. 103: 7055-7067. https://doi.org/10.3168/jds.2019-17790.

Oliver, P., A. Caimari, R. Díaz-Rúa, and A. Palou. 2012. Diet-induced obesity affects expression of adiponutrin/PNPLA3 and adipose triglyceride lipase, two members of the same family. Int. J. Obes. 2005 36:225–232. https://doi.org/10.1038/ijo.2011.92.

Pingitore, P., and S. Romeo. 2019. The role of PNPLA3 in health and disease. Biochim. Biophys. Acta BBA - Mol. Cell Biol. Lipids 1864:900–906. https://doi.org/10.1016/j.bbalip.2018.06.018.

Polson, D.A., and M.P. Thompson. 2003. Adiponutrin mRNA expression in white adipose tissue is rapidly induced by meal-feeding a high-sucrose diet. Biochem. Biophys. Res. Commun. 301:261–266. https://doi.org/10.1016/S0006-291X(02)03027-9.

Rae-Whitcombe, S.M., D. Kennedy, M. Voyles, and M.P. Thompson. 2010. Regulation of the promoter region of the human adiponutrin/PNPLA3 gene by glucose and insulin. Biochem. Biophys. Res. Commun. 402:767–772. https://doi.org/10.1016/j.bbrc.2010.10.106.

Reid, I.M. 1980. Incidence and severity of fatty liver in dairy cows. Vet Rec. 107:281-284. https://doi.org/10.1136/vr.107.12.281

Romeo, S., J. Kozlitina, C. Xing, A. Pertsemlidis, D. Cox, L.A. Pennacchio, E. Boerwinkle, J.C. Cohen, and H.H. Hobbs. 2008. Genetic variation in PNPLA3 confers susceptibility to nonalcoholic fatty liver disease. Nature Genetics 40:1461–1465. https://doi.org/10.1038/ng.257.

Rotman, Y., C. Koh, J.M. Zmuda, D.E. Kleiner, T.J. Liang, and NASH CRN. 2010. The association of genetic variability in patatin-like phospholipase domain-containing protein 3 (PNPLA3) with histological severity of nonalcoholic fatty liver disease. Hepatol. Baltim. Md. 52:894–903. https://doi.org/10.1002/hep.23759.

Ruhanen, H., J. Perttilä, M. Hölttä-Vuori, Y. Zhou, H. Yki-Järvinen, E. Ikonen, R. Käkelä, and V.M. Olkkonen. 2014. PNPLA3 mediates hepatocyte triacylglycerol remodeling. J. Lipid Res. 55:739–746. https://doi.org/10.1194/jlr.M046607.

Rukkwamsuk, T., M.J.H. Geelen, T.A.M. Kruip, and T. Wensing. 2000. Interrelation of fatty acid composition in adipose tissue, serum, and liver of dairy cows during the development of fatty liver postpartum. J. Dairy Sci. 83:52–59. https://doi.org/10.3168/jds.S0022-0302(00)74854-5.

Taylor, S.C., and A. Posch. 2014. The design of a quantitative western blot experiment. Accessed June 16, 2020. https://www.hindawi.com/journals/bmri/2014/361590/.

Trinder, P. 1969. Determination of glucose in blood using glucose oxidase with an alternative oxygen acceptor. Ann. Clin. Biochem. 6:24–27. https://doi.org/10.1177/000456326900600108.

Trout, D.L., E.H. Estes, and S.J. Friedberg. 1960. Titration of free fatty acids of plasma: A study of current methods and a new modification. J. Lipid Res. 1:199–202.

Vandehaar, M.J., G. Yousif, B.K. Sharma, T.H. Herdt, R.S. Emery, M.S. Allen, and J.S. Liesman. 1999. Effect of energy and protein density of prepartum diets on fat and protein metabolism of dairy cattle in the periparturient period. J. Dairy Sci. 82:1282–1295. https://doi.org/10.3168/jds.S0022-0302(99)75351-8.

Walker, C.G., M.A. Crookenden, K.M. Henty, R.R. Handley, B. Kuhn-Sherlock, H.M. White, S.S. Donkin, R.G. Snell, S. Meier, A. Heiser, J.J. Loor, M.D. Mitchell, and J.R. Roche. 2016. Epigenetic regulation of pyruvate carboxylase gene expression in the postpartum liver. J. Dairy Sci. 99:5820–5827. https://doi.org/10.3168/jds.2015-10331.

Wang, Y., N. Kory, S. BasuRay, J.C. Cohen, and H.H. Hobbs. 2019. PNPLA3, CGI-58, and inhibition of hepatic triglyceride hydrolysis in mice. Hepatol. Baltim. Md. 69:2427–2441. https://doi.org/10.1002/hep.30583.

White, H.M. 2015. The role of tca cycle anaplerosis in ketosis and fatty liver in periparturient dairy cows. Anim. Open Access J. MDPI 5:793–802. https://doi.org/10.3390/ani5030384.

White, H.M. 2020. ADSA Foundation Scholar Award: Influencing hepatic metabolism: Can nutrient partitioning be modulated to optimize metabolic health in the transition dairy cow? J. Dairy Sci. 8: 6741-6750. https://doi.org/10.3168/jds.2019-18119.

Yang, A., E.P. Mottillo, L. Mladenovic-Lucas, L. Zhou, and J.G. Granneman. 2019. Dynamic interactions of ABHD5 with PNPLA3 regulate triacylglycerol metabolism in brown adipocytes. Nature Metab. 1:560–569. https://doi.org/10.1038/s42255-019-0066-3.

TABLES AND FIGURES

Table 2.1. Ingredient and nutrient composition of the pre- and postpartum experimental diets.

Diet Component	Prepartum[1]	Postpartum[2]
Ingredient, % DM		—
Straw	29.63	—
Corn silage	51.12	28.36
Concentrate Mix[3]	19.25	36.07
Alfalfa silage	—	29.78
Cottonseed	—	5.80
Chemical composition		
DM, %	43.70	48.71
CP, % DM	12.65	17.00
NDF, % DM	43.55	29.90
Lignin, % DM	4.62	4.18
EE, % DM	2.63	5.05
NFC, % DM	34.36	42.69
Ash, % DM	7.34	7.36
NE_L, Mcal/kg DM	1.42	1.65

[1]Cows assigned to the fatty liver induction protocol received 6 kg of dry cracked corn (90.2 % DM, 1.82 Mcal/kg DM) as a top-dress from -28 expected days relative to calving to parturition.

[2]Control and fatty liver induction treatments received the same postpartum diet; however, fatty liver induction cows were feed restricted to 80% of *ad libitum* intake from +14 days relative to calving until their blood β-hydroxybutyrate concentration was ≥ 3.0 mmol/L.

[3]Prepartum concentrate mix: Soybean meal 46 % CP (86.3 %), $CaCO_3$ (3.37 %), $Ca(H_2PO_4)_2$ (1.65 %), and a premix (8.68 %) composed of: $CaSO_4$ (23.20 %), NaCl (13.85 %), $CaCO_3$ (12.00 %), MgO (11.85 %), $MgSO_4$ (11.80 %), $CaHPO_4$ (21.0 %), mineral oil (1.0 %), selenium yeast 3000 (0.56 %, Prince Agri Products, Teaneck, NJ), Rumensin-90 (0.43%, Elanco Animal Health, Greenfield, IN), biotin (0.42%, DSM Nutritional Products, Belvidere, NJ), vitamin A (439.1 KIU/kg), vitamin D_3 (132.7 KIU/kg), and vitamin E (6.4 KIU/kg). Postpartum concentrate mix: contained fine ground corn (55.78 %), canola meal (14.75 %), distillers grain (8.88 %), soy hull pellet (4.38 %), exceller meal 8.88 %, Quality Roasting Inc., Valders, WI), $CaCO_3$ (2.25 %), $NaHCO_3$ (2.25 %), yellow grease (0.88 %), Urea (0.53 %), MgO (0.40 %), and a premix (1.05 %) composed of: Cl (51.2 %), Na (34 %), Ca (0.5 %), S (0.09 %), Co (78.2 ppm), Cu (4,871 ppm), I (469 ppm), Mn (14,382 ppm), Se (89.5 ppm), Zn (20,708 ppm), vitamin A (2055.7 KIU/kg), vitamin D_3 (411.1 KIU/kg), vitamin E (8.7 KUI/kg), Rumensin-90 (1.8%, Elanco Animal Health, Greenfield, IN), and biotin (0.8%, DSM Nutritional Products, Belvidere, NJ).

Table 2.2. Least squares means (LSM) and 95% confidence intervals (CI) of body weight, body condition score, dry matter intake, milk and milk component yield, milk composition, and energy balance for cows exposed to a control (CTL) or fatty liver induction (FLI) treatment.

	CTL		FLI		*P*-value[2]		
Response[1]	LSM	95% CI	LSM	95% CI	TRT	DRTC	T×D
BW, kg	715.4	[705.6, 725.0]	716.0	[705.9, 726.2]	0.92	<0.01	0.94
ΔBW, kg							
Prepartum	2.9	[-7.5, 13.3]	3.5	[-7.3, 14.4]	0.93	—	—
Postpartum	-75.0	[-90.6, -59.6]	-80.4	[-96.5, -64.2]	0.63	—	—
BCS, pts	3.30	[3.17, 3.44]	3.39	[3.25, 3.54]	0.17	<0.01	0.19
ΔBCS, pts							
Prepartum	-0.33	[-0.49, -0.17]	-0.01	[-0.18, 0.15]	0.01	—	—
Postpartum	-0.82	[-1.00, -0.63]	-1.13	[-1.33, -0.94]	0.03	—	—
DMI, kg							
Prepartum	14.3	[12.7, 15.7]	15.9	[14.5, 17.1]	0.01	<0.01	0.78
Postpartum	24.2	[23.2, 25.3]	22.9	[21.7, 24.0]	0.05	<0.01	<0.01
Milk yield							
Total, kg	45.8	[44.1, 47.4]	43.4	[41.5, 45.2]	0.06	<0.01	0.62
Fat, kg	2.2	[2.0, 2.3]	2.2	[2.0, 2.3]	0.96	<0.01	0.08
Protein, kg	1.3	[1.2, 1.4]	1.2	[1.1, 1.3]	0.19	<0.01	0.98
Lactose, kg	2.2	[2.2, 2.3]	2.2	[2.1, 2.2]	0.16	<0.01	0.76
Energy, Mcal	36.3	[34.0, 38.6]	35.7	[33.2, 38.0]	0.65	<0.01	0.10
Milk composition							
Fat, %	4.66	[4.32, 5.07]	4.92	[4.55, 5.37]	0.25	<0.01	0.81
Protein, %	2.83	[2.75, 2.92]	2.83	[2.75, 2.92]	0.97	<0.01	0.04
Lactose, %	4.88	[4.80, 4.95]	4.94	[4.86, 5.01]	0.19	<0.01	0.53
SnF, %	8.75	[8.61, 8.90]	8.81	[8.67, 8.96]	0.51	<0.01	0.15
MUN, mg/dL	11.29	[10.82, 11.80]	11.26	[10.77, 11.79]	0.92	<0.01	0.78
SCC	70.06	[32.43, 150.04]	61.99	[27.73, 137.10]	0.82	<0.01	0.16
EB, Mcal							
Prepartum	7.9	[5.1, 10.3]	12.6	[10.4, 14.6]	<0.01	0.04	0.27
Postpartum	-7.8	[-10.1, -5.5]	-9.2	[-11.6, -6.8]	0.39	<0.01	0.04

[1]BW = bodyweight, ΔBW = BW change, BCS = body condition score, prepartum changes are from -28 to +1 expected days relative to calving (DRTC) and postpartum are from +1 to +56 DRTC, SnF = solids not fat, MUN = milk urea nitrogen, somatic cell count (SCC) is expressed as cells/mL × 1,000, milk energy and energy balance (EB) were calculated using published equations (NRC, 2001)

[2]Statistics for fixed effects are treatment (TRT), DRTC, and the interaction of TRT and DRTC (T×D)

Table 2.3. Least squares means (LSM) and 95% confidence intervals (CI) of blood fraction metabolites, liver triglyceride (TG) content, and tissue patatin-like phospholipase domain-containing protein 3 (PNPLA3) protein abundance for cows exposed to a control (CTL) or fatty liver induction (FLI) treatment.

	CTL		FLI		*P*-value[2]		
Response[1]	LSM	95% CI	LSM	95% CI	TRT	DRTC	T×D
Plasma glucose, mg/dL	65.27	[63.65, 66.89]	64.67	[62.97, 66.37]	0.61	<0.01	0.42
Serum BHB, mmol/L	0.55	[0.51, 0.60]	0.59	[0.54, 0.66]	0.25	<0.01	0.15
Plasma FA, mEq/L							
Prepartum	0.18	[0.15, 0.23]	0.14	[0.12, 0.17]	0.03	<0.01	0.44
Postpartum	0.38	[0.32, 0.46]	0.40	[0.33, 0.48]	0.66	<0.01	0.07
Serum TG, mg/dL							
Prepartum	23.48	[18.42, 28.55]	24.58	[19.45, 29.70]	0.68	0.16	0.97
Postpartum	9.02	[8.02, 10.15]	9.70	[8.61, 10.93]	0.23	0.04	0.97
Liver TG, % DM	5.35	[4.12, 6.95]	4.59	[3.50, 6.03]	0.41	<0.01	0.75
PNPLA3							
Liver, AU × 100,000	133.84	[120.78, 148.32]	123.68	[111.07, 137.75]	0.29	<0.01	0.93
Adipose, AU × 10,000	129.84	[99.45, 169.51]	117.17	[89.45, 153.50]	0.55	0.34	0.78

[1]BHB = β-hydroxybutyrate, FA =fatty acid, prepartum analysis included samples collected from -28 to 0 expected days relative to calving, postpartum analysis included samples collected from +1 to +56 days relative to calving

[2]Statistics for fixed effects are treatment (TRT), day relative to calving (DRTC), and the interaction of TRT and DRTC (T×D)

Table 2.4. Spearman correlations (r) between -28 days relative to calving (DRTC) patatin-like phospholipase domain-containing protein 3 protein abundance and patatin-like phospholipase domain-containing protein 3 protein abundance at other timepoints within tissue.

	Liver		Adipose	
DRTC	r	*P*-value	r	*P*-value
- 14	0.77	< 0.01	0.50	0.01
+ 1	0.63	< 0.01	0.46	0.02
+14	0.62	< 0.01	0.55	0.03
+28	0.71	< 0.01	–	–
+42	0.70	< 0.01	–	–
+56	0.64	< 0.01	0.40	0.05

Table 2.5. Spearman correlations between tissue protein abundance of patatin-like phospholipase domain-containing protein (PNPLA3), tissue metabolite concentrations, animal performance variables, and energy balance within expected days relative to calving.

	Liver PNPLA3							Adipose PNPLA3				
Variable[1]	-28	-14	+ 1	+14	+28	+42	+56	-28	-14	+ 1	+14	+56
PNPLA3, AU	-0.24	-0.15	-0.11	-0.29	–	–	0.28	-0.24	-0.15	-0.11	-0.29	0.28
P-value	0.26	0.48	0.59	0.18	–	–	0.20	0.26	0.48	0.59	0.18	0.20
Liver TG, % DM	0.18	-0.36	-0.11	-0.50	-0.18	-0.25	-0.15	-0.12	-0.02	-0.07	0.09	-0.37
P-value	0.39	0.08	0.59	0.01	0.40	0.22	0.50	0.58	0.92	0.73	0.66	0.07
Serum BHB, mmol/L	-0.03	-0.48	-0.14	0.02	-0.01	-0.14	-0.08	0.26	-0.17	0.07	0.12	-0.02
P-value	0.89	0.02	0.50	0.93	0.96	0.51	0.73	0.23	0.44	0.75	0.58	0.93
Plasma glc, mg/dL	0.06	0.04	0.13	0.14	0.06	0.14	-0.03	-0.15	0.34	0.06	-0.09	0.13
P-value	0.76	0.84	0.53	0.50	0.77	0.49	0.90	0.46	0.10	0.78	0.66	0.54
Plasma FA, mEq/L	0.16	-0.47	-0.18	-0.47	-0.24	-0.38	0.13	-0.09	-0.04	0.05	-0.03	0.13
P-value	0.43	0.02	0.38	0.02	0.25	0.06	0.58	0.68	0.84	0.80	0.89	0.52
Serum TG, mg/dL	0.01	-0.15	-0.11	-0.07	-0.05	0.10	0.07	-0.26	-0.18	0.06	-0.27	-0.14
P-value	0.98	0.49	0.60	0.73	0.83	0.65	0.75	0.22	0.41	0.77	0.19	0.49
Body weight, kg	-0.23	-0.25	-0.24	0.05	-0.04	0.03	0.07	-0.01	-0.28	0.00	-0.06	-0.35
P-value	0.27	0.24	0.24	0.82	0.86	0.89	0.74	0.96	0.19	0.99	0.77	0.09
BCS, points	-0.31	-0.36	-0.14	-0.12	0.26	-0.34	-0.05	0.12	-0.21	-0.19	-0.15	-0.22
P-value	0.14	0.08	0.52	0.60	0.24	0.10	0.83	0.58	0.33	0.37	0.49	0.29
Energy balance, Mcal	0.05	0.10	0.00	0.36	-0.01	0.12	-0.06	0.04	-0.37	0.29	-0.17	0.32
P-value	0.80	0.63	0.98	0.08	0.98	0.58	0.81	0.86	0.08	0.17	0.41	0.13

[1]PNPLA3 refers to protein abundance correlations between tissues, TG = triglyceride, DM = dry matter, BHB = β-hydroxybutyrate, glc = glucose, FA = fatty acid, BCS = body condition score

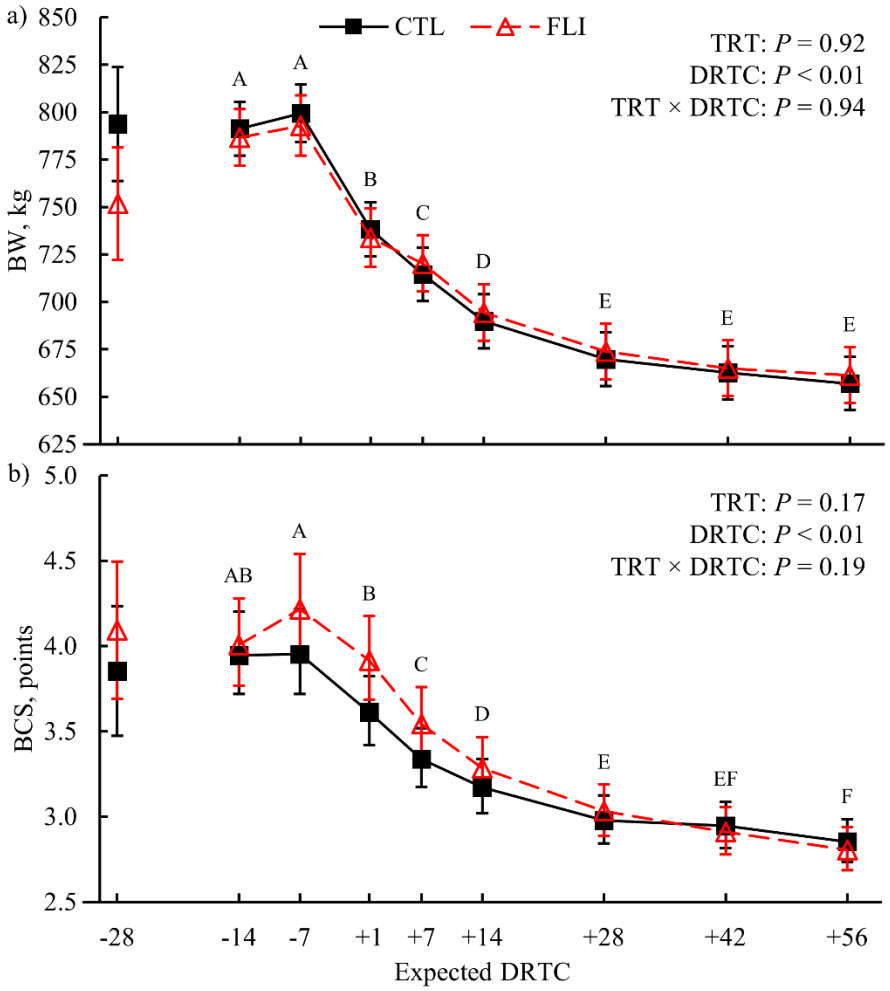

Figure 2.1. Body weight (BW) and body condition score (BCS) across the experimental period for control (CTL) and fatty liver induction (FLI) treatments (TRT). Error bars represent the 95% confidence limits of the least squares mean. The -28 expected days relative to calving (DRTC) values were included as model covariates for their respective response; values graphically represented for -28 expected DRTC are the arithmetic means and 95% confidence limits. differences across DRTC ($P \leq 0.05$, Tukey's adjustment) are indicated when alphabetic superscripts do not share characters.

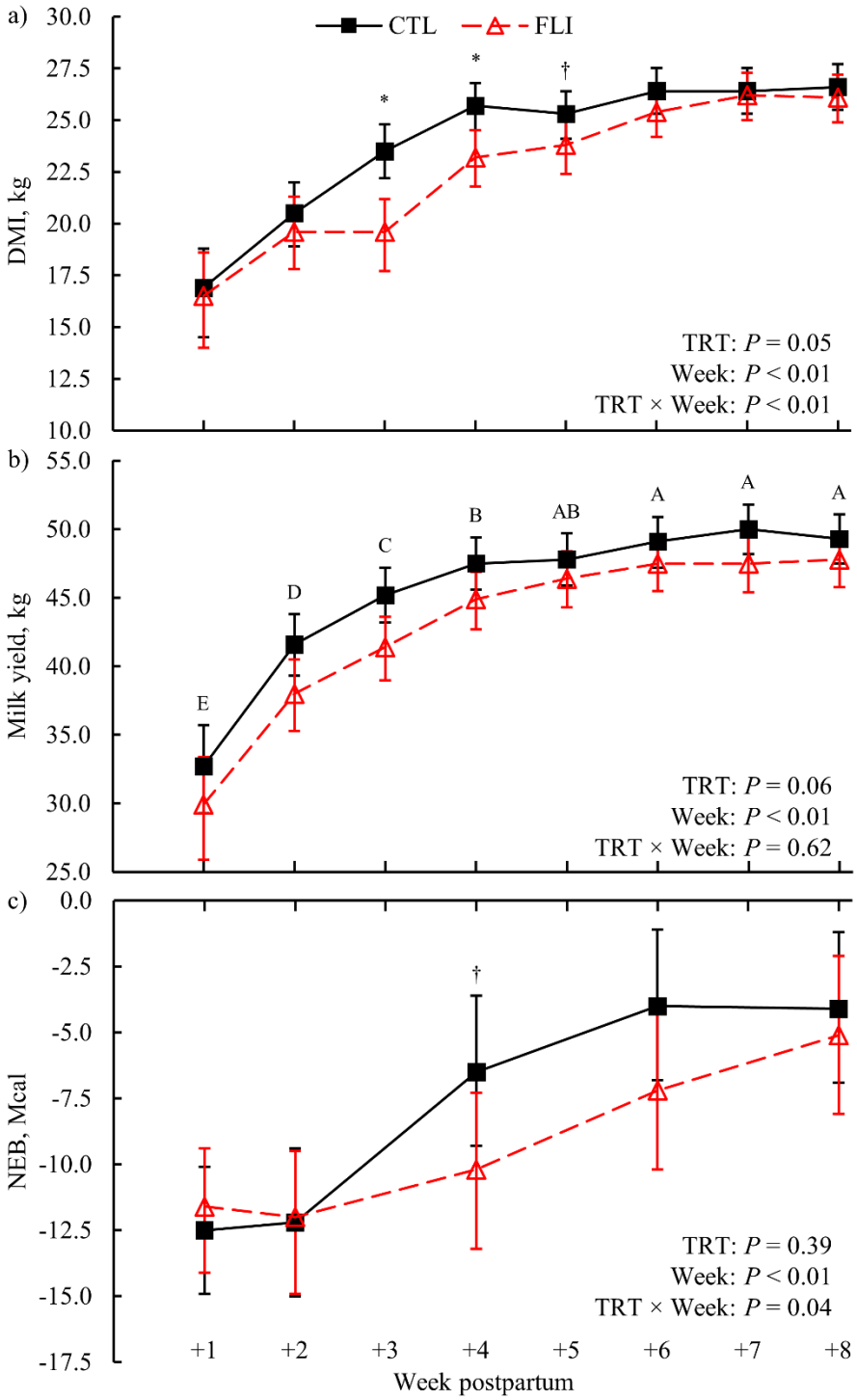

Figure 2.2. Dry matter intake (DMI; panel a), milk yield (panel b), and calculated net energy balance (NEB; panel c) for control (CTL) and fatty liver induction (FLI) treatments (TRT). Error bars represent the 95% confidence limits of the least squares mean. Differences across weeks ($P \leq 0.05$, Tukey's adjustment) are indicated when alphabetic superscripts do not share characters. Symbols represent significant (*; $P \leq 0.05$) and marginal (†; $0.05 < P \leq 0.10$) simple effect differences for treatment × time interactions after multiplicity correction (Bonferroni).

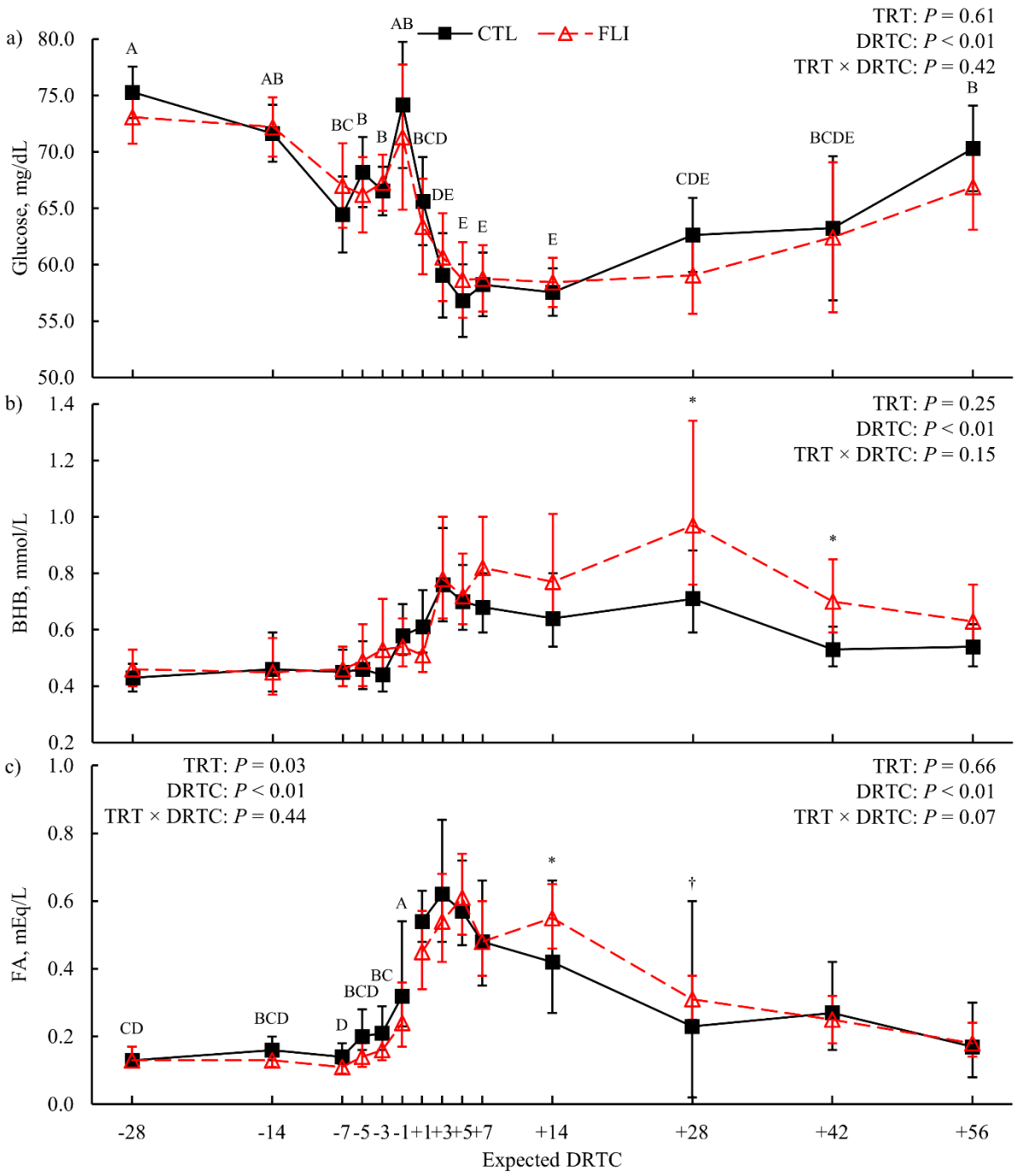

Figure 2.3. Plasma glucose (panel a), serum β-hydroxybutyrate (BHB; panel b), and plasma fatty acids (FA; panel c) during the experimental period for control (CTL) and fatty liver induction (FLI) treatments (TRT). Error bars represent the 95% confidence limits of the least squares mean. Differences across days relative to calving (DRTC, $P \leq 0.05$, Tukey's adjustment) are indicated when alphabetic superscripts do not share characters. Symbols represent significant (*; $P \leq 0.05$) and marginal (†; $0.05 < P \leq 0.10$) simple effect differences for treatment by time interactions after multiplicity correction (Bonferroni).

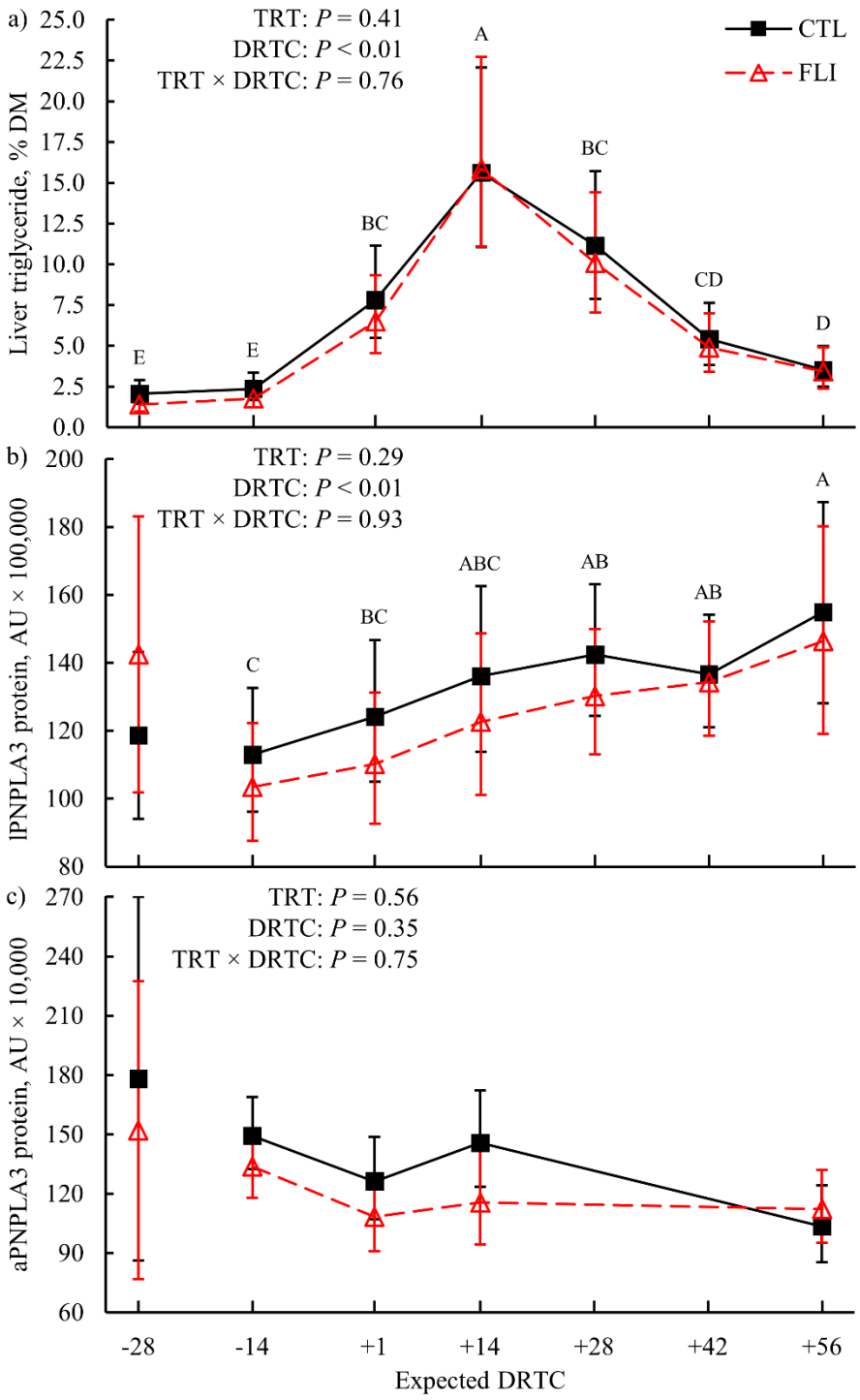

Figure 2.4. Liver triglyceride (TG; panel a), liver patatin-like phospholipase domain-containing protein 3 (lPNPLA3; panel b), adipose PNPLA3 (aPNPLA3; panel c), during the experimental period for control (CTL) and fatty liver induction (FLI) treatments (TRT). Error bars represent the 95% confidence limits of the least squares mean. Differences across expected days relative to calving (DRTC; $P \leq 0.05$, Tukey's adjustment) are indicated when alphabetic superscripts do not share characters.

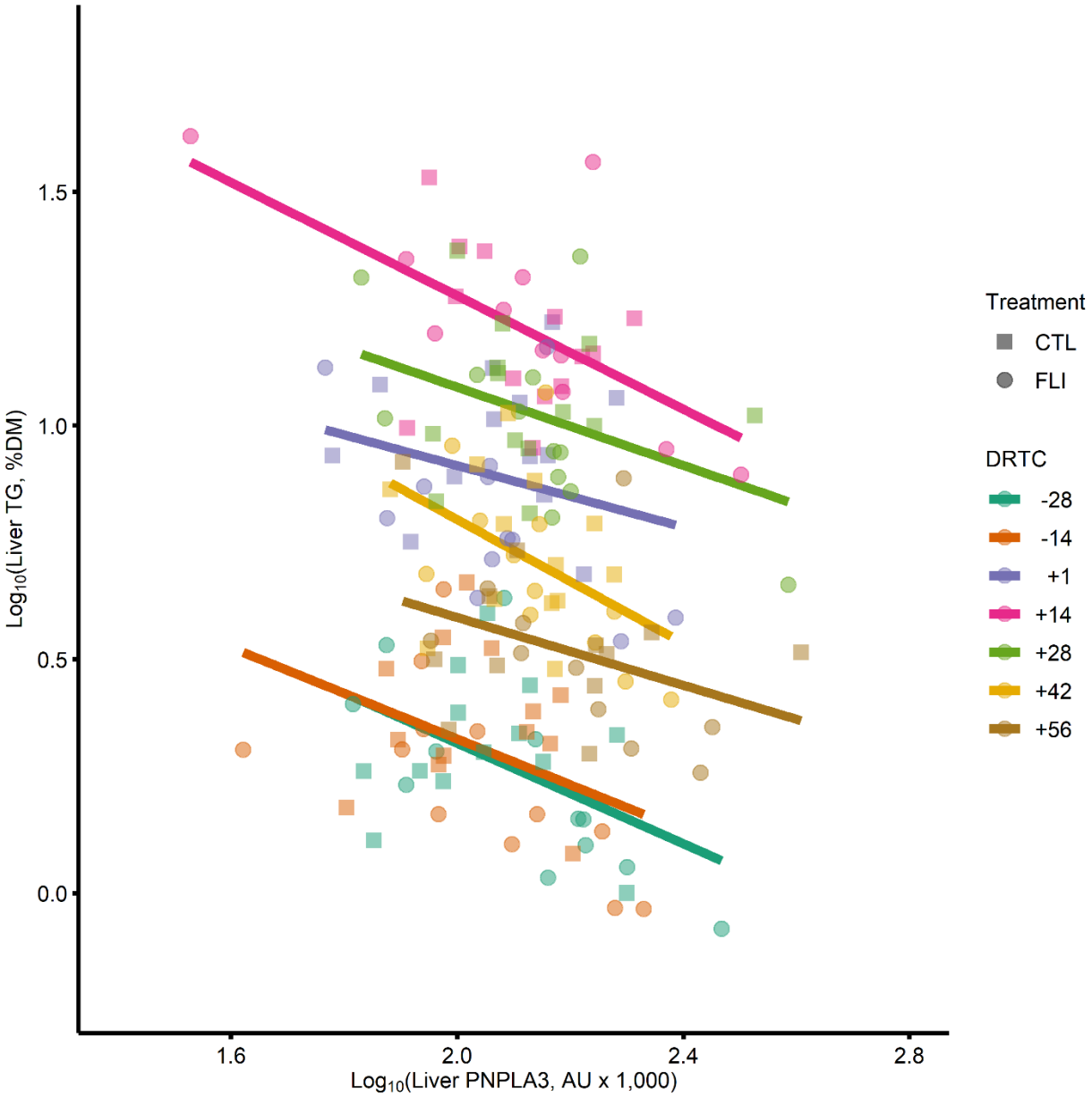

Figure 2.5. A representative plot for mixed effect regression analysis associating liver patatin-like phospholipase domain-containing protein 3 (PNPLA3) to liver triglyceride (TG) content. Liver PNPLA3 was negatively associated (β = -0.31; *P* = 0.03) with liver TG when controlling for experimental design factors including treatment, days relative to calving (DRTC), the interaction of treatment and time, and block effects. Magnitude of liver PNPLA3 abundance effect on liver TG content is represented by trendlines for the linear predictor within DRTC.

CHAPTER 3: NOVEL FACETS OF THE LIVER TRANSCRIPTOME ARE ASSOCIATED WITH THE SUSCEPTIBILITY AND RESISTANCE TO LIPID-RELATED METABOLIC DISORDERS IN PERIPARTURIENT HOLSTEIN COWS

ABSTRACT

Lipid-related metabolic disorders (**LRMD**) are prevalent in early lactation dairy cows and represent a significant financial burden to the dairy production system. While progress has been made in our understanding of the gross pathology of LRMD, there is limited knowledge as to what divergent metabolic regulation determines progression of LRMD pathology. We hypothesized that LRMD pathology is regulated by metabolic pathways conferring susceptibility (disposition to LRMD occurrence during typical conditions) and resistance (disposition to LRMD onset and severity when presented a challenge). Our objectives were to leverage an experiment with cows subjected to a control dietary treatment or fatty liver induction protocol (**FLI**) to discover differentially expressed genes and metabolic pathways within the liver associated with LRMD susceptibility and resistance via whole transcriptome RNA-sequencing. Clustering cows based on postpartum lipid metabolite concentrations (*i.e.* blood β-hydroxybutyrate and liver triglyceride) within original dietary treatment identified groups of cows less susceptible (**LS**) and more susceptible (**MS**) to LRMD within the control treatment, as well as groups more resistant (**MR**) and less resistant (**LR**) to LRMD within the FLI treatment. Cows within the MS and LR clusters had greater concentrations of the lipid metabolites than LS and MR clusters, respectively. Additionally, the LR cluster appeared to achieve a clinical hyperketonemia threshold earlier postpartum than the MR cluster. Comparing the liver transcriptomes (LS vs MS and MR vs LR) on -28, +1, and +14 days relative to calving revealed numerous differentially expressed genes related to the innate immune response and

inflammation, potentially mediating the adaptation to oxidative stress peripartum. Inferred differential metabolism supports unique roles for glutathione metabolism and eicosanoid metabolism for modulating LRMD susceptibility and resistance, respectively. Additionally, major histocompatibility complex molecules and interferon inducible proteins appear to participate in the metabolic control of susceptibility and resistance to LRMD. Overall, this research provides novel insight into the role of immunometabolism in LRMD pathology and suggests potential for unique control points for LRMD progression and severity.

INTRODUCTION

Physiological adaptations necessary to make the transition from a gravid, non-lactating state through parturition and into a lactating state represents several metabolic challenges for periparturient dairy cows. The principal challenges include onset of negative net energy balance spurred by a reduction in voluntary feed intake and increasing lactation energy requirements, insulin resistance, immunosuppression, and mineral imbalance (Bauman and Bruce Currie, 1980; Wankhade et al., 2017; Wilkens et al., 2020). Maladaptation to these challenges can result in numerous pathologies including the lipid-related metabolic disorders (**LRMD**) hyperketonemia (**HYK**) and fatty liver syndrome (**FLS**). These comorbid disorders are prevalent in early lactation dairy cows with an incidence of 43 to 53% and 50% for HYK and FLS, respectively (Jorritsma et al., 2000, 2001; McArt et al., 2012; Mahrt et al., 2015). Hyperketonemia, elevated concentrations of blood β-hydroxybutyrate (**BHB**), and bovine FLS, characterized by a substantial accumulation of liver triglyceride (**TG**), have been associated with unfavorable performance outcomes including greater risk of comorbidities, decreased reproductive efficiency, productive losses, and premature culling (Jorritsma et al., 2000; Bobe et al., 2004; Walsh et al., 2007; McArt et al., 2012). The deterministic estimate for total cost per case of

hyperketonemia is $375 US and $256 US for primiparous and multiparous cows, respectively (McArt et al., 2015). Fiscal impact of fatty liver on dairy production is difficult to determine, but expected to cost the industry at least $60 million US annually (Bobe et al., 2004). Therefore, these LRMD not only represent a concern for the health and wellness of dairy cows, but the cost of dairy production.

Our understanding of the pathology for these disorders has historically focused on understanding the liver metabolism of long chain fatty acids (**FA**) mobilized from adipose tissue TG (Grummer, 1993; Bobe et al., 2004). An apparent excess of liver uptake of endogenous FA surpasses the oxidative and secretory capacity of hepatocytes, promoting ketogenesis and storage of re-esterified FA (Grummer, 1993; Bobe et al., 2004; White, 2015). Thus, most research regarding prevention and treatment of HYK and FLS have focused on limiting FA substrate through managing dairy cow prepartum obesity or excessive mobilization of FA during the postpartum period (Contreras et al., 2004; Vailati-Riboni et al., 2016; Zenobi et al., 2018). An alternative approach has been focused on nutritional interventions to support oxidation via TCA (DeFrain et al., 2004; Soltan, 2010; Caputo Oliveira et al., 2019) or improve liver TG secretion (Piepenbrink and Overton, 2003; Chandler and White, 2017; Bollatti et al., 2019).

The advent of genome-wide gene expression profiling using microarray or RNAseq techniques has expanded our capability to identify and understand the underpinning regulatory mechanisms of physiological states. With respect to the liver transcriptome, research concerning LRMD has focused on comparing prepartum dietary treatments (Loor et al., 2006; McCarthy et al., 2010; McCabe et al., 2012; Shahzad et al., 2014) or feed restriction models (Loor et al., 2007; Akbar et al., 2013) to either increase risk of metabolic disorders or induce negative energy balance. In addition, the liver transcriptome has been compared between cows overfed dietary

energy achieving subclinical HYK and those not progressing to HYK (Shahzad et al., 2019). These papers have given insight into the pathogenesis of LRMD, such as highlighting the role of key transcription factors (i.e. peroxisome proliferator-activated receptor) and the contributions of steroid biosynthesis (Loor et al., 2006, 2007; McCarthy et al., 2010; McCabe et al., 2012; Shahzad et al., 2014). However, the liver transcriptome of periparturient dairy cows experiencing LRMD absent of a challenge protocol has not been compared to apparently healthy contemporaries. Additionally, there has been no evaluation of whether the differential biology observed during these experiments is representative of any differential biology in LRMD that occurs without a challenge protocol.

We hypothesize that periparturient cows have divergent physiological adaptations to lactation that affect their susceptibility or resistance to LRMD. Also, we hypothesize that there are unique genes and metabolic pathways responsible for LRMD susceptibility and resistance. Our presupposition is that dairy cows developing LRMD pathologies absent of a challenge represent a LRMD susceptible population of cows, while cows with delayed onset or severity of LRMD when challenged represent a population of LRMD resistant cows. To evaluate our hypotheses, we clustered periparturient cows based on postpartum lipid metabolite concentrations within a control treatment (**CTL**) and FLS induction treatment (**FLI**; oversupply of energy prepartum and some postpartum feed restriction). Within the CTL treatment we identified a cluster apparently less susceptible (**LS**) to LRMD and a cluster more susceptible (**MS**) to LRMD; additionally, we determined an apparently more resistant (**MR**) to LRMD cluster and a cluster less resistant (**LR**) to LRMD in the FLI treatment. Our objectives were to evaluate the liver transcriptome of these clusters via RNA-sequencing within original treatment for differentially expressed genes (**DEG**) and enriched metabolic pathways (**EMP**), as well as to

evaluate the common and unique liver transcriptome features of the susceptibility and resistance models.

MATERIALS AND METHODS

Animal Experimental Design

This research was part of a previously detailed experiment which enrolled multiparous Holstein cows (n = 25) at the University of Wisconsin-Madison Dairy Cattle Instruction and Research Center (Chapter 2). All animal use and handling protocols were approved by the University of Wisconsin-Madison College of Agricultural and Life Sciences Animal Care and Use Committee. Blocked by expected calving date, cows were randomly assigned to a CTL (n =13) or a FLI (n = 12) treatment. The treatment period began at -28 days relative to calving (**DRTC**) and ended at +56 DRTC. Control cows were allowed *ad libitum* intake of diets formulated to meet the needs of dry or lactating cows, respectively (Chapter 2). The FLI cows were offered a daily top-dress of dry, cracked corn (6 kg) in addition to *ad libitum* access to the dry cow ration. Post-calving, FLI cows were offered *ad libitum* access to the lactating cow ration until +14 DRTC, at which time feed intake was restricted to 80% of *ad libitum* intake, based on the average voluntary intake from the 3 days preceding restriction (Chapter 2). Blood BHB was monitored daily for all postpartum cows with a BHBCheck meter (PortaCheck, Moorestown, NJ); cows that achieved a blood BHB ≥ 3.0 mmol/L were treated for clinical ketosis, re-alimented to feed, and allowed *ad libitum* intake for the remainder of the experiment (Chapter 2).

Methods regarding sample collection and analysis are detailed in-depth in the companion manuscript (Chapter 2) and are briefly described here. Feed intake and milk yield data were recorded daily; composition analysis was performed on monthly composites of feed samples and on milk samples collected weekly (Chapter 2). Sampling occurred at -28, -14, +1, +14, +28, +42,

and +56 DRTC for body weight (**BW**), body condition score (**BCS**), blood samples, and liver biopsies. Additional body weights and BCS were evaluated at -7 and +7 DRTC, and additional blood samples were collected at -7, -5, -3, +3, +5, +7 DRTC. Blood fractions (serum or plasma) were quantified for BHB and glucose, respectively, using Catachem VETSPEC reagents on the Catachem Well-T AutoAnalyzer (Catachem, Oxford, CT). Plasma FA concentration and liver TG concentration were determined using colorimetric, enzymatic assays (Folch et al., 1957; Caputo Oliveira et al., 2019; Chapter 2).

K-means Clustering and Retrospective Selection

To avoid subjectively choosing cows representing differential susceptibility or resistance to LRMD, a K-means clustering algorithm (R, version 3.5.2) was used to empirically group cows based on metabolic characteristics. Variables supplied to the algorithm included concentrations of plasma FA, serum BHB, and liver TG from +1, +14, and +28 DRTC, as well as the maximum postpartum concentration of each lipid metabolite from any DRTC timepoint. This allowed for a longitudinal assessment of LRMD status and the maximum concentrations served as a proxy for LRMD severity. All variables were tested for normality ($P \leq 0.05$, Shapiro-Wilk test) and transformed (Log_{10} or reciprocal) to an empirically Gaussian distribution ($P > 0.05$, Shapiro-Wilk test). Clustering was performed within original dietary treatment (CTL or FLI) to promote groupings that reflected our study hypotheses and objectives. For each original treatment, we evaluated algorithms allowing for 2 to 5 clusters, 1000 iterations, and 1000 random starts. Based on silhouette plot evaluation (R package: cluster, version 2.1.0) (Mächler et al., 2015) and the number of cows within the largest 2 clusters ($n \geq 4$), the optimal number of clusters was 2 and 4 for CTL and FLI, respectively. Two of the clusters from within the FLI treatment had too few cows to be considered for RNAseq ($n \leq 2$) and were excluded. From the clusters within CTL and

FLI treatments, cows (n = 4 per cluster) were randomly selected to represent the cluster and proceeded to RNA isolation and library preparation for RNAseq. Poor RNA integrity on one or more samples, detailed subsequently, resulted in the elimination of one cow per cluster; therefore, each cluster was represented by 3 randomly selected cows (n = 6 per original treatment) with adequate RNA integrity. Assignment of clusters as LS or MS in the CTL treatment and LR or MR in the FLI treatment was based on the statistical evaluation of the metabolites supplied for clustering (see *Statistical Analysis*). Greater concentrations of LRMD biomarkers suggest progressed pathology and increased risk of negative performance outcomes (Grummer, 1993; Bobe et al., 2004; Ospina et al., 2010; Overton et al., 2017, 100); therefore, the clusters with greater blood BHB, blood FA, or liver TG where designate MS and LR within the CTL and FLI treatments, respectively..

RNA Isolation, Library Preparation, Sequencing, and Mapping

Liver tissue samples (~50 mg) were homogenized into fine powders in liquid nitrogen using a mortar and pestle. Sample RNA was extracted following the miRNeasy protocol with a QIAcube instrument (Qiagen, Foster City, CA). The RNA integrity number was determined via Bioanalyzer using the RNA 6000 nano kit (Agilent, Santa Clara, CA) for all samples (n = 48). To improve overall RNA integrity for the experiment, one cow per cluster was dropped due to excessively low integrity. For the remaining samples (n = 36), RNA integrity was 6.0 ± 1.2 (SD). Library preparation for RNA sequencing was done using Illumina TruSeq ribo-zero gold kit (Illumina, San Diego, CA, US) following manufacturer's instructions. For each sample, 1 μg of total RNA was used as the input. The fragment distribution of prepared libraries was assessed with Bioanalyzer DNA 1000 kit (Agilent, Santa Clara, CA, US). Quantification of prepared libraries was performed using a Kapa quantification kit (Kapa biosystems, Darmstadt, Germany)

with a QuantStudio5 quantitative PCR instrument (Thermo Fisher, Waltham, MA). Libraries were further normalized to ensure equal quantity before sequencing. Normalized, pooled samples were sequenced on an Illumina NextSeq 500 instrument (Illumina, San Diego, CA, US) to obtain paired-end, 2 × 75 bp reads using a 150 high-output kit. Quality of reads was assessed by FastQC (https://www.bioinformatics.babraham.ac.uk/projects/fastqc/). Before sequence alignment, raw reads were filtered to remove those shorter than 50 bp. For alignment, the genome reference and annotation files for *Bos taurus* (release 106, ARS-UCD 1.2) were downloaded from NCBI (https://www.ncbi.nlm.nih.gov/assembly/GCF_002263795.1) for use. Raw reads from the whole transcriptome RNA-seq libraries were aligned to the *Bos taurus* reference genome using STAR (2.5.2b). Read count quantification was done using cufflinks (Trapnell et al., 2012) with sorted bam file generated by STAR as the input file. The expression level of mRNAs in each sample were normalized to fragments per kilobase of transcript per million mapped reads (**FPKM**) by cufflinks (Trapnell et al., 2012).

Statistical Analysis

Due to the dependence of the retrospective cluster assignments on the original dietary treatment (CTL or FLI), the complete data (n = 12, selected cows) was divided into data sets based on original dietary treatment. Therefore, all statistical analyses compared either LS vs MS or LR vs MR. Any comparisons between original dietary treatments should be considered subjective assessments.

Biometric, Productivity, and Metabolite Data. Analysis of biometric (*i.e.* BCS), productive (*i.e.* milk energy yield), and metabolite data (*i.e.* serum BHB) was performed using SAS (version 9.4; SAS Institute Inc., Cary, NC) procedures UNIVARIATE and GLIMMIX. Several response variables had non-Gaussian distributions based on the Shapiro-Wilk test ($P <$

0.05). For those responses, data transformations were systematically evaluated and transformations providing Gaussian distributions were selected either empirically, by Shapiro-Wilk test ($P > 0.05$), or subjectively, by histogram visualization (when empirical solutions were not found). The bimodal nature of calculated net energy balance necessitated downstream analysis to be performed on prepartum and postpartum timepoints separately. Linear mixed models were used to evaluate responses for evidence of differences between clusters (LS vs MS or LR vs MR, n = 3 cows/cluster), using the systematic model building procedure previously outlined (Chapter 2). The typical fixed effects included cluster, time, and cluster×time; the typical random effects included cow, cow nested within week of lactation (models with subsampling), and repeated measures of cow across time (when applicable). Due to the limited sample size for analyzing these performance responses, we considered fixed effects with $P \leq 0.10$ as having significant evidence for differences and effects with $0.10 < P \leq 0.15$ as having marginal evidence for differences. Whenever a cluster×time effect had evidence ($P \leq 0.15$) we made simple-effect comparisons of treatment within timepoint and corrected for multiplicity by the Bonferroni method. Treatment means are expressed as least squares means and the 95% confidence interval denoted as [lower limit, upper limit].

Liver Whole-Transcriptome Analysis. Differential gene expression analysis was done using the cuffdiff function of cufflinks (Trapnell et al., 2012) within each DRTC for LS vs MS and MR vs LR. *P*-values were corrected for multiplicity by false discovery rate (Benjamini and Hochberg, 1995) and are here-in referred to as *Q*-values. The Database for Annotation, Visualization and Integrated Discovery (**DAVID**) web-based software was used to evaluate gene ontologies and EMP (Huang et al., 2009a; b) for DEG within a DRTC comparison. Genes supplied to the test list (termed gene list by DAVID) had $Q \leq 0.10$ within the respective DRTC

timepoint comparison. A customized background list was supplied to DAVID, which included all sequenced genes successfully tested within each DRTC. Fischer's exact statistics were extracted and corrected for multiplicity by false discovery rate (Benjamini and Hochberg, 1995). Our evidence criteria for DEG, gene ontologies, and EMP was $Q \leq 0.05$ and $0.05 < Q \leq 0.10$ for significant and marginal evidence, respectively.

RESULTS

Phenotypic Characterization of Clusters

Clusters Within the Control Cows: Less or More Susceptible to LRMD. Biometric indicators of obesity, BW and BCS, were not different between LS and MS cows ($P \geq 0.85$; Figures 3.1a and 3.1c). There was marginal evidence for time-dependent difference between clusters for BCS ($P = 0.14$) but was not separable by simple effects comparisons at any DRTC ($P \geq 0.15$). Milk energy output and dry matter intake (**DMI**) did not differ between susceptibility clusters, $P = 0.59$ and $P = 0.41$, respectively. Thus, net energy balance did not differ between susceptibility clusters pre- ($P = 0.89$) or postpartum ($P = 0.28$; Figure 3.1e). Plasma glucose (Figure 3.2a) and FA concentration (Figure 3.2b) did not differ ($P = 0.62$ and $P = 0.39$, respectively) between LS and MS cows either. Serum BHB concentration was greater ($P = 0.08$) for the MS cows than the LS cows (Figure 3.2c). In addition, liver TG content was greater ($P = 0.02$; Figure 3.4a) for the MS cows than the LS cows.

Clusters Within the FLI Cows: More or Less Resistant to LRMD. Cows in the MR cluster were individually feed restricted for 4, 8, and 13 d, respectively, while the LR cows were feed restricted 0, 2, and 8 d, respectively. Resistance clusters did not differ in BCS ($P = 0.91$; Figure 3.1d), but the MR cows had greater BW from +7 to +56 DRTC ($P \leq 0.07$ for simple effects; Figure 3.1b) compared to LS cows. Milk energy output and milk lactose yield were

similar ($P > 0.99$ and $P = 0.52$, respectively) between resistance clusters. Evidence of greater postpartum DMI ($P = 0.09$, contrast) for MR cows compared to LR cows was observed, contributing to the significantly ($P = 0.01$) attenuated negative energy balance observed for MR cows compared to LR cows (Figure 3.1f). Plasma glucose concentrations were greater postpartum ($P = 0.07$, contrast) for MR cows than LR cows (Figure 3.3a). Compared to their LR contemporaries, MR cows had lower concentrations of postpartum plasma FA ($P = 0.06$, contrast; Figure 3.3b), serum BHB ($P = 0.10$; Figure 3.3c), and liver TG ($P = 0.03$; Figure 3.4b).

Differentially Expressed Genes and Enriched Metabolic Pathways

Clusters Within the Control Cows: Less or More Susceptible to LRMD. For the comparison of LS and MS clusters, there were 13,151 genes at -28 DRTC, 13,011 genes at +1 DRTC, and 13,211 genes at +14 DRTC tested for differential expression (Table 3.1). Genes with significant (marginal) evidence on -28, +1, and +14 DRTC totaled 165 (58), 116 (31), and 199 (39), respectively. A selection of genes differentially expressed across all DRTC within the susceptibility cluster comparisons are listed in Table 3.2. Metabolic pathways enriched within the DEG with significant (marginal) evidence number 0 (2), 4 (3), and 5 (2) for -28, +1, and +14 DRTC, respectively (Table 3.3).

Clusters Within the FLI Cows: More or Less Resistant to LRMD. For the comparison of MR and LR cows, there were 13,139 genes at -28 DRTC, 13,150 genes at +1 DRTC, and 12,718 genes at +14 DRTC tested for differential expression (Table 3.1). Significant (marginal) evidence for differential expression was found for 127 (30), 142 (50), and 102 (31) genes at -28, +1, and +14 DRTC, respectively. A selection of genes differentially expressed across all DRTC within the resistance cluster comparisons are listed in Table 3.4. Metabolic pathways enriched

within the DEG with significant (marginal) evidence number 0 (5), 6 (2), and 0 (0) for -28, +1, and +14 DRTC, respectively (Table 3.5).

DISCUSSION

The purpose of this work is to provide novel insight into the genes and metabolic pathways integral to the pathology of LRMD. To that end, we retrospectively identified groups of peripartum dairy cows within a relatively normal dietary scenario and within a metabolically challenging dietary scenario with apparently different metabolic statuses. These differences in metabolic status were determined via K-means clustering of cows based on postpartum liver and blood characterization as indicators of HYK and FLS (Grummer, 1993; Drackley, 1999; Overton et al., 2017). Sequencing of the liver transcriptomes at several peripartum time-points suggested numerous genes and metabolic pathways associated with LRMD at one or more timepoints. Therefore, this discussion will only concern the phenotypic characterization of the clusters within original dietary treatment and a selection of genes, gene families, and metabolic pathways.

Phenotypic Characterization of Clusters

Clusters Within the Control Cows: Less or More Susceptible to LRMD. Cows within the CTL treatment were subject to pre- and postpartum diets typical for dairy cows, without additional imposed challenges (Chapter 2). Differential regulation of genes and metabolic pathways may underly facets of liver metabolism that may predispose and individual cow to the progression of LRMD. The principal metabolic differences between the LS and MS cows were the greater serum BHB ($P = 0.08$; Figure 3.2c) and liver TG ($P = 0.02$; Figure 3.3a) concentrations observed for the MS cows. As mentioned, these metabolites serve as the primary biomarkers for HYK and FLS, with greater concentrations suggesting pathology (Grummer,

1993; Drackley, 1999; Overton et al., 2017). Thus, the MS cluster appears to be in a less favorable metabolic condition and prone to LRMD. Greater plasma FA concentration is also a biomarker of LRMD and would be expected in the MS cluster (Ospina et al., 2010; Chapinal et al., 2012). Although plasma FA was numerically greater for MS cows postpartum (Figure 3.2b), it was not significantly different from the LS cows. This lack of difference in FA is corroborated by the similar BW and BCS between the susceptibility clusters peripartum (Figure 3.1), suggesting unappreciable differences in the lipolysis of adipose TG between clusters. Additionally, these clusters did not differ in DMI, milk energy output, energy balance (Figure 3.1e), or plasma glucose (Figure 3.2a). Although these differences are in contrast to the present dogma of insufficient nutrient supply and over-mobilization of body energy reserves leading to LRMD (Grummer, 1993; Drackley, 1999; White, 2015), it is important to remember that the lack of differences here may be due to the small sample size in regards to metabolite analysis. Conversely, these data may suggest that some cows are susceptible to onset of LRMD despite the lack of energetic challenges that are classically associated with the dogma and may be susceptible due to independent risk factors.

Clusters Within the FLI Cows: More or Less Resistant to LRMD. The FLI treatment imposed on the cows in the resistance clusters (MR and LR) was intended to predispose cows to LRMD. All cows in the FLI treatment progressed to a clinical HYK blood BHB threshold (BHB ≥ 3.0 mmol/L; Chapter 2). Thus, the aim of metabolic clustering was to identify cows more resistant to the FLI treatment, with lower metabolite concentrations (plasma FA, serum BHB, and liver TG) or greater feed restriction d until blood BHB ≥ 3.0 mmol/L. Consistent with this goal, dairy cows in the MR cluster had lower concentrations of serum BHB ($P = 0.10$; Figure 3.3c) and liver TG postpartum ($P = 0.03$; Figure 3.3b) compared to the LR cluster. Furthermore,

MR cows required more feed restriction d to achieve BHB ≥ 3.0 mmol/L. Together these data suggest cows in the MR cluster were more resistant to LRMD than LR cows. The MR cows compared to LR cows had greater postpartum BW (Figure 3.1b) and less negative energy balance postpartum (Figure 3.1f), suggesting that the MR cows did not mobilize as much endogenous energy reserves to support lactation nutrient requirements as the LR cows. Greater plasma FA concentration for the LR cows (Figure 3.3b) corroborates greater lipolysis of adipose tissue TG. The greater plasma glucose concentration for the MR cows postpartum (Figure 3.3a), with similar milk lactose output, may suggest MR cows had greater hepatic gluconeogenesis or decrease peripheral glucose utilization compared to LR cows (Bauman and Bruce Currie, 1980; Baumgard et al., 2017; Kvidera et al., 2017). Overall, the MR cows appeared to experience a more favorable adaptation to lactation when a dietary challenge was imposed than LR cows.

Inferred Differential Regulation of the Liver Transcriptome

Greater Glutathione Mediated Antioxidation for Less Susceptible Cows. Mobilization of adipose tissue TG as FA and their linear uptake by the liver results in a tremendous supply of liver FA for metabolism in dairy cows (Thompson and Darling, 1975; Emery et al., 1992). Oxidation of these FA in the hepatocyte mitochondria and peroxisomes to produce energy can also produce reactive oxygen species (**ROS**). Accumulation of hepatic ROS in early postpartum dairy cows and can induce oxidative stress, characterized by excessive oxidation of proteins and lipids and induction of apoptosis (Sordillo and Aitken, 2009; Mavangira and Sordillo, 2018). Glutathione is a protein that can serve as an antioxidant, protecting cells from ROS-induced oxidative damage (Sordillo and Aitken, 2009; Chandler and White, 2017; Du et al., 2017). In the present experiment, the KEGG pathway glutathione metabolism was enriched in the DEG identified in the comparison of susceptibility clusters on +1 DRTC (Table 3.3). The LS cows had

greater expression of genes in the glutathione-center antioxidant defense system than MS cows: *GSTA4* (2.6-fold), *GSTT1*(2.0-fold), and *GSTA1* (2.5-fold). These genes catalyze glutathione conjugations with electrophilic compounds (*i.e.* drugs, xenobiotics, lipid hydroperoxides) and some have glutathione peroxidase activity (Strange et al., 2001; Tsuchida, 2002; Townsend and Tew, 2003). Thus, the LS cows appear to have improved their antioxidation capacity compared to their MS contemporaries.

Greater Eicosanoid Synthesis for Less Resistant Cows. Eicosanoids, a subcategory of oxylipids, are signaling molecules made by the enzymatic or non-enzymatic oxidation of arachidonic acid or other polyunsaturated fatty acids (Dennis and Norris, 2015; Mavangira and Sordillo, 2018). These molecules can have either pro- or anti-inflammatory properties, while influencing oxidative stress (Mavangira and Sordillo, 2018). Eicosanoids can directly promote oxidative stress through the production of ROS or indirectly via production of ROS during biosynthesis. Some eicosanoids, such as 15-deoxy-delta 12, 14-Prostaglandin J_2 exert antioxidant effects by directly or indirectly targeting and decreasing ROS production by other cellular metabolic processes (*i.e.* mitochondrial oxidation; Dennis and Norris, 2015; Mavangira and Sordillo, 2018). At +1 DRTC, the KEGG pathways linoleic acid metabolism, alpha-linoleic metabolism, and arachidonic acid metabolism were enriched for the comparison of LRMD resistance cluster (Table 5). All the specific DEG were expressed more in the livers of LR cows: *PLB1* (36.8-fold), *PLA2* (∞-fold), *PLA2G2A* (∞-fold), *CYP2B6* (2.6-fold), and *CYP2J2* (4.3-fold).The inferred promotion of eicosanoid synthesis may be a byproduct of the greater ROS production and pathology of LRMD. However, the greater eicosanoid production may be an adaptation by the LR to accelerate the termination of the liver's inflammatory state.

Apparently Greater Innate Immunity for Cows Less Susceptible and Less Resistant.

The role of the immune system in the progression of metabolic syndrome is an emerging scientific field in dairy science (Hotamisligil, 2006; Sordillo and Mavangira, 2014). In humans, there appeared to be crosstalk between metabolism and the immune response which furthers the progress of non-alcoholic fatty liver to steatohepatitis and cirrhosis (Vidali et al., 2008). In the present experiment, many of the most consistently DEG across DRTC were the immunity-related genes involved in expressing components of the major histocompatibility complex (**MHC**; classes I and II) and genes in the interferon inducible protein (**IFI**) family for LRMD susceptibility and resistance comparisons.

The MHC molecules are responsible for the presentation of antigens on the cell surface and recruit other mechanisms of the initiate immune response when antigens represent "non-self" proteins (Herkel et al., 2003). Expression of MHC molecules, particularly MHC class II, have been implicated in the pathology of liver metabolic and inflammatory disease in humans (Herkel et al., 2003; Vidali et al., 2008). In our data, the expression of MHC elements was found in the cell adhesion molecules pathway at -28 and +1 DRTC for the susceptibility clusters and -28 DRTC for the resistance cluster comparison. Of note, *bovine lymphocyte antigen - DQB* (***BOLA-DQB***), an MHC class II protein, was one of the few DEG observed at every DRTC for the LRMD susceptibility and resistance cluster comparisons. Expression of MHC II molecules is typically restricted to professional antigen presenting cell types and not hepatocytes (Ting and Trowsdale, 2002); however, hepatocytes from humans with clinical hepatitis do express MHC class II molecules (Dienes et al., 1987), which may be capable of attracting CD_4^+ T lymphocytes (Herkel et al., 2003). It is theorized that ROS induced peroxidation of cellular components, such as proteins and lipids, can induce MHC expression and presentation of the oxidized component

antigens to the cell surface (Vidali et al., 2008). The subsequent recruitment of CD_4^+ T lymphocytes and cytokine expression promotes the apoptosis and clearance of ROS-damaged hepatocytes by the immune system (Herkel et al., 2003; Vidali et al., 2008). Interestingly, *BOLA-DBQ* and other MHC components generally had greater expression for the LS and LR cows than MS and MR, respectively. Considering the LS group was the metabolically preferable group within the susceptibility cluster, we did not expect the relative directionality of the DEG to be similar to LR, the less preferable resistance cluster. It may be that cows not experiencing additional dietary challenges benefit from a more efficient clearance of ROS damaged hepatocytes, while cows challenged with additional prepartum energy may suffer from an excessive quantity of ROS damaged cells or oversensitive presentation of antigen, resulting in disproportional apoptosis and clearance.

Interferons are cytokines that are best known for their secretion in response to viral infections but have been implicated in the pathology of non-alcoholic fatty liver disease in humans (Honda et al., 2010; Møhlenberg et al., 2019). The IFI and other interferon stimulated genes are downstream effectors of interferon (Takaoka and Yanai, 2006). Similar to the MHC genes, IFI genes, specifically *IFI6*, *IFI27*, *IFI44*, and *IFI44L*, had greater relative expression (range of 2.0- to 5.6-fold) for LS and LR cows than the MS and MR cows, respectively, across all DRTC. It is possible that the IFI serve as the upstream regulators promoting the expression of the MHC molecules (Takaoka and Yanai, 2006) and promote the clearance of ROS-damaged hepatocytes as previously discussed.

Serum Amyloid A Was Differentially Expressed Within Susceptibility and Resistance Clusters. Serum amyloid A (**SAA**) is an acute phase response protein associated with the inflammatory cascade which has been previously associated with HYK (Saremi et al., 2013;

Abuajamieh et al., 2016; Sack, 2018). The isoforms *SAA1* and *SAA2* are generally considered the predominant pro-inflammatory protein expressed in the liver, while *SAA3* has generally been viewed as an adipokine (Saremi et al., 2013; Sack, 2018). Expression of *SAA3* was significantly greater for LS cows at -28 DRTC (6.1-fold) than MS, but LS cows had significantly lower *SAA3* expression (3.2-fold) at +1 DRTC than MS cows. At +14 DRTC, the LS cluster had greater expression of *SAA2* (6.1-fold), *SAA4* (1.7-fold), and *LOC104968478* (21.1-fold) than the MS cluster. The LR cluster had consistently greater expression of all *SAA* isoforms than the MR, ranging from 4- to 9.8-fold. Comparison of resistance clusters agrees with previous work associating greater abundance of SAA and states with LRMD (Abuajamieh et al., 2016; Bradford and Swartz, 2020). However, the susceptibility cluster comparison suggests a more nuanced regulation of SAA in the absence of additional dietary challenges. It has been previously suggested that a priming of the inflammatory response may exert protective effects in peripartum dairy cows (Loor, 2010), which the relative expression pattern of *SAA3* for the susceptibility clusters may support.

Insight into LRMD Pathology

There is considerable variation in the metabolic health of dairy cows peripartum; this is evident in the variable prevalence of LRMD and their comorbidities (Jorritsma et al., 2001; Suthar et al., 2013; Overton et al., 2017). In addition, the variation in occurrence and severity of LRMD is still evident when cows are subjected to a dietary challenge (Loor et al., 2007; Chapter 2). Our retrospective clustering of dairy cows based on lipid metabolites within the CTL and FLI dietary treatments (Chapter 2) empirically identified groups of cows with divergent metabolic health, as previously discussed. The apparent presence of these divergent groups within both dietary conditions indicated two potential control points for LRMD pathology, susceptibility to

LRMD incidence and resistance to LRMD severity. Even though the gross pathology of LRMD pertaining to lipid metabolism and gluconeogenesis has been investigated, there has been limited investigation into the divergent metabolic regulation responsible for these LRMD susceptibility or resistance control points. The evaluation of the liver transcriptome through RNA-sequencing allowed for a more holistic evaluation of what unique and shared metabolic pathways underpin these control points (Loor et al., 2013).

The select genes and metabolic pathways presented in this work appear to be centered around hepatic adaptation to the lipotoxic effects of ROS through the innate immune system and inflammatory response. As discussed, the intersection of nutrient metabolism, immunity, and inflammation in the peripartum physiological adaptations and LRMD pathology has been a growing discipline in dairy science (Sordillo and Mavangira, 2014; Bradford and Swartz, 2020). These observations support further investigation into immunometabolism, specifically on the contributions of glutathione metabolism, eicosanoid metabolism, and MHC molecules in liver tissue. The observed regulation for these pathways is summarized in Figure 3.5. Interestingly, the susceptibility and resistance comparisons each had a unique inferred metabolic pathway on +1 DRTC. Glutathione metabolism was unique to the susceptibility comparison, while eicosanoid metabolism was a unique to the resistance comparison (Tables 3.3 and 3.5). Of course, these differences could be due to differences in the expressed genes available for testing between these +1 DRTC comparisons (Table 3.1). Apparently, the relevance of MHC molecules and the innate immune response is shared across the susceptibility and resistance comparisons. However, the relative expression of the DEG and EMP (*i.e. BOLA-DQB*) was greater for the metabolically preferable susceptibility cluster (LS) and the metabolically less preferable resistance cluster (LR). This discordant direction of expression across LRMD susceptibility and resistance

comparisons suggests that research experiments implementing dietary challenges to evaluate LRMD pathology should be interpreted with caution. While some differentially regulated genes and pathways may be shared, the observed response directionality may reflect adaptive mechanisms to limit the severity of LRMD rather than the direct pathology. Additionally, there may be unique mechanisms to the natural pathology of LRMD and those mechanisms that resist progression of LRMD.

CONCLUSIONS

There is substantial individual variation in the metabolic response of dairy cows to peripartum conditions, suggesting the underpinning regulation of key metabolic pathways may confer susceptibility or resistance to LRMD. We empirically grouped multiparous Holstein cows within normal and challenged peripartum dietary conditions based on their blood lipid metabolite profile and liver TG content. This approach revealed two metabolic health groups within each dietary condition, suggesting differential susceptibility to LRMD incidence or resistance to LRMD induced by a dietary challenge. These metabolic differences were realized in the liver transcriptomes of these cow groups with the inferred differential metabolism highlighting the role of the inflammatory response and innate immunity in LRMD pathology. Novel insights included the differential regulation of MHC molecules and IFI, which may aid the response to the ROS-induced cellular damage that occurs in liver tissue peripartum. Furthermore, the contributions of liver glutathione and eicosanoid metabolism to LRMD pathology immediately postpartum appear to be of greater biological importance relative to dietary condition, normal and challenged, respectively. Future work should build on the contributions of these specific mechanisms and delineate their dependence on specific dietary conditions.

ACKNOWLEDGEMENTS

This work was made possible due to collaboration with Dr. Wenli Li and Brianna Murphy (US Dairy Forage Research Center, Madison, WI). For the original animal experiment, the authors acknowledge and appreciate the support of D. Rieman, manager at the UW-Madison Dairy Cattle Center, and the UW-Madison Dairy Cattle Instruction and Research Center staff (University of Wisconsin-Madison, Madison, WI). Furthermore, the authors recognize the valued assistance from H. M. White laboratory members T. L. Chandler, C. R. Seely, and M. R. Moede, as well as laboratory manager S. J. Bertics. This project was supported by the Agricultural Food Research Initiative of the National Institute of Food and Agriculture, USDA, Grant # 2016-67015-24573, USDA Hatch Grant # WIS01736, and the Land O'Lakes John Brandt Memorial Scholarship.

REFERENCES

Abuajamieh, M., S.K. Kvidera, M.V.S. Fernandez, A. Nayeri, N.C. Upah, E.A. Nolan, S.M. Lei, J.M. DeFrain, H.B. Green, K.M. Schoenberg, W.E. Trout, and L.H. Baumgard. 2016. Inflammatory biomarkers are associated with ketosis in periparturient Holstein cows. Res. Vet. Sci. 109:81–85. https://doi.org/10.1016/j.rvsc.2016.09.015.

Akbar, H., M. Bionaz, D.B. Carlson, S.L. Rodriguez-Zas, R.E. Everts, H.A. Lewin, J.K. Drackley, and J.J. Loor. 2013. Feed restriction, but not l-carnitine infusion, alters the liver transcriptome by inhibiting sterol synthesis and mitochondrial oxidative phosphorylation and increasing gluconeogenesis in mid-lactation dairy cows. J. Dairy Sci. 96:2201–2213. https://doi.org/10.3168/jds.2012-6036.

Bauman, D.E., and W. Bruce Currie. 1980. Partitioning of nutrients during pregnancy and lactation: A review of mechanisms involving homeostasis and homeorhesis. J. Dairy Sci. 63:1514–1529. https://doi.org/10.3168/jds.S0022-0302(80)83111-0.

Baumgard, L.H., R.J. Collier, and D.E. Bauman. 2017. A 100-Year Review: Regulation of nutrient partitioning to support lactation. J. Dairy Sci. 100:10353–10366. https://doi.org/10.3168/jds.2017-13242.

Benjamini, Y., and Y. Hochberg. 1995. Controlling the false discovery rate: A practical and powerful approach to multiple testing. J. Royal Stat. Soc. Series B (Methodological) 57:289–300.

Bobe, G., J.W. Young, and D.C. Beitz. 2004. Invited review: Pathology, etiology, prevention, and treatment of fatty liver in dairy cows. J. Dairy Sci. 87:3105–3124. https://doi.org/10.3168/jds.S0022-0302(04)73446-3.

Bollatti, J.M., M.G. Zenobi, N.A. Artusso, A.M. Lopez, C.D. Nelson, B.A. Barton, C.R. Staples, and J.E.P. Santos. 2020. Effects of rumen-protected choline on the inflammatory and metabolic status and health of dairy cows during the transition period. J. Dairy Sci. 103(5):4192-4205. https://doi.org/10.3168/jds.2019-17294.

Bradford, B.J., and T.H. Swartz. 2020. Review: Following the smoke signals: Inflammatory signaling in metabolic homeostasis and homeorhesis in dairy cattle. Animal 14:s144–s154. https://doi.org/10.1017/S1751731119003203.

Caputo Oliveira, R., K.J. Sailer, H.T. Holdorf, C.R. Seely, R.S. Pralle, M.B. Hall, N.M. Bello, and H.M. White. 2019. Postpartum supplementation of fermented ammoniated condensed whey improved feed efficiency and plasma metabolite profile. J. Dairy Sci. 102:2283–2297. https://doi.org/10.3168/jds.2018-15519.

Chandler, T.L., and H.M. White. 2017. Choline and methionine differentially alter methyl carbon metabolism in bovine neonatal hepatocytes. PLoS ONE 12:e0171080. https://doi.org/10.1371/journal.pone.0171080.

Chapinal, N., M.E. Carson, S.J. LeBlanc, K.E. Leslie, S. Godden, M. Capel, J.E.P. Santos, M.W. Overton, and T.F. Duffield. 2012. The association of serum metabolites in the transition period with milk production and early-lactation reproductive performance. J. Dairy Sci. 95:1301–1309. https://doi.org/10.3168/jds.2011-4724.

Contreras, L.L., C.M. Ryan, and T.R. Overton. 2004. Effects of dry cow grouping strategy and prepartum body condition score on performance and health of transition dairy cows. J. Dairy Sci. 87:517–523. https://doi.org/10.3168/jds.S0022-0302(04)73191-4.

DeFrain, J.M., A.R. Hippen, K.F. Kalscheur, and P.W. Jardon. 2004. Feeding glycerol to transition dairy cows: Effects on blood metabolites and lactation performance. J. Dairy Sci. 87:4195–4206. https://doi.org/10.3168/jds.S0022-0302(04)73564-X.

Dennis, E.A., and P.C. Norris. 2015. Eicosanoid storm in infection and inflammation. Nature Reviews Immunol. 15:511–523. https://doi.org/10.1038/nri3859.

Dienes, H.P., T. Hütteroth, G. Hess, and S.C. Meuer. 1987. Immunoelectron microscopic observations on the inflammatory infiltrates and HLA antigens in hepatitis B and non-A, non-B. Hepatology 7:1317–1325. https://doi.org/10.1002/hep.1840070623.

Drackley, J.K. 1999. Biology of dairy cows during the transition period: The final frontier?. J. Dairy Sci. 82:2259–2273. https://doi.org/10.3168/jds.S0022-0302(99)75474-3.

Du, X., Z. Shi, Z. Peng, C. Zhao, Y. Zhang, Z. Wang, X. Li, G. Liu, and X. Li. 2017. Acetoacetate induces hepatocytes apoptosis by the ROS-mediated MAPKs pathway in ketotic cows. J.Cell. Physiol. 232:3296–3308. https://doi.org/10.1002/jcp.25773.

Emery, R.S., J.S. Liesman, and T.H. Herdt. 1992. Metabolism of long chain fatty acids by ruminant liver. J. Nutr. 122:832–837. https://doi.org/10.1093/jn/122.suppl_3.832.

Folch, J., M. Lees, and G.H. Sloane Stanley. 1957. A simple method for the isolation and purification of total lipids from animal tissues. J. Biol. Chem. 226:497–509.

Grummer, R.R. 1993. Etiology of lipid-related metabolic disorders in periparturient dairy cows. J. Dairy Sci. 76:3882–3896. https://doi.org/10.3168/jds.S0022-0302(93)77729-2.

Herkel, J., B. Jagemann, C. Wiegard, J.F.G. Lazaro, S. Lueth, S. Kanzler, M. Blessing, E. Schmitt, and A.W. Lohse. 2003. MHC class II-expressing hepatocytes function as antigen-presenting cells and activate specific CD4 T lymphocytes. Hepatology 37:1079–1085. https://doi.org/10.1053/jhep.2003.50191.

Honda, M., A. Sakai, T. Yamashita, Y. Nakamoto, E. Mizukoshi, Y. Sakai, T. Yamashita, M. Nakamura, T. Shirasaki, K. Horimoto, Y. Tanaka, K. Tokunaga, M. Mizokami, and S. Kaneko. 2010. Hepatic ISG expression is associated with genetic variation in interleukin 28B and the outcome of IFN therapy for chronic hepatitis C. Gastroenterology 139:499–509. https://doi.org/10.1053/j.gastro.2010.04.049.

Hotamisligil, G.S. 2006. Inflammation and metabolic disorders. Nature 444:860–867. https://doi.org/10.1038/nature05485.

Huang, D.W., B.T. Sherman, and R.A. Lempicki. 2009a. Systematic and integrative analysis of large gene lists using DAVID bioinformatics resources. Nature Protocols. 4:44–57. https://doi.org/10.1038/nprot.2008.211.

Huang, D.W., B.T. Sherman, and R.A. Lempicki. 2009b. Bioinformatics enrichment tools: Paths toward the comprehensive functional analysis of large gene lists. Nucleic Acids Res. 37:1–13. https://doi.org/10.1093/nar/gkn923.

Jorritsma, R., H. Jorritsma, Y.H. Schukken, P.C. Bartlett, T. Wensing, and G.H. Wentink. 2001. Prevalence and indicators of post partum fatty infiltration of the liver in nine commercial dairy herds in the Netherlands. Livest. Prod. Sci. 68:53–60. https://doi.org/10.1016/S0301-6226(00)00208-6.

Jorritsma, R., H. Jorritsma, Y.H. Schukken, and G.H. Wentink. 2000. Relationships between fatty liver and fertility and some periparturient diseases in commercial Dutch dairy herds. Theriogenology 54:1065–1074. https://doi.org/10.1016/S0093-691X(00)00415-5.

Kvidera, S.K., E.A. Horst, M. Abuajamieh, E.J. Mayorga, M.V.S. Fernandez, and L.H. Baumgard. 2017. Glucose requirements of an activated immune system in lactating Holstein cows. J. Dairy Sci. 100:2360–2374. https://doi.org/10.3168/jds.2016-12001.

Loor, J.J. 2010. Genomics of metabolic adaptations in the peripartal cow. Animal 4:1110–1139. https://doi.org/10.1017/S1751731110000960.

Loor, J.J., M. Bionaz, and J.K. Drackley. 2013. Systems physiology in dairy cattle: Nutritional genomics and beyond. Annu. Rev. Anim. Biosci. 1:365–392. https://doi.org/10.1146/annurev-animal-031412-103728.

Loor, J.J., H.M. Dann, N.A.J. Guretzky, R.E. Everts, R. Oliveira, C.A. Green, N.B. Litherland, S.L. Rodriguez-Zas, H.A. Lewin, and J.K. Drackley. 2006. Plane of nutrition prepartum alters hepatic gene expression and function in dairy cows as assessed by longitudinal transcript and metabolic profiling. Physiol. Genomics 27:29–41. https://doi.org/10.1152/physiolgenomics.00036.2006.

Loor, J.J., R.E. Everts, M. Bionaz, H.M. Dann, D.E. Morin, R. Oliveira, S.L. Rodriguez-Zas, J.K. Drackley, and H.A. Lewin. 2007. Nutrition-induced ketosis alters metabolic and signaling gene networks in liver of periparturient dairy cows. Physiol. Genomics 32:105–116. https://doi.org/10.1152/physiolgenomics.00188.2007.

Mächler, M., P. Rousseeuw, A. Struyf, and M. Hubert. 2015. “Finding groups in data”: Cluster analysis extended Rousseeuw et al. | Semantic Scholar. Accessed February 27, 2020. /paper/%22Finding-Groups-in-Data%22%3A-Cluster-Analysis-Extended-M%C3%A4chler-Rousseeuw/17a188e028a95d003144fcfd3a0839fe622deb79.

Mahrt, A., O. Burfeind, and W. Heuwieser. 2015. Evaluation of hyperketonemia risk period and screening protocols for early-lactation dairy cows. J. Dairy Sci. 98:3110–3119. https://doi.org/10.3168/jds.2014-8910.

Mavangira, V., and L.M. Sordillo. 2018. Role of lipid mediators in the regulation of oxidative stress and inflammatory responses in dairy cattle. Res. Vet. Sci. 116:4–14. https://doi.org/10.1016/j.rvsc.2017.08.002.

McArt, J.A.A., D.V. Nydam, and G.R. Oetzel. 2012. Epidemiology of subclinical ketosis in early lactation dairy cattle. J. Dairy Sci. 95:5056–5066. https://doi.org/10.3168/jds.2012-5443.

McArt, J.A.A., D.V. Nydam, and M.W. Overton. 2015. Hyperketonemia in early lactation dairy cattle: A deterministic estimate of component and total cost per case. J. Dairy Sci. 98:2043–2054. https://doi.org/10.3168/jds.2014-8740.

McCabe, M., S. Waters, D. Morris, D. Kenny, D. Lynn, and C. Creevey. 2012. RNA-seq analysis of differential gene expression in liver from lactating dairy cows divergent in negative energy balance. BMC Genomics 13:193. https://doi.org/10.1186/1471-2164-13-193.

McCarthy, S.D., S.M. Waters, D.A. Kenny, M.G. Diskin, R. Fitzpatrick, J. Patton, D.C. Wathes, and D.G. Morris. 2010. Negative energy balance and hepatic gene expression patterns in high-yielding dairy cows during the early postpartum period: A global approach. Physiol. Genomics 42A:188–199. https://doi.org/10.1152/physiolgenomics.00118.2010.

Møhlenberg, M., E. Terczynska-Dyla, K.L. Thomsen, J. George, M. Eslam, H. Grønbæk, and R. Hartmann. 2019. The role of IFN in the development of NAFLD and NASH. Cytokine 124:154519. https://doi.org/10.1016/j.cyto.2018.08.013.

Ospina, P.A., D.V. Nydam, T. Stokol, and T.R. Overton. 2010. Evaluation of nonesterified fatty acids and beta-hydroxybutyrate in transition dairy cattle in the northeastern United States: Critical thresholds for prediction of clinical diseases. J. Dairy Sci. 93:546–554. https://doi.org/10.3168/jds.2009-2277.

Overton, T.R., J.A.A. McArt, and D.V. Nydam. 2017. A 100-Year Review: Metabolic health indicators and management of dairy cattle. J. Dairy Sci. 100:10398–10417. https://doi.org/10.3168/jds.2017-13054.

Piepenbrink, M.S., and T.R. Overton. 2003. Liver metabolism and production of cows fed increasing amounts of rumen-protected choline during the periparturient period. J. Dairy Sci. 86:1722–1733. https://doi.org/10.3168/jds.S0022-0302(03)73758-8.

Sack, G.H. 2018. Serum amyloid A – a review. Mol. Med. 24:46-71. https://doi.org/10.1186/s10020-018-0047-0.

Saremi, B., M. Mielenz, M.M. Rahman, A. Hosseini, C. Kopp, S. Dänicke, F. Ceciliani, and H. Sauerwein. 2013. Hepatic and extrahepatic expression of serum amyloid A3 during

lactation in dairy cows. J. Dairy Sci. 96:6944–6954. https://doi.org/10.3168/jds.2013-6495.

Shahzad, K., M. Bionaz, E. Trevisi, G. Bertoni, S.L. Rodriguez-Zas, and J.J. Loor. 2014. Integrative analyses of hepatic differentially expressed genes and blood biomarkers during the peripartal period between dairy cows overfed or restricted-fed energy prepartum. PLoS One 9. https://doi.org/10.1371/journal.pone.0099757.

Shahzad, K., V. Lopreiato, Y. Liang, E. Trevisi, J.S. Osorio, C. Xu, and J.J. Loor. 2019. Hepatic metabolomics and transcriptomics to study susceptibility to ketosis in response to prepartal nutritional management. J. Anim. Sci. Biotechnol. 10:96-112. https://doi.org/10.1186/s40104-019-0404-z.

Soltan, M.A. 2010. Effect of dietary chromium supplementation on productive and reproductive performance of early lactating dairy cows under heat stress. J. Anim. Physiol.Anim. Nutr. 94:264–272. https://doi.org/10.1111/j.1439-0396.2008.00913.x.

Sordillo, L.M., and S.L. Aitken. 2009. Impact of oxidative stress on the health and immune function of dairy cattle. Vet. Immunol. Immunopathol. 128:104–109. https://doi.org/10.1016/j.vetimm.2008.10.305.

Sordillo, L.M., and V. Mavangira. 2014. The nexus between nutrient metabolism, oxidative stress and inflammation in transition cows. Anim. Prod. Sci. 54:1204–1214. https://doi.org/10.1071/AN14503.

Strange, R.C., M.A. Spiteri, S. Ramachandran, and A.A. Fryer. 2001. Glutathione-S-transferase family of enzymes. Mutation Research/Fundamental Mol. Mechanisms Mutagenesis 482:21–26. https://doi.org/10.1016/S0027-5107(01)00206-8.

Suthar, V.S., J. Canelas-Raposo, A. Deniz, and W. Heuwieser. 2013. Prevalence of subclinical ketosis and relationships with postpartum diseases in European dairy cows. J. Dairy Sci. 96:2925–2938. https://doi.org/10.3168/jds.2012-6035.

Takaoka, A., and H. Yanai. 2006. Interferon signalling network in innate defense. Cellular Microbiol. 8:907–922. https://doi.org/10.1111/j.1462-5822.2006.00716.x.

Thompson, G.E., and F. Darling. 1975. The hepatic uptake of individual free fatty acids in sheep during noradrenaline infusion. Res. Vet. Sci. 18:325–327. https://doi.org/10.1016/S0034-5288(18)33586-0.

Ting, J.P.-Y., and J. Trowsdale. 2002. Genetic control of MHC class II expression. Cell 109 Suppl:S21-33. https://doi.org/10.1016/s0092-8674(02)00696-7.

Townsend, D.M., and K.D. Tew. 2003. The role of glutathione- S -transferase in anti-cancer drug resistance. Oncogene 22:7369–7375. https://doi.org/10.1038/sj.onc.1206940.

Trapnell, C., A. Roberts, L. Goff, G. Pertea, D. Kim, D.R. Kelley, H. Pimentel, S.L. Salzberg, J.L. Rinn, and L. Pachter. 2012. Differential gene and transcript expression analysis of

RNA-seq experiments with TopHat and Cufflinks. Nature Protocols 7:562–578. https://doi.org/10.1038/nprot.2012.016.

Tsuchida, S. 2002. Glutathione Transferases. J.R. Bertino, ed. Academic Press, New York.

Vailati-Riboni, M., S. Meier, C.R. Burke, J.K. Kay, M.D. Mitchell, C.G. Walker, M.A. Crookenden, A. Heiser, S.L. Rodriguez-Zas, J.R. Roche, and J.J. Loor. 2016. Prepartum body condition score and plane of nutrition affect the hepatic transcriptome during the transition period in grazing dairy cows. BMC Genomics 17:854. https://doi.org/10.1186/s12864-016-3191-3.

Vidali, M., S.F. Stewart, and E. Albano. 2008. Interplay between oxidative stress and immunity in the progression of alcohol-mediated liver injury. Trends Mol. Med. 14:63–71. https://doi.org/10.1016/j.molmed.2007.12.005.

Walsh, R.B., J.S. Walton, D.F. Kelton, S.J. LeBlanc, K.E. Leslie, and T.F. Duffield. 2007. The effect of subclinical ketosis in early lactation on reproductive performance of postpartum dairy cows. J. Dairy Sci. 90:2788–2796. https://doi.org/10.3168/jds.2006-560.

Wankhade, P.R., A. Manimaran, A. Kumaresan, S. Jeyakumar, K.P. Ramesha, V. Sejian, D. Rajendran, and M.R. Varghese. 2017. Metabolic and immunological changes in transition dairy cows: A review. Vet World 10:1367–1377. https://doi.org/10.14202/vetworld.2017.1367-1377.

White, H.M. 2015. The role of TCA cycle anaplerosis in ketosis and fatty liver in periparturient dairy cows. Animals (Basel) 5:793–802. https://doi.org/10.3390/ani5030384.

Wilkens, M.R., C.D. Nelson, L.L. Hernandez, and J.A.A. McArt. 2020. Symposium review: Transition cow calcium homeostasis—Health effects of hypocalcemia and strategies for prevention. J. Dairy Sci. 103: 2909-2927. https://doi.org/10.3168/jds.2019-17268.

Zenobi, M.G., R. Gardinal, J.E. Zuniga, A.L.G. Dias, C.D. Nelson, J.P. Driver, B.A. Barton, J.E.P. Santos, and C.R. Staples. 2018. Effects of supplementation with ruminally protected choline on performance of multiparous Holstein cows did not depend upon prepartum caloric intake. J. Dairy Sci. 101:1088–1110. https://doi.org/10.3168/jds.2017-13327.

TABLES AND FIGURES

Table 3.1. The number of genes tested within day relative to calving (DRTC; diagonal) that are shared within and across comparison of clusters.[1]

		Susceptibility			Resistance		
	DRTC	-28	+ 1	+14	-28	+ 1	+14
Susceptibility	-28	13,151	12,752	12,837	12,833	12,757	12,519
	+ 1	21,009	13,011	12,784	12,670	12,744	12,512
	+14	20,891	20,978	13,211	12,768	12,774	12,620
Resistance	-28	20,962	20,939	20,834	13,139	12,736	12,518
	+ 1	20,874	21,001	20,828	20,865	13,150	12,525
	+14	21,065	21,198	21,103	21,076	21,071	12,718

[1]The number of tested genes shared (pairwise) across DRTC and across cluster comparisons (susceptibility or resistance) are above the diagonal, while the number of not-tested genes shared are below the diagonal. There were 34,411 genes that were potentially tested across the *Bos taurus* genome (release 106, ARS-UCD 1.2).

Table 3.2. Genes differentially expressed at all days relative to calving in liver samples from cows less or more susceptible to lipid-related metabolic disorders.[1]

Gene	Symbol	-28	+1	+14
BOLA class I histocompatibility antigen, alpha chain BL3-6	*BOLA*	-1.3	-1.3	-1.4
major histocompatibility complex, class II, DQ beta	*BOLA-DQB*	-2.2	-3.0	-3.0
coiled-coil domain containing 80	*CCDC80*	-5.0	-1.4	-3.4
C-C motif chemokine 14 precursor	*CCL14*	-1.7	-1.9	-1.6
B-cell receptor CD22	*CD22*	1.4	1.1	0.9
acetylcholine receptor subunit epsilon	*CHRNE*	2.3	1.3	1.5
C-type lectin domain family 4 member F	*CLEC4F*	-1.3	-1.3	-1.5
GTPase IMAP family member 6	*GIMAP6*	-1.3	-1.7	-1.7
GTPase IMAP family member 8	*GIMAP8*	-2.2	-2.0	-2.4
ISG15 ubiquitin-like modifier	*ISG15*	-1.6	-1.0	1.1
methylenetetrahydrofolate dehydrogenase 1 like	*MTHFD1L*	-1.4	-1.3	-1.6
olfactory receptor 4X2	*OR4S1*	1.0	0.9	0.8
prodynorphin	*PDYN*	-2.4	-2.9	-2.2
secreted frizzled related protein 2	*SFRP2*	5.6	4.4	2.0
pulmonary surfactant-associated protein A precursor	*SFTPA1*	-3.7	-2.1	-1.6
teneurin transmembrane protein 1	*TENM1*	-2.1	-1.3	-0.9

[1]Genes were considered differentially expressed within day relative to calving (-28, +1, and +14) when $Q \leq 0.10$ (*P*-value corrected for multiplicity by false discovery rate). Values represent the $\log_2$-transformed fold change within each timepoint (more susceptible/less susceptible).

Table 3.3. Kyoto Encyclopedia of Genes and Genomes metabolic pathways enriched within the differentially expressed genes in liver samples from cows less or more susceptible to lipid-related metabolic disorders.[1]

DRTC	ID	Metabolic Pathway	FE	*Q*-value	Gene Symbols[2]
-28	bta04514	Cell adhesion molecules (CAMs)	5	0.098	*MGC126945, ITGAV, NRCAM, LOC534578, CD22, BOLA-DQB, LOC100848815*
	bta04145	Phagosome	4	0.098	*SEC61G, SFTPA1, MRC2, MGC126945, ITGAV, SEC61B, BOLA-DQB*
	bta03320	PPAR signaling pathway	6	0.136	*SCD, CYP8B1, APOA5, SLC27A6, FADS2*
+ 1	bta05204	Chemical carcinogenesis	7	0.023	*LOC615303, CYP1A1, GSTA4, GSTT1, GSTA1, CYP2C87*
	bta00480	Glutathione metabolism	8	0.026	*ODC1, GSTA4, GSTT1, ANPEP, GSTA1*
	bta00980	Metabolism of xenobiotics by cytochrome P450	7	0.026	*LOC615303, CYP1A1, GSTA4, GSTT1, GSTA1*
	bta05164	Influenza A	4	0.04	*RSAD2, OAS1X, DDX39B, DDX58, LOC784541, BOLA-DQB, LOC100848815*
	bta04141	Protein processing in endoplasmic reticulum	3	0.079	*CKAP4, HSPA5, HYOU1, DNAJB11, MOGS, SEC23B, WFS1*
	bta00982	Drug metabolism - cytochrome P450	6	0.079	*LOC615303, GSTA4, GSTT1, GSTA1*
	bta04514	Cell adhesion molecules (CAMs)	4.0	0.085	*NRCAM, LOC534578, CD22, BOLA-DQB, LOC100848815*
+14	bta04512	ECM-receptor interaction	9	6.3×10^{-5}	*COL6A3, COL6A1, COL5A1, COL5A3, COL3A1, COL1A1, COL1A2, COL5A2, VWF, TNXB*
	bta04974	Protein digestion and absorption	10	6.8×10^{-5}	*COL6A3, COL6A1, COL5A1, COL5A3, COL3A1, COL1A1, COL1A2, COL5A2, COL15A1*
	bta04611	Platelet activation	4.0	0.046	*COL5A1, COL5A3, ADCY1, COL3A1, COL1A1, COL1A2, COL5A2, VWF*
	bta04510	Focal adhesion	3	0.046	*COL6A3, COL6A1, COL5A1, COL5A3, COL3A1, COL1A1, COL1A2, COL5A2, VWF, TNXB*
	bta05146	Amoebiasis	5	0.046	*COL5A1, COL5A3, ADCY1, COL3A1, COL1A1, COL1A2, COL5A2*
	bta04923	Regulation of lipolysis in adipocytes	7	0.058	*PTGER3, ADCY1, FABP4, LIPE, IRS2*
	bta04151	PI3K-Akt signaling pathway	3	0.058	*IFNAR1, COL6A3, COL6A1, COL5A1, COL5A3, LPAR1, COL3A1, COL1A1, COL1A2, COL5A2, VWF, TNXB*

[1]Enrichment analysis was performed within day relative to calving (DRTC) using the Database for Annotation, Visualization, and Integrated Discovery (version 6.8) by comparing a list of differentially expressed genes ($Q \leq 0.10$) to a custom background list including all tested genes. Fold enrichment (FE) and Fischer's exact statistics were extracted; tests were corrected for multiplicity by the false discovery rate method (*Q*-value).

[2]Annotation of gene transcripts and affiliated gene symbols are based on the *Bos taurus* reference genome (release 106, ARS-UCD 1.2)

Table 3.4. Genes differentially expressed at all days relative to calving in liver samples from cows more or less resistant to lipid-related metabolic disorders.[1]

Gene	Symbol	-28	+1	+14
major histocompatibility complex, class II, DQ beta	*BOLA-DQB*	1.9	2.1	2.6
GTPase IMAP family member 4	*GIMAP4*	-0.8	-1.2	-1.2
17-beta-hydroxysteroid dehydrogenase 13	*HSD17B13*	1.2	1.8	1.2
interferon induced protein 44	*IFI44*	1.3	1.8	1.3
interferon alpha inducible protein 6	*IFI6*	1.8	2.6	1.0
MHC Class I JSP.1	*JSP.1*	0.8	1.1	0.7
myomesin 1	*MYOM1*	0.9	1.8	0.8
2',5'-oligoadenylate synthetase 1, 40/46kDa	*OAS1X*	2.3	1.8	1.4
proto-oncogene tyrosine-protein kinase ROS	*ROS1*	-1.1	-1.4	-3.0

[1]Genes were considered differentially expressed within day relative to calving (-28, +1, and +14) when $Q \leq 0.10$ (*P*-value corrected for multiplicity by false discovery rate). Values represent the $\log_2$-transformed fold change within each timepoint (less resistant/more resistant).

Table 3.5. Kyoto Encyclopedia of Genes and Genomes metabolic pathways enriched within the differentially expressed genes in liver samples from cows more or less resistant to lipid-related metabolic disorders.[1]

Metabolic Pathway	FE	*Q*-value	Gene Symbols
Cytokine-cytokine receptor interaction	4.6	0.099	*PF4, CXCR2, CXCR1, IL1R2, CCR1, CSF2RB*
Cell adhesion molecules (CAMs)	4.5	0.099	*VCAN, JSP.1, SELL, LOC534578, BOLA-DQB*
Viral myocarditis	6.4	0.099	*JSP.1, MYH7, CD55, BOLA-DQB*
Chemokine signaling pathway	3.5	0.099	*PF4, NCF1, CXCR2, CXCR1, CCR1, CCL24*
Hematopoietic cell lineage	5.7	0.099	*MS4A1, LOC515418, IL1R2, CD55*
Metabolic pathways	14.1	0.041	*IDI1, HAL, SDS, LOC511161, KYAT1, ALPI, FOLH1B, LOC615045, BCO1, OAT, GCSH, ASAH2, PLB1, FDPS, FUT1, HDC, AKR1B10, MBOAT2, ACSS2, MTHFD1L, ADH4, ENPP3, B4GALT4, PLA2G2A, CYP2J2, LOC100125266, CYP2B6*
Arachidonic acid metabolism	2.6	0.041	*PLB1, LOC615045, PLA2G2A, CYP2B6, CYP2J2*
Linoleic acid metabolism	2.1	0.041	*PLB1, LOC615045, PLA2G2A, CYP2J2*
Autoimmune thyroid disease	2.1	0.041	*JSP.1, LOC524810, LOC100300716, BOLA-DQB*
Allograft rejection	2.1	0.041	*JSP.1, LOC524810, LOC100300716, BOLA-DQB*
Viral myocarditis	2.6	0.041	*JSP.1, LOC524810, LOC100300716, CD55, BOLA-DQB*
Intestinal immune network for IgA production	2.1	0.083	*LOC524810, PIGR, LOC100300716, BOLA-DQB*
alpha-Linolenic acid metabolism	1.6	0.086	*PLB1, LOC615045, PLA2G2A*
Pentose and glucuronate interconversions	10.6	0.253	*LOC100296421, AKR1B10, UGT2B10*
HTLV-I infection	2.7	0.253	*EGR1, JSP.1, MYC, ATF3, SLC25A6LOC534578, BOLA-DQB*
Circadian rhythm	9.0	0.253	*ARNTL, PER1, RORC*
Retinol metabolism	6.0	0.316	*LOC100296421, UGT2B10, CYP26B1*
Herpes simplex infection	2.9	0.316	*OAS1X, ARNTL, PER1, JSP.1, BOLA-DQB*
Protein processing in endoplasmic reticulum	2.6	0.316	*CKAP4, PDIA4, PDIA3, CRYAB, PDIA6*
Antigen processing and presentation	4.9	0.316	*PDIA3, JSP.1, BOLA-DQB*
Influenza A	2.6	0.380	*RSAD2, OAS1X, DDX39B, BOLA-DQB*
Cell adhesion molecules (CAMs)	3.0	0.458	*JSP.1, LOC534578, BOLA-DQB*

[1]Enrichment analysis was performed within day relative to calving (DRTC) using the Database for Annotation, Visualization, and Integrated Discovery (version 6.8) by comparing a list of differentially expressed genes ($Q \leq 0.10$) to a custom background list including all tested genes. Fold enrichment (FE) and Fischer's exact statistics were extracted; tests were corrected for multiplicity by the false discovery rate method (*Q*-value).

[2]Annotation of gene transcripts and affiliated gene symbols are based on the *Bos taurus* reference genome (release 106, ARS-UCD 1.2)

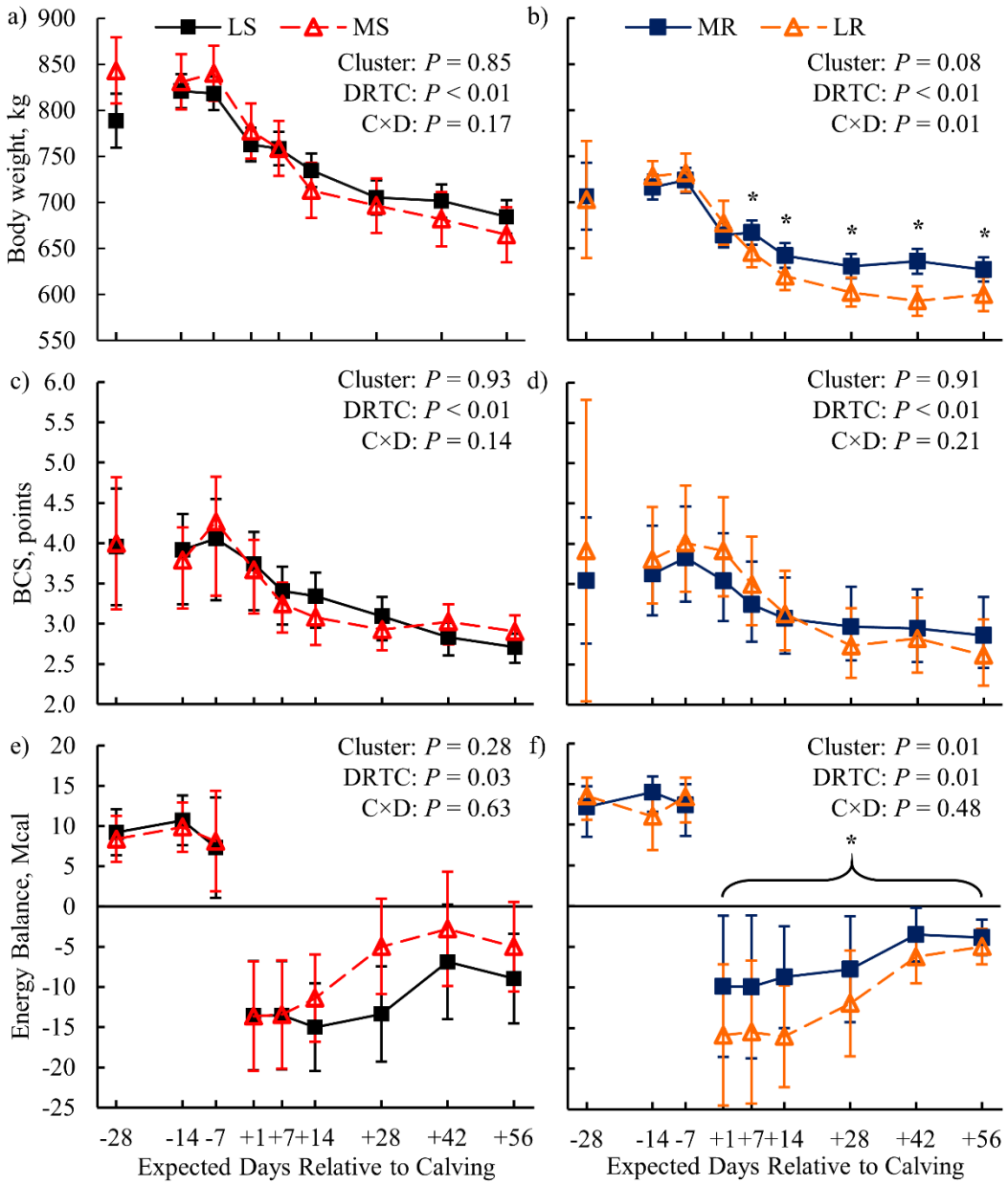

Figure 3.1. Body weight, body condition score (BCS), and calculated energy balance for dairy cows clustered based on postpartum lipid metabolites within original dietary treatment. Left-hand panels compare cows less (LS) or more susceptible (MS) to lipid-related metabolic disorders, while right-hand panels compare cows more (MR) or less resistant (LR) to lipid-related metabolic disorders. Statistics for the fixed effects of cluster, day relative to calving (DRTC), and their interaction (C×D) across the experimental period (panels a through d) or the postpartum period (panels e and f) are displayed in the top-right corner of each panel. Asterisks denote significant ($P \leq 0.10$; Bonferroni adjusted) simple effects of cluster within DRTC or contrast of cluster across postpartum samples (bracketed).

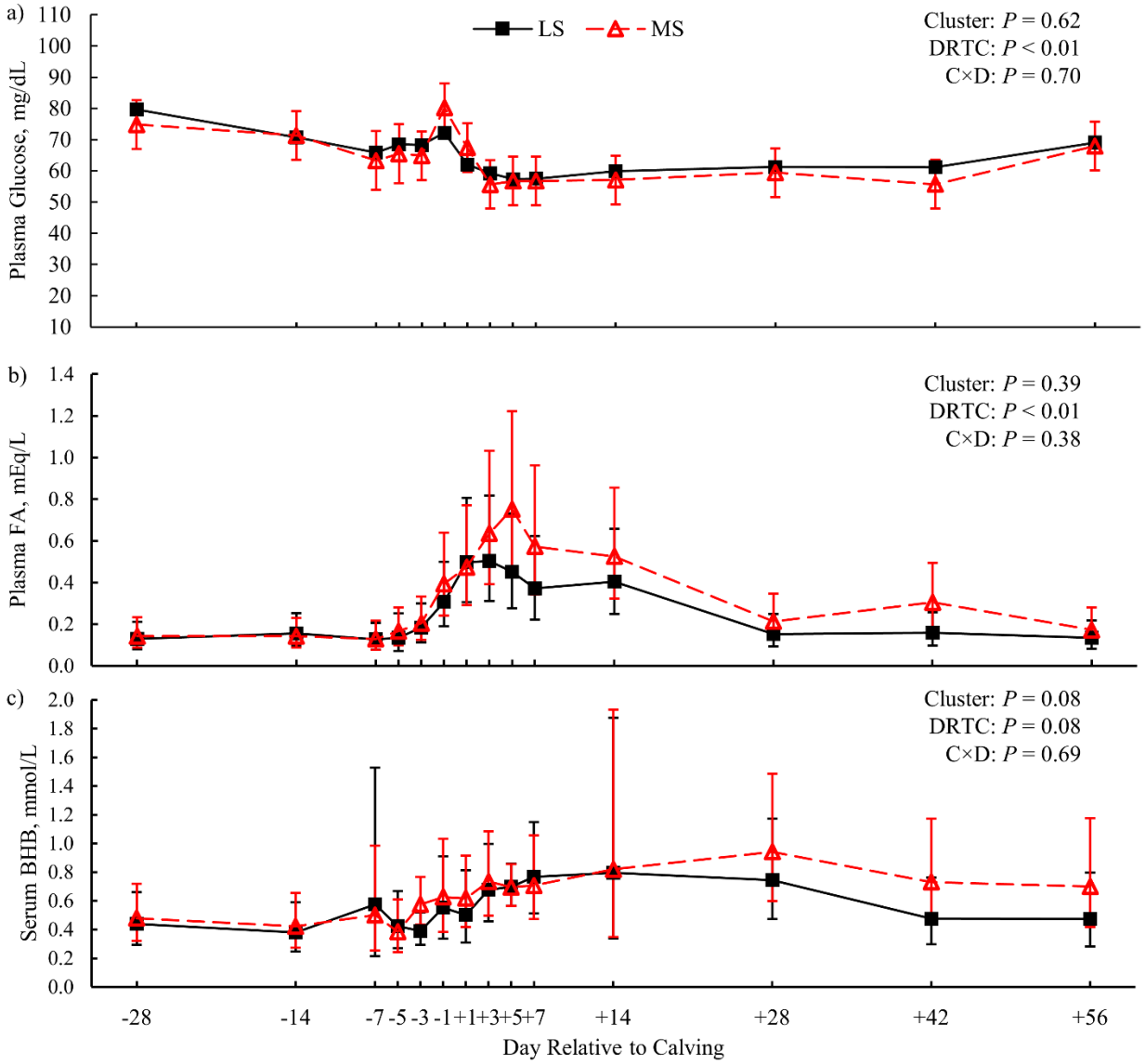

Figure 3.2. Blood fraction concentrations of glucose, fatty acids (FA), and β-hydroxybutyrate (BHB) for dairy cows less (LS) or more susceptible (MS) to lipid-related metabolic disorders. Statistics for the fixed effects of cluster, day relative to calving (DRTC), and their interaction (C×D) are displayed in the top-right corner of each panel. There were no significant contrasts of cluster across postpartum samples ($P > 0.10$).

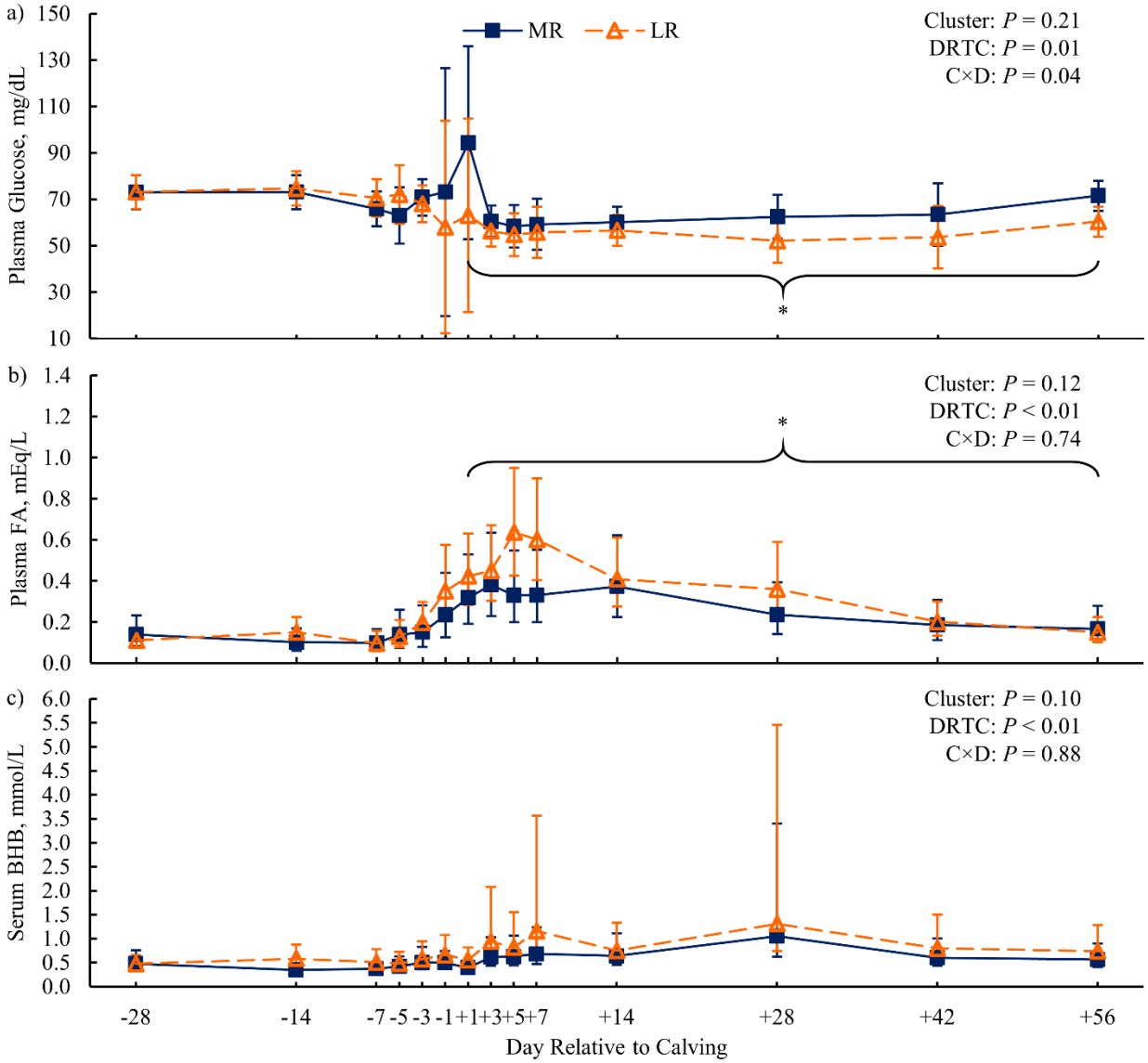

Figure 3.3. Blood fraction concentrations of glucose, fatty acids (FA), and β-hydroxybutyrate (BHB) for dairy cows more resistant (MR) or less resistant (LR) to lipid-related metabolic disorders. Statistics for the fixed effects of cluster, day relative to calving (DRTC), and their interaction (C×D) are displayed in the top-right corner of each panel. Asterisks and brackets denote significant contrasts of cluster across postpartum samples ($P \leq 0.10$).

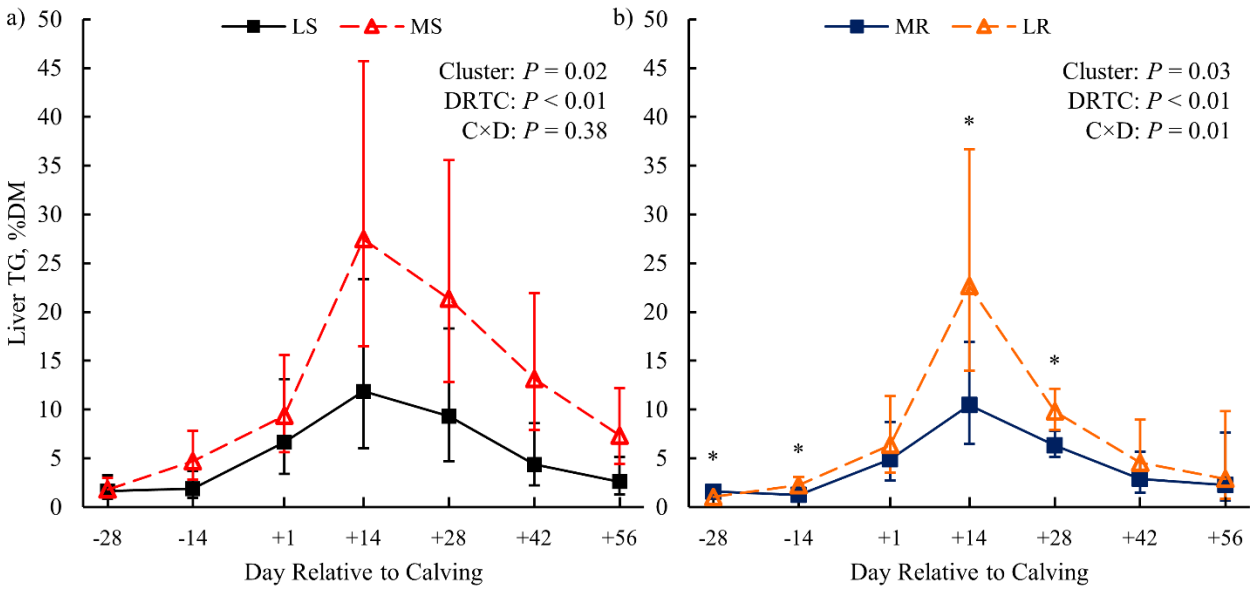

Figure 3.4. Liver triglyceride (TG) content for dairy cows clustered based on postpartum lipid metabolites within original dietary treatment. Panel a depicts cows less (LS) or more susceptible (MS) to lipid-related metabolic disorders, while panel b compares cows more (MR) or less resistant (LR) to lipid-related metabolic disorders. Statistics for the fixed effects of cluster, day relative to calving (DRTC), and their interaction (C×D) are displayed in the top-right corner of each panel. Asterisks denote significant ($P \leq 0.10$; Bonferroni adjusted) simple effects of cluster within DRTC.

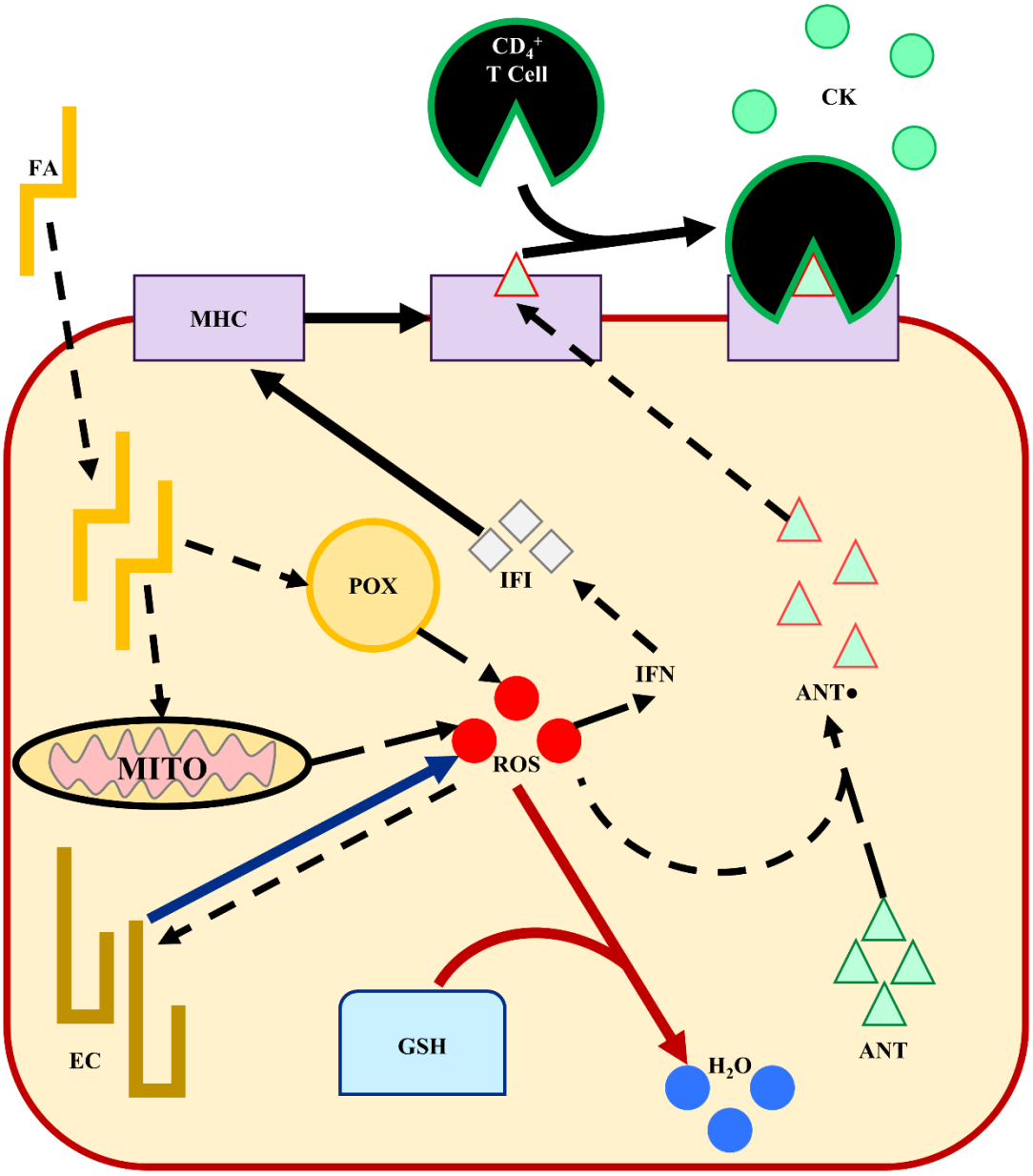

Figure 3.5. A working model of differentially regulated metabolic pathways in the liver of dairy cows that contribute to the pathology of lipid-related metabolic disorders. Fatty acids (FA) entering the hepatocyte are oxidized in the mitochondria (MITO) and peroxisomes (POX), producing energy and reactive oxygen species (ROS). Interferon (IFN) production is promoted by ROS, stimulating major histocompatibility complex (MHC) expression. Antigens (ANT) are oxidized (ANT●) by ROS. The ANT● are presented by the MHC promoting CD_4^+ T lymphocyte recruitment and cytokine (CK) production. Eicosanoids (EC) are formed by FA oxidation by ROS and may promote ROS production. Glutathione (GSH) reduces ROS and other oxidized products. Arrows demonstrate the directionality and specificity of metabolic pathways: not differentially regulated pathways are dashed lines (----), pathways upregulated in cows less susceptible to LRMD are blue (——), pathways upregulated in cows less resistant to LRMD are red (——), and pathways upregulated in cows less susceptible and more resistant are solid, black (——).

CHAPTER 4: LITERATURE PART 2: BIG DATA, BIG PREDICTIONS: UTILIZING MILK FOURIER-TRANSFORM INFRARED AND GENOMICS TO IMPROVE HYPERKETONEMIA MANAGEMENT

ABSTRACT

Negative animal health and performance outcomes are associated with disease incidences that can be labor intensive, costly, and cumbersome for many farms. Amelioration of unfavorable outcomes through early detection and treatment of disease has emphasized the value of improving health monitoring. Although the value is recognized, detecting hyperketonemia (**HYK**) is still difficult for many farms to do practically and efficiently. Increasing data streams available to farms presents opportunities to use data to better monitor cow and herd health; however, challenges remain with regard to validating, integrating, and interpreting data. During the transition to lactation period, useful data are presented in the form of milk production and composition, milk Fourier-transform infrared (**FTIR**) wavelength absorbance, cow management records, and genomics, which have been employed to monitor postpartum onset of HYK. Attempts to predict postpartum HYK from test-day milk and performance variables incorporated into multiple linear regression models have demonstrated sufficient accuracy to monitor monthly herd prevalence; however, they lacked the sensitivity and specificity for individual cow diagnostics. Subsequent artificial neural network prediction models employing FTIR data and milk composition variables achieved 83 and 81% sensitivity and specificity for individual cow diagnostics. Although these results fail to reach the diagnostic goals of 90%, they are achieved without individual cow blood samples, which may justify acceptance of lower performance. The caveat is that these models depend on milk analysis, which is traditionally done every 4 weeks.

This infrequent sampling allows for a single diagnostic sample for about half of the fresh cows. Benefits to farms are greatly improved if postpartum cows can be milk tested weekly. Additionally, this allows for close monitoring of somatic cell count and may open the door for use of other herd health monitoring tools. Future improvements in these models may be achievable by maximizing sensitivity at the expense of specificity and may be most economical in disorders for which the cost of treatment is less than that of mistreating (e.g., HYK). Genomic predictions for HYK may be improved by incorporating genome-wide associated SNP and further utilized for precision management of HYK risk groups. Development and validation of HYK prediction models may provide producers with individual cow and herd-level management tools.

INTRODUCTION

Advances in dairy cattle management, nutrition, genetics, and reproduction not only represent improvements in knowledge of dairy cattle biology but are reflective of availability and timeliness of data. Routine analysis of milk samples started as a way to monitor milk fat and protein and has progressed to other complex traits and monitoring of herd health indicators. Other data are now available to farms from numerous sources, including feeding systems, rumination sensors, activity monitors, robotic milking systems, and weather stations, to name a few (Wathes et al., 2008; Wolfert et al., 2017). Furthermore, management systems incorporating advanced technology can be accessed by off-farm management team members and can send real-time alerts.

Although undoubtedly a wealth of knowledge and potential exists in the pool of data from the aforementioned systems, a great need remains to sort, validate, and integrate these data into forms that are user friendly, consistent across platforms and manufacturers, and practically

applicable. For many research teams, an obvious place to start has been with detection of health events or monitoring of high-risk physiological periods. Development of individual diagnostic and herd-level management tools for these disorders can yield economic, production, and animal health benefits. Of particular interest to us and others is monitoring animal health during the transition to lactation period. This is a period of increased risk for metabolic disorders such as hyperketonemia (**HYK**), hypocalcemia, and fatty liver. The purpose of this review is to recognize the progress that has been made, as well as highlight future opportunities, in using "big data" to monitor herd health, specifically with regard to HYK.

HYPERKETONEMIA PREDICTION FROM MILK AND MANAGEMENT DATA

The reference test for HYK diagnosis is the quantification of blood serum or plasma β-hydroxybutyrate (**BHB**) concentration via enzymatic assay (Iwersen et al., 2009; McArt et al., 2013). The establishment of current blood or blood fraction BHB thresholds based on the increased risk of unfavorable animal health and performance outcomes has been thoroughly reviewed (McArt et al., 2013; Overton et al., 2017), with thresholds of BHB ≥ 1.2 mmol/L and BHB ≥ 1.4 mmol/L being the most frequently used. Although evidence suggests that dietary and management factors affect basal blood BHB concentration (DeFrain et al., 2006; Roche et al., 2010), BHB ≥ 1.2 mmol/L has been suggested as a universal standard for HYK diagnosis (Suthar et al., 2013).

Despite the availability of handheld BHB meters that can be used cowside, diagnostic protocols based on blood BHB are costly and labor-intensive, presenting application challenges (McArt et al., 2014; Denis-Robichaud et al., 2014; Sailer et al., 2018). Alternatively, collection of a milk sample is noninvasive and can be incorporated into milking routines, and concentrations of milk ketone bodies are correlated with their blood concentrations (Marstorp et

al., 1983; Andersson, 1984; Denis-Robichaud et al., 2014). Fourier-transform infrared (**FTIR**) spectrometry has provided a practical method of predicting milk ketone body concentrations, and although it is not currently as accurate as chemical quantification of the molecules using gas-liquid chromatography, flow injection analysis, or enzymatic assays, it can be implemented on a larger scale, given that it is already used for routine dairy herd improvement (**DHI**) milk testing (de Roos et al., 2007). Furthermore, predicted concentrations of milk acetone or BHB from FTIR correlate ($r = 0.80$) with chemically analyzed milk concentrations (de Roos et al., 2007).

Attempts to evaluate the efficacy of milk ketone body concentrations for HYK diagnosis have been challenged in the establishment of diagnostic thresholds. A range of milk BHB and acetone thresholds have been suggested based on concordance with blood or blood fraction BHB diagnosis. Enjalbert et al. (2001) suggested thresholds of milk acetone, as determined via gas-liquid chromatography, of ≥160 μmol/L and enzymatically determined milk BHB ≥70 μmol/L for sensitive (91.7%) HYK screening; however, accuracy was low at 64.0% and 69.4% for milk acetone and milk BHB, respectively. Similar thresholds were determined by van der Drift et al. (2012b) using FTIR-predicted milk acetone (131.5 μmol/L) and milk BHB (76.3 μmol/L), with accuracies of 87.1 and 76.8%, respectively. Conversely, van Knegsel et al. (2010) reported that much lower thresholds of FTIR-predicted milk acetone of ≥70 μmol/L and milk BHB of ≥23 μmol/L maximized accuracy of HYK diagnosis, 71.6 and 70.7%, respectively. Comparison of FTIR-predicted milk BHB (≥1.2 mmol/L as the diagnostic threshold) with blood BHB resulted in overall sensitivity and specificity of 81 and 92%, respectively (Renaud et al., 2019). Similar sensitivity and specificity were achieved when FTIR-predicted BHB and acetone were analyzed in primiparous, but not multiparous, Holstein and Jersey cows (Chandler et al., 2018). Additional incorporation of performance variables including dry period length, gestation length, and

lactation number to milk analysis results (fat, protein, FTIR-predicted acetone and BHB) improved accuracy of models to predict HYK but still lacked the sensitivity to provide an individual cow diagnostic tool (Chandler et al., 2018). Regardless of the lack of sensitivity of these models compared with enzymatic blood BHB quantification, a role remains for these models in herd-level diagnostics and monitoring (Denis-Robichaud et al., 2014; Chandler et al., 2015). Routine (*i.e.*, monthly) implementation of these herd- level HYK predictions can aid farms in monitoring prevalence and identifying patterns and farm-specific risk factors. Additional benefits may derive from observing herd health consequences from intentional or unintentional management and environment changes.

Efforts to increase reliability of model predictions have involved the use of more advanced statistical modeling techniques, larger sample sets, and raw FTIR wavelength data (Pralle et al., 2018). Using a data set of more than 3,600 samples (divided into training and external testing sample sets), artificial neural network models based on milk analysis (such as milk fat, protein, FTIR-predicted acetone and BHB), and raw FTIR wavelengths resulted in improved HYK prediction models compared with models using either FTIR data or milk analysis data alone, or models built using multiple linear or partial least squares regression (Pralle et al., 2018). Despite failing to reach the diagnostic accuracy of cowside enzymatic blood tests such as the Precision Xtra (Abbott Diabetes Care, Alameda, CA) and BHBCheck (PortaCheck, Moorestown, NJ) meters (Iwersen et al., 2009; Sailer et al., 2018), these models are considered to have “very good” diagnostic capacity based on general thresholds of diagnostic accuracy (Šimundić, 2009). When we recall that the goal of using FTIR milk analysis to diagnose HYK was to reduce the cost and labor necessary to employ blood-based diagnostics on farm, we may be willing to accept slightly lower diagnostic capacity in exchange for the reduced intensity and

cost of FTIR-based diagnostics (Pralle et al., 2018). A positive case of HYK is likely to be treated with oral propylene glycol, a low-cost treatment that requires no milk withdrawal (McArt et al., 2012a, 2014), resulting in minimal consequence to treating a false-positive case. Given this, an opportunity may exist to maximize prediction model sensitivity, at the expense of specificity, while maintaining cost-effectiveness and promoting animal welfare.

GENETIC AND GENOMIC MANAGEMENT OF KETOSIS

Investigations into genetic selection for HYK susceptibility have predominately relied on voluntary records provided by dairy producers. Threshold model heritability estimates have ranged from 0.02 to 0.17 in Holstein cows (Kadarmideen et al., 2000; Zwald et al., 2004; Parker Gaddis et al., 2014; Klein et al., 2019). Presently, Zoetis Genetics (Kalamazoo, MI) is the only provider of genomic evaluations for HYK susceptibility, which is marketed as ketosis resistance, based on voluntary records in the United States (Vukasinovic et al., 2017); however, misclassification of HYK cases as controls (or as nonevents) is a problem with voluntary records, especially when considering subclinical cases and the variation in HYK diagnosis criteria (Oetzel, 2004; Pryce et al., 2016). Weigel et al. (2017) explored the heritability of HYK based on intensive sampling of blood BHB concentration at 4 time points between 5 and 18 days in milk (**DIM**; inclusive), and the estimated heritability for the binary assignment of HYK was 0.07, which was within the range reported for voluntary records. The authors were unable to evaluate the effectiveness of voluntary records as an indicator of an intensively sampled HYK phenotype because farm managers were not blind to HYK assessment. Nonetheless, it was proposed that a reference population of cows could be established for population-wide genomic predictions of HYK susceptibility (Weigel et al., 2017).

Milk ketone body concentration, predicted from FTIR and collected during routine DHI testing, has been proposed as an indicator trait for HYK susceptibility. These traits are heritable, with milk acetone heritability ranging from 0.10 to 0.28 (van der Drift et al., 2012a; Ranaraja et al., 2018) and milk BHB heritability ranging from 0.067 to 0.19 (van der Drift et al., 2012a; Koeck et al., 2014; Jamrozik et al., 2016; Ranaraja et al., 2018). Genetic correlations between clinical HYK records and FTIR-predicted ketone bodies are moderate, ranging from 0.25 to 0.48 (Koeck et al., 2014; Jamrozik et al., 2016). Although these results suggest that FTIR-predicted milk ketone bodies are promising HYK indicator traits, the correlation between these test-day milk BHB or acetone traits and the more intensively sampled HYK phenotypes has not been explored. Further investigation into these associations will inform on the adequacy of monthly milk ketone body concentration records as the basis for genomic management strategies of subclinical HYK susceptibility.

Incorporation of genetic and genomic evaluations of HYK susceptibility into management through animal breeding programs is intuitive. A potential concern for directly breeding against HYK susceptibility is the unintentional elimination of compensatory metabolism (*i.e.*, ketogenesis), at least with respect to the subclinical phenotype. Use of genomics as a tool for precision health management is a largely unexplored alternative. Genome-guided management of HYK would be analogous to personalized human medicine, where estimated breeding values for HYK, alone or coupled with other on-farm data streams such as test-day prediction models (Chandler et al., 2018; Pralle et al., 2018), could be used to stratify cows into risk groups for group-specific management (Weigel et al., 2017).

The scheme we propose is based on polygenic risk, because complex traits reflect numerous small effects from loci across the genome. A subset of single nucleotide

polymorphisms (**SNP**) may explain an effective amount of variance that can augment HYK management. Indeed, Nani et al. (2019) found that genomic predictions incorporating a subset of genome-wide significant SNP considerably improved the predictive ability of whole-genome models for sire conception rate. Therefore, genome-wide association studies (**GWAS**) for HYK may indicate a subset of SNP worthy of increased weighting in genomic evaluation of HYK susceptibility [e.g., weighted genomic best linear unbiased prediction (**GBLUP**)]. Previous GWAS for HYK based on voluntary records have not identified SNP with genome-wide significant associations (Parker Gaddis et al., 2018; Klein et al., 2019). We believe the present lack of genome-wide associations is due to voluntary record HYK phenotypes having variation in trait definition across herds (*i.e.*, subclinical vs. clinical, urine vs. blood ketone body metrics) and having high misclassification rates caused by insufficient assessment frequency (*i.e.*, only 1 blood BHB measurement within the first 21 DIM). A preliminary GWAS in Holstein cows, specifically for a subclinical HYK phenotype based on multiple blood BHB measurements, has marginal genome-wide evidence for a single SNP as- sociation and significant evidence for SNP associations dependent on parity status (Pralle et al., 2019 a, b). Further validation of these findings would justify use of specific SNP genotypes for HYK risk assessment, potentially in a parity-dependent manner.

ON-FARM INTEGRATION OF HERD-HEALTH DIAGNOSTICS, CHALLENGES, AND OPPORTUNITIES

Although the collective body of research has generated diagnostic tools, on-farm integration and implementation remain difficult. A few key challenges present hurdles and deserve our vested interest. Here we address 4 that appear to be limiting progress at this point: the nature of “monthly” DHI milk testing on farm, differences in proprietary FTIR predictions

across FTIR equipment manufacturers, challenges in implementing advanced computational models and integrating data streams for farm usability, and validation of the accuracy of prediction models within experiments and across dairy operations.

Historically, DHI milk sampling has been performed about every 4 weeks on privately owned dairy farms (Weigel et al., 2017). Based on the at-risk period and duration for HYK, a farm would test only half of the fresh cows during the peak risk period (3 to 18 DIM; McArt et al. 2012b), and those cows would be tested only once. The 2 intuitive ways to address this challenge are (1) to produce equations based on in-line measurement systems and (2) to implement weekly milk testing of fresh cows. Current in-line systems include Herd Navigator (DeLaval International AB, Tumba, Sweden) and AfiLab (Afimilk, Kibbutz Afikim, Israel); however, only the former provides milk BHB predictions for monitoring HYK (Blom et al., 2015). For farms that do not have in-line measurement systems, the second option could be viable. In this system, all early-postpartum cows would be milk sampled weekly, resulting in fresh cows being sampled twice during the at-risk period. Use of prediction models on these samples would allow for either treatment of cows predicted positive or generation of a list of cows that warrant blood BHB testing. Beyond detection of HYK, these weekly milk samples could have additional benefits. Reporting somatic cell count (**SCC**) or differential SCC could provide valuable information in this postpartum period, to help identify cases of mastitis earlier (Fourdraine et al., 2019). As the technology continues to improve (e.g., differential SCC), it may also be a means to flag cows with increased inflammatory markers. Furthermore, if a group of cows are being milk tested weekly, it is not beyond reason that other subgroups would be selectively milk sampled that day, which opens the door further for using milk FTIR to determine energy balance (McParland et al., 2015; Grelet et al., 2016), evaluate likelihood of

conception (Ho et al., 2019), test for pregnancy in mid-lactation cows (Lainé et al., 2017; Toledo-Alvarado et al., 2018), or monitor cows within treatment pens. Milk analysis does not occur without cost, but analysis from postpartum cows may provide more valuable information than analysis from cows in late lactation, allowing us to envision that DHI programs of the future may shift to more frequent testing of cows in periods of interest. The second challenge, differences in FTIR equipment and proprietary predictions across manufacturers, is apparent to collaborative research teams when working across DHI organizations or trying to reconcile compiled results as discrepancies arise throughout growing data sets. Although the equipment is based on the same technology, standards are still primarily used for controlling the basic components (e.g., fat, protein) across the industry. Given the proprietary nature of the predictions offered by companies, we may not be able to compare FTIR-predicted characteristics (such as short-chain fatty acids) across manufacturers. Furthermore, these proprietary predictions change over time, even within a manufacturer. Standardization efforts can reduce background noise and prediction errors and are sensitive to milk composition shifts (Tiplady et al., 2019). These differences may not be as evident to producers viewing results from a single DHI laboratory, but if research is based on separate platforms, there may be limitations to on-farm application based on the equipment used by the DHI or in-line system.

As discussed herein, prediction of complex metabolic disorders will likely have marginal improvements in precision and accuracy when utilizing computation- ally advanced methods, such as artificial neural networks. Appreciable gains in model performance were observed when incorporating more data from several sources (*i.e.,* farm management software, milk components, and milk FTIR output), regardless of prediction method (Pralle et al., 2018). Further improvement to model performance could be made by incorporating other data streams, such as

rumination collars and accelerometers, which may provide additional insight into animal health and wellness; however, the inclusion of multiple data streams increases the technical difficulty for data alignment and quality control for the DHI and dairy producer. For the ultimate value of these tools to be achieved by the farm, the outcome of these models must also be returned in a timely manner from the time sampled. In the case of HYK, the ideal turnaround time from milk sampling to results being returned to the farm would be 24 h, for cows to be treated. This challenge also extends far beyond monitoring HYK, or even general herd health, into whole-farm monitoring. Farms have countless data streams available to them. Many of these data sources are not discussed here but fall into attempts by industry and university collaborators to integrate into useful, proactive decision-making tools (Cabrera et al., 2020).

Model validation is of paramount importance in affirming the efficacy of any big data tools applied in practice. Most of the work in trait or outcome prediction relies on random cross-validation methods, where a random subset (or subsets) of data is excluded from model training and used for evaluation. Recently, Wang and Bovenhuis (2019) predicted cow methane emission from milk mid-infrared spectrum and demonstrated how this strategy can result in overoptimistic evaluation of model accuracy compared with block cross-validation. Block cross-validation partitions data into training and evaluation data sets strategically by factors causing data dependence (e.g., farm); therefore, underestimated prediction error rates are avoided in data with systematic differences between blocks (Qin et al., 2016). In their study, Wang and Bovenhuis (2019) observed coefficients of determination of 0.49 and 0.01 in the validation sets for random cross-validation and block cross-validation, respectively. This is a massive difference that would mislead conclusions and potential application. With respect to HYK, this systematic confounding could occur due to previously alluded differences in diet composition and management practices

altering basal concentrations of blood BHB or other milk characteristics. Furthermore, we believe this demonstrates the importance of collecting data from a diverse portfolio of herds and production systems for model training and validation.

Besides the progress made in using big data from on-farm data streams to improve cow health and disease management, omics technologies have provided big data mining opportunities for systems biologists to unravel the underlying mechanisms of physiological states (Loor et al., 2013). These applications interrogate the coordinated changes in biological processes and networks in a family of molecules, such as RNA (transcriptomics), proteins (proteomics), and molecules involved in cellular metabolism (metabolomics). Unlike reductionist approaches, omics techniques allow for unguided discovery of novel biological elements that can be incorporated into knowledge of the physiological state, such as metabolic disorders. For example, a microarray of the liver transcriptome from cows with nutrient-induced HYK highlighted the roles of transcription factors, protein ubiquitination, and inflammation, and suggested several novel genes (e.g., *LPIN1*, *LPIN3*, *ANGPTL4*) related to HYK etiology (Loor et al., 2007). Overall, this work is still in infancy, but it may augment our precision management strategies through greater appreciation of essential metabolic pathways, shifting toward a metabolic engineering approach.

CONCLUSIONS

The wealth of data available to dairy farms today presents immense opportunities. Substantial progress has been made in predicting HYK with management records, milk FTIR analysis, and genomics, which demonstrates the capacity of using a “big data” approach to derive practical solutions that can be implemented on farm. Moving forward, researchers will continue to push the capacity of big data to diagnose and perhaps predict future cases of health incidences.

To effectively implement these tools for on-farm use, research and industry need to address the timeliness of data availability, the standardization of equipment measurements, and frameworks for data stream integration. Nonetheless, big data–oriented management strategies have great potential for improving animal health and productivity, ultimately improving dairy farm profit-ability through strategic management.

ACKNOWLEDGMENTS

This chapter is a reproduction of a published manuscript authored by Pralle and White (2020). The authors gratefully acknowledge the countless undergraduate and graduate students, farm and research staff, and collaborators who make our research contributions to this field possible. We recognize funding for the projects completed by the H. M. White research group referenced here: USDA AFRI Critical Agriculture Research and Extension (CARE; 2015-67028-23572); USDA Hatch (WIS01877 and WISC01878) from the Wisconsin Agricultural Experiment Station (Madison, WI); Cooperative Research Program for Agriculture Science and Technology Development (Project No. PJ012078) Rural Development Administration, Jeonju-si, Jeollabuk-do, Republic of Korea; AgSource Cooperative Services (research funding support and collaborative efforts; Verona, WI); Purina Animal Nutrition LLC (St. Louis, MO) graduate student fellowships; VitaPlus Corporation (Madison, WI) graduate student fellowship; and the Wisconsin Alumni Research Foundation (Madison, WI).

REFERENCES

Andersson, L. 1984. Concentrations of blood and milk ketone bodies, blood isopropanol and plasma glucose in dairy cows in relation to the degree of hyperketonaemia and clinical signs. Zentralbl. Veterinarmed. A. 31:683–693. https://doi.org/10.1111/j.1439-0442.1984.tb01327.x.

Blom, J.Y., J.M. Christensen, and C. Ridder. 2015. Real-time analyses of BHB in milk can monitor ketosis and its impact on reproduction in dairy cows. Pages 263–272 in Precision Livestock Farming Applications. I. Halachmi, ed. Wageningen Academic Publishers, Wageningen, the Netherlands.

Cabrera, V., L. Fadul-Pacheco, J. Barrientos, and H. Delgado. 2020. Real-time continuous decision making using big data. J. Dairy Sci. https://doi.org/10.3168/jds.2019-17145.

Chandler, T.L., R.S. Pralle, J.R.R. Dórea, S.E. Poock, G. R. Oetzel, R. H. Fourdraine, and H. M. White. 2018. Predicting hyperketonemia by logistic and linear regression using test-day milk and performance variables in early-lactation Holstein and Jersey cows. J. Dairy Sci. 101:2476–2491. https://doi.org/10.3168/jds.2017-13209.

Chandler, T.L., R.S. Pralle, G.R. Oetzel, R.H. Fourdraine, and H.M. White. 2015. Development of a ketosis prevalence detection tool in Holstein dairy cows based on milk component data and cow test-day information. J. Dairy Sci. 98 (Suppl. 3):507. (Abstr.)

de Roos, A.P.W., H.J.C.M. van den Bijgaart, J. Hørlyk, and G. de Jong. 2007. Screening for subclinical ketosis in dairy cattle by Fourier transform infrared spectrometry. J. Dairy Sci. 90:1761–1766. https://doi.org/10.3168/jds.2006-203.

DeFrain, J.M., A.R. Hippen, K.F. Kalscheur, and D.J. Schingoethe. 2006. Feeding lactose to increase ruminal butyrate and the metabolic status of transition dairy cows. J. Dairy Sci. 89:267–276. https://doi.org/10.3168/jds.S0022-0302(06)72091-4.

Denis-Robichaud, J., J. Dubuc, D. Lefebvre, and L. DesCôteaux. 2014. Accuracy of milk ketone bodies from flow-injection analysis for the diagnosis of hyperketonemia in dairy cows. J. Dairy Sci. 97:3364– 3370. https://doi.org/10.3168/jds.2013-6744.

Enjalbert, F., M.C. Nicot, C. Bayourthe, and R. Moncoulon. 2001. Ketone bodies in milk and blood of dairy cows: Relationship between concentrations and utilization for detection of subclinical ketosis. J. Dairy Sci. 84:583–589. https://doi.org/10.3168/jds.S0022-0302(01)74511-0.

Fourdraine, R.H., A. Samia Kalantari, J. Amdall, and A.D. Coburn. 2019. Using differential somatic cell count to improve udder health. ICAR Conference, Prague, Czech Republic. S12(T)-PP-05.

Grelet, C., C. Bastin, M. Gelé, J.B. Davière, M. Johan, A. Werner, R. Reding, J.A. Fernandez Pierna, F.G. Colinet, P. Dardenne, N. Gengler, H. Soyeurt, and F. Dehareng. 2016. Development of Fourier transform mid-infrared calibrations to predict acetone, β-

hydroxybutyrate, and citrate contents in bovine milk through a European dairy network. J. Dairy Sci. 99:4816–4825. https://doi.org/10.3168/jds.2015-10477.

Ho, P.N., V. Bonfatti, T.D. W. Luke, and J.E. Pryce. 2019. Classifying the fertility of dairy cows using milk mid-infrared spectroscopy. J. Dairy Sci. 102:10460–10470. https://doi.org/10.3168/jds.2019-16412.

Iwersen, M., U. Falkenberg, R. Voigtsberger, D. Forderung, and W. Heuwieser. 2009. Evaluation of an electronic cowside test to detect subclinical ketosis in dairy cows. J. Dairy Sci. 92:2618–2624. https://doi.org/10.3168/jds.2008-1795.

Jamrozik, J., A. Koeck, G.J. Kistemaker, and F. Miglior. 2016. Multiple-trait estimates of genetic parameters for metabolic disease traits, fertility disorders, and their predictors in Canadian Holsteins. J. Dairy Sci. 99:1990–1998. https://doi.org/10.3168/jds.2015-10505.

Kadarmideen, H., R. Thompson, and G. Simm. 2000. Linear and threshold model genetic parameters for disease, fertility and milk production in dairy cattle. Anim. Sci. 71:411–419. https://doi.org/10.1017/S1357729800055338.

Klein, S.L., C. Scheper, K. Brügemann, H.H. Swalve, and S. König. 2019. Phenotypic relationships, genetic parameters, genome-wide associations, and identification of potential candidate genes for ketosis and fat-to-protein ratio in German Holstein cows. J. Dairy Sci. 102:6276–6287. https://doi.org/10.3168/jds.2019-16237.

Koeck, A., J. Jamrozik, F.S. Schenkel, R. K. Moore, D.M. Lefebvre, D.F. Kelton, and F. Miglior. 2014. Genetic analysis of milk β-hydroxybutyrate and its association with fat-to-protein ratio, body condition score, clinical ketosis, and displaced abomasum in early first lactation of Canadian Holsteins. J. Dairy Sci. 97:7286– 7292. https://doi.org/10.3168/jds.2014-8405.

Lainé, A., C. Bastin, C. Grelet, H. Hammami, F.G. Colinet, L.M. Dale, A. Gillon, J. Vandenplas, F. Dehareng, and N. Gengler. 2017. Assessing the effect of pregnancy stage on milk composition of dairy cows using mid-infrared spectra. J. Dairy Sci. 100:2863– 2876. https://doi.org/10.3168/jds.2016-11736.

Loor, J.J., M. Bionaz, and J.K. Drackley. 2013. Systems physiology in dairy cattle: Nutritional genomics and beyond. Annu. Rev. Anim. Biosci. 1:365–392. https://doi.org/10.1146/annurev-animal-031412-103728.

Loor, J.J., R.E. Everts, M. Bionaz, H. Dann, D.E. Morin, R. Oliveira, S.L. Rodriguez-Zas, J.K. Drackley, and H.A. Lewin. 2007. Nutrition-induced ketosis alters metabolic and signaling gene networks in liver of periparturient dairy cows. Physiol. Genomics 32:105–116. https://doi.org/10.1152/physiolgenomics.00188.2007.

Marstorp, P., T. Anfält, and L. Andersson. 1983. Determination of oxidized ketone bodies in milk by flow injection analysis. Anal. Chim. Acta 149:281–289. https://doi.org/10.1016/S0003-2670(00)83184-0.

McArt, J.A.A., D.V. Nydam, G.R. Oetzel, T.R. Overton, and P.A. Ospina. 2013. Elevated non-esterified fatty acids and β-hydroxybutyrate and their association with transition dairy cow performance. Vet. J. 198:560–570. https://doi.org/10.1016/j.tvjl.2013.08.011.

McArt, J.A.A., D.V. Nydam, and G.R. Oetzel. 2012a. A field trial on the effect of propylene glycol on displaced abomasum, removal from herd, and reproduction in fresh cows diagnosed with subclinical ketosis. J. Dairy Sci. 95:2505–2512. https://doi.org/10.3168/jds.2011-4908.

McArt, J.A.A., D.V. Nydam, and G.R. Oetzel. 2012b. Epidemiology of subclinical ketosis in early lactation dairy cattle. J. Dairy Sci. 95:5056–5066. https://doi.org/10.3168/jds.2012-5443.

McArt, J.A.A., D.V. Nydam, G.R. Oetzel, and C.L. Guard. 2014. An economic analysis of hyperketonemia testing and propylene glycol treatment strategies in early lactation dairy cattle. Prev. Vet. Med. 117:170–179. https://doi.org/10.1016/j.prevetmed.2014.06.017.

McParland, S., E. Kennedy, E. Lewis, S.G. Moore, B. McCarthy, M. O'Donovan, and D.P. Berry. 2015. Genetic parameters of dairy cow energy intake and body energy status predicted using mid- infrared spectrometry of milk. J. Dairy Sci. 98:1310–1320. https://doi.org/10.3168/jds.2014-8892.

Nani, J.P., F.M. Rezende, and F. Peñagaricano. 2019. Predicting male fertility in dairy cattle using markers with large effect and functional annotation data. BMC Genomics 20:258. https://doi.org/10.1186/s12864-019-5644-y.

Oetzel, G.R. 2004. Monitoring and testing dairy herds for metabolic disease. Vet. Clin. North Am. Food Anim. Pract. 20:651–674. https://doi.org/10.1016/j.cvfa.2004.06.006.

Overton, T.R., J.A.A. McArt, and D.V. Nydam. 2017. A 100-Year Review: Metabolic health indicators and management of dairy cattle. J. Dairy Sci. 100:10398–10417. https://doi.org/10.3168/jds.2017-13054.

Parker Gaddis, K.L., J.B. Cole, J.S. Clay, and C. Maltecca. 2014. Genomic selection for producer-recorded health event data in US dairy cattle. J. Dairy Sci. 97:3190–3199. https://doi.org/10.3168/ jds.2013-7543.

Parker Gaddis, K.L., J.H. Megonigal Jr., J.S. Clay, and C.W. Wolfe. 2018. Genome-wide association study for ketosis in US Jerseys using producer-recorded data. J. Dairy Sci. 101:413–424. https://doi.org/10.3168/jds.2017-13383.

Pralle, R.S. and H.M. White. 2020. Symposium review: Big data, big predictions: Utilizing milk Fourier-transform infrared and genomics to improve hyperketonemia management. J. Dairy Sci. 103:3867-3873. https://doi.org/10.3168/jds.2019-17379.

Pralle, R.S., K.W. Weigel, N.E. Schultz, and H.M. White. 2019a. Hyperketonemia genome-wide association study in Holstein cows. Page 538 in Proc. European Association for Animal Production. (Abstr.) Wageningen Academic, Wageningen, the Netherlands.

Pralle, R.S., K.W. Weigel, N.E. Schultz, and H.M. White. 2019b. Hyperketonemia SNP by parity group genome-wide interaction study in Holstein cows. Page 541 in Proc. European Association for Animal Production. (Abstr.) Wageningen Academic, Wageningen, the Netherlands.

Pralle, R.S., K.W. Weigel, and H.M. White. 2018. Predicting blood β-hydroxybutyrate using milk Fourier transform infrared spectrum, milk composition, and producer-reported variables with multiple linear regression, partial least squares regression, and artificial neural network. J. Dairy Sci. 101:4378–4387. https://doi.org/10.3168/jds.2017-14076.

Pryce, J.E., K.L. Parker Gaddis, A. Koeck, C. Bastin, M. Abdelsayed, N. Gengler, F. Miglior, B. Heringstad, C. Egger-Danner, K.F. Stock, A.J. Bradley, and J.B. Cole. 2016. Invited review: Opportunities for genetic improvement of metabolic diseases. J. Dairy Sci. 99:6855–6873. https://doi.org/10.3168/jds.2016-10854.

Qin, L.X., H.C. Huang, and C.B. Begg. 2016. Cautionary note on using cross-validation for molecular classification. J. Clin. Oncol. 34:3931–3938. https://doi.org/10.1200/JCO.2016.68.1031.

Ranaraja, U., K. Cho, M. Park, S. Kim, S. Lee, and C. Do. 2018. Genetic parameter estimation for milk β-hydroxybutyrate and acetone in early lactation and its association with fat to protein ratio and energy balance in Korean Holstein cattle. Asian-Australas. J. Anim. Sci. 31:798–803. https://doi.org/10.5713/ajas.17.0443.

Renaud, D. L., D. F. Kelton, and T. F. Duffield. 2019. Short communication: Validation of a test-day milk test for β-hydroxybutyrate for identifying cows with hyperketonemia. J. Dairy Sci. 102:1589–1593. https://doi.org/10.3168/jds.2018-14778.

Roche, J.R., J.K. Kay, C.V.C. Phyn, S. Meier, J.M. Lee, and C.R. Burke. 2010. Dietary structural to nonfiber carbohydrate concentration during the transition period in grazing dairy cows. J. Dairy Sci. 93:3671–3683. https://doi.org/10.3168/jds.2009-2868.

Sailer, K.J., R.S. Pralle, R.C. Oliveira, S.J. Erb, G.R. Oetzel, and H.M. White. 2018. Technical note: Validation of the BHBCheck blood β-hydroxybutyrate meter as a diagnostic tool for hyperketonemia in dairy cows. J. Dairy Sci. 101:1524–1529. https://doi.org/10.3168/jds.2017-13583.

Šimundić, A.M. 2009. Measures of diagnostic accuracy: Basic definitions. EJIFCC 19:203–211.

Suthar, V.S., J. Canelas-Raposo, A. Deniz, and W. Heuwieser. 2013. Prevalence of subclinical ketosis and relationships with postpartum diseases in European dairy cows. J. Dairy Sci. 96:2925–2938. https://doi.org/10.3168/jds.2012-6035.

Tiplady, K.M., R.G. Sherlock, M.D. Littlejohn, J.E. Pryce, S.R. Davis, D.J. Garrick, R.J. Spelman, and B.L. Harris. 2019. Strategies for noise reduction and standardization of milk mid-infrared spectra from dairy cattle. J. Dairy Sci. 102:6357–6372. https://doi.org/10.3168/jds.2018-16144.

Toledo-Alvarado, H., A.I. Vazquez, G. de los Campos, R.J. Tempelman, G. Gabai, A. Cecchinato, and G. Bittante. 2018. Changes in milk characteristics and fatty acid profile during the estrous cycle in dairy cows. J. Dairy Sci. 101:9135–9153. https://doi.org/10.3168/jds.2018-14480.

van der Drift, S.G.A., R. Jorritsma, J.T. Schonewille, H.M. Knijn, and J.A. Stegeman. 2012b. Routine detection of hyperketonemia in dairy cows using Fourier transform infrared spectroscopy analysis of β-hydroxybutyrate and acetone in milk in combination with test-day information. J. Dairy Sci. 95:4886–4898. https://doi.org/10.3168/jds.2011-4417.

van der Drift, S.G.A., K.J.E. van Hulzen, T.G. Teweldemedhn, R. Jorritsma, M. Nielen, and H.C.M. Heuven. 2012a. Genetic and nongenetic variation in plasma and milk β-hydroxybutyrate and milk acetone concentrations of early-lactation dairy cows. J. Dairy Sci. 95:6781–6787. https://doi.org/10.3168/jds.2012-5640.

van Knegsel, A.T.M., S.G.A. van der Drift, M. Horneman, A.P.W. de Roos, B. Kemp, and E.A.M. Graat. 2010. Short communication: Ketone body concentration in milk determined by Fourier transform infrared spectroscopy: Value for the detection of hyperketonemia in dairy cows. J. Dairy Sci. 93:3065–3069.

Vukasinovic, N., N. Bacciu, C.A. Przybyla, P. Boddhireddy, and S.K. DeNise. 2017. Development of genetic and genomic evaluation for wellness traits in US Holstein cows. J. Dairy Sci. 100:428–438. https://doi.org/10.3168/jds.2016-11520.

Wang, Q., and H. Bovenhuis. 2019. Validation strategy can result in an overoptimistic view of the ability of milk infrared spectra to predict methane emission of dairy cattle. J. Dairy Sci. 102:6288–6295. https://doi.org/10.3168/jds.2018-15684.

Wathes, C.M., H.H. Kristensen, J.M. Aerts, and D. Berckmans. 2008. Is precision livestock farming an engineer's daydream or nightmare, an animal's friend or foe, and a farmer's panacea or pitfall? Comput. Electron. Agric. 64:2–10. https://doi.org/10.1016/j.compag.2008.05.005.

Weigel, K.A., P.M. VanRaden, H.D. Norman, and H. Grosu. 2017. A 100-Year Review: Methods and impact of genetic selection in dairy cattle—From daughter–dam comparisons to deep learning algorithms. J. Dairy Sci. 100:10234–10250. https://doi.org/10.3168/ jds.2017-12954.

Wolfert, S., L. Ge, C. Verdouw, and M.-J. Bogaardt. 2017. Big data in smart farming—A review. Agric. Syst. 153:69–80. https://doi.org/10.1016/j.agsy.2017.01.023.

Zwald, N.R., K.A. Weigel, Y.M. Chang, R.D. Welper, and J.S. Clay. 2004. Genetic selection for health traits using producer-recorded data. I. Incidence rates, heritability estimates, and sire breeding values. J. Dairy Sci. 87:4287–4294. https://doi.org/10.3168/jds.S0022-0302(04)73573-0.

CHAPTER 5: HYPERKETONEMIA GWAS AND PARITY DEPENDENT SNP ASSOCIATIONS IN HOLSTEIN DAIRY COWS INTENSIVELY SAMPLED FOR BLOOD β-HYDROXYBUTYRATE CONCENTRATION

ABSTRACT

Hyperketonemia (**HYK**) is a metabolic disorder that affects early postpartum dairy cows; however, there has been limited success in identifying genomic variants contributing to HYK susceptibility. We conducted a genome-wide association study (**GWAS**) using HYK phenotypes based on an intensive screening protocol, interrogated genotype interactions with parity group (**GWIS**), and evaluated the enrichment of annotated metabolic pathways. Holstein cows were enrolled onto the experiment after parturition and blood samples were collected at 4 timepoints between 5 to 18 days postpartum. Concentration of blood β-hydroxybutyrate (**BHB**) was quantified cow-side via a handheld BHB meter. Cows were labeled as a HYK case when at least one blood sample had BHB ≥ 1.2 mmol/L and all other cows considered non-HYK controls. After quality control procedures, 1,710 cows and 58,699 genotypes were available for further analysis. The GWAS and GWIS were performed using the forward feature select linear mixed model method. There was evidence for an association between *ARS-BFGL-NGS-91238* and HYK susceptibility, as well as parity-dependent associations to HYK for *BovineHD0600024247* and *BovineHD1400023753*. Candidate genes annotated to these SNP associations have been previously associated with obesity, diabetes, insulin resistance, and fatty liver in humans and rodent models. Enrichment analysis revealed focal adhesion and axon guidance as metabolic pathways contributing to HYK etiology, while genetic variation in pathways related to insulin secretion and sensitivity may affect HYK susceptibility in a parity dependent matter. In

conclusion, the present work proposes several novel marker associations and metabolic pathways contributing to genetic risk for HYK susceptibility.

INTRODUCTION

Hyperketonemia (**HYK**) is a common metabolic disorder in early postpartum dairy cows, with prevalence ranging from 10.3 to 53.2% across studies (McArt et al., 2012; van der Drift et al., 2012; Garro et al., 2014; Mahrt et al., 2015; Chandler et al., 2018). The progression of HYK is driven by early postpartum negative energy balance (Baird, 1982; Grummer, 1993; Herdt, 2000), which promotes adipose lipolysis and hepatic ketogenesis (Grummer, 1993; Koltes and Spurlock, 2011; White, 2015). Blood β-hydroxybutyrate (**BHB**), a product of ketogenesis, is the reference metabolite for HYK with BHB concentrations ≥ 1.2 mmol/L considered positive HYK cases (Chapinal et al., 2012; McArt et al., 2012; Suthar et al., 2013). Negative consequences associated with HYK include greater risk of comorbidities, decreased reproductive efficiency, productive losses, and premature culling (Walsh et al., 2007; Duffield et al., 2009; McArt et al., 2012; Rutherford et al., 2016). These associated consequences culminate to a total economic loss of $375 and $256 per HYK case for primiparous and multiparous cows, respectively (McArt et al., 2015).

Improving dairy cow profitability and health through genetic management has led to several investigations assessing the heritability of HYK. Most investigations have relied on voluntary (self-recorded) producer records, estimating heritability between 0.02 to 0.17 in Holstein cows (Kadarmideen et al., 2000; Zwald et al., 2004; Parker Gaddis et al., 2014; Klein et al., 2019). This large range in heritability may reflect voluntary records not providing consistent, accurate phenotypes for HYK because of variability in diagnostic protocols, protocol compliance, and recording procedures. Furthermore, the short resolution time, variable day of

incidence, and subclinical nature of HYK requires repeated quantification of blood BHB in early lactation to accurately diagnose HYK (Oetzel, 2004; McArt et al., 2012; Mahrt et al., 2015). Heritability estimation of a binary HYK phenotype based on repeated blood BHB sampling has provided an estimate of 0.07 (Weigel et al., 2017).

Genome-wide association (**GWAS**), genome-wide interaction studies (**GWIS**), and metabolic pathway enrichment analyses are methods to further dissect trait genetic architecture. These analyses can aid in discovery of genetic variants, genes, and pathways essential to disease etiology, providing candidates for reductionist experiments (Visscher et al., 2017). Furthermore, refinement of the essential genetic components to HYK risk may be utilized for improved genetic selection and integrated into targeted HYK management schemes based on genetic risk (Zhang et al., 2014; Weigel et al., 2017). Using a population of US Jersey cows, Parker Gaddis et al. (2018) proposed several single nucleotide polymorphisms (**SNP**) associated with HYK based on standardized effect size. The proximal genes and subsequent pathway analysis suggested insulin regulation, lipid metabolism, and immune response as contributing metabolic pathways to HYK susceptibility. Klein et al. (2019) identified candidate SNP associations with HYK in a population of German Holsteins, with proximal genes related to diabetes and obesity. However, neither of these studies identified SNP or metabolic pathways that were significant after multiple-test correction (Parker Gaddis et al., 2014; Klein et al., 2019). Both studies relied on convenience phenotypes without standardized HYK diagnostic practices (Parker Gaddis et al., 2014; Klein et al., 2019). Yepes et al. (2019) conducted GWAS for a HYK phenotype based on repeated BHB sampling on a small number of Holstein cows (n = 128) and suggested several SNP associations. Their proposed candidate genes generally related to the regulation of energy metabolism and lipoprotein metabolism.

We hypothesized a genomic survey of HYK susceptibility using phenotypes based on an intensive HYK screening protocol would result in detection of genome-wide significant SNP and metabolic pathways. The objectives of the present work were to use a population of Holstein cows with a HYK phenotype based on multiple early lactation blood BHB measurements to 1) discover any SNP associated with HYK susceptibility, 2) identify SNP associations with HYK dependent on parity group (primiparous vs. multiparous), and 3) to infer gene pathways enriched within SNP associated with HYK susceptibility.

MATERIALS AND METHODS

All experimental protocols were approved by the Animal Care and Use Committee of the College of Agriculture and Life Sciences at the University of Wisconsin-Madison.

Holstein dairy cows (n = 1,903) from three privately-owned dairy farms in southern Wisconsin and the University of Wisconsin-Madison Emmons Blaine Dairy Cattle Research Center were enrolled for HYK phenotype assessment (Rathbun et al., 2017; Weigel et al. 2017). Cows were assigned to a herd-year-season (**HYS**) contemporary group (10 levels) with seasons defined as a parturition date within the range of January to March, April to June, July to September, or October to December. A blood sample from a coccygeal vessel was obtained from each cow immediately after returning to freestall housing from the morning milk harvest and within 1 hour of feed access. Frequency of sampling was twice per week, three or four days apart, such that four measurements were available for each cow between 5 and 18 days postpartum, inclusive. Each blood sample was tested cowside for BHB concentration with the Precision Xtra Blood Glucose and Ketone Meter (Abbott Diabetes Care, Alameda, CA; 8 HYS groups) or BHBCheck blood ketone meter (PortaCheck, Moorestown, NJ; 2 HYS groups), which have been validated for use in dairy cattle with similar diagnostic performance (Iwersen et al.,

2009; Bach et al., 2016; Sailer et al., 2018). Cows were diagnosed with HYK if blood BHB ≥ 1.2 mmol/L and reported to farm staff for treatment of HYK per the respective farm's standard operating procedure. A binary HYK phenotype was assigned to each cow, where cows with a maximum observed blood BHB ≥ 1.2 mmol/L were labeled HYK [1] and the remaining cows labeled as non-HYK controls [0].

Imputed SNP genotypes were provided by the Council on Dairy Cattle Breeding (Bowie, MD) and represented 60,671 SNP routinely implemented in genomic evaluations within the United States of America. The original cow genotypes were analyzed using a variety of genotyping platforms: Illumina BovineLD BeadChip (32% of genotyped cows; Illumina, San Diego, CA, USA), Zoetis Low Density (23% of genotyped cows; Zoetis, Parsippany, NJ, USA), Zoetis Low Density Version 4 (20% of genotyped cows; Zoetis), Zoetis Low Density Version 2 (10% of genotyped cows; Zoetis), Illumina BovineSNP50 BeadChip Version 2 (5% of genotyped cows; Illumina), and GeneSeek Genomic Profiler LD Version 4 (5% of genotyped cows; Neogen, Lincoln, NE, USA). Genomic coordinates of the provided SNP were updated to the most recent release of the *Bos taurus* genome assembly (release 106, ARS-UCD 1.2).

Genotype quality control procedures were performed in the R statistical environment (version 3.4.5), using procedures within the GenABEL (version 1.8) package (Aulchenko et al., 2007). Phenotyped cows with unavailable genotypes (n = 100), registered as a crossbred (n = 9), a twin (n = 4 pairs, random exclusion of one cow within each pair), or a genotype call rate < 95% (n = 80) were discarded. Subsequently, SNP were sequentially discarded based on the following criteria: call rate < 93% (n = 876), monomorphic (n = 43), minor allele frequency < 0.01 (n = 858), and lack of genomic coordinates (n = 195). Hardy-Weinberg Equilibrium statistics were corrected for multiple testing using the false discovery rate method (Benjamini and Hochberg,

1995) and suggested no SNP violated Hardy-Weinberg Equilibrium ($Q > 0.15$). After quality control, 1,710 purebred Holstein cows with 58,699 quality SNP remained for GWAS.

Genome-Wide Association Study

Association testing was performed using the Feature Forward Selection (**FFselect**) method to test for additive SNP effects across the genome (Schultz and Weigel, 2020). Briefly, the FFselect method extends the improved linear mixed model for GWAS proposed by Widmer et al. (2014) by incorporating a shared environment relationship matrix in addition to the genomic relationship matrix (GRM) comprised of a mixture of two component GRMs (one constructed from all SNP and one constructed from select SNP that well predict the phenotype). This method improves power to detect associations by more accurately modeling the effect of large effect loci while retention of the all SNP GRM reduces false positives due to confounding population structure or cryptic relatedness. Execution was performed with the lrgprApply function from the R-package lrgpr (Hoffman et al., 2014) and the following general statistical model was used:

$$y_{ijk} = \mu + parity_i + SNP_j + u_k + \varepsilon_{ijk}$$

where $\boldsymbol{y_{ijk}}$ is the binary HYK phenotype for a given cow with overall mean $\boldsymbol{\mu}$; $\boldsymbol{parity_j}$ is the fixed effect covariate of parity number; $\boldsymbol{SNP_j}$ is the additive SNP substitution effect; $\boldsymbol{u_k}$ is a random effect having a distribution mean equal to zero and covariance matrix equal to $\boldsymbol{RM_{weighted}\sigma^2_{rm}}$, where **RM** is a relationship matrix consisting of a mixture of three component relationship matrices. Relationship Matrix 1 (RM1) is an environmental relationship matrix with element $RM1_{lm}$ (l, m = 1, 2, ..., n) equal to 1 for individuals who share the same HYS and 0 for individuals from different HYS groups. Relationship Matrix 2 (RM2) is a genomic relationship matrix with element $RM2_{lm}$ (l, m = 1, 2, ..., n) calculated from a subset of select trait associated

genetic markers. Relationship Matrix 3 (RM3) is a genomic relationship matrix with element $RM3_{lm}$ (l, m = 1, 2, ..., n) calculated from all genetic markers. RM2 and RM3 are centered genomic relationship matrices calculated by multiplying the centered genotype matrix by its transpose and dividing by the number of markers. RM1, RM2, and RM3 are weighted by their contributions to the unknown variance ($\boldsymbol{\sigma_{rm}^2}$). The random effect $\mathbf{u}$ is equivalent to the sum of HYS and additive genetic effects. For GWAS purposes, it is unnecessary to explicitly estimate each of these effects. The random residual error is denoted as $\boldsymbol{\varepsilon_{ijk}}$. Variance components were estimated by maximum likelihood. SNP within 1 MB of an individual test SNP were excluded from RM2 to avoid proximal contamination (*i.e.* double counting). Significance of a SNP effect was tested using the Wald statistic. Genomic inflation ($\boldsymbol{\lambda}$) of SNP test statistics for each GWAS was computed using the median method of the estlambda() function within the GenABEL (version 1.8) R-package (Aulchenko et al., 2007). Individual SNP associations were considered statistically significant after false discovery rate correction (p.adjust, R) when $Q \leq 0.05$ and marginally significant when $0.05 < Q \leq 0.10$. Additionally, we report associations with nominal evidence using the minimum threshold suggested by the Wellcome Trust Case Control Consortium ($P \leq 5.0 \times 10^{-5}$; Burton et al., 2007), which has been used as a suggestive threshold in previous bovine GWAS (Sallam et al., 2017; Seabury et al., 2017; Higgins et al., 2018).

Genome-Wide Interaction Study

Interaction testing was performed using the above described FFselect method to test the interaction between additive SNP effects and parity group (primiparous vs. multiparous). To increase power of detection, a two-step GWIS method was implemented as proposed by Kooperberg and LeBlanc (2008). First, SNP were filtered based on disease-genotype associations where SNP with GWAS *P*-values < 0.001 proceeded to the second step. Then, the

SNP passing step 1 had their dependence on parity group evaluated based on the following general statistical model

$$y_{ijkl} = \mu + parity\ group_i + SNP_j + parity\ group \times SNP_{ij} + u_k + \varepsilon_{ijk}$$

where y_{ijk} is the binary HYK phenotype for a given cow with overall mean μ; $parity\ group_i$ is the binary fixed effect of parity group (primiparous vs. multiparous); SNP_j is the additive SNP substitution effect; $parity\ group \times SNP_{ij}$ is the interaction between parity group and SNP effect; u_k denotes the summed random effects of HYS and additive genetic effects; and the random residual error was denoted as ε_{ijk}. Significance of the combined effect of SNP and the parity group by SNP interaction (**P×G**) was tested using the Wald statistic (Kooperberg and Leblanc, 2008) and were considered statistically significant when $Q \leq 0.05$ and marginally significant when $0.05 < Q \leq 0.10$.

Candidate Gene and Pathway Enrichment Analysis

As mentioned previously, the SNP in this experiment were selected for routine use in genetic evaluations of dairy cows. Due to the selection criteria, these SNP have relatively low linkage disequilibrium on a population-wide level (Wiggans et al., 2009, 2010; VanRaden et al., 2011, 2013). Thus, the potential candidate genes for SNP associated to HYK susceptibility were determined based on proximity. All SNP (n = 58,699) were annotated to genes within 500 KB, based on *Bos taurus* annotation release 106 (assembly ARS-UCD 1.2), using BEDTools version 2.27 (Quinlan and Hall, 2010).

Enrichment analysis of metabolic pathways from the Kyoto Encyclopedia of Genes and Genomes (**KEGG**; 29, 30) was performed to give biological context to SNP associated with HYK. For enrichment analysis, every SNP was assigned to the closest gene that was within a 15 KB window. This resulted in a list of 16,499 unique genes that were supplied as a reference (or

background) list to the Database for Annotation, Visualization and Integrated Discovery (**DAVID**) software, which was the software used to perform the KEGG pathway enrichment analysis (27, 47, 48). The test lists (termed gene lists by DAVID) for the enrichment analysis was determined based on the lowest observed GWAS or GWIS *P*-value for SNP within 15 KB of each gene on the reference list. For the purpose of identifying metabolic pathways whose genetic contribution to HYK depends on parity, the previously described GWIS model was used to test the P×G for all SNP regardless of GWAS (first step) *P*-values. Genes annotated to SNP with $P < 0.05$ comprised the enrichment test lists for the GWAS (n = 1,356 genes) and the GWIS (n= 1,265 genes). Fisher exact statistics produced by DAVID were corrected for multiple testing by the false discovery rate method (p.adjust, R), with statistical significance and marginal significance declared at thresholds of $Q \leq 0.05$ and $0.05 < Q \leq 0.10$, respectively.

RESULTS

Incidence of HYK was 33.6% overall and ranged from 15.4 to 59.0% across HYS groups (Table 5.1). The mean parity number was 2.3 ± 1.2 standard deviations overall and ranged from 2.1 to 2.7 across HYS groups. Additionally, the proportion of multiparous cows ranged from 54.7 to 84.9% across HYS groups, with a proportion of 68.9% overall. Primiparous cows had a lower HYK incidence (19.7%; n = 559) than multiparous cows (39.4%; n = 1,213).

Genome-Wide Association Study of Hyperketonemia

A Quantile-Quantile plot of observed versus expected *P*-values demonstrated adequate accounting for population structure by the FFselect GWAS ($\lambda = 1.01$, Figure 1). No SNP associations achieved genome-wide significance ($Q \leq 0.05$). Marginal evidence for an association to HYK susceptibility ($P = 1.5\times10^{-6}$, $Q = 0.09$) was detected for *ARS-BFGL-NGS-91238* (Table 5.2; Figure 5.2). Nominal evidence for an association was found for

BovineHD1600004315 ($P = 2.2\times10^{-5}$, $Q = 0.55$) and *BTB-00318749* ($P = 2.8\times10^{-5}$, $Q = 0.55$). Genes within 500 KB of these SNP are reported in Table 5.3.

The genes proximal to low *P*-value SNP identified during the GWAS were enriched within 11 KEGG pathways (Table 5.4). Focal adhesion (bta04510, $P = 6.5 \times 10^{-4}$, $Q = 0.03$) and axon guidance (bta04360, $P = 1.5 \times 10^{-3}$, $Q = 0.03$) were the only pathways exhibiting significant evidence for enrichment. The remaining 9 pathways had marginal evidence for enrichment ($0.05 < Q \leq 0.09$; Table 5.4). Two marginal pathways are relatively concordant in their gene annotations with focal adhesion: regulation of actin cytoskeleton (bta04540, $Q = 0.06$, $\kappa = 0.54$) and PI3K-Akt signaling pathway (bta04730, $Q = 0.06$, $\kappa = 0.54$). The marginal pathway long-term potentiation (bta04015, $P = 5.9 \times 10^{-3}$, $Q = 0.06$) had some concordance with the following pathways: Rap1 signaling pathway (bta04720), platelet activation (bta04611), long-term depression (bta04151), gap junction (bta04810), and vascular smooth muscle contraction (bta04270).

Genome-Wide Interaction Study of Hyperketonemia for Parity Group

After filtering based on disease-genotype association, 64 SNP were available for evaluation of their P×G interaction. A significant parity P×G interaction was detected for *BovineHD0600024247* ($P = 5.3\times10^{-4}$, $Q = 0.03$; Table 5.2) and marginal evidence for a P×G interaction was detected for *BovineHD1400023753* ($P = 2.7\times10^{-3}$, $Q = 0.09$; Table 5.2). Genes within 500 KB of these SNP are reported in Table 5.3; notably, *BovineHD1400023753* was found within the coding sequence of *Collagen Type XIV Alpha 1 Chain* (***COL14A1***).

Evidence of enrichment for 20 KEGG pathways was detected for genes proximal to PxG GWIS identified SNP, with 14 and 6 demonstrating significant ($Q \leq 0.05$) or marginal ($0.07 \leq Q \leq 0.10$) evidence, respectively (Table 5.5). Interestingly, 16 pathways share gene annotations

with 6 or more other pathways with κ values ranging from 0.30 to 0.69 (Figure 5.3). The metabolic pathways with the most overlap were cAMP signaling pathway (bta04024, $P = 2.2\times10^{-3}$, $Q = 0.02$), insulin secretion (bta04911, $P = 4.1\times10^{-3}$, $Q = 0.02$), and aldosterone synthesis and secretion (bta04925, $P = 7.6\times10^{-3}$, $Q = 0.04$). Protein digestion and absorption (bta04974, $P = 0.01$, $Q = 0.05$) was the only pathway that did not share genes with any other pathway detailed in Table 5.5.

DISCUSSION

In this study, our objective was to discover genomic variants, biological processes, and metabolic pathways associated with HYK susceptibility through GWAS, GWIS, and enrichment analysis. This was conducted using an intensive HYK phenotype determined by repeatedly sampling blood BHB concentrations of cows in the high-risk early lactation period.

Occurrence of HYK cases is difficult to compare across experiments because the proportion of subclinical cases is a function of the frequency of tests and the days postpartum eligibility window for testing (Oetzel, 2004; McArt et al., 2012; Mahrt et al., 2015). The precedent for high-quality assessment of HYK incidence is repeated blood BHB concentration tests, occurring on 2 (or more) days per weeks for the first 2 to 3 weeks postpartum (Oetzel, 2004; McArt et al., 2012, 2015; Mahrt et al., 2015). Experiments with fewer weekly blood BHB measurements, that use HYK diagnostics other than blood BHB concentration, or that rely on voluntary reporting of cases could significantly underreport HYK incidence in comparison (Oetzel, 2004; Mahrt et al., 2015; McArt et al., 2015); thus, we refer to these experiments proportion of HYK cases as prevalence. Prevalence estimates for HYK based on blood BHB range from 10.3 to 21.8% (Suthar et al., 2013; Garro et al., 2014; Chandler et al., 2018). Lower HYK prevalence is reported in experiments using voluntary records provided by dairy owners,

ranging from 0.2% to 10.0% (Kadarmideen et al., 2000; Zwald et al., 2004; Koeck et al., 2012; Klein et al., 2019). McArt et al. (2012) and Mahrt et al. (2015) implemented intensive blood BHB testing protocols and observed greater HYK incidences than the present study, 43.2% and 53.2%, respectively. Their greater HYK incidences could be due to more frequent BHB sampling or differences in environmental conditions, particularly farm management. In addition, Mahrt et al (2015) monitored BHB for a longer period, 3 to 42 days postpartum, and their greater incidence could reflect a longer observation time. However, the blood BHB monitoring procedure used in the present work was expected to diagnose 95% of HYK cases (Oetzel, unpublished data). Therefore, we believe our HYK incidence is representative and has minimal misclassification.

Genome-Wide Association Study of Hyperketonemia

A GWAS performed for HYK using voluntary records from US Jersey dairy cows observed the largest SNP effect sizes on chromosomes 6, 10, 11, 14, and 23 (Parker Gaddis et al., 2018). Significance testing for these SNP associations was not performed. Klein et al. (2019) proposed 5 candidate SNP associations for HYK based on a population of primiparous Holstein cows, contained on chromosomes 5, 8, 9, and 15. In a smaller GWAS (128 cows), SNP associations with a similar HYK phenotype (repetitive BHB sampling) were identified on chromosomes 5, 8, 10, and X (Leal Yepes et al., 2019). None of the SNP in the present study where exact replications of these previously reported candidate SNP associations. Furthermore, we did not replicate any proximal genes identified in previous studies (Parker Gaddis et al., 2018; Klein et al., 2019; Leal Yepes et al., 2019). There are numerous reasons why SNP associations might not be replicated between experiments (Chanock et al., 2007; Kraft et al., 2009); we expect breed differences and the use of a less accurate phenotype where the major

contributors to the lack of SNP replication between studies (Kraft et al., 2009; Sluis et al., 2010; Evangelou et al., 2011).

Genome-Wide Interaction Study of Hyperketonemia for Parity Group

Parity is an established risk factor for HYK, with advanced parity increasing the odds or relative risk for a HYK case (McArt et al., 2013; Garro et al., 2014; Vergara et al., 2014). The presently identified interactions (Table 2) are novel evidence of genetic susceptibility for HYK to be dependent on parity group, at least for some genomic variants. While we acknowledge that the prepartum environment and management of primiparous cows are typically different from multiparous, the biology of postpartum cows is different between parity groups. These biological differences could underly the parity-dependence of SNP effects on HYK susceptibility. This may justify the inclusion of P×G in the routine genetic evaluations of HYK for animal breeding and highlights the impact of parity in more reductionist experiments.

Candidate Genes for HYK Susceptibility

Proximal gene annotations to SNP suggest specific genes that have important roles in HYK etiology. Genomic markers with evidence for HYK associations or parity group dependent associations were annotated to all genes with start or end positions within 500 KB of the SNP location (Table 5.3). Many of the annotated genes have a “LOC” designation with no known gene orthologs and were generally considered pseudogenes. While pseudogenes can be transcriptionally active and may participate in the regulation of the respective gene’s expression (Balakirev and Ayala, 2003), our discussion of candidate genes will focus on those with evidence in other species for biological importance. Bovine HYK and fatty liver, a comorbid disorder (Grummer, 1993; Herdt, 2000), have metabolic features in common with human disorders, such as obesity, Type 2 Diabetes Mellitus (**T2D**), and nonalcoholic fatty liver disease (**NAFLD**).

Among the metabolic features in common are adiposity, hepatic steatosis, and insulin resistance (Grummer, 1993; Bobe et al., 2004; Bernabucci et al., 2005; Sung et al., 2012; Mu et al., 2019); therefore, candidate genes previously associated with these disorders or metabolic features are discussed.

There were several candidate genes generally related to adipogenesis and obesity, including *neuropeptide FF receptor 2* (***NPFFR2***), *Ectonucleotide Pyrophosphatase/Phosphodiesterase 2* (***ENPP2***), *DEP domain-containing mTOR-interacting protein* (***DEPTOR***) and *COL14A1*. The expression of *ENPP2* prohibits adipogenesis in mice with diet-induced obesity (Dusaulcy et al., 2011; Nishimura et al., 2014). Polymorphisms annotated to *NPFFR2* have been associated to body mass index in humans (Hunt et al., 2011). In addition, *NPFFR2* has been implicated as a pharmacological target for managing obesity, particularly by reducing dietary intake (Maletínská et al., 2015; Pražienková et al., 2017). There is some controversy in the role of *DEPTOR* in the regulation of adipogenesis and obesity, where hypothalamic specific and systemic overexpression of *DEPTOR* in mice demonstrated protective against diet induced obesity in transgenic mice (Caron et al., 2016a), but these results were not recapitulated when specifically overexpressed in mouse proopiomelanocortin neurons of the hypothalamus (Caron et al., 2016b). In a doxycycline-inducible *DEPTOR* transgenic mouse model, adiposity was promoted by induced overexpression of *DEPTOR* (Laplante et al., 2012). Furthermore, DEPTOR protein content of white adipose tissue was greater in obese than lean humans (Laplante et al., 2012). Microarray studies have demonstrated upregulated *COL14A1* expression in the liver and adipose of mice with diet induced obesity (Long et al., 2017; Kwon and Choi, 2018; Kwon et al., 2018). In dairy cows, body condition score and extensive body condition loss peripartum are established risk factors for HYK incidence (Bernabucci et al.,

2005; Garro et al., 2014; Rathbun et al., 2017); therefore, these candidate genes suggest genetic predisposition to HYK was mediated in part through cow obesity.

Candidate genes associated with T2D and insulin resistance included *GC Vitamin D Binding Protein* (***GC***), *Tripartite Motif Containing 36* (***TRIM36***), and *ENPP2*. In humans, genomic variants in *GC* have been associated with fasting plasma insulin concentration (Szathmary, 1987; Hirai et al., 2000) and oral glucose tolerance (Baier et al., 1998); in addition, plasma vitamin D binding protein was inversely associated with indices of insulin resistance in adolescent females (Ashraf et al., 2014). Co-expression network analysis of liver microarray data suggested *TRIM36* as a seed gene; however, *TRIM36* mRNA expression was not altered in insulin resistant liver models (Li et al., 2019). Differential methylation of *TRIM36* in adipose tissue has been associated with T2D status as well (Nilsson et al., 2014). Previously discussed for a role in adipogenesis, *ENPP2* mRNA expression was increased in the adipose tissue of individuals with T2D (Boucher et al., 2005) and associated with insulin resistance in mice with diet-induced obesity (Nishimura et al., 2014). Overall, these candidate genes demonstrate the genetic susceptibility for HYK and parity group dependent genetic effects may have mechanistic similarity to T2D in humans, particularly via insulin resistance.

Most SNP with evidence for an association to HYK or a P×G effect had one (or more) candidate genes previously associated to NAFLD or hepatic steatosis. These genes include Mitochondrial Ribosomal Protein L13 (***MRPL13***), Solute Carrier Family 4 Member 4 (***SLC4A4***), *GC*, *DEPTOR* and *COL14A1*. Differential expression of *MRPL13* and *COL14A1* mRNA was observed in the liver tissue of humans with steatosis (Wang et al., 2016), while *SLC4A4* was differentially expressed in rodents with steatosis (Teufel et al., 2016; Li et al., 2019). Genomic variants within *GC* have been associated to NAFLD, as well as lower hepatic

GC mRNA expression and serum vitamin D binding protein concentration for NAFLD patients compared to controls (Adams et al., 2013). Systemic overexpression and proopiomelanocortin neuron specific overexpression of *DEPTOR* in transgenic mouse models was associated with greater hepatic steatosis (Laplante et al., 2012; Caron et al., 2016b). Generally, these gene annotations suggest mechanistic similarity in the progression of NAFLD in humans and the genomic susceptibility for HYK in dairy cows. It is interesting to speculate whether these candidate gene annotations related to NAFLD suggest shared genomic susceptibility between the HYK and fatty liver phenotypes in dairy cows.

Enrichment Analysis of Annotated Polymorphisms

Pathway enrichment analysis explores the polygenic effect of GWAS by assessing the association of curated gene-phenotype observations to a subset of annotated SNP associated with the trait. Thus, we gain functional insight into the numerous small effects that contribute to complex traits, such as HYK susceptibility (Huang et al., 2009; Mooney et al., 2014). Furthermore, assessment of metabolic pathways enriched within the P×G interactions from the GWIS can provide insight into which pathways have differential importance for HYK between parity groups.

Enrichment of the focal adhesion pathway suggests an important role for cell-matrix adhesions in the etiology of HYK across parity groups. There is tremendous diversity in the components of focal adhesions, including scaffolding molecules, GTPases, kinases, phosphatases, lipases, and proteases (Wozniak et al., 2004). Additionally, focal adhesion plays a pivotal role in numerous biological processes, such as the regulation of gene expression, cell differentiation, cell proliferation, cell motility, and cell survival (Wozniak et al., 2004). The ubiquity and diversity of focal adhesions influence across cell types and tissues provides a

challenge to contextualize it within HYK etiology. However, future HYK research may benefit from investigating the role of focal adhesion related genes and pathways.

Axon guidance refers to a crucial stage in the formation of neuronal networks, where the growth cone of a developing neurite receives guidance from chemotropic signals to extend to an appropriate axon target (Dickson, 2002). As with focal adhesion, innervation of tissues is ubiquitous and has not been extensively studied in the context of dairy cow HYK etiology. Several tissues responsible for regulating energy homeostasis have demonstrated responsiveness to neural signals including the liver (Xia et al., 2006; de Lartigue, 2016), adipose (Bowers et al., 2004; Foster and Bartness, 2006; Nguyen et al., 2016), and pancreas (Gilon, 2001; Molina et al., 2014). Therefore, the role of neural development and neural regulation of tissues related to HYK etiology could be a rich area of discovery.

The numerous enriched pathways (Table 5.5) within P×G associations may indicate biological differences in HYK etiology between primi- and multiparous, which is currently unexplored within reductionist research. Many of the enriched pathways with stronger evidence ($Q \leq 0.01$) are related to neurological function and signaling (*i.e.* cholinergic synapse and retrograde endocannabinoid signaling), which we previously discussed as an uninvestigated aspect of HYK etiology. However, the substantial amount of concordance in annotated genes between pathways (Figure 5.3) suggests that a broader aspect of biology may be targeted. This may indicate a genetic basis for cows belonging to different parity groups adapting differently to the early postpartum insulin resistance necessary to support lactation (Bauman and Currie, 1980; De Koster and Opsomer, 2013). Pathways supporting this opinion include insulin secretion, estrogen signaling pathway, and aldosterone synthesis and secretion. Glucose-stimulated insulin secretion is impaired in insulin-resistant humans and mice (Jones et al., 1997; Asghar et al.,

2006); in addition, estrogen and aldosterone have demonstrated capacity to modulate insulin sensitivity (Abate et al., 2002; Luther, 2014). In fact, mice with aldosterone deficiency have increased glucose stimulated insulin secretion (Luther et al., 2011). In terms of HYK etiology, insulin resistance has been suggested as a predisposing factor for HYK because it would promote excessive postpartum adipose TG lipolysis (Grummer, 1993; Holtenius et al., 2003; De Koster and Opsomer, 2013), potentially overwhelming the hepatic oxidative capacity of dairy cows and promoting ketogenesis (White, 2015). In fact, cows with HYK have reduced quantitative insulin sensitivity check index values (Youssef et al., 2017) and reduced glucose stimulated insulin secretion during intravenous glucose tolerance test (Djoković et al., 2017). Together, these results reinforce the importance of insulin resistance in HYK etiology and suggests the relative importance of genetic factors may be parity group dependent.

CONCLUSIONS

In the present work, the genetic architecture of HYK susceptibility in early postpartum Holstein cows was dissected by GWAS, GWIS, and pathway enrichment analysis. These analyses were performed on a HYK phenotype determined by repeated blood BHB concentration measurements, which is essential for accurate HYK assessment. Marginal evidence for an association between marker *ARS-BFGL-NGS-91238* (chromosome 10, base pair 3856662) and HYK susceptibility was observed. Furthermore, novel evidence for parity-dependent SNP associations was discovered with markers *BovineHD0600024247* (chromosome 6, base pair 86882515) and *BovineHD1400023753* (chromosome 14, base pair 81538205) having significant and marginal evidence, respectively. Numerous candidate genes were annotated to the SNP and parity-dependent SNP associations that have been previously associated with human metabolic disorders and pathologies, such as obesity, T2D, insulin resistance, and NAFLD. Enrichment

analysis revealed that focal adhesion related pathways and axon guidance might contribute to HYK etiology. Furthermore, genetic variation in pathways related to insulin secretion and sensitivity may affect HYK susceptibility in a parity dependent matter. In conclusion, the present work proposes several novel SNP associations and metabolic pathways contributing to genetic risk for HYK susceptibility.

ACKNOWLEDGEMENTS

This chapter is a reproduction of a published manuscript (Pralle et al., 2020). The authors recognize and appreciate the support of the owners and herdsman at the privately-owned dairies, as well as the research staff at the University of Wisconsin-Madison Emmons Blaine Dairy Research Center. Furthermore, this work would not have been possible without the assistance of numerous graduate and undergraduate students, especially R. C. Oliveira and F. M. Rathbun. Finally, the authors thank G. R. Wiggans from the Council on Dairy Cattle Breeding for providing the imputed genotypes used in this work. This research was supported by the National Institute of Food and Agriculture (Washington, DC) through the USDA Agriculture and Food Research Initiative Critical Agricultural Research and Extension (CARE; 2015-67028-23572) and USDA Hatch grants (No. WIS01878) from the Wisconsin Agricultural Experiment Station (Madison, WI). Additional funding was provided by the Cooperative Research Program for Agriculture Science and Technology Development (Project No. PJ012078, Rural Development Administration, Republic of Korea).

REFERENCES

Abate, N., S.M. Haffner, A. Garg, R.M. Peshock, and S.M. Grundy. 2002. Sex steroid hormones, upper body obesity, and insulin resistance. J. Clin. Endocrinol. Metab. 87:4522–4527. https://doi.org/10.1210/jc.2002-020567.

Adams, L.A., S.W. White, J.A. Marsh, S.J. Lye, K.L. Connor, R. Maganga, O.T. Ayonrinde, J.K. Olynyk, T.A. Mori, L.J. Beilin, L.J. Palmer, J.M. Hamdorf, and C.E. Pennell. 2013. Association between liver-specific gene polymorphisms and their expression levels with nonalcoholic fatty liver disease. Hepatol. Baltim. Md. 57:590–600. https://doi.org/10.1002/hep.26184.

Asghar, Z., D. Yau, F. Chan, D. LeRoith, C.B. Chan, and M.B. Wheeler. 2006. Insulin resistance causes increased beta-cell mass but defective glucose-stimulated insulin secretion in a murine model of type 2 diabetes. Diabetologia 49:90–99. https://doi.org/10.1007/s00125-005-0045-y.

Ashraf, A.P., C. Huisingh, J.A. Alvarez, X. Wang, and B.A. Gower. 2014. Insulin resistance indices are inversely associated with Vitamin D binding protein concentrations. J. Clin. Endocrinol. Metab. 99:178–183. https://doi.org/10.1210/jc.2013-2452.

Aulchenko, Y.S., S. Ripke, A. Isaacs, and C.M. van Duijn. 2007. GenABEL: An R library for genome-wide association analysis. Bioinforma. Oxf. Engl. 23:1294–1296. https://doi.org/10.1093/bioinformatics/btm108.

Bach, K.D., W. Heuwieser, and J.A.A. McArt. 2016. Technical note: Comparison of 4 electronic handheld meters for diagnosing hyperketonemia in dairy cows. J. Dairy Sci. 99:9136–9142. https://doi.org/10.3168/jds.2016-11077.

Baier, L.J., A.M. Dobberfuhl, R.E. Pratley, R.L. Hanson, and C. Bogardus. 1998. Variations in the vitamin D-binding protein (Gc locus) are associated with oral glucose tolerance in nondiabetic Pima Indians. J. Clin. Endocrinol. Metab. 83:2993–2996. https://doi.org/10.1210/jcem.83.8.5043.

Balakirev, E.S., and F.J. Ayala. 2003. Pseudogenes: Are they “junk” or functional DNA? Annu. Rev. Genet. 37:123–151. https://doi.org/10.1146/annurev.genet.37.040103.103949.

Bauman, D.E., and W. B. Currie. 1980. Partitioning of nutrients during pregnancy and lactation: A review of mechanisms involving homeostasis and homeorhesis. J. Dairy Sci. 63:1514–1529. https://doi.org/10.3168/jds.S0022-0302(80)83111-0.

Benjamini, Y., and Y. Hochberg. 1995. Controlling the false discovery rate: A practical and powerful approach to multiple testing. J. Royal Stat. Soc. Ser. B Methodol. 57:289–300.

Bernabucci, U., B. Ronchi, N. Lacetera, and A. Nardone. 2005. Influence of body condition score on relationships between metabolic status and oxidative stress in periparturient dairy cows. J. Dairy Sci. 88:2017–2026. https://doi.org/10.3168/jds.S0022-0302(05)72878-2.

Bobe, G., J.W. Young, and D.C. Beitz. 2004. Invited review: Pathology, etiology, prevention, and treatment of fatty liver in dairy cows. J. Dairy Sci. 87:3105–3124. https://doi.org/10.3168/jds.S0022-0302(04)73446-3.

Boucher, J., D. Quilliot, J.P. Pradères, M.F. Simon, S. Grès, C. Guigné, D. Prévot, G. Ferry, J.A. Boutin, C. Carpéné, P. Valet, and J.S. Saulnier-Blache. 2005. Potential involvement of adipocyte insulin resistance in obesity-associated up-regulation of adipocyte lysophospholipase D/autotaxin expression. Diabetologia 48:569–577. https://doi.org/10.1007/s00125-004-1660-8.

Bowers, R.R., W.T.L. Festuccia, C.K. Song, H. Shi, R.H. Migliorini, and T.J. Bartness. 2004. Sympathetic innervation of white adipose tissue and its regulation of fat cell number. Am. J. Physiol. Regul. Integr. Comp. Physiol. 286:R1167–R1175. https://doi.org/10.1152/ajpregu.00558.2003.

Burton, P.R., D.G. Clayton, L.R. Cardon, N. Craddock, P. Deloukas, A. Duncanson, D.P. Kwiatkowski, M.I. McCarthy, W.H. Ouwehand, N.J. Samani, J.A. Todd, P. Donnelly, J.C. Barrett, P.R. Burton, D. Davison, P. Donnelly, D. Easton, D. Evans, H.-T. Leung, J.L. Marchini, A.P. Morris, C.C.A. Spencer, M.D. Tobin, L.R. Cardon, D.G. Clayton, A.P. Attwood, J.P. Boorman, B. Cant, U. Everson, J.M. Hussey, J.D. Jolley, A.S. Knight, K. Koch, E. Meech, S. Nutland, C.V. Prowse, H.E. Stevens, N.C. Taylor, G.R. Walters, N.M. Walker, N.A. Watkins, T. Winzer, J.A. Todd, W.H. Ouwehand, R.W. Jones, W.L. McArdle, S.M. Ring, D.P. Strachan, M. Pembrey, G. Breen, D. St Clair, S. Caesar, K. Gordon-Smith, L. Jones, C. Fraser, E.K. Green, D. Grozeva, M.L. Hamshere, P.A. Holmans, I.R. Jones, G. Kirov, V. Moskvina, I. Nikolov, M.C. O'Donovan, M.J. Owen, N. Craddock, D.A. Collier, A. Elkin, A. Farmer, R. Williamson, P. McGuffin, A.H. Young, I.N. Ferrier, S.G. Ball, A.J. Balmforth, J.H. Barrett, D.T. Bishop, M.M. Iles, A. Maqbool, N. Yuldasheva, A.S. Hall, P.S. Braund, P.R. Burton, R.J. Dixon, M. Mangino, S. Stevens, M.D. Tobin, J.R. Thompson, N.J. Samani, F. Bredin, M. Tremelling, M. Parkes, H. Drummond, C.W. Lees, E.R. Nimmo, J. Satsangi, S.A. Fisher, A. Forbes, C.M. Lewis, C.M. Onnie, N.J. Prescott, J. Sanderson, C.G. Mathew, J. Barbour, M.K. Mohiuddin, C.E. Todhunter, J.C. Mansfield, T. Ahmad, F.R. Cummings, D.P. Jewell, J. Webster, M.J. Brown, D.G. Clayton, G.M. Lathrop, J. Connell, A. Dominiczak, N.J. Samani, C.A.B. Marcano, B. Burke, R. Dobson, J. Gungadoo, K.L. Lee, P.B. Munroe, S.J. Newhouse, A. Onipinla, C. Wallace, M. Xue, M. Caulfield, M. Farrall, A. Barton, T.B. in R.G. and Genomics (BRAGGS), I.N. Bruce, H. Donovan, S. Eyre, P.D. Gilbert, S.L. Hider, A.M. Hinks, S.L. John, C. Potter, A.J. Silman, D.P.M. Symmons, W. Thomson, J. Worthington, D.G. Clayton, D.B. Dunger, S. Nutland, H.E. Stevens, N.M. Walker, B. Widmer, J.A. Todd, T.M. Frayling, R.M. Freathy, H. Lango, J.R.B. Perry, B.M. Shields, M.N. Weedon, A.T. Hattersley, G.A. Hitman, M. Walker, K.S. Elliott, C.J. Groves, C.M. Lindgren, N.W. Rayner, N.J. Timpson, E. Zeggini, M.I. McCarthy, M. Newport, G. Sirugo, E. Lyons, F. Vannberg, A.V.S. Hill, L.A. Bradbury, C. Farrar, J.J. Pointon, P. Wordsworth, M.A. Brown, J.A. Franklyn, J.M. Heward, M.J. Simmonds, S.C.L. Gough, S. Seal, B.C. Susceptibility Collaboration (UK), M.R. Stratton, N. Rahman, M. Ban, A. Goris, S.J. Sawcer, A. Compston, D. Conway, M. Jallow, M. Newport, G. Sirugo, K.A. Rockett, D.P. Kwiatkowski, S.J. Bumpstead, A. Chaney, K. Downes, M.J.R. Ghori, R. Gwilliam, S.E. Hunt, M. Inouye, A. Keniry, E. King, R.

McGinnis, S. Potter, R. Ravindrarajah, P. Whittaker, C. Widden, D. Withers, P. Deloukas, H.-T. Leung, S. Nutland, H.E. Stevens, N.M. Walker, J.A. Todd, D. Easton, D.G. Clayton, P.R. Burton, M.D. Tobin, J.C. Barrett, D. Evans, A.P. Morris, L.R. Cardon, N.J. Cardin, D. Davison, T. Ferreira, J. Pereira-Gale, I.B. Hallgrimsdóttir, B.N. Howie, J.L. Marchini, C.C.A. Spencer, Z. Su, Y.Y. Teo, D. Vukcevic, P. Donnelly, D. Bentley, M.A. Brown, L.R. Cardon, M. Caulfield, D.G. Clayton, A. Compston, N. Craddock, P. Deloukas, P. Donnelly, M. Farrall, S.C.L. Gough, A.S. Hall, A.T. Hattersley, A.V.S. Hill, D.P. Kwiatkowski, C.G. Mathew, M.I. McCarthy, W.H. Ouwehand, M. Parkes, M. Pembrey, N. Rahman, N.J. Samani, M.R. Stratton, J.A. Todd, J. Worthington, The Wellcome Trust Case Control Consortium, Management Committee, Data and Analysis Committee, UK Blood Services and University of Cambridge Controls, 1958 Birth Cohort Controls, Bipolar Disorder, Coronary Artery Disease, Crohn's Disease, Hypertension, Rheumatoid Arthritis, Type 1 Diabetes, Type 2 Diabetes, Tuberculosis, Ankylosing Spondylitis, Autoimmune Thyroid Disease, Breast Cancer, Multiple Sclerosis, Gambian Controls, G. DNA Data QC and Informatics, Statistics, and Primary Investigators. 2007. Genome-wide association study of 14,000 cases of seven common diseases and 3,000 shared controls. Nature 447:661–678. https://doi.org/10.1038/nature05911.

Caron, A., S.M. Labbé, D. Lanfray, P.-G. Blanchard, R. Villot, C. Roy, D.M. Sabatini, D. Richard, and M. Laplante. 2016a. Mediobasal hypothalamic overexpression of DEPTOR protects against high-fat diet-induced obesity. Mol. Metab. 5:102–112. https://doi.org/10.1016/j.molmet.2015.11.005.

Caron, A., S.M. Labbé, M. Mouchiroud, R. Huard, D. Lanfray, D. Richard, and M. Laplante. 2016b. DEPTOR in POMC neurons affects liver metabolism but is dispensable for the regulation of energy balance. Am. J. Physiol. Regul. Integr. Comp. Physiol. 310:R1322–R1331. https://doi.org/10.1152/ajpregu.00549.2015.

Chandler, T.L., R.S. Pralle, J.R.R. Dórea, S.E. Poock, G.R. Oetzel, R.H. Fourdraine, and H.M. White. 2018. Predicting hyperketonemia by logistic and linear regression using test-day milk and performance variables in early-lactation Holstein and Jersey cows. J. Dairy Sci. 101:2476–2491. https://doi.org/10.3168/jds.2017-13209.

Chanock, S.J., T. Manolio, M. Boehnke, E. Boerwinkle, D.J. Hunter, G. Thomas, J.N. Hirschhorn, G. Abecasis, D. Altshuler, J.E. Bailey-Wilson, L.D. Brooks, L.R. Cardon, M. Daly, P. Donnelly, J.F. Fraumeni, N.B. Freimer, D.S. Gerhard, C. Gunter, A.E. Guttmacher, M.S. Guyer, E.L. Harris, J. Hoh, R. Hoover, C.A. Kong, K.R. Merikangas, C.C. Morton, L.J. Palmer, E.G. Phimister, J.P. Rice, J. Roberts, C. Rotimi, M.A. Tucker, K.J. Vogan, S. Wacholder, E.M. Wijsman, D.M. Winn, F.S. Collins, and NCI-NHGRI Working Group on Replication in Association Studies. 2007. Replicating genotype–phenotype associations. Nature 447:655–660. https://doi.org/10.1038/447655a.

Chapinal, N., M.E. Carson, S.J. LeBlanc, K.E. Leslie, S. Godden, M. Capel, J.E.P. Santos, M.W. Overton, and T.F. Duffield. 2012. The association of serum metabolites in the transition period with milk production and early-lactation reproductive performance. J. Dairy Sci. 95:1301–1309. https://doi.org/10.3168/jds.2011-4724.

Baird, G.D. 1982. Primary ketosis in the high-producing dairy cow: Clinical and subclinical disorders, treatment, prevention, and outlook. J. Dairy Sci. 65:1–10. https://doi.org/10.3168/jds.S0022-0302(82)82146-2.

De Koster, J.D., and G. Opsomer. 2013. Insulin resistance in dairy cows. Vet. Clin. North Am. Food Anim. Pract. 29:299–322. https://doi.org/10.1016/j.cvfa.2013.04.002.

Dickson, B.J. 2002. Molecular mechanisms of axon guidance. Science 298:1959–1964. https://doi.org/10.1126/science.1072165.

Djoković, R., V. Dosković, M. Cincović, B. Belić, N. Fratrić, B. Jašović, and M. Lalović. 2017. Estimation of insulin resistance in healthy and ketotic cows during an intravenous glucose tolerance test. Pak. Vet. J. 37:387-392.

van der Drift, S.G.A., R. Jorritsma, J.T. Schonewille, H.M. Knijn, and J.A. Stegeman. 2012. Routine detection of hyperketonemia in dairy cows using Fourier transform infrared spectroscopy analysis of β-hydroxybutyrate and acetone in milk in combination with test-day information. J. Dairy Sci. 95:4886–4898. https://doi.org/10.3168/jds.2011-4417.

Duffield, T.F., K.D. Lissemore, B.W. McBride, and K.E. Leslie. 2009. Impact of hyperketonemia in early lactation dairy cows on health and production. J. Dairy Sci. 92:571–580. https://doi.org/10.3168/jds.2008-1507.

Dusaulcy, R., C. Rancoule, S. Grès, E. Wanecq, A. Colom, C. Guigné, L.A. van Meeteren, W.H. Moolenaar, P. Valet, and J.S. Saulnier-Blache. 2011. Adipose-specific disruption of autotaxin enhances nutritional fattening and reduces plasma lysophosphatidic acid. J. Lipid Res. 52:1247–1255. https://doi.org/10.1194/jlr.M014985.

Evangelou, E., J. Fellay, S. Colombo, J. Martinez-Picado, N. Obel, D.B. Goldstein, A. Telenti, and J.P.A. Ioannidis. 2011. Impact of phenotype definition on genome-wide association signals: Empirical evaluation in human immunodeficiency virus type 1 infection. Am. J. Epidemiol. 173:1336–1342. https://doi.org/10.1093/aje/kwr024.

Foster, M.T., and T.J. Bartness. 2006. Sympathetic but not sensory denervation stimulates white adipocyte proliferation. Am. J. Physiol. Regul. Integr. Comp. Physiol. 291:R1630–R1637. https://doi.org/10.1152/ajpregu.00197.2006.

Garro, C.J., L. Mian, and M. Cobos Roldán. 2014. Subclinical ketosis in dairy cows: Prevalence and risk factors in grazing production system. J. Anim. Physiol. Anim. Nutr. 98:838–844. https://doi.org/10.1111/jpn.12141.

Gilon, P. 2001. Mechanisms and physiological significance of the cholinergic control of pancreatic cell function. Endocr. Rev. 22:565–604. https://doi.org/10.1210/er.22.5.0440.

Grummer, R.R. 1993. Etiology of lipid-related metabolic disorders in periparturient dairy cows. J. Dairy Sci. 76:3882–3896. https://doi.org/10.3168/jds.S0022-0302(93)77729-2.

Herdt, T.H. 2000. Ruminant adaptation to negative energy balance. Influences on the etiology of ketosis and fatty liver. Vet. Clin. North Am. Food Anim. Pract. 16:215–230, https://doi.org/10.1016/s0749-0720(15)30102-x.

Higgins, M.G., C. Fitzsimons, M.C. McClure, C. McKenna, S. Conroy, D.A. Kenny, M. McGee, S.M. Waters, and D.W. Morris. 2018. GWAS and eQTL analysis identifies a SNP associated with both residual feed intake and GFRA2 expression in beef cattle. Sci. Rep. 8:14301-14312. https://doi.org/10.1038/s41598-018-32374-6.

Hirai, M., S. Suzuki, Y. Hinokio, A. Hirai, M. Chiba, H. Akai, C. Suzuki, and T. Toyota. 2000. Variations in vitamin D-binding protein (group-specific component protein) are associated with fasting plasma insulin levels in Japanese with normal glucose tolerance. J. Clin. Endocrinol. Metab. 85:1951–1953. https://doi.org/10.1210/jcem.85.5.6569.

Hoffman, G.E., J.G. Mezey, and E.E. Schadt. 2014. lrgpr: interactive linear mixed model analysis of genome-wide association studies with composite hypothesis testing and regression diagnostics in R. Bioinforma. Oxf. Engl. 30:3134–3135. https://doi.org/10.1093/bioinformatics/btu435.

Holtenius, K., S. Agenäs, C. Delavaud, and Y. Chilliard. 2003. Effects of feeding intensity during the dry period. 2. Metabolic and hormonal responses. J. Dairy Sci. 86:883–891. https://doi.org/10.3168/jds.S0022-0302(03)73671-6.

Huang, D.W., B.T. Sherman, and R.A. Lempicki. 2009. Bioinformatics enrichment tools: Paths toward the comprehensive functional analysis of large gene lists. Nucleic Acids Res. 37:1–13. https://doi.org/10.1093/nar/gkn923.

Hunt, S.C., S.J. Hasstedt, Y. Xin, B.K. Dalley, B.A. Milash, E. Yakobson, R.E. Gress, L.E. Davidson, and T.D. Adams. 2011. Polymorphisms in the NPY2R gene show significant associations with BMI that are additive to FTO, MC4R, and NPFFR2 gene effects. Obesity 19:2241–2247. https://doi.org/10.1038/oby.2011.239.

Iwersen, M., U. Falkenberg, R. Voigtsberger, D. Forderung, and W. Heuwieser. 2009. Evaluation of an electronic cowside test to detect subclinical ketosis in dairy cows. J. Dairy Sci. 92:2618–2624. https://doi.org/10.3168/jds.2008-1795.

Jones, C.N.O., D. Pei, P. Staris, K.S. Polonsky, Y.D.-I. Chen, and G.M. Reaven. 1997. Alterations in the glucose-stimulated insulin secretory dose-response curve and in insulin clearance in nondiabetic insulin-resistant individuals. J. Clin. Endocrinol. Metab. 82:1834–1838. https://doi.org/10.1210/jcem.82.6.3979.

Kadarmideen, H.N., R. Thompson, and G. Simm. 2000. Linear and threshold model genetic parameters for disease, fertility and milk production in dairy cattle. Anim. Sci. 71:411–419. https://doi.org/10.1017/S1357729800055338.

Klein, S.-L., C. Scheper, K. Brügemann, H.H. Swalve, and S. König. 2019. Phenotypic relationships, genetic parameters, genome-wide associations, and identification of

potential candidate genes for ketosis and fat-to-protein ratio in German Holstein cows. J. Dairy Sci. 102:6276–6287. https://doi.org/10.3168/jds.2019-16237.

Koeck, A., F. Miglior, D.F. Kelton, and F.S. Schenkel. 2012. Health recording in Canadian Holsteins: Data and genetic parameters. J. Dairy Sci. 95:4099–4108. https://doi.org/10.3168/jds.2011-5127.

Koltes, D.A., and D.M. Spurlock. 2011. Coordination of lipid droplet-associated proteins during the transition period of Holstein dairy cows. J. Dairy Sci. 94:1839–1848. https://doi.org/10.3168/jds.2010-3769.

Kooperberg, C., and M. Leblanc. 2008. Increasing the power of identifying gene x gene interactions in genome-wide association studies. Genet. Epidemiol. 32:255–263. https://doi.org/10.1002/gepi.20300.

Kraft, P., E. Zeggini, and J.P.A. Ioannidis. 2009. Replication in genome-wide association studies. Stat. Sci. Rev. J. Inst. Math. Stat. 24:561–573. https://doi.org/10.1214/09-STS290.

Kwon, E.Y., and M.S. Choi. 2018. Luteolin targets the toll-like receptor signaling pathway in prevention of hepatic and adipocyte fibrosis and insulin resistance in diet-induced obese mice. Nutrients. 10:1450-1416. https://doi.org/10.3390/nu10101415.

Kwon, E.Y., S.K. Shin, and M.-S. Choi. 2018. Ursolic acid attenuates hepatic steatosis, fibrosis, and insulin resistance by modulating the circadian rhythm pathway in diet-induced obese mice. Nutrients. 1719-1733. https://doi.org/10.3390/nu10111719.

Laplante, M., S. Horvat, W.T. Festuccia, K. Birsoy, Z. Prevorsek, A. Efeyan, and D.M. Sabatini. 2012. DEPTOR cell-autonomously promotes adipogenesis, and its expression is associated with obesity. Cell Metab. 16:202–212. https://doi.org/10.1016/j.cmet.2012.07.008.

de Lartigue, G. 2016. Role of the vagus nerve in the development and treatment of diet-induced obesity. J. Physiol. 594:5791–5815. https://doi.org/10.1113/JP271538.

Leal Yepes, F.A., D.V. Nydam, S. Mann, L. Caixeta, J.A.A. McArt, T.R. Overton, J.J. Wakshlag, and H.J. Huson. 2019. Longitudinal phenotypes improve genotype association for hyperketonemia in dairy cattle. Anim. Open Access J. MDPI 9. https://doi.org/10.3390/ani9121059.

Li, L., Z. Pan, and X. Yang. 2019. Key genes and co-expression network analysis in the livers of type 2 diabetes patients. J. Diabetes Investig. 10:951–962. https://doi.org/10.1111/jdi.12998.

Long, Z., M. Cao, S. Su, G. Wu, F. Meng, H. Wu, J. Liu, W. Yu, K. Atabai, and X. Wang. 2017. Inhibition of hepatocyte nuclear factor 1b induces hepatic steatosis through DPP4/NOX1-mediated regulation of superoxide. Free Radic. Biol. Med. 113:71–83. https://doi.org/10.1016/j.freeradbiomed.2017.09.016.

Luther, J.M. 2014. Effects of aldosterone on insulin sensitivity and secretion. Steroids 91:54–60. https://doi.org/10.1016/j.steroids.2014.08.016.

Luther, J.M., P. Luo, M.T. Kreger, M. Brissova, C. Dai, T.T. Whitfield, H.S. Kim, D.H. Wasserman, A.C. Powers, and N.J. Brown. 2011. Aldosterone decreases glucose-stimulated insulin secretion in vivo in mice and in murine islets. Diabetologia 54:2152–2163. https://doi.org/10.1007/s00125-011-2158-9.

Mahrt, A., O. Burfeind, and W. Heuwieser. 2015. Evaluation of hyperketonemia risk period and screening protocols for early-lactation dairy cows. J. Dairy Sci. 98:3110–3119. https://doi.org/10.3168/jds.2014-8910.

Maletínská, L., V. Nagelová, A. Tichá, J. Zemenová, Z. Pirník, M. Holubová, A. Špolcová, B. Mikulášková, M. Blechová, D. Sýkora, Z. Lacinová, M. Haluzík, B. Železná, and J. Kuneš. 2015. Novel lipidized analogs of prolactin-releasing peptide have prolonged half-lives and exert anti-obesity effects after peripheral administration. Int. J. Obes. 39:986–993. https://doi.org/10.1038/ijo.2015.28.

McArt, J.A.A., D.V. Nydam, and G.R. Oetzel. 2013. Dry period and parturient predictors of early lactation hyperketonemia in dairy cattle. J. Dairy Sci. 96:198–209. https://doi.org/10.3168/jds.2012-5681.

McArt, J.A.A., D.V. Nydam, and G.R. Oetzel. 2012. Epidemiology of subclinical ketosis in early lactation dairy cattle. J. Dairy Sci. 95:5056–5066. https://doi.org/10.3168/jds.2012-5443.

McArt, J.A.A., D.V. Nydam, and M.W. Overton. 2015. Hyperketonemia in early lactation dairy cattle: A deterministic estimate of component and total cost per case. J. Dairy Sci. 98:2043–2054. https://doi.org/10.3168/jds.2014-8740.

Molina, J., R. Rodriguez-Diaz, A. Fachado, M.C. Jacques-Silva, P.-O. Berggren, and A. Caicedo. 2014. Control of insulin secretion by cholinergic signaling in the human pancreatic islet. Diabetes 63:2714–2726. https://doi.org/10.2337/db13-1371.

Mooney, M.A., J.T. Nigg, S.K. McWeeney, and B. Wilmot. 2014. Functional and genomic context in pathway analysis of GWAS data. Trends Genet. 30:390–400. https://doi.org/10.1016/j.tig.2014.07.004.

Mu, W., X. Cheng, Y. Liu, Q. Lv, G. Liu, J. Zhang, and X. Li. 2019. Potential nexus of non-alcoholic fatty liver disease and Type 2 diabetes mellitus: Insulin resistance between hepatic and peripheral tissues. Front. Pharmacol. 9:1566-1575. https://doi.org/10.3389/fphar.2018.01566.

Nguyen, N.L.T., C.L. Barr, V. Ryu, Q. Cao, B. Xue, and T.J. Bartness. 2016. Separate and shared sympathetic outflow to white and brown fat coordinately regulates thermoregulation and beige adipocyte recruitment. Am. J. Physiol.-Regul. Integr. Comp. Physiol. 312:R132–R145. https://doi.org/10.1152/ajpregu.00344.2016.

Nilsson, E., P.A. Jansson, A. Perfilyev, P. Volkov, M. Pedersen, M.K. Svensson, P. Poulsen, R. Ribel-Madsen, N.L. Pedersen, P. Almgren, J. Fadista, T. Rönn, B. Klarlund Pedersen, C. Scheele, A. Vaag, and C. Ling. 2014. Altered DNA methylation and differential expression of genes influencing metabolism and inflammation in adipose tissue from subjects with type 2 diabetes. Diabetes 63:2962–2976. https://doi.org/10.2337/db13-1459.

Nishimura, S., M. Nagasaki, S. Okudaira, J. Aoki, T. Ohmori, R. Ohkawa, K. Nakamura, K. Igarashi, H. Yamashita, K. Eto, K. Uno, N. Hayashi, T. Kadowaki, I. Komuro, Y. Yatomi, and R. Nagai. 2014. ENPP2 contributes to adipose tissue expansion and insulin resistance in diet-induced obesity. Diabetes 63:4154–4164. https://doi.org/10.2337/db13-1694.

Oetzel, G.R. 2004. Monitoring and testing dairy herds for metabolic disease. Vet. Clin. North Am. Food Anim. Pract. 20:651–674. https://doi.org/10.1016/j.cvfa.2004.06.006.

Parker Gaddis, K.L., J.B. Cole, J.S. Clay, and C. Maltecca. 2014. Genomic selection for producer-recorded health event data in US dairy cattle. J. Dairy Sci. 97:3190–3199. https://doi.org/10.3168/jds.2013-7543.

Parker Gaddis, K.L., J.H. Megonigal, J.S. Clay, and C.W. Wolfe. 2018. Genome-wide association study for ketosis in US Jerseys using producer-recorded data. J. Dairy Sci. 101:413–424. https://doi.org/10.3168/jds.2017-13383.

Pralle, R.S., N.E. Schultz, H.M. White, and K.A. Weigel. 2020. Hyperketonemia GWAS and parity dependent SNP associations in Holstein dairy cows intensively sampled for blood β-hydroxybutyrate concentration. Physiol. Genomics. In Press. https://doi.org/10.1152/physiolgenomics.00016.2020.

Pražienková, V., M. Holubová, H. Pelantová, M. Bugáňová, Z. Pirník, B. Mikulášková, A. Popelová, M. Blechová, M. Haluzík, B. Železná, M. Kuzma, J. Kuneš, and L. Maletínská. 2017. Impact of novel palmitoylated prolactin-releasing peptide analogs on metabolic changes in mice with diet-induced obesity. PLoS ONE 12. https://doi.org/10.1371/journal.pone.0183449.

Quinlan, A.R., and I.M. Hall. 2010. BEDTools: A flexible suite of utilities for comparing genomic features. Bioinforma. Oxf. Engl. 26:841–842. https://doi.org/10.1093/bioinformatics/btq033.

Rathbun, F.M., R.S. Pralle, S.J. Bertics, L.E. Armentano, K. Cho, C. Do, K.A. Weigel, and H.M. White. 2017. Relationships between body condition score change, prior mid-lactation phenotypic residual feed intake, and hyperketonemia onset in transition dairy cows. J. Dairy Sci. 100:3685–3696. https://doi.org/10.3168/jds.2016-12085.

Rutherford, A.J., G. Oikonomou, and R.F. Smith. 2016. The effect of subclinical ketosis on activity at estrus and reproductive performance in dairy cattle. J. Dairy Sci. 99:4808–4815. https://doi.org/10.3168/jds.2015-10154.

Sailer, K.J., R.S. Pralle, R.C. Oliveira, S.J. Erb, G.R. Oetzel, and H.M. White. 2018. Technical note: Validation of the BHBCheck blood β-hydroxybutyrate meter as a diagnostic tool for hyperketonemia in dairy cows. J. Dairy Sci. 101:1524–1529. https://doi.org/10.3168/jds.2017-13583.

Sallam, A.M., Y. Zare, F. Alpay, G.E. Shook, M.T. Collins, S. Alsheikh, M. Sharaby, and B.W. Kirkpatrick. 2017. An across-breed genome wide association analysis of susceptibility to paratuberculosis in dairy cattle. J. Dairy Res. 84:61–67. https://doi.org/10.1017/S0022029916000807.

Schultz, N., and K. Weigel. 2020. FFselect: An improved linear mixed model for genome-wide association study in populations featuring shared environments confounded by relatedness. bioRxiv. https://doi.org/ 10.1101/2020.01.01.892455.

Seabury, C.M., D.L. Oldeschulte, M. Saatchi, J.E. Beever, J.E. Decker, Y.A. Halley, E.K. Bhattarai, M. Molaei, H.C. Freetly, S.L. Hansen, H. Yampara-Iquise, K.A. Johnson, M.S. Kerley, J. Kim, D.D. Loy, E. Marques, H.L. Neibergs, R.D. Schnabel, D.W. Shike, M.L. Spangler, R.L. Weaber, D.J. Garrick, and J.F. Taylor. 2017. Genome-wide association study for feed efficiency and growth traits in U.S. beef cattle. BMC Genomics 18:386-410. https://doi.org/10.1186/s12864-017-3754-y.

Sluis, S. van der, M. Verhage, D. Posthuma, and C.V. Dolan. 2010. Phenotypic complexity, measurement bias, and poor phenotypic resolution contribute to the missing heritability problem in genetic association studies. PLOS ONE 5:e13929. https://doi.org/10.1371/journal.pone.0013929.

Sung, K.-C., W.-S. Jeong, S.H. Wild, and C.D. Byrne. 2012. Combined influence of insulin resistance, overweight/obesity, and fatty liver as risk factors for Type 2 diabetes. Diabetes Care 35:717–722. https://doi.org/10.2337/dc11-1853.

Suthar, V.S., J. Canelas-Raposo, A. Deniz, and W. Heuwieser. 2013. Prevalence of subclinical ketosis and relationships with postpartum diseases in European dairy cows. J. Dairy Sci. 96:2925–2938. https://doi.org/10.3168/jds.2012-6035.

Szathmary, E.J. 1987. The effect of Gc genotype on fasting insulin level in Dogrib Indians. Hum. Genet. 75:368–372. https://doi.org/10.1007/bf00284110.

Teufel, A., T. Itzel, W. Erhart, M. Brosch, X.Y. Wang, Y.O. Kim, W. von Schönfels, A. Herrmann, S. Brückner, F. Stickel, J.-F. Dufour, T. Chavakis, C. Hellerbrand, R. Spang, T. Maass, T. Becker, S. Schreiber, C. Schafmayer, D. Schuppan, and J. Hampe. 2016. Comparison of gene expression patterns between mouse models of nonalcoholic fatty liver disease and liver tissues from patients. Gastroenterology 151:513-525. https://doi.org/10.1053/j.gastro.2016.05.051.

VanRaden, Paul M., O'Connell Jeffrey R., G.R. Wiggans, and K.A. Weigel. 2011. Genomic evaluations with many more genotypes. Genet. Sel. Evol. 43:10-20. https://doi.org/10.1186/1297-9686-43-10.

VanRaden, P.M., D.J. Null, M. Sargolzaei, G.R. Wiggans, M.E. Tooker, J.B. Cole, T.S. Sonstegard, E.E. Connor, M. Winters, J.B.C.H.M. van Kaam, A. Valentini, B.J. Van Doormaal, M.A. Faust, and G.A. Doak. 2013. Genomic imputation and evaluation using high-density Holstein genotypes. J. Dairy Sci. 96:668–678. https://doi.org/10.3168/jds.2012-5702.

Vergara, C.F., D. Döpfer, N.B. Cook, K.V. Nordlund, J.A.A. McArt, D.V. Nydam, and G.R. Oetzel. 2014. Risk factors for postpartum problems in dairy cows: Explanatory and predictive modeling. J. Dairy Sci. 97:4127–4140. https://doi.org/10.3168/jds.2012-6440.

Visscher, P.M., N.R. Wray, Q. Zhang, P. Sklar, M.I. McCarthy, M.A. Brown, and J. Yang. 2017. 10 years of GWAS discovery: Biology, function, and translation. Am. J. Hum. Genet. 101:5–22. https://doi.org/10.1016/j.ajhg.2017.06.005.

Walsh, R.B., J.S. Walton, D.F. Kelton, S.J. LeBlanc, K.E. Leslie, and T.F. Duffield. 2007. The effect of subclinical ketosis in early lactation on reproductive performance of postpartum dairy cows. J. Dairy Sci. 90:2788–2796. https://doi.org/10.3168/jds.2006-560.

Wang, R., X. Wang, and L. Zhuang. 2016. Gene expression profiling reveals key genes and pathways related to the development of non-alcoholic fatty liver disease. Ann. Hepatol. 15:190–199. https://doi.org/10.5604/16652681.1193709.

Weigel, K.A., R.S. Pralle, H. Adams, K. Cho, C. Do, and H.M. White. 2017. Prediction of whole-genome risk for selection and management of hyperketonemia in Holstein dairy cattle. J. Anim. Breed. Genet. Z. Tierzuchtung Zuchtungsbiologie 134:275–285. https://doi.org/10.1111/jbg.12259.

White, H.M. 2015. The role of TCA cycle anaplerosis in ketosis and fatty liver in periparturient dairy cows. Anim. Open Access J. MDPI 5:793–802. https://doi.org/10.3390/ani5030384.

Wiggans, G.R., T.S. Sonstegard, P.M. VanRaden, L.K. Matukumalli, R.D. Schnabel, J.F. Taylor, F.S. Schenkel, and C.P. Van Tassell. 2009. Selection of single-nucleotide polymorphisms and quality of genotypes used in genomic evaluation of dairy cattle in the United States and Canada. J. Dairy Sci. 92:3431–3436. https://doi.org/10.3168/jds.2008-1758.

Wiggans, G.R., P.M. VanRaden, L.R. Bacheller, M.E. Tooker, J.L. Hutchison, T.A. Cooper, and T.S. Sonstegard. 2010. Selection and management of DNA markers for use in genomic evaluation. J. Dairy Sci. 93:2287–2292. https://doi.org/10.3168/jds.2009-2773.

Wozniak, M.A., K. Modzelewska, L. Kwong, and P.J. Keely. 2004. Focal adhesion regulation of cell behavior. Biochim. Biophys. Acta 1692:103–119. https://doi.org/10.1016/j.bbamcr.2004.04.007.

Xia, F., Z. He, K. Li, X. Wang, and J. Dong. 2006. Evaluation of the role of sympathetic denervation on hepatic function. Hepatol. Res. 36:259–264. https://doi.org/10.1016/j.hepres.2006.08.009.

Youssef, M.A., M.R. El-Ashker, and M.S. Younis. 2017. The effect of subclinical ketosis on indices of insulin sensitivity and selected metabolic variables in transition dairy cattle. Comp. Clin. Pathol. 26:329–334. https://doi.org/10.1007/s00580-016-2377-z.

Zhang, Z., U. Ober, M. Erbe, H. Zhang, N. Gao, J. He, J. Li, and H. Simianer. 2014. Improving the accuracy of whole genome prediction for complex traits using the results of genome wide association studies. PLOS ONE 9:e93017. https://doi.org/10.1371/journal.pone.0093017.

Zwald, N.R., K.A. Weigel, Y.M. Chang, R.D. Welper, and J.S. Clay. 2004. Genetic selection for health traits using producer-recorded data. I. Incidence rates, heritability estimates, and sire breeding values. J. Dairy Sci. 87:4287–4294. https://doi.org/10.3168/jds.S0022-0302(04)73573-0.

TABLES AND FIGURES

Table 5.1. Descriptive statistics of hyperketonemia (HYK) observations stratified by herd and herd-year-season groups[1].

Herd	Year-Season	Sample Size	Parity[2]	Multiparous[3], %	HYK[4], %
A		559	2.6 ± 1.2	81.4	22.2
	A1	102	2.6 ± 1.3	76.5	18.6
	A2	155	2.6 ± 1.2	80.6	20.0
	A3	130	2.5 ± 1.1	80.8	26.9
	A4	146	2.7 ± 1.2	84.9	24.0
	A5	26	2.4 ± 0.9	88.5	15.4
B		1185	2.2 ± 1.2	63.5	40.0
	B1	522	2.1 ± 1.1	61.9	33.9
	B2	256	2.1 ± 1.2	59.4	22.3
	B3	407	2.3 ± 1.2	68.3	59.0
C		53	2.1 ± 1.2	54.7	37.7
D		106	2.3 ± 1.2	70.8	20.8
	Overall	1903	2.3 ± 1.2	68.9	33.6

[1]Herds are anonymized to A, B, C, and D. A single year-season was observed for herds C and D. Seasons were defined as a parturition date within the range of January to March, April to June, July to September, or October to December.

[2]Average parity number ± standard deviation

[3]Cows with parity number ≥ 2

[4]HYK incidence based on four, spaced blood β-hydroxybutyrate concentration tests between 5 to 18 days postpartum, where a cow with a test β-hydroxybutyrate concentration ≥ 1.2 mmol/L is considered a HYK case

Table 5.2. Association statistics for the hyperketonemia genome-wide association study (GWAS) and genome-wide parity group by genotype interaction study (GWIS)[1].

Model Covariate[3]	Single Nucleotide Polymorphism			*P*-value		*Q*-value[2]	
	Name	Chr[4]	Position	GWAS	GWIS	GWAS	GWIS
Parity							
	ARS-BFGL-NGS-91238	10	3856662	1.54×10^{-6}		0.09	
	BovineHD1600004315	16	15375298	2.25×10^{-5}		0.55	
	BTB-00318749	7	70336255	2.82×10^{-5}		0.55	
Parity Group							
	BovineHD0600024247	6	86882515	5.29×10^{-4}	5.33×10^{-4}		0.03
	BovineHD1400023753	14	81538205	2.02×10^{-4}	2.73×10^{-3}		0.09

[1]GWAS and GWIS were executed using the feature forward select method. Statistics for GWAS represent the association of the additive genotype effect on hyperketonemia, while GWIS statistics represent the interaction of parity group and genotype on hyperketonemia.
[2]False discovery rate corrected *P*-value (p.adjust function, R version 3.4.5)
[3]Designation of how the covariate fixed effect was coded where parity is continuous and parity group is binary (primiparous vs. multiparous)
[4]*Bos taurus* chromosome

Table 5.3. Candidate genes based on proximity to genomic markers with evidence for genome-wide associations (GWAS) or parity group dependent associations (GWIS) for hyperketonemia susceptibility[1].

Single Nucleotide Polymorphism				Gene[2]			
Name	Chr[3]	Position	Significance[4]	Symbol	Start Position	End Position	Distance
BovineHD0600024247	6	86882515	GWIS	*LOC782958*	86910219	86912212	27704
				SLC4A4	86449494	86813499	69016
				GC	86955729	87007189	73214
				NPFFR2	87248988	87326152	366473
				LOC112447099	86362772	86420117	462398
ARS-BFGL-NGS-91238	10	3856662	GWAS	*LOC787395*	3911953	3912623	55291
				TRIM36	3972432	4015587	115770
				PGGT1B	4050987	4104900	194325
				LOC781719	3638172	3638722	217940
				CCDC112	4107467	4317609	250805
				LOC112448357	4124240	4125580	267578
				LOC787551	4244056	4244754	387394
				KCNN2	2932155	3428630	428032
BovineHD1400023753	14	81538205	GWIS	*COL14A1*	81469694	81730369	0
				LOC112449642	81527029	81527135	11070
				DEPTOR	81286798	81449393	88812
				MRPL13	81745768	81786691	207563
				MTBP	81786823	81864708	248618
				DSCC1	81263986	81276602	261603
				TAF2	81173269	81261603	276602
				SNTB1	81870562	82009881	332357
				LOC104974144	81115751	81120903	417302
				ENPP2	80982686	81118688	419517

[1]GWAS and GWIS were executed using the feature forward select method. Statistics for GWAS represent the association of the additive genotype effect on hyperketonemia, while GWIS statistics represent the interaction of parity group and genotype on hyperketonemia.

[2]Gene symbol and genomic coordinates (in base pairs) are based on release 106 of the *Bos taurus* genome assembly. All reported genes have a start or end position within 500 KB of the respective single nucleotide polymorphism. Distance refers to the number of base pairs between the polymorphism and the nearest gene coordinate, start or end position. A distance of 0 base pairs indicates the SNP resides within the respective gene.

[3]*Bos taurus* chromosome

[4]Identifies the genomic survey the single nucleotide polymorphism had evidence for association with hyperketonemia susceptibility. Association statistics are reported in Table 2 and in text.

Table 5.4. Kyoto encyclopedia of genes and genomes (KEGG) metabolic pathways enriched for hyperketonemia based on genes proximal to associated single nucleotide polymorphisms.[1]

Term	KEGG	FE[2]	*P*-value	*Q*-value[3]
Focal adhesion	bta04510	1.9	6.5×10-4	0.03
Axon guidance	bta04360	2.1	1.5×10-3	0.03
Long-term potentiation	bta04015	2.3	5.9×10-3	0.06
Rap1 signaling pathway	bta04720	1.7	7.5×10-3	0.06
Platelet activation	bta04611	1.9	7.8×10-3	0.06
Long-term depression	bta04151	2.3	8.3×10-3	0.06
Gap junction	bta04810	2.1	8.4×10-3	0.06
Regulation of actin cytoskeleton	bta04540	1.7	0.01	0.06
PI3K-Akt signaling pathway	bta04730	1.5	0.01	0.06
Vascular smooth muscle contraction	bta04270	1.8	0.02	0.07
Ubiquitin mediated proteolysis	bta04120	1.8	0.02	0.09

[1]Polymorphisms associated with hyperketonemia where determined by genome-wide association ($P < 0.05$). Gene annotation to polymorphisms was performed using BEDTools (v. 2.27) and release 106 of the *Bos taurus* genome assembly. Enrichment analysis was conducted using the Database for Annotation, Visualization and Integrated Discovery.

[2]Fold enrichment

[3]False discovery rate corrected *P*-value (p.adjust function, R version 3.4.5)

Table 5.5. Kyoto encyclopedia of genes and genomes (KEGG) metabolic pathways enriched within parity group dependent genotype associations for hyperketonemia.[1]

Term	KEGG[2]	FE[3]	*P*-value	*Q*-value[4]
Cholinergic synapse	bta04725	2.6	9.4×10^{-5}	3.0×10^{-3}
Glutamatergic synapse	bta04724	2.3	4.6×10^{-4}	9.0×10^{-3}
Retrograde endocannabinoid signaling	bta04723	2.4	6.0×10^{-4}	9.0×10^{-3}
Dopaminergic synapse	bta04728	2.1	1.3×10^{-3}	0.01
Circadian entrainment	bta04713	2.3	1.3×10^{-3}	0.01
cAMP signaling pathway	bta04024	1.8	2.2×10^{-3}	0.02
Estrogen signaling pathway	bta04915	2.3	2.2×10^{-3}	0.02
Adrenergic signaling in cardiomyocytes	bta04261	2.0	3.0×10^{-3}	0.02
Amphetamine addiction	bta05031	2.5	3.5×10^{-3}	0.02
Insulin secretion	bta04911	2.2	4.1×10^{-3}	0.02
Aldosterone synthesis and secretion	bta04925	2.2	7.6×10^{-3}	0.04
cGMP-PKG signaling pathway	bta04022	1.8	0.01	0.05
Protein digestion and absorption	bta04974	2.1	0.01	0.05
Glioma	bta05214	2.2	0.01	0.05
GABAergic synapse	bta04727	2.0	0.02	0.07
Glucagon signaling pathway	bta04922	2.0	0.02	0.07
Dilated cardiomyopathy	bta05414	2.0	0.02	0.07
Progesterone-mediated oocyte maturation	bta04914	2.0	0.03	0.08
Neuroactive ligand-receptor interaction	bta04080	1.5	0.03	0.09
Rap1 signaling pathway	bta04015	1.5	0.04	0.10

[1]Interactions between parity status (primiparous vs. multiparous) and genotypes for hyperketonemia where determined by a genome-wide interaction study ($P < 0.05$). Gene annotation to single nucleotide polymorphisms was performed using BEDTools (v. 2.27) and release 106 of the *Bos taurus* genome assembly. Enrichment analysis was conducted using the Database for Annotation, Visualization and Integrated Discovery.

[2]Fold enrichment

[3]False discovery rate corrected *P*-value (p.adjust function, R version 3.4.5)

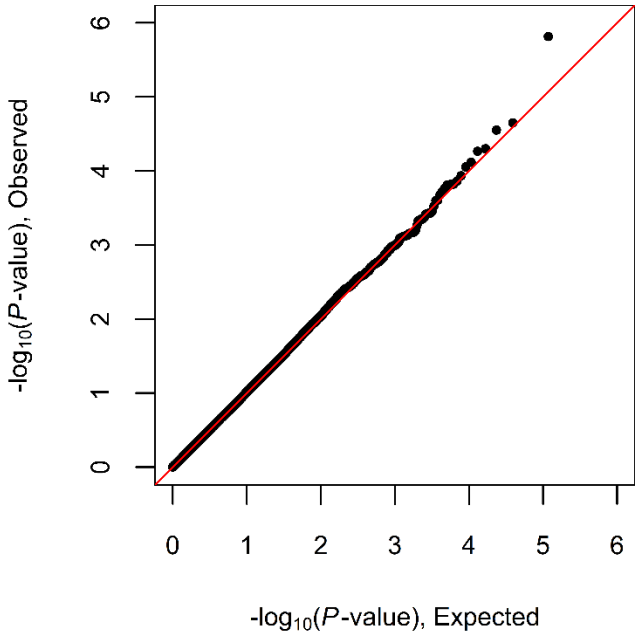

Figure 5.1. Quantile-quantile plot comparing the observed and expected *P*-value distributions to theoretically assess the correction for population structure in a genome-wide association study (GWAS) for hyperketonemia in early lactation Holstein cows (n = 1,710) using the feature forward select linear mixed model methodology.

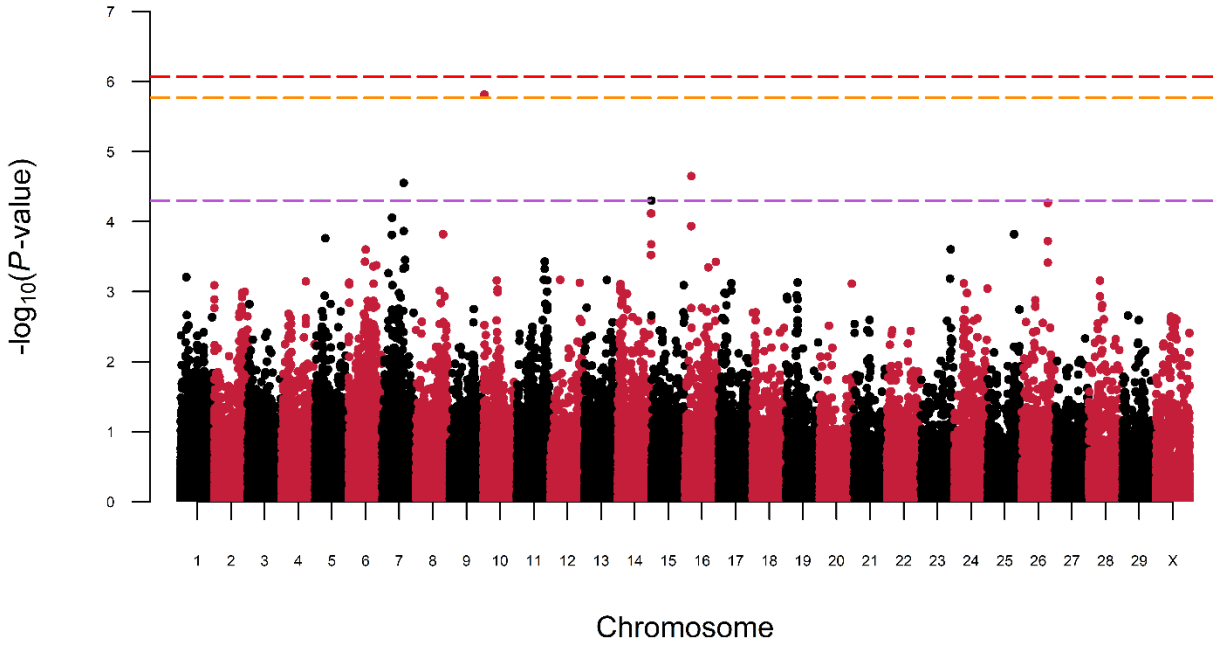

Figure 5.2. Manhattan plot depicting the negative decadic logarithm of single nucleotide polymorphism *P*-values from a genome-wide association study for hyperketonemia in early lactation Holstein cows (n = 1,710) using the feature forward select linear mixed model methodology. Horizontal dashed lines indicating significance thresholds are lavender, orange, and red for putative ($P \leq 5.0 \times 10^{-5}$), marginal ($0.05 < Q \leq 0.10$), and significant ($Q \leq 0.05$) genome-wide associations, respectively.

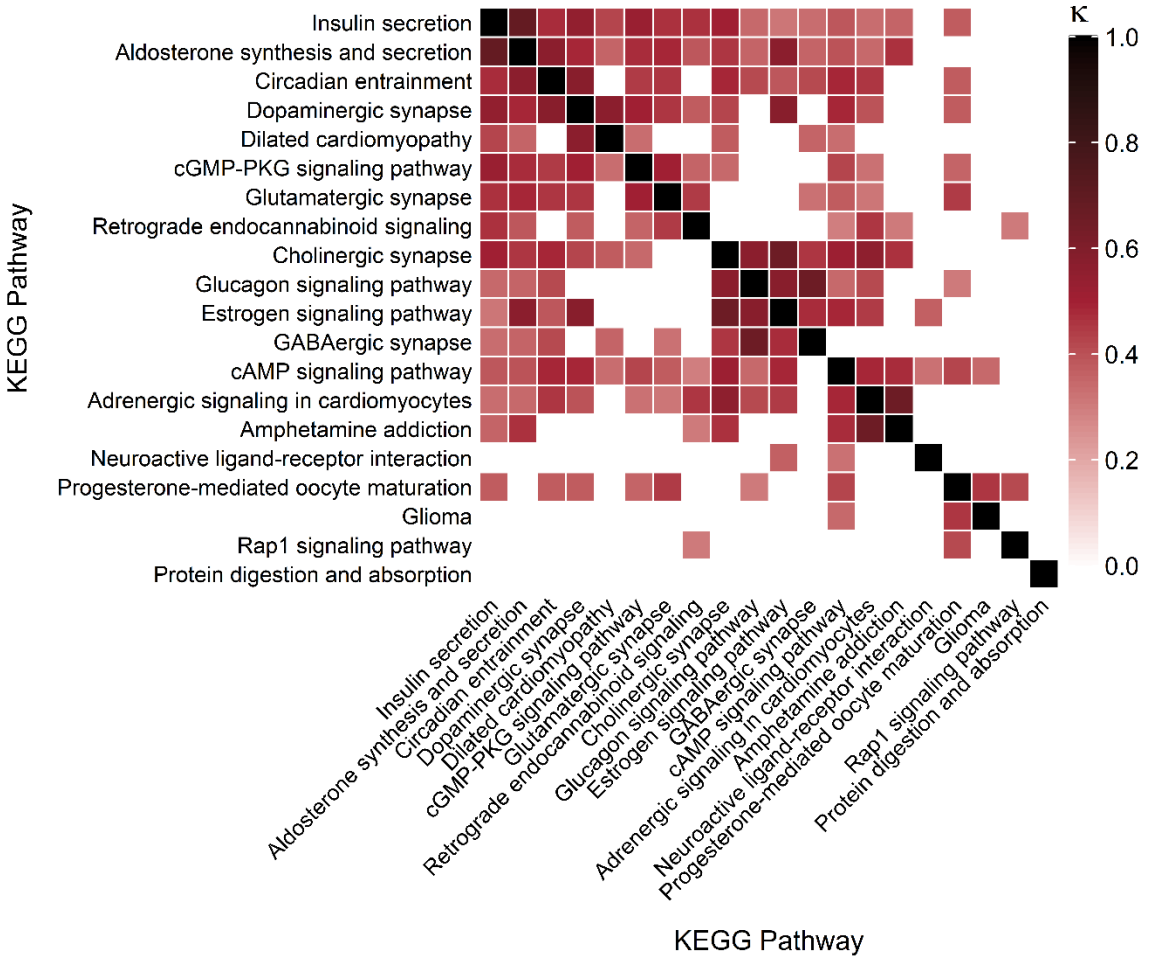

Figure 5.3. Heat map of concordance (κ) between Kyoto Encyclopedia of Genes and Genomes (KEGG) metabolic pathways enriched within parity group dependent genotype associations for hyperketonemia.

CHAPTER 6: PREDICTING BLOOD β-HYDROXYBUTYRATE USING MILK FOURIER TRANSFORM INFRARED SPECTRUM, MILK COMPOSITION, AND PRODUCER-REPORTED VARIABLES WITH MULTIPLE LINEAR REGRESSION, PARTIAL LEAST SQUARES REGRESSION, AND ARTIFICIAL NEURAL NETWORK

ABSTRACT

Prediction of postpartum hyperketonemia (**HYK**) using Fourier transform infrared (**FTIR**) spectrometry analysis could be a practical diagnostic option for farms because these data are now available from routine milk analysis during Dairy Herd Improvement testing. The objectives of this study were to (1) develop and evaluate blood β-hydroxybutyrate (**BHB**) prediction models using multivariate linear regression (**MLR**), partial least squares regression (**PLS**), and artificial neural network (**ANN**) methods and (2) evaluate whether milk FTIR spectrum (**mFTIR**) based models are improved with the inclusion of test-day variables (**mTest**; milk composition and producer-reported data). Paired blood and milk samples were collected from multiparous cows 5 to 18 d postpartum at 3 Wisconsin farms (3,629 observations from 1,013 cows). Blood BHB concentration was determined by a Precision Xtra meter (Abbott Diabetes Care, Alameda, CA), and milk samples were analyzed by a privately-owned laboratory (AgSource, Menomonie, WI) for components and FTIR spectrum absorbance. Producer-recorded variables were extracted from farm management software. A blood BHB ≥1.2 mmol/L was considered HYK. The data set was divided into a training set (n = 3,020) and an external testing set (n = 609). Model fitting was implemented with JMP 12 (SAS Institute, Cary, NC). A 5-fold cross-validation was performed on the training data set for the MLR, PLS, and ANN prediction methods, with square root of blood BHB as the dependent variable. Each method was fitted

using 3 combinations of variables: mFTIR, mTest, or mTest + mFTIR variables. Models were evaluated based on coefficient of determination, root mean squared error, and area under the receiver operating characteristic curve. Four models (PLS–mTest + mFTIR, ANN–mFTIR, ANN–mTest, and ANN–mTest + mFTIR) were chosen for further evaluation in the testing set after fitting to the full training set. In the cross-validation analysis, model fit was greatest for ANN, followed by PLS and MLR. Diagnostic strength after cross-validation was poorest for MLR and was similar for ANN and PLS. Models that used mTest + mFTIR variables performed marginally better than models that used only mFTIR or mTest variables. These results suggest that blood BHB prediction models that use mFTIR + mTest variables may be useful additions to existing HYK diagnostic and management programs.

INTRODUCTION

Hyperketonemia (**HYK**) is a metabolic disorder that impairs milk production, reproduction, and health outcomes in lactating dairy cows (Duffield, 2000; McArt et al., 2012). The postpartum prevalence of HYK ranges worldwide from 15 to 22%, although it can vary greatly between farms (Suthar et al., 2013; Santschi et al., 2016; Chandler et al., 2018). Measurement of blood β-hydroxybutyrate (**BHB**) concentration early postpartum is the predominant diagnostic method, and HYK is commonly defined as blood BHB ≥1.2 mmol/L (Iwersen et al., 2009; McArt et al., 2012; Gordon et al., 2017). Milk ketone body concentrations have been considered for HYK diagnosis because they are correlated with blood concentrations (Marstorp et al., 1983; Andersson, 1984; Enjalbert et al., 2001). The most accurate methods for detecting milk ketone bodies are flow-injection analysis, gas-liquid chromatography, and enzymatic assays; however, these techniques are expensive, time consuming, and difficult to automate. Fourier transform infrared (**FTIR**) spectrometry could provide a practical alternative

for predicting concentrations of milk ketone bodies because it is already used to evaluate milk composition in DHI milk testing programs (Rutten et al., 2009, 2011).

Studies in which milk FTIR data have been used to predict milk ketone body concentrations have reported moderate correlations between predicted and assayed milk concentrations (Hansen, 1999; Heuer et al., 2001; de Roos et al., 2007). However, correlation of FTIR-based milk ketone body concentration predictions with blood BHB concentration is low (Chandler et al., 2018), and use of FTIR-predicted milk ketone bodies for HYK diagnosis has produced tests with insufficient sensitivity to diagnose individual cows (van der Drift et al., 2012; Chandler et al., 2018). Marginal improvement of FTIR-predicted milk ketone bodies used as an HYK diagnostic was made by including FTIR-predicted milk ketone bodies with cow test-day information in logistic (van der Drift et al., 2012) and multiple linear regression (**MLR**; Chandler et al., 2018) models predicting blood BHB concentration. At this time, these predictions of blood BHB concentration are recommended as a tool for monitoring HYK prevalence at the herd level, but sensitivity and specificity are insufficient for use as an individual cow diagnostic tool (van der Drift et al., 2012; Chandler et al., 2018).

Inclusion of milk FTIR spectrum data, combined with FTIR-predicted milk ketone body concentrations and milk composition in models, could generate more robust models with enhanced prediction of blood BHB and HYK diagnosis by capturing residual spectrum predictive abilities. Furthermore, advancements in computing technology have made flexible and computationally demanding methods, such as machine learning, increasingly available for such applications. Artificial neural networks (**ANN**) are a type of machine-learning prediction method with the ability to self-learn relationships from labeled experimental data and generalize to unlabeled situations. This advanced modeling technique may allow optimization of blood BHB

concentration prediction from milk FTIR spectrum, milk component, and producer-reported variables.

We hypothesized that the use of more advanced modeling techniques, such as partial least squares regression (**PLS**) and ANN, would result in improved predictions of HYK status from producer-reported and milk composition variables compared with MLR. Furthermore, we hypothesized that predictions of blood BHB could be optimized by inclusion of milk FTIR spectrum, milk component, and producer-reported variables. Based on these hypotheses, our objectives were to (1) develop and evaluate blood BHB prediction models using MLR, PLS, and ANN methods and (2) evaluate whether milk FTIR spectrum–based models are improved by the inclusion of milk composition and producer-reported variables.

MATERIALS AND METHODS

Cows from 2 privately owned Holstein dairy farms in southern Wisconsin and the University of Wisconsin– Madison Emmons Blaine Dairy Cattle Research Center were enrolled in the study. Dairy farms were selected based on the following criteria: early-lactation cows grouped in a separate pen, availability of headlocks for blood sampling, capability of proportional milk sampling, use of management software, and willingness to participate. All animal use and handling protocols were approved by the University of Wisconsin–Madison College of Agricultural and Life Sciences Animal Care and Use Committee. Farms were visited twice a week for regular sampling of paired blood and milk samples from multiparous Holstein cows (n = 1,013) between 5 and 18 days in milk (**DIM**). This provided an opportunity to collect up to 4 paired blood and milk samples per cow within the 2-wk sampling period. Routine HYK testing within the first 10 DIM at the University of Wisconsin–Madison farm allowed some cows to contribute 5 samples as described by Rathbun et al. (2017).

Sample Collection and Analysis

Morning milk samples were collected by an International Committee on Animal Recordings–approved sampling system using a proportional sampler that had been calibrated within the previous 12 mo. Animal identification numbers were recorded by automatic radio-frequency identification collection and verified by visual identification of animal identification tags to prevent inaccurate identification recording. Samples were preserved with 2-bromo-2-nitropropane-1,3-diol (Advanced Instruments Inc., Norwood, MA) and transported to AgSource Cooperative Services (Menomonie, WI) for analysis according to standard test-day procedures. In brief, all milk samples were preheated to 40°C and mixed before analysis of milk fat and milk protein by FTIR using the Foss MilkoScan FT+ (Foss Analytical, Hillerød, Denmark) in accordance with the instrument manufacturer's instructions and ISO 9622/ IDF 141:2013 (AOAC official method 972.16; AOAC International, 2016). Analysis of somatic cell count (**SCC**) was performed using Fossomatic FC (Foss Analytical). Milk BHB and milk acetone concentrations were predicted by FTIR using Foss Ketolab (Foss Analytical) based on the calibrations of de Roos et al. (2007). Additionally, the Foss MilkoScan FT+ analysis of milk samples provided predictions for the proportions of saturated, unsaturated, trans- , short-, medium-, and long-chain fatty acid (**FA**) in milk based on Foss FTIR FA prediction models (Foss Analytical). Per the DHI's standard operating procedures, milk samples were analyzed on equipment that is calibrated weekly with 12 standards, and standards are rechecked daily and hourly with a subset of 6 of the 12 standards. Intra-assay coefficients of variation for all variables were maintained at <7%. Interassay coefficients of variation are not available for all variables; however, interassay coefficients of variation for fat and protein are maintained at <2 and <1.5%, respectively. Immediately following the morning milk sampling, each cow was confined to a

headlock along the feed alley before or during the morning feeding. At this time, a blood sample was collected from a coccygeal vessel into an evacuated Vacutainer serum collection tube containing clot activator (BD Diagnostics, Franklin Lakes, NJ). Whole-blood BHB concentration was quantified cowside with the hand-held Precision Xtra blood glucose and ketone meter (Abbott Diabetes Care, Alameda, CA). This meter has been validated for use in dairy cattle (Iwersen et al., 2009; Bach et al., 2016; Sailer et al., 2018). Cows were diagnosed with HYK for a given sampling if blood BHB was ≥1.2 mmol/L. Incidences of HYK were reported to farm staff for treatment per the respective farm's standard operating procedures.

Data Collection

Milk sample composition was obtained from AgSource Cooperative Services (Menomonie, WI) and included variables routinely predicted from milk FTIR spectrum: protein percentage, fat percentage, fat:protein ratio, solids not fat percentage, SCC, milk urea nitrogen, FA categories (detailed above), acetone, and BHB. Prediction accuracy and precision of the preceding milk components were not evaluated in the present study; rather, variables were used as provided to represent data as available during routine analysis. The FTIR spectrum absorbance (1,060 wavenumbers per sample) was exported separate from the milk composition variables and provided by AgSource Cooperative Services. Producer-recorded variables regarding the previous and current lactation, which are routinely exported during milk test, were exported from DairyComp305 (Valley Ag Services, Tulare, CA) for all cows in the study. These variables included calving date, parity, DIM, age at first calving, previous lactation length, previous lactation 305-d mature equivalent milk, gestation length, and dry period length. A single observation comprised a blood BHB measurement and a paired milk sample composition and FTIR spectrum from a single sample collection day. For each observation, producer-reported

variables listed above for each cow were aligned with the observational data. A total of 4,147 observations were collected, but some were excluded due to missing blood BHB (n = 26), failure to capture FTIR spectrum (n = 462), missing producer-reported data (n = 25), and misreported data (n = 5), leaving 3,629 observations for further analysis.

Model Fitting and Validation

All model fitting was performed with JMP Pro 12 (SAS Institute Inc., Cary, NC). Blood BHB concentration did not have a normal distribution, which is an assumption of MLR; therefore, the square root transformation of blood BHB concentration was the dependent variable for all models to better satisfy MLR assumptions and provide consistency. Modeling methods used in this study included MLR, PLS, and ANN. Each method was fitted with 3 different groups of potential explanatory variables: producer-reported and milk composition variables (**mTest**), FTIR spectrum absorbance variables (**mFTIR**), and the union of mTest and mFTIR variables (**mTest + mFTIR**). This resulted in 9 method–variable (e.g., MLR–mFTIR) combinations.

Observations within cow were considered independent and randomly assigned to a training set (n = 3,020) and a testing set (n = 609) before analysis. Observations in the training set were used to perform a 5-fold cross-validation for all 9 method–group combinations as described below. Data within the testing set were maintained separately and not used until external model validation.

MLR

For the MLR method, an initial model was fitted to predict blood BHB from potential explanatory variables in mTest, mFTIR, and mTest + mFTIR using the stepwise fit function and minimum corrected Akaike information criterion stopping rule. When explanatory variables with

$P > 0.15$ were included in the model, the variable with the greatest *P*-value was removed and the model was refitted. This was repeated until all variables were significant at $P \leq 0.15$. Then, collinearity was evaluated for each variable using a variable inflation factor (**VIF**), and variables with VIF ≥10 were considered collinear. When collinearity was present, the variable with the greatest VIF was removed and the model was refitted. This process was repeated until all variables had a VIF <10. Removing collinear variables can drastically alter the *P*-values of retained variables, and previously significant variables can become nonsignificant. In those instances, nonsignificant variables were removed successively, and once only significant variables remained the collinearity check was repeated.

PLS Regression

An initial PLS model was fitted with potential explanatory variables in mTest, mFTIR, and mTest + mFTIR, and the model was fitted with 15 factors (latent variables). After the initial fitting, the model was refitted using variables with variable importance projection values >0.8, again with 15 factors.

ANN

For ANN models, the neural predictive modeling function was implemented. A single hidden layer with 15 nodes and a tangent activation identity provided the framework for the ANN with the following specifications: least absolute values of residuals, weight decay penalty method, and 750 tours (epochs). When too many variables of low predictive ability are fitted with ANN, computing time increases, model robustness decreases, and the risk of overfitting increases. Therefore, only explanatory variables with variable importance projection values >0.8 in the PLS analyses were included in the respective ANN models using mTest, mFTIR, and mTest + mFTIR explanatory variables.

Cross-Validation and External Validation

In this study, cross-validation was performed by randomly dividing observations from the training data set into 5 subsets or folds (A through E), each with 604 observations. Each subset was used to develop MLR, PLS, and ANN models using mTest, mFTIR, and mTest + mFTIR variables independently. The resulting models were fitted to the other 4 subsets, in turn, and the following statistics were recorded: coefficient of determination (**R^2**), root mean squared error (**RMSE**), and area under the receiver operating characteristic curve (**AUC**). Of the 9 models evaluated by cross-validation, 4 models were chosen for further evaluation based on R^2, RMSE, and AUC. These models were fitted to the full training data set and validated externally using the aforementioned testing set. Statistics used to evaluate model fit in the external validation included the concordance correlation coefficient (**CCC**) and mean squared error (**MSE**) of predicted blood BHB concentrations (Tedeschi, 2006). In addition, accuracy, sensitivity, specificity, positive predictive value (**PPV**), and negative predictive value (**NPV**) of predicted HYK diagnoses were evaluated for each model using the optimal diagnostic thresholds that were determined as the predicted BHB value that maximized the difference between sensitivity and 1 – specificity.

RESULTS AND DISCUSSION

In the full data set, a total of 24, 97, 182, 685, and 25 individual cows contributed 1, 2, 3, 4, and 5 samples, respectively. The proportion of samples diagnosed with HYK was 12.3, 12.1, and 13.6% for the full data set (n = 3,629), training set (n = 3,020), and testing set (n = 609), respectively. Mean blood BHB concentrations were 0.78, 0.77, and 0.81 for the full data set, training set, and testing set, respectively. Within specific folds of the training set, the proportion of samples diagnosed with HYK ranged from 10.8 to 13.4%, and mean blood BHB concentration

ranged from 0.75 to 0.80 mmol/L (Table 6.1). The means and standard errors of producer-reported and milk composition variables are reported in Tables 6.2 and 6.3, respectively. It is likely that the proportion of HYK samples and BHB concentration was reduced by the inclusion of multiple samples from individual healthy cows as well as the inclusion of samples from HYK cows collected after treatment.

Model Development and Cross-Validation in the Training Set

Prediction Methods. Relative fit of models was the greatest for ANN, with mean R^2 of 0.44 ± 0.01, 0.36 ± 0.01, and 0.27 ± 0.02 for ANN, PLS, and MLR methods, respectively, when averaged across the mTest, mFTIR, and mTest + mFTIR groups of explanatory variables (Table 6.4). Similarly, relative performance based on average RMSE was 0.16 ± 0.003, 0.18 ± 0.003, and 0.27 ± 0.06 for ANN, PLS, and MLR, respectively. To our knowledge, no previous studies have investigated the use of advanced statistical modeling, such as PLS and ANN, to develop blood BHB prediction models. In the current study, diagnostic ability of the ANN and PLS methods was similar, with an average AUC of 0.85 ± 0.007, whereas MLR had poorer diagnostic ability, with an average AUC of 0.81 ± 0.012.

Explanatory Variables. When averaged across methods, models that used mTest + mFTIR potential explanatory variables provided the greatest R^2 (0.39 ± 0.02) as shown in Table 4. However, average RMSE for models with mTest + mFTIR explanatory variables was similar to that of models with mTest explanatory variables, and average AUC values were similar for models with mTest, mFTIR, or mTest + mFTIR explanatory variables (Table 6.4). Models that used only mFTIR variables had the least favorable fit statistics, with a mean R^2 of 0.33 ± 0.02 and RMSE of 0.27 ± 0.061. Improvement of R2 by using mTest + mFTIR explanatory variables is expected because the inclusion of more variables generally improves relative fit. The poorer fit

of mFTIR variables compared with mTest + mFTIR and mTest variables should be interpreted with caution. Model fit statistics are noticeably poorer for the MLR models with mFTIR variables compared with all other models (Table 6.4). This decreased the mean performance of models based on mFTIR variables. When comparing PLS and ANN models fit with mFTIR variables (0.38 ± 0.02, 0.17 ± 0.004, and 0.86 ± 0.006 for R^2, RMSE, and AUC, respectively) with those fit with mTest variables (0.38 ± 0.02, 0.17 ± 0.004, and 0.84 ± 0.008 for R^2, RMSE, and AUC, respectively) or mTest + mFTIR variables (0.43 ± 0.02, 0.16 ± 0.003, and 0.86 ± 0.008 for R2, RMSE, and AUC, respectively), mean performance of mFTIR variables was similar to mTest variables. Both mFTIR and mTest variables were marginally poorer than mTest + mFTIR variables (Table 6.4). This study supports and expands upon the work of Chandler et al. (2018), who reported improvements in correlation, AUC, and accuracy of MLR models by incorporating additional milk composition and producer-reported variables into models based on individual FTIR milk ketone body tests. Previously, van der Drift et al. (2012) also proposed utilizing producer-reported and milk composition variables to augment milk FTIR–based predictions of milk ketone bodies when predicting blood BHB and diagnosing HYK. Neither of these previous studies explored use of mFTIR data in prediction models. Results from this study support mFTIR variables being able to explain a marginal amount of additional variation in models already containing mTest data.

Evaluation of Method–Variable Group Combination. A summary of the R^2, RMSE, and AUC of all 9 prediction method–variable group combinations is provided in Table 6.4. Overall, the model with the best fit was ANN–mTest + mFTIR, with R^2, RMSE, and AUC of 0.46 ± 0.01, 0.16 ± 0.002, and 0.86 ± 0.005, respectively. However, RMSE and AUC of ANN–mTest + mFTIR were improved only marginally relative to ANN–mTest (0.17 ± 0.001 and 0.85 ± 0.004,

respectively), ANN–mFTIR (0.17 ± 0.002 and 0.86 ± 0.004, respectively), and PLS–mTest + mFTIR (0.17 ± 0.002 and 0.86 ± 0.005, respectively). Based on the differences in predictive ability between methods and groups of explanatory variables in the cross-validation analysis, 4 models (ANN–mTest + mFTIR, ANN–mTest, ANN–mFTIR, and PLS–mTest + mFTIR) were chosen for external validation in the testing set.

External Validation of the Testing Set. Overall, the ANN–mTest + mFTIR model provided greater fit in the independent testing set, with R^2, RMSE, and CCC of 0.56, 0.16, and 0.69, respectively. The other model–explanatory variable combinations, namely PLS–mTest + mFTIR, ANN–mFTIR, and ANN-mTest, performed similarly in the testing set based on R^2, RMSE, and CCC (Table 5; Figure 6.1). Decomposition of MSE revealed minimal mean and slope bias for all models, with 99.0, 98.9, 98.3, and 99.0% of MSE attributed to error for PLS–mTest + mFTIR, ANN–mFTIR, ANN– mTest, and ANN–mTest + mFTIR, respectively (Table 6.5). Model AUC values were 0.88, 0.83, 0.87, and 0.88 for PLS–mTest + mFTIR, ANN–mFTIR, ANN–mTest, and ANN–mTest + mFTIR, respectively (Table 6.6). The PLS–mTest + mFTIR method–variable combination had the lowest accuracy (0.73) of HYK diagnosis due to low specificity (0.71), but it provided the greatest sensitivity (0.89). Meanwhile, ANN–mTest + mFTIR and ANN–mTest had equal accuracy (0.80), although ANN–mTest + mFTIR had marginally greater sensitivity, specificity, and NPV (Table 6.6). Despite the lowest AUC (0.83), ANN–mFTIR had intermediate accuracy, sensitivity, specificity, PPV, and NPV values of 0.78, 0.76, 0.78, 0.35, and 0.95, respectively, compared with other model–variable combinations.

Comparison of the PLS–mTest + mFTIR and ANN–mTest + mFTIR to determine whether the added complexity of the ANN method was advantageous indicated that ANN marginally improved fit statistics for blood BHB prediction. In addition, ANN improved

accuracy, specificity, and PPV of HYK diagnosis compared with PLS–mTest + mFTIR (Table 6.6). Based on the models developed herein, it appears that the added complexity of the ANN method may improve HYK diagnosis compared with PLS–mTest + mFTIR. However, the improvement in goodness of fit statistics for ANN compared with PLS may be marginal. Inclusion of mTest + mFTIR explanatory variables in ANN models provided marginal improvements in fit and diagnostic statistics, although ANN–mTest + mFTIR was most preferable and ANN–mFTIR was least preferable (Tables 6.5 and 6.6). This indicates that ANN with milk composition and producer-reported variables are somewhat better than ANN with milk FTIR spectrum for prediction of blood BHB, and fitting ANN with all explanatory variables seems to confer marginal improvement. This could be due to residual effects within the milk FTIR data not captured by mTest variables, which include FTIR-predicted milk ketone body concentrations. However, it is important to note that some of the between-samples variation in milk FTIR spectrum may be captured in the milk composition variables represented in the mTest data. For example, milk-based predictions of the concentrations of acetone, saturated FA, or unsaturated FA may explain some of the variation present in the milk FTIR data, and this could diminish the difference in prediction accuracy between models that were developed from mTest explanatory variables and those that were developed with mTest + mFTIR explanatory variables. The ANN–mTest model performance was only marginally reduced compared with ANN–mTest + mFTIR and was slightly improved compared with ANN–mFTIR, which may indicate that the addition of FTIR spectrum data is not essential. Use of mTest data may also be a more practical solution from a data management perspective because mTest models would not require the additional capture of FTIR spectrum data and merging of the spectrum data with mTest data by cow. However, models fitted only with milk FTIR spectrum may be more reliable and ubiquitous

for application in the field than models including producer-reported variables. Producer-recorded variables rely heavily on input from farm staff: they must use herd management software regularly, record potential explanatory variables accurately, and allow the milk testing service provider to access these data freely. Precision and accuracy of these data are also likely to be variable across dairy farms. Conversely, models based solely on milk FTIR spectrum do not require farms to record or provide management data and can be readily implemented by analysis of proportionally collected milk samples, but are dependent on the type of equipment and quality control of sample analysis at the milk testing laboratory.

Prediction Models as an HYK Diagnosis Strategy

Diagnosis of HYK on privately owned dairy operations can be hampered by the expense and labor associated with cowside and enzymatic tests. Predictions of blood BHB using data retrieved from weekly or monthly milk samples and recorded herd management data could provide a high-throughput, efficient, and cost-effective means of diagnosis and monitoring HYK. A potential limitation of implementing blood BHB prediction models using milk FTIR variables may be the frequency of routine DHI milk testing, which is typically every 4 to 5 wk. At this frequency, half of the cows would not have a single milk sample collected during the high HYK risk period (5–18 DIM; McArt et al., 2012), and the remaining cows would have only 1 milk sample during the high-risk period from which to predict blood BHB and HYK risk. It may be feasible for some large dairy farms to implement weekly milk sampling of cows in early lactation (5–18 DIM), especially if these cows are grouped separately. Frequent sampling of these cows would allow prediction of individual cow HYK based on FTIR data, with or without producer-reported variables, as an effective diagnostic and monitoring tool. This tool could be

particularly valuable if other diagnostics (e.g., SCC) were provided for these early-lactation cows.

All models validated externally in the testing set (PLS–mTest + mFTIR, ANN–mFTIR, ANN–mTest, and ANN–mTest + mFTIR) had "very good" diagnostic capacity (AUC ≥0.83; Šimundić, 2009) for HYK; however, no model achieved the "excellent" diagnostic strength that is typical with ideal reference tests (AUC ≥0.90; Šimundić, 2009). Furthermore, none achieved the sensitivity and specificity of currently available cowside blood tests (88 and 96%, respectively; Iwersen et al., 2009). The relatively low PPV values (ranging from 0.32 to 0.39; Table 6.6) imply the potential for misdiagnosis of some healthy cows as HYK, which could result in unnecessary treatments and increased costs. Alternatively, the cost-effectiveness and labor efficiency of milk-based prediction models for HYK diagnosis may justify the reduced diagnostic strength compared with enzymatic and cowside assays, especially when the cost of an untreated HYK case is much greater than the cost of HYK treatment (McArt et al., 2014). Milk-based prediction models could also be used for HYK screening programs, with predicted positives undergoing more precise cowside or enzymatic tests. In this instance, models with lower specificity and PPV may be of less concern because there would be further testing, and the primary goal of screening would be to identify all cows that are potentially HYK positive.

CONLUSIONS

Blood BHB prediction models developed from producer-reported variables, milk composition, and milk FTIR spectrum may be adequate for HYK diagnosis and monitoring due to reasonable diagnostic strength and efficient implementation. Overall, ANN provided the most favorable fit statistics and diagnostic performance, although improvement over PLS was marginal. Inclusion of mTest + mFTIR variables in prediction models improved HYK diagnostic

strength slightly compared with mTest or mFTIR variables separately, but there may be technical advantages to predicting HYK status solely from mFTIR or mTest variables without merging these data sets by cow.

ACKNOWLEDGEMENTS

The writing in this chapter is a reproduction of a published manuscript (Pralle et al., 2017). This research is based on work that was supported by the National Institute of Food and Agriculture, USDA Agriculture and Food Research Initiative Critical Agricultural Research and Extension (CARE; 2015-67028-23572) and Early Concept Grants for Exploratory Research (EAGER; 2017-67007-25947). Additional funding was from the USDA Hatch grant number WIS01878 from the Wisconsin Agricultural Experiment Station (Madison). The authors recognize and appreciate the support of the owners and herdsmen at the privately-owned dairies as well as the research staff at the University of Wisconsin–Madison Emmons Blaine Dairy Research Center. Furthermore, this work would not have been possible without the assistance of the following individuals: F. M. Rathbun, R. C. Oliveira, C. A. Getschel, L. C. Resende, C. H. Nova, K. J. Sailer, and T. Mack (all individuals from University of Wisconsin-Madison).

REFERENCES

Andersson, L. 1984. Concentrations of blood and milk ketone bodies, blood isopropanol and plasma glucose in dairy cows in relation to the degree of hyperketonaemia and clinical signs. Zentralbl. Veterinarmed. A 31:683–693. https://doi.org/10.1111/j.1439-0442.1984.tb01327.x.

AOAC International. 2016. Official Methods of Analysis. 20th ed. AOAC International, Gaithersburg, MD.

Bach, K.D., W. Heuwieser, and J.A.A. McArt. 2016. Technical note: Comparison of 4 electronic handheld meters for diagnosing hyper- ketonemia in dairy cows. J. Dairy Sci. 99:9136–9142. https://doi.org/10.3168/jds.2016-11077.

Chandler, T.L., R.S. Pralle, J.R.R. Dórea, S.E. Poock, G.R. Oetzel, R.H. Fourdraine, and H.M. White. 2018. Predicting hyperketonemia by logistic and linear regression using test-day milk and performance variables in early-lactation Holstein and Jersey cows. J. Dairy Sci. 101:2476–2491. https://doi.org/10.3168/jds.2017-13209.

de Roos, A.P., H. Van Den Bijgaart, J. Hørlyk, and G. de Jong. 2007. Screening for subclinical ketosis in dairy cattle by Fourier transform infrared spectrometry. J. Dairy Sci. 90:1761–1766. https:// doi.org/10.3168/jds.2006-203.

Duffield, T. 2000. Subclinical ketosis in lactating dairy cattle. Vet. Clin. North Am. Food Anim. Pract. 16:231–253. https://doi.org/10.1016/S0749-0720(15)30103-1.

Enjalbert, F., M.C. Nicot, C. Bayourthe, and R. Moncoulon. 2001. Ketone bodies in milk and blood of dairy cows: Relationship between concentrations and utilization for detection of subclinical ketosis. J. Dairy Sci. 84:583–589. https://doi.org/10.3168/jds.S0022-0302(01)74511-0.

Gordon, J.L., T.F. Duffield, T.H. Herdt, D.F. Kelton, L. Neuder, and S.J. LeBlanc. 2017. Effects of a combination butaphosphan and cyanocobalamin product and insulin on ketosis resolution and milk production. J. Dairy Sci. 100:2954–2966. https://doi.org/10.3168/jds.2016-11925.

Hansen, P. W. 1999. Screening of dairy cows for ketosis by use of infrared spectroscopy and multivariate calibration. J. Dairy Sci. 82:2005–2010. https://doi.org/10.3168/jds.S0022-0302(99)75437-8.

Heuer, C., H.J. Luinge, E. Lutz, and Y.H. Schukken. 2001. Determination of acetone in cow milk by Fourier transform infrared spectroscopy for the detection of subclinical ketosis. J. Dairy Sci. 84:575–582. https://doi.org/10.3168/jds.S0022-0302(01)74510-9.

Iwersen, M., U. Falkenberg, R. Voigtsberger, D. Forderung, and W. Heuwieser. 2009. Evaluation of an electronic cowside test to detect subclinical ketosis in dairy cows. J. Dairy Sci. 92:2618–2624. https://doi.org/10.3168/jds.2008-1795.

Marstorp, P., T. Anfält, and L. Andersson. 1983. Determination of oxidized ketone bodies in milk by flow injection analysis. J. Dairy Sci. 149:281–289. https://doi.org/10.1016/S0003-2670(00)83184-0.

McArt, J.A.A., D.V. Nydam, and G.R. Oetzel. 2012. Epidemiology of subclinical ketosis in early lactation dairy cattle. J. Dairy Sci. 95:5056–5066. https://doi.org/10.3168/jds.2012-5443.

McArt, J.A.A., D.V. Nydam, G.R. Oetzel, and C.L. Guard. 2014. An economic analysis of hyperketonemia testing and propylene glycol treatment strategies in early lactation dairy cattle. Prev. Vet. Med. 117:170–179. https://doi.org/10.1016/j.prevetmed.2014.06.017.

Pralle, R.S., K.A. Weigel, H.M., White. 2017. Predicting blood β-hydroxybutyrate using milk Fourier transform infrared spectrum, milk composition, and producer-reported variables with multiple linear regression, partial least squares regression, and artificial neural network. J. Dairy Sci. 101:4378-4387. https://doi.org/10.3168/jds.2017-14076.

Rathbun, F.M., R.S. Pralle, S.J. Bertics, L.E. Armentano, K. Cho, C. Do, K.A. Weigel, and H.M. White. 2017. Relationships between body condition score change, prior mid-lactation phenotypic residual feed intake, and hyperketonemia onset in transition dairy cows. J. Dairy Sci. 100:3685–3696. https://doi.org/ 10.3168/jds.2016-12085.

Rutten, M.J.M., H. Bovenhuis, J.M.L. Heck, and J.A.M. van Arendonk. 2011. Predicting bovine milk protein composition based on Fourier transform infrared spectra. J. Dairy Sci. 94:5683–5690. https://doi.org/10.3168/jds.2011-4520.

Rutten, M.J.M., H. Bovenhuis, K.A. Hettinga, H.J.F. van Valenberg, and J.A.M. van Arendonk. 2009. Predicting bovine milk fat composition using infrared spectroscopy based on milk samples collected in winter and summer. J. Dairy Sci. 92:6202–6209. https://doi.org/10.3168/jds.2009-2456.

Sailer, K.J., R.S. Pralle, R.C. Oliveira, G.R. Oetzel, and H.M. White. 2018. Technical note: Validation of BHBCheck blood β-hydroxybutyrate meter as a diagnostic tool for hyperketonemia. J. Dairy Sci. 101:1524–1529. https://doi.org/10.3168/jds.2017-13583.

Santschi, D.E., R. Lacroix, J. Durocher, M. Duplessis, R.K. Moore, and D.M. Lefebvre. 2016. Prevalence of elevated milk β-hydroxybutyrate concentrations in Holstein cows measured by Fourier-transform infrared analysis in Dairy Herd Improvement milk samples and association with milk yield and components. J. Dairy Sci. 99:9263–9270. https://doi.org/10.3168/jds.2016-11128.

Šimundić, A.M. 2009. Measures of diagnostic accuracy: Basic definitions. EJIFCC 19:203–211.

Suthar, V. S., J. Canelas-Raposo, A. Deniz, and W. Heuwieser. 2013. Prevalence of subclinical ketosis and relationships with postpartum diseases in European dairy cows. J. Dairy Sci. 96:2925–2938. https://doi.org/10.3168/jds.2012-6035.

Tedeschi, L.O. 2006. Assessment of the adequacy of mathematical models. Agric. Syst. 89:225–247. https://doi.org/10.1016/j.agsy.2005.11.004.

van der Drift, S.G.A., R. Jorritsma, J.T. Schonewille, H.M. Knijn, and J.A. Stegeman. 2012. Routine detection of hyperketonemia in dairy cows using Fourier transform infrared spectroscopy analysis of β-hydroxybutyrate and acetone in milk in combination with test-day information. J. Dairy Sci. 95:4886–4898. https://doi.org/10.3168/jds.2011-4417.

Table 6.1. Blood β-hydroxybutyrate (BHB) concentration, proportion of samples diagnosed with hyperketonemia (HYK), and proportion of samples from each farm for the training set and cross-validation subsets used for model development and the testing set used for external validation.

	Cross-validation Subsets[1]						
Variable	A	B	C	D	E	Training Set	Testing Set
Sample size	604	604	604	604	604	3020	609
Blood BHB, mmol/L							
Mean[2]	0.8	0.8	0.8	0.8	0.8	0.77	0.81
Minimum	0.1	0.1	0.1	0.2	0.2	0.1	0.1
Maximum	4.7	3.9	4.5	3.6	3.8	4.7	5.4
HYK, %	11	13	12	13	12	12.12	13.63
Farm[3], %							
X	51.7	48.0	48.7	46.2	48.5	48.6	47.5
Y	41.4	43.7	44.2	46.7	45.4	44.3	45.8
Z	6.9	8.3	7.1	7.1	6.1	7.1	6.7

[1]Training set observations were randomly assigned to 1 of 5 data subsets (A through E), which were used to perform 5-fold cross-validation during model development.

[2]BHB standard error ± 0.02 mmol/L

[3]Proportion of samples contributed from each farm, anonymized as X, Y, and Z

Table 6.2. Sample means and standard errors (SE) of producer-recorded variables extracted from DairyComp305 (Valley Agricultural Software, Tulare, CA, USA) for the training set and cross-validation subsets used for model development and the testing set used for external validation.

	Cross-validation Subsets[1]									
Variable	A	B	C	D	E	SE	Training Set	SE	Testing Set	SE
DIM[2]	11.5	11.1	11.8	11.3	11.5	0.2	11.5	0.1	11.7	0.2
Parity	2.9	2.9	3.0	3.0	2.9	0.1	3.0	0.0	3.0	0.1
AGEFC[3], mo	23.0	23.2	23.2	23.2	23.1	0.1	23.1	0.0	23.4	0.2
PLACT[4], d	338.7	337.6	339.2	337.5	333.5	2.1	337.3	1.0	336.3	2.3
PME305[5], kg	15778	15774	15739	15836	15657	94	15757	43	15608	96
Gestation, d	276.8	277.0	277.2	277.0	276.8	0.7	277.0	0.3	277.7	0.5
Dry period, d	56.3	55.3	56.0	56.4	56.2	0.5	56.0	0.2	55.9	0.5

[1]Training set observations were randomly assigned to 1 of 5 data subsets (A through E), which were used to perform a 5-fold cross-validation during model development.
[2]Days in milk
[3]Age at first calving
[4]Previous lactation length
[5]Previous 305 d mature equivalent milk

Table 6.3. Sample means and standard errors (SE) of milk composition variables provided by AgSource Cooperative Services (Menomonie, WI, USA) for datasets and cross-validation subsets used for model fitting and evaluation.

	Cross-validation Subsets[1]									
Variables[2]	A	B	C	D	E	SE	Training Set	SE	Testing Set	SE
Yield, kg	41.16	39.93	40.32	39.58	39.21	0.54	40.05	0.23	40.10	0.54
Fat, %	4.31	4.43	4.31	4.35	4.34	0.04	4.35	0.02	4.33	0.04
Protein, %	3.43	3.45	3.41	3.46	3.42	0.02	3.43	0.01	3.40	0.02
F:P[3]	1.27	1.30	1.28	1.27	1.28	0.01	1.28	0.01	1.29	0.01
Lactose, %	4.76	4.73	4.74	4.74	4.74	0.01	4.74	0.004	4.75	0.01
SnF[4], %	9.25	9.25	9.22	9.26	9.24	0.02	9.24	0.01	9.21	0.02
SCC[5]	217.13	208.47	198.02	223.16	218.75	26.73	213.11	13.85	154.43	15.92
MUN[6]	11.05	11.51	11.45	11.23	11.37	0.11	11.32	0.05	11.51	0.10
Acetone	0.09	0.09	0.09	0.09	0.09	0.004	0.09	0.002	0.10	0.01
BHB[7]	0.08	0.08	0.08	0.08	0.08	0.003	0.08	0.001	0.08	0.003
Fatty acids[8]										
MUFA	1.35	1.41	1.38	1.38	1.37	0.02	1.38	0.01	1.37	0.02
PUFA	0.30	0.30	0.30	0.30	0.30	0.002	0.30	0.001	0.30	0.002
SFA	2.58	2.64	2.55	2.60	2.59	0.03	2.59	0.01	2.59	0.03
SCFA	0.40	0.41	0.39	0.40	0.40	0.01	0.40	0.002	0.40	0.01
MCFA	1.86	1.92	1.85	1.88	1.86	0.03	1.87	0.01	1.85	0.02
LCFA	1.67	1.74	1.71	1.70	1.69	0.02	1.70	0.01	1.69	0.02

[1]Training set observations were randomly assigned to 1 of 5 data subsets (A through E), which were used to perform a 5-fold cross-validation during model development.

[2]Milk composition variables were measured in composite milk samples preserved with 2-bromo-2-nitropropane-1,3-diol (Advanced Instruments, Inc., Norwood, MA, USA) collected during the A.M. milking. Milk fat %, protein %, lactose %, solids not fat %, and milk urea nitrogen were determined by the FOSS MilkoScan FT+ (FOSS Analytical, Eden Prairie, MN, USA). Somatic cell count was determined by the Fossomatic FC (FOSS Analytical). Acetone and BHB concentration was determined using FOSS KETOLAB (FOSS Analytical, Hillerød, Denmark). Milk fatty acid groups were determined by FOSS MilkoScan FT+ (FOSS Analytical)

[3]Fat to protein ratio

[4]Solids not fat

[5]Somatic cell count x1,000 cells/mL

[6]Milk urea nitrogen, mg/dL

Table 6.3. *Continued.*

[7]β-hydroxybutyrate

[8]Monounsaturated fatty acids (MUFA), polyunsaturated fatty acids (PUFA), short chain fatty acids (SCFA), medium chain fatty acids (MCFA), and long chain fatty acids (LCFA) in g/100 g milk

170

Table 6.4. Fit statistic means and standard errors (SE) for five-fold cross-validation of blood β-hydroxybutyrate prediction models in the training set during model development.

Method[1]	Variables[3]	r^2	SE	RMSE[4]	SE	AUC[5]	SE
MLR	*(averaged across variables)*	0.27	0.02	0.27	0.060	0.81	0.012
PLS		0.36	0.01	0.18	0.003	0.85	0.007
ANN		0.44	0.01	0.16	0.003	0.85	0.005
(averaged across methods)	mFTIR	0.33	0.02	0.27	0.061	0.84	0.012
	mTest	0.35	0.02	0.18	0.003	0.83	0.007
	mTest+mFTIR	0.39	0.02	0.18	0.003	0.83	0.010
MLR	mFTIR	0.23	0.02	0.45	0.072	0.81	0.014
MLR	mTest	0.29	0.01	0.19	0.001	0.82	0.006
MLR	mTest+mFTIR	0.31	0.01	0.18	0.002	0.82	0.008
PLS	mFTIR	0.34	0.01	0.18	0.002	0.86	0.004
PLS	mTest	0.33	0.01	0.18	0.002	0.84	0.006
PLS	mTest+mFTIR	0.40	0.01	0.17	0.002	0.86	0.005
ANN	mFTIR	0.42	0.01	0.17	0.002	0.86	0.004
ANN	mTest	0.43	0.01	0.17	0.001	0.85	0.004
ANN	mTest+mFTIR	0.46	0.01	0.16	0.002	0.86	0.005

[1]Model prediction methodology: artificial neural network (ANN), partial least squares (PLS), multiple linear regression (MLR)
[2]Coefficient of determination
[3]Potential explanatory variable group: producer-recorded and milk composition variables (mTEST), milk Fourier transform infrared absorbance variables (mFTIR), and all collected variables (mTest+mFTIR)
[4]Root mean square error
[5]Area under the curve of the receiver operating characteristic curve

Table 6.5. Model fit statistics for blood β-hydroxybutyrate prediction models in external validation using the testing set.

	Model[1]			
Fit Statistics	PLS-mTest+mFTIR	ANN-mFTIR	ANN-mTest	ANN-mTest+mFTIR
R^2	0.50	0.50	0.51	0.56
RMSE[3]	0.17	0.17	0.17	0.16
CCC[4]	0.66	0.66	0.67	0.69
Mean bias	0.00004	0.00027	0.00029	0.00001
MSE Decomp[5]				
Mean	0.0	1.0	1.0	0.0
Slope	1.0	0.1	0.7	1.0
Error	99.0	98.9	98.3	99.0

[1] Partial least squares regression with milk test and milk Fourier transform infrared spectrum absorbance variables (PLS-mTest+mFTIR), artificial neural network with Fourier transform infrared spectrum absorbance variables (ANN-mFTIR), artificial neural network with milk test variables (ANN-mTest), artificial neural network with milk test and milk Fourier transform infrared spectrum absorbance variables (ANN-mTest+mFTIR)

[2]Coefficient of determination

[3]Root mean square error

[4]Concordance correlation coefficient

[5]Mean square error decomposition, %

Table 6.6. Accuracy, sensitivity, specificity, and predictive values of blood β-hydroxybutyrate prediction models for hyperketonemia[1] diagnosis in external validation using the testing set.

	Model[2]			
Diagnostic Statistics[3]	PLS-mTest+mFTIR	ANN-mFTIR	ANN-mTest	ANN-mTest+mFTIR
AUC[4]	0.88	0.83	0.87	0.88
Accuracy[5]	0.73	0.78	0.80	0.80
Sensitivity	0.89	0.76	0.80	0.83
Specificity	0.71	0.78	0.80	0.81
Positive predictive value	0.32	0.35	0.39	0.38
Negative predictive value	0.98	0.95	0.96	0.97

[1]Hyperketonemia diagnosed as blood β-hydroxybutyrate concentration ≥ 1.2 mmol/L as quantified cowside by the Precision Xtra meter (Abbott Diabetes Care, Alameda, CA)

[2]Partial least squares regression with milk test and milk Fourier transform infrared spectrum absorbance variables (PLS-mTest+mFTIR), artificial neural network with Fourier transform infrared spectrum absorbance variables (ANN-mFTIR), artificial neural network with milk test variables (ANN-mTest), and artificial neural network with milk test and milk Fourier transform infrared spectrum absorbance variables (ANN-mTest+mFTIR)

[3]Predicted blood β-hydroxybutyrate threshold for hyperketonemia diagnosis was determined as the value which maximized the formula: sensitivity - (1 - specificity)

[4]Area under the curve of the receiver operating characteristic curve

[5]Calculated as the proportion of correctly identified observations among all observations tested

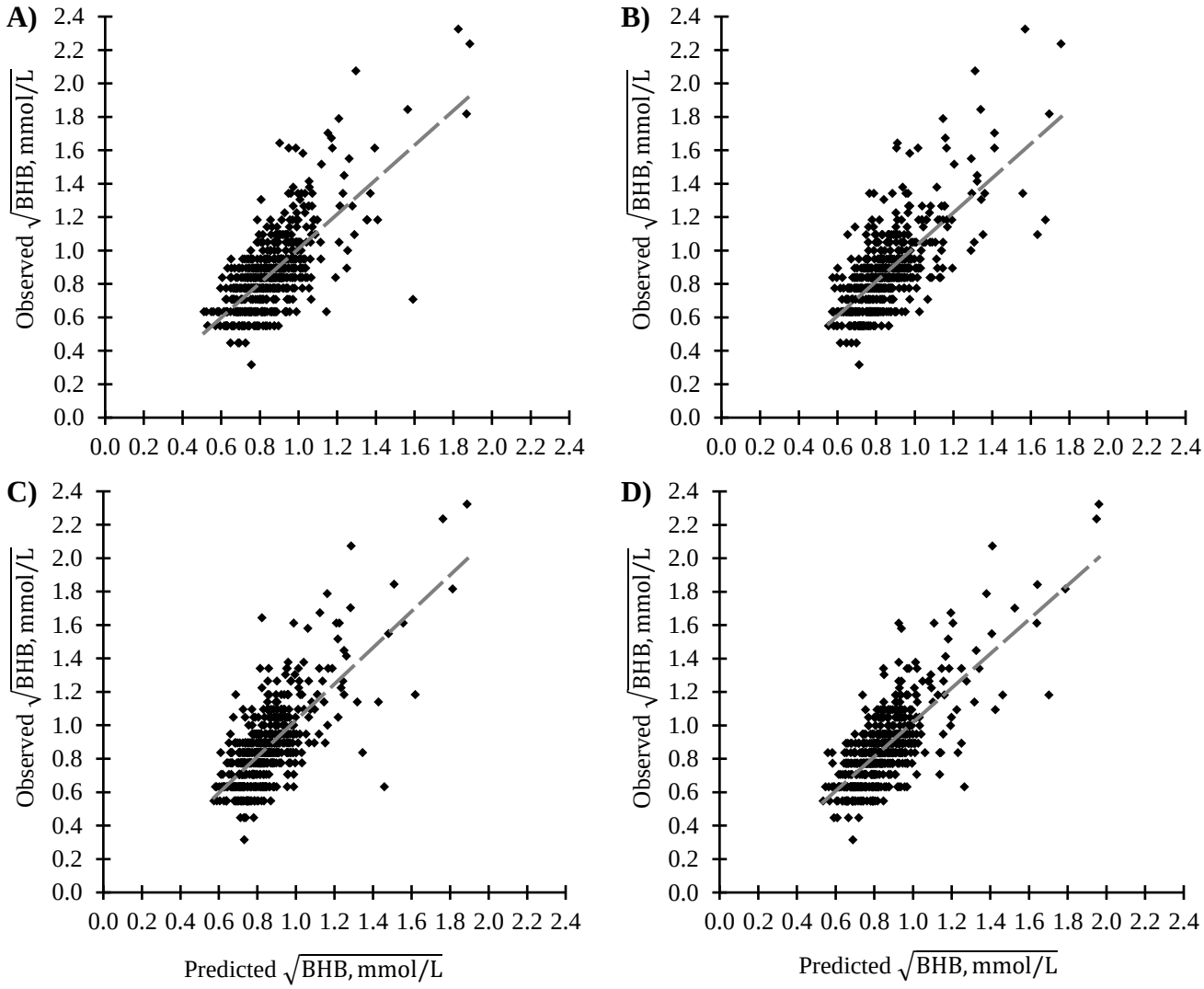

Figure 6.1. Observed versus predicted plots of the square root of β-hydroxybutyrate (BHB, mmol/L; best fit line = gray and dashed) for A) partial least squares regression with milk test and milk Fourier transform infrared spectrum absorbance variables (PLS-mTest+mFTIR), B) artificial neural network with Fourier transform infrared spectrum absorbance variables (ANN-mFTIR), C) artificial neural network with milk test variables (ANN-mTest), and D) artificial neural network with milk test and milk Fourier transform infrared spectrum absorbance variables (ANN-mTest+mFTIR) from external validation in the testing set.

CHAPTER 7: DAIRYING FORWARD

Hyperketonemia (**HYK**) and fatty liver syndrome (**FLS**) are prevalent lipid-related metabolic disorders (**LRMD**) in early lactation dairy cows, that represent a significant financial burden to the dairy production system and animal welfare concern. Therefore, an improved understanding of these metabolic disorders pathology and the proper application of this knowledge in a data-driven management system has tremendous potential for optimizing dairy production systems profitability. Additionally, innovative approaches to diagnose, treat, or prevent LRMD will improve animal health and demonstrate the ongoing commitment to improving animal health and welfare, an essential element to ensuring the dairy industry's social license to operate. This dissertation has pursued several lines of inquiry that expanded our knowledge of HYK and FLS: targeted reductionist research (Chapter 2), discovery-driven inference (Chapters 3 and 5), and development of data-driven management tools (Chapter 6). In this chapter, we will ruminate on the future directions for the research detailed in the preceding chapters and their amalgamation into precision metabolic health management.

Patatin-like Phospholipase Domain-Containing Protein 3

The contribution of liver lipases to FLS and HYK has been largely ignored by previous literature, which made our inquiry into the contributions of the candidate gene patatin-like phospholipase domain-containing protein 3 (**PNPLA3**) exceptionally novel. We were able to detect an inverse relationship between liver PNPLA3 and liver triglyceride (**TG**), despite the FLS induction treatment not reducing liver PNPLA3 abundance or increasing liver TG compared to the control treatment (Chapter 2). This *in vivo* evidence suggests a potential role for liver PNPLA3 in the pathology of FLS. Although not a part of this dissertation, an *in vitro* experiment within the H. M. White lab used small interfering RNA to knockdown *PNPLA3* in primary

bovine hepatocytes, resulting in a reduction of PNPLA3 protein abundance and greater accumulation of cellular TG (unpublished data). This confirmed a direct mechanistic relationship where greater liver PNPLA3 reduces liver TG accumulation. To leverage liver PNPLA3 to improve animal health, future investigations will need to interrogate the regulation of PNPLA3 protein abundance by nutritional factors. In particular, the feed-forward regulatory loop mediated by FA that was proposed by Dr. Helen Hobbs and colleagues (Howard Hughes Medical Institute) needs to be confirmed and its conservation in dairy cows may allow for strategically feeding protected FA to prevent LRMD. Additionally, it has been suggested by Stefano Romeo and colleagues (University of Gothenburg) that impaired or reduced liver PNPLA3 activity may reduce liver capacity to assemble and secrete liver TG as very-low density lipoproteins (**VLDL**). Considering the limited capacity for the ruminant liver to secrete VLDL, liver PNPLA3 abundance may be an important factor to consider in the success or failure of nutritional interventions expected to promote VLDL secretion (*i.e.* choline) and should be studied further.

Variation in LRMD Pathology

Cow metabolism does not uniformly respond to dietary or environmental conditions peripartum across individuals. This is apparent in the epidemiological surveys of LRMD, where only a portion of cows within a herd develop LRMD. Another example is the experiment in Chapter 2, where the FLS induction and control treatments produced overlapping ranges of lipid metabolite concentrations, particularly liver TG. We were able to group these cows in Chapter 3 within dietary condition into distinct metabolic states for both treatments. These observations highlight the need for dairy science research, especially regarding LRMD, to be reproduced across a variety of experimental conditions, so that we have a nuanced, comprehensive understanding of cow biology. It also raises the question of whether we should retrospectively

evaluate metabolic health research in a “responder vs. non-responder” framework within treatments? Research subjects are routinely excluded because of the variation a LRMD case and comorbidities can cause, providing a “cleaner” data set that is often claimed as more representative and sensitive. These so-called outlier exclusions may exclude important biological variation and do not address the underlying biology that drives these “responder vs. non-responder” differences. This research question could be invaluable to the unraveling of the unique mechanisms that diverge to determine treatment success or failure. However, reproducibility of defining a “responder” and “non-responder” presents a serious challenge because the definition of a metabolic health response would need to be stable within and across experimental treatments. An example of this reproducibility challenge is blood β-hydroxybutyrate (**BHB**). Blood BHB concentrations ≥ 1.2 mmol/L have been widely accepted as a diagnostic indicator of HYK. However, there are dietary treatments (*i.e.* lactose or lactate supplementation) that may promote BHB production from butyrate by the rumen epithelium, which could raise blood BHB concentration to meet the HYK diagnostic threshold despite relatively low hepatic ketogenesis. This challenge becomes exponentially more difficult when considering additional LRMD biomarkers (*i.e.* blood FA and liver TG). Our approach using K-means clustering in Chapter 3 provided an empirical solution to considering a multidimensional LRMD phenotype, but the reproducibility challenge remained because clustering was dependent on the original treatment. The solution to the reproducibility challenge is likely more data; either future epidemiological research could establish more thresholds across variable environmental conditions or research that performs clustering should utilize larger sample sizes in an attempt to better represent the greater population of dairy cows.

Integrating Immunometabolism

The intersection of metabolic health, inflammation, and immunity has been a growing field of interest in dairy science. Most of this research has focused on how this immune-metabolic interface has been mediated by gastrointestinal tract and adipose tissue. Our work in Chapter 3 contributed to the limited work suggesting that the liver innate immune response is divergent for cows of different LRMD dispositions. The inferred metabolism of select metabolic pathways in Chapter 3 indicates reactive oxygen species (**ROS**), which are a product of FA oxidation in hepatocytes, may be associated with the liver immune response. Future research could interrogate this hypothesis by exposing cultured hepatocytes in factorial to H_2O_2 and substantial FA concentrations, measuring ROS, oxidized products (*i.e.* proteins and lipids), and the expression of the immunity related genes indicated in Chapter 3 (*i.e.* major histocompatibility complex molecules). The greater question that arises from the associations of immunometabolism to LRMD is whether we should integrate biomarkers of oxidative stress, inflammation, and the immune response into our metabolic health evaluations? If so, what biomarkers do we include? Epidemiological investigations to date have focused on the use of single pro-inflammatory biomarkers (i.e. haptoglobin) as indicators of cow health and productivity. Considering the potential causative role of ROS and oxidative stress, serum markers of protein damage (*i.e.* protein carbonyl content), lipid damage (*i.e.* malonialdehyde), or antioxidant status (*i.e.* superoxide dismutase activity) may be more informative. In addition, LRMD biomarker predictive potentials may be enhanced by considering lipid, inflammation, and immunity metabolites together as an index or predictive model.

Genetics and Phenotyping with Milk Infrared Spectra

Recently, quantitative genetic research has been emphasizing the use of genomic technologies to provide genetic evaluations of health outcomes and leveraging the abundant milk infrared absorbance data to predict novel phenotypic traits (*i.e.* feed efficiency and metabolic health). Our dissection of the HYK genetic architecture (Chapter 5) was especially novel because it was based on HYK phenotypes with low case-control misclassification. This was due to the frequent, repeated sampling of blood BHB in early lactation for each cow. Also, the genetic analysis revealed routinely assessed genomic markers were associated with HYK, some in a parity dependent manner. Of course, future genomic dissections can (and should) be performed with more marker genotypes and a greater number of cows in an effort to replicate our findings and discover new genomic regions of interest. However, it is valuable to consider and incorporate these associated genotypes into HYK genetic evaluations to improve accuracy (detailed in Chapter 4). The parity group × genotype interaction associations provide a particularly interesting challenge for genetic evaluation of HYK. It is possible that a subset of interactions could be considered in HYK genetic evaluations, but the low power of interaction tests makes it difficult to appreciate what interactions and how many need to be considered. Relatively simple methods to address this issue are providing parity group specific genetic evaluations or interrogating the improvement of HYK genetic evaluation accuracy through cross-validation of models with different interaction inclusion parameters. Moving forward, the largest challenge for genomic management of HYK is the generation of accurate phenotypes, because the variation in day in milk at first positive HYK test and short resolution window (days until first negative HYK test) necessitates frequent blood BHB testing. The ideal blood BHB testing frequency would be every other day for the first 3 weeks of lactation. For many lactation traits,

Dairy Herd Improvement milk testing has convenient and reliable mechanism to generate phenotype records for genetic evaluation, which is why we interrogated the use of the data to predict HYK in Chapter 6. The HYK prediction models developed as a part of this dissertation (Chapter 6) may be accurate enough to produce a HYK screening or diagnosis list. However, the frequency of routine Dairy Herd Improvement testing (once a month) is inadequate to diagnose the majority of HYK cases. Presently, some privately-owned WI dairy herds are trialing weekly milk testing of early lactation cows, a timeline consistent with low intensity blood BHB sampling, to determine whether it is efficacious for HYK monitoring. The advent of in-line milk infrared capture by technology, such as AfiLab milk analyzer or the Lely robotic milking systems, provides the opportunity for future development of metabolic health prediction models that can diagnose cows daily. Sufficiently accurate in-line HYK prediction models would rectify sampling intensity issues and allow herds employing that technology to serve as accurate HYK reference populations for genetic evaluation.

Data-Driven Metabolic Health Management

There has been considerable growth in the interest of leveraging technology and data resources to develop decision support tools for dairy farm management that has been concomitant with the increase in farm generated data. With an increasingly technology savvy workforce that is diminishing in size, there is a tremendous opportunity and need to innovate data-driven solutions that utilize labor more strategically and efficiently. Additionally, these data-driven husbandry schemes can allow for individualized managements of cows on large-scale operations. While this dissertation's multifaceted research has provided several novel insights into LRMD pathology and management, it did not directly address the integration and use of the physiological, genomic, and milk infrared data into a data-driven management scheme

for cow metabolic health (Figure 7.1). We previously mentioned the value of integrating HYK prediction models based on Dairy Herd Improvement testing and farm data streams to improve health trait genetic evaluations. Genetic evaluations could also serve as a tool, independently or integrated with other data, to assess risk of LRMD, allowing for management decisions to be made prepartum and selective management postpartum. For example, cows at relatively high risk for HYK could be prophylactically treated, while low risk individual may receive low frequency HYK assessment. Also, there has been substantial adaptation of other technologies, such as rumination collars and activity monitors, that could be integrated into daily data-based health evaluations.

When considering LRMD research and the discussed future directions, we must remember that the metabolic, immune, and nutritive changes across the peripartum period are a part of the orchestrated adaptations that lead to a successful transition. Although maladaptation can lead to LRMD or other unfavorable outcomes, the complete elimination of these responses (e.g. no increase in blood FA or BHB, no mounted immune response) would be detrimental to the cow. Within this context, it is our overall goal to understand the physiological and genomic underpinnings of these adaptations, as well as the animal variation that determine a cow's successful transition, in order to mitigate metabolic failure, generate interventions that optimize cow performance and health, and generate LRMD management and detection tools that are accurate, efficient, and cost-effective.

TABLES AND FIGURES

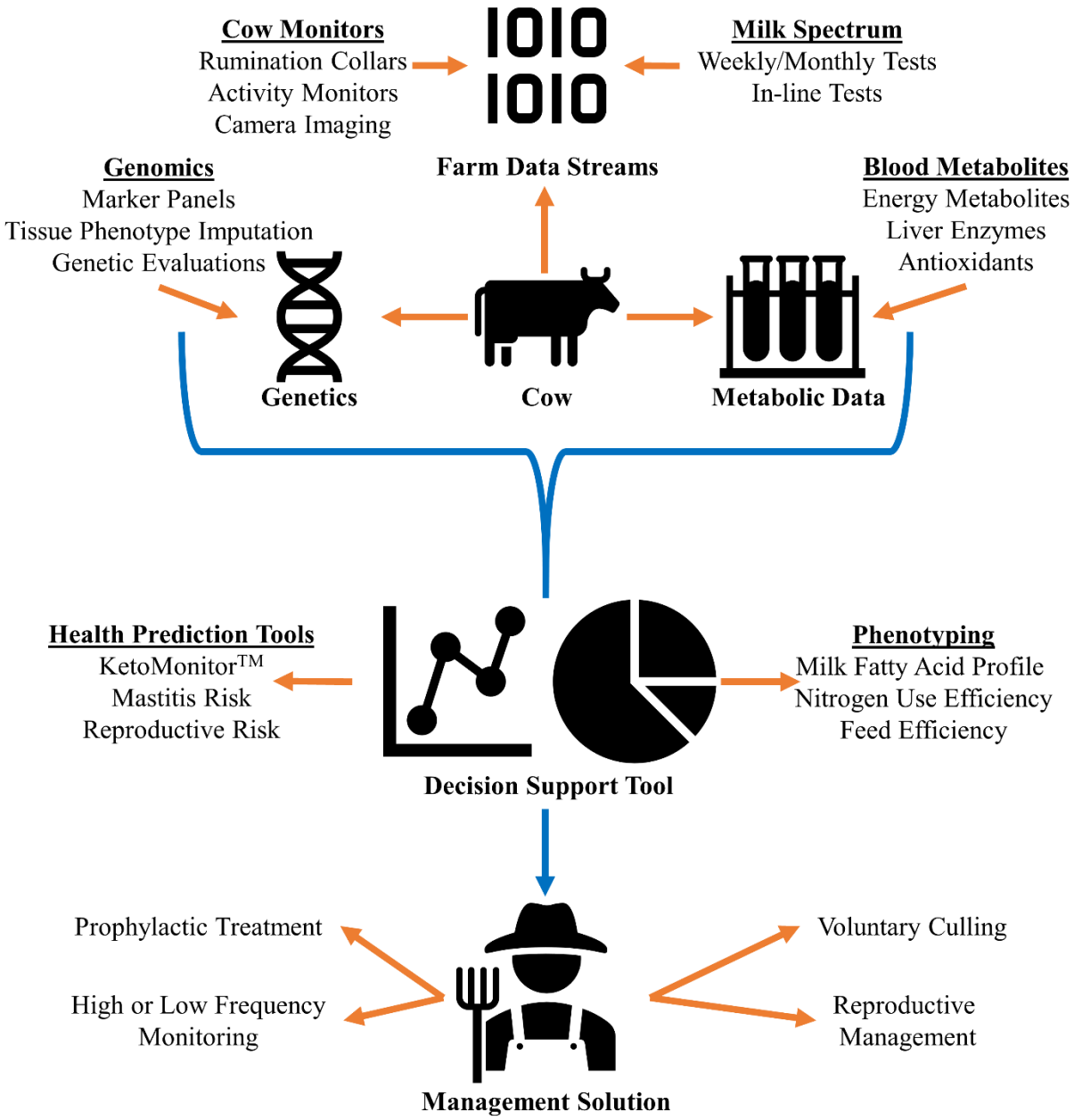

Figure 7.1. A data flow scheme for the data-driven management dairy cows. Orange lines indicate data generation and potential outcomes. Blue lines indicate the directionality of the integration and use of data.